



ADVANCES IN QUANTUM CHEMISTRY

Volume 22

Per-Olov Löwdin

EDITORIAL BOARD

David P. Craig (Canberra, Australia)
Raymond Daudel (Paris, France)
Ernst R. Davidson (Bloomington, Indiana)
Inga Fischer-Hjalmars (Stockholm, Sweden)
Kenichi Fukui (Kyoto, Japan)
George G. Hall (Kyoto, Japan)
Masao Kotani (Tokyo, Japan)
Frederick A. Matsen (Austin, Texas)
Roy McWeeney (Pisa, Italy)
Joseph Paldus (Waterloo, Canada)
Ruben Pauncz (Haifa, Israel)
Siegfried Peyerimhoff (Bonn, Germany)
John A. Pople (Pittsburgh, Pennsylvania)
Alberte Pullman (Paris, France)
Bernard Pullman (Paris, France)
Klaus Ruedenberg (Ames, Iowa)
Henry F. Schaefer III (Athens, Georgia)
Au-Chin Tang (Kirin, Changchun, China)
Rudolf Zahradnik (Prague, Czechoslovakia)

ADVISORY EDITORIAL BOARD

David M. Bishop (Ottawa, Canada)
Jean-Louis Calais (Uppsala, Sweden)
Giuseppe del Re (Naples, Italy)
Fritz Grein (Fredericton, Canada)
Andrew Hurley (Clayton, Australia)
Mu Shik Jhon (Seoul, Korea)
Mel Levy (New Orleans, Louisiana)
Jan Linderberg (Århus, Denmark)
William H. Miller (Berkeley, California)
Keiji Morokuma (Okazaki, Japan)
Jens Oddershede (Odense, Denmark)
Pekka Pyykkö (Helsinki, Finland)
Leo Radom (Canberra, Australia)
Mark Ratner (Evanston, Illinois)
Dennis R. Salahub (Montreal, Canada)
Isaiah Shavitt (Columbus, Ohio)
Per Siegbahn (Stockholm, Sweden)
Harel Weinstein (New York, New York)
Robert E. Wyatt (Austin, Texas)
Tokio Yamabe (Kyoto, Japan)

ADVANCES IN QUANTUM CHEMISTRY

EDITOR-IN-CHIEF

PER-OLOV LÖWDIN

ASSOCIATE EDITORS

JOHN R. SABIN AND MICHAEL C. ZERNER

QUANTUM THEORY PROJECT
UNIVERSITY OF FLORIDA
GAINESVILLE, FLORIDA

VOLUME 22



ACADEMIC PRESS, INC.

Harcourt Brace Jovanovich, Publishers

San Diego New York Boston London Sydney Tokyo Toronto

Academic Press Rapid Manuscript Reproduction

This book is printed on acid-free paper. (∞)

Copyright © 1991 by ACADEMIC PRESS, INC.

All Rights Reserved.

No part of this publication may be reproduced or transmitted in any form or by any means, electronic or mechanical, including photocopy, recording, or any information storage and retrieval system, without permission in writing from the publisher.

Academic Press, Inc.
San Diego, California 92101

United Kingdom Edition published by
Academic Press Limited
24-28 Oval Road, London NW1 7DX

Library of Congress Catalog Number: 64-8029

International Standard Book Number: 0-12-034822-5

PRINTED IN THE UNITED STATES OF AMERICA

91 92 93 94 95 9 8 7 6 5 4 3 2 1

Contributors

Numbers in parentheses indicate the pages on which the authors' contributions begin.

Jan Almlöf (301), Department of Chemistry, Minnesota Supercomputer Institute, University of Minnesota, Minneapolis, Minnesota 55455

H.-P. Cheng (125), Department of Physics and Astronomy, and Materials Research Center, Northwestern University, Evanston, Illinois 60208

D. E. Ellis (125), Department of Physics and Astronomy, and Materials Research Center, Northwestern University, Evanston, Illinois 60208

Steffen Eriksen (167), Department of Chemistry, Odense University, DK-5230 Odense M, Denmark

Shridhar R. Gadre (211), Department of Chemistry, University of Poona, Pune 411 007, India

Jan Geertsen (167), Department of Chemistry, Odense University, DK-5230 Odense M, Denmark

Horacio Grinberg (9), Departamento de Fisica, Facultad de Ciencias Exactas y Naturales, Universidad de Buenos Aires, 1428 Buenos Aires, Republica Argentina

J. Guo (125), Department of Physics and Astronomy, and Materials Research Center, Northwestern University, Evanston, Illinois 60208

George G. Hall (1), Shell Center for Mathematical Education, University of Nottingham, Nottingham NG7 2RD, England

J. J. Low (125), UOP Research Center, Des Plaines, Illinois 60017

Julio Mara  n (9), Departamento de Fisica, Facultad de Ciencias Exactas, Universidad Nacional de La Plata, 1900 La Plata, Republica Argentina

Jens Oddershede (167), Department of Chemistry, Odense University, DK-5230 Odense M, Denmark

Rajeev K. Pathak (211), Department of Chemistry, University of Poona, Pune 411 007, India

Peter R. Taylor (301), ELORET Institute, Palo Alto, California 94303

Preface

In investigating the highly different phenomena in nature, scientists have always tried to find some fundamental principles that can explain the variety from a basic unity. Today they have not only shown that all the various kinds of matter are built up from a rather limited number of atoms, but also that these atoms are constituted of a few basic elements of building blocks. It seems possible to understand the innermost structure of matter and its behavior in terms of a few elementary particles: electrons, protons, neutrons, photons, etc., and their interactions. Since these particles obey not the laws of classical physics but the rules of modern quantum theory of wave mechanics established in 1925, there has developed a new field of “quantum science” which deals with the explanation of nature on this ground.

Quantum chemistry deals particularly with the electronic structure of atoms, molecules, and crystalline matter and describes it in terms of electronic wave patterns. It uses physical and chemical insight, sophisticated mathematics, and high-speed computers to solve the wave equations and achieve its results. Its goals are great, and today the new field can boast of both its conceptual framework and its numerical accomplishments. It provides a unification of the natural sciences that was previously inconceivable, and the modern development of cellular biology shows that the life sciences are now, in turn, using the same basis. “Quantum biology” is a new field which describes the life processes and the functioning of the cell on a molecular and submolecular level.

Quantum chemistry is hence a rapidly developing field which falls between the historically established areas of mathematics, physics, chemistry, and biology. As a result there is a wide diversity of backgrounds among those interested in quantum chemistry. Since the results of the research are reported in periodicals of many different types, it has become increasingly difficult for both the expert and the nonexpert to follow the rapid development in this new borderline area.

The purpose of this serial publication is to try to present a survey of the current development of quantum chemistry as it is seen by a number of the internationally leading research workers in various countries. The authors have been invited to give their personal points of view of the subject freely and without severe space limitations. No attempts have been made to avoid overlap—on the contrary, it has seemed desirable to have certain important research areas reviewed from different points of view.

The response from the authors and the referees has been so encouraging that a series of new volumes is being prepared. However, in order to control production costs and speed publication time, a new format involving camera-ready manuscripts is being

used from Volume 20. A special announcement about the new format was published in that volume (page xiii).

In the volumes to come, special attention will be devoted to the following subjects: the quantum theory of closed states, particularly the electronic structure of atoms, molecules, and crystals; the quantum theory of scattering states, dealing also with the theory of chemical reactions; the quantum theory of time-dependent phenomena, including the problem of electron transfer and radiation theory; molecular dynamics; statistical mechanics and general quantum statistics; condensed matter theory in general; quantum biochemistry and quantum pharmacology; the theory of numerical analysis and computational techniques.

As to the content of Volume 22, the Editors would like to thank the authors for their contributions, which give an interesting picture of part of the current state of the art of the quantum theory of matter: from a historical survey of the foundations of molecular orbital theory, over the Feynman path integral method and its applications to the electronic structure of atoms and molecules, a study of transition metal clusters, investigations of the coupled cluster based polarization propagators and some basic inequalities in quantum chemistry as applied to bounds for energy functionals, to a survey of quantum mechanical calculations based on atomic natural orbitals.

It is our hope that the collection of surveys of various parts of quantum chemistry and its advances presented here will prove to be valuable and stimulating, not only to the active research workers but also to the scientists in neighboring fields of physics, chemistry, and biology who are turning to the elementary particles and their behavior to explain the details and innermost structure of their experimental phenomena.

PER-OLOF LÖWDIN

The Lennard-Jones paper of 1929 and the foundations of Molecular Orbital Theory

George G. Hall

Shell Centre for Mathematical Education,
University of Nottingham,
Nottingham NG7 2RD

ABSTRACT

The 1929 paper by Lennard-Jones is the first one to treat Molecular Orbital theory in a quantitative way. It introduced the Linear Combination of Atomic Orbitals approximation for the molecular orbitals. Its derivation of the electronic structure of the oxygen molecule from quantum principles convinced many chemists that quantum mechanics could contribute something new to their subject. The rigour and computational success of the theory today owe much to this paper and his subsequent developments of it.

1. Introduction

In 1929 a Discussion of the Faraday Society was held in Bristol. It was organized by W.E. Garner and J.E. Lennard-Jones, both local Professors. The subject was Molecular Spectra and Molecular Structure and it brought together many of those most active in these fields at that time including F. Hund, R.S. Mulliken, C.V. Raman, V. Henri and G. Herzberg. To this specialist audience Lennard-Jones presented his first paper on the Theory of Molecular Structure (1). To appreciate the significance of this paper it is necessary to see it in the context of the subject at that time. From today's vantage point, some parts of it may appear conventional and others dated. It is equally important to realise its role in making known to the chemical community the relevance and potential utility of Quantum Mechanical calculation.

The Discussion itself brought together both theorists and experimentalists and, following a trenchant paper by O.W. Richardson, much of the discussion centred on problems of notation and usage of symbols for various quantum numbers. Several of our presently accepted conventions were fixed during that meeting. As is typical of that time, papers on various kinds of spectra predominated and most of these concerned the interpretation of experimental spectra. In these circumstances the Lennard-Jones paper stood out as purely quantum mechanical and highly original.

2. Background

In 1926 Schrödinger published his epoch-making papers (2) on wave mechanics. Then Heisenberg applied perturbation theory (3) to the two-electron problem and showed how "resonance" arising from electron exchange could explain "exchange forces". Heitler and London (4) used this idea to explain the covalent bond as exemplified in the hydrogen molecule. From this beginning the electron-pair, or resonance, treatment of molecular structure developed rapidly. It took over so many of the earlier ideas of the Lewis model of chemical bonding that it was easily accepted by many chemists and became the preferred mode of explanation.

At the same time Hund began to formulate, as an alternative, the Molecular Orbital (MO) theory (5). His objective was to determine the quantum numbers of all the electrons in a molecule and specify its state by vector coupling them, as had proved so successful for atoms. He postulated that each electron should have four quantum numbers which remained invariant with inter-nuclear distance R . Since the electronic structure of atoms could be assumed known, he considered the two limiting cases when R was infinite, giving separated atoms, or zero, giving the united atom. He drew correlation diagrams connecting the electron levels as a function of R and judged that levels going to unoccupied levels of the united atom would be unfavourable to bonding and those remaining occupied for all R would be favourable. With these ideas, and considerable experimental information from spectra of various kinds, he could assign the electron configurations of some diatomics. It emerged from his work that the conservation of the number of nodes in each orbital as R changed was very significant.

A very similar stand-point was taken by Mulliken (6) who adapted Hund's assignments and made more use of atomic data. His extensive

spectroscopic experience enabled him to suggest electronic structures for many diatomics. In particular Mulliken emphasised the importance of the group theory classifications and his distinction between σ , π and δ bonds remains vital to us.

3. The Lennard-Jones paper

The starting-point of Lennard-Jones paper is his uncompromising insistence on the *auf-bau* principle. Just as Bohr built up atoms by adding electrons one by one, so molecules should be built up in the same way. (Mulliken had considered this possibility but thought it impractical.) He then considered what the Schrödinger equation for a typical electron in a diatomic would be. Since he was concerned only with homonuclear diatomics the differential equation can be written out in full but with unknown potentials expressing the effect of all the other electrons on the selected one. By treating these as perturbations he could start with the hydrogen molecular ion equation. Already an approximate solution for this was known using + and - combinations of the separated atomic orbitals. Thus his first approximation to the molecular orbital is a linear combination of H-like atomic orbitals suitably normalized using the overlap integral. The screening constants are adjusted to allow for the other electrons. From his evaluation of the integrals he then gave a correlation diagram having some quantitative significance and showing how different levels could both rise and fall with R .

For the diatomics with few electrons, this approach was quite successful and confirmed many of the assignments already made by Hund and Mulliken. For larger molecules Lennard-Jones introduced another idea. He accepted that atoms with the inert gas structure of completed outer shells could not show bonding. Except for the London force, they must repel one another. By starting from pairs of such atoms and removing electrons one by one he could arrive at the structure of these larger systems. Thus two Ne atoms repelled but the removal of two electrons and the reduction of the nuclear charges gave fluorine molecule with an "inverted H system" in the perturbation to the orbital equation. Thus the single bond of fluorine is due to the removal of two anti-bonding electrons. This gave a fast and easy explanation both for fluorine and oxygen molecules. His argument for the $^3\Sigma$ ground state structure of oxygen was the first to be based on quantum mechanical principles rather than on the interpretation of spectra. His assignment of $^1\Sigma$ for the ground state of the carbon dimer contrasted with the $^3\Pi$ given by Mulliken (6) and

experiment confirmed him, though the separation between the two states is small.

In effect, this Lennard-Jones approach implied that the inner electrons in these molecules remained in atomic orbitals and only the valence electrons needed to be in MO involving both nuclei. This distinction was earlier made by Hund whereas Mulliken thought all electrons should be MO. Mulliken (7) eventually agreed that, while, strictly speaking, all should be in MO, it might be accurate enough to put the inner ones in AO.

As a final contribution, the paper also argued that the notation for the MO should begin with the principal quantum number of the atomic orbital of the separated atom instead of using that of the united atom, as was the custom at that time.

4. The follow-up to the paper

Lennard-Jones himself did not rush to build on his beginning. He was involved in moving to Cambridge. By the time of the next Faraday Discussion on the subject, in 1933, the molecular orbital theory had become much more accepted as a valid and useful theory. In that discussion he presented a paper (8) on hydrocarbon free radicals, including CH_2 , in which group theory is used to help assign the order of the orbital energies and explain the electronic and geometrical structures. E.Hückel attended that meeting and, in the course of the discussion, acknowledged (9) that the first quantitative use of molecular orbital theory was the 1929 paper of Lennard-Jones. Perhaps this contact with Hückel prompted his next molecular paper (10) on the treatment of conjugated hydrocarbons. In this paper he introduced the concepts of compression energy of the σ bonds and the variation of β with distance, which opened up the whole subject of variable CC distances in conjugated hydrocarbons. This paper is still quoted as the formative paper in the treatment of polyacetylene since it allowed for the persistent alternation of double and single bond character despite the length of the molecule.

The first accurate calculation of a molecular orbital wavefunction was the Coulson (11) calculation on the hydrogen molecule. Although the method was then extended to the lithium molecule (12) it relied on the high symmetry of the homonuclear diatomic and did not generalize.

Although Lennard-Jones gave partial explanations much earlier, the final resolution of the problem of justifying the use of atomic orbitals for the inner electrons and diatomic orbitals only for the valence electrons was not achieved until twenty years later when he showed (13) that the determinantal wavefunction had unitary transformations which left it invariant but could be used to transform the molecular orbitals into localized equivalent orbitals without loss of accuracy. In these two papers he gave a rigorous derivation of the orbital equations from the Schrödinger equation using a method he had introduced (14) for the atomic SCF equations. It was not until the third paper in this series (15) that the MOs were completely defined as eigenfunctions of the SCF Hamiltonian. At this point the MO theory became fully rigorous and consistent.

5. Conclusion

By any standards Lennard-Jones must be considered an outstanding scientist. He worked on many problems which continue to interest us and contributed his share of good ideas in each case. Perhaps his work on intermolecular forces is best known today though his theories of liquids and of surface catalysis are still quoted and influence our thinking. His molecular structure work is represented in a relatively small number of papers but shows him trying to understand the fundamental aspects of the subject and injecting ideas which we still find useful.

Lennard-Jones has an important place in the history of theoretical studies in this country. N.F.Mott said (16) of him "If in his Bristol appointment he was the first man in this country to hold a Chair of Theoretical Physics within a Physics Department, certainly he was the first man to hold a chair of Theoretical Chemistry anywhere in the world." He set the style of the subject here and tried very hard, with some success, to explain it to experimental chemists in a very simple way.

References

- 1 Lennard-Jones, J.E. (1929) *Trans.Faraday Soc.* **25**,668
- 2 Schrödinger, E. (1926) *Ann.d.Phys* **79**,361,489,734.

- 3 Heisenberg, W. (1926) *Z.Phys.* **38**,411
- 4 Heitler, W. and London, F. (1927) *Z.Phys.* **44**,455
- 5 Hund, F. (1926) *Z.Phys.* **36**,657
- 6 Mulliken, R.S. (1927) *Phys.Rev.* **32**,186
- 7 Mulliken, R.S. and Rieke, C.A. (1941) *Rep.Progress Phys.* **8**,231
- 8 Lennard-Jones, J.E. (1934) *Trans.Faraday Soc.* **30**,70
- 9 Hückel, E. (1934) *Trans.Faraday Soc.* **30**,59
- 10 Lennard-Jones, J.E. (1937) *Proc.Roy.Soc.* **A158**,280
- 11 Coulson, C.A. (1938) *Proc.Camb.Phil.Soc.* **34**,204
- 12 Coulson, C.A. and Duncanson, W.E. (1943) *Proc.Roy.Soc.* **A181**,378
- 13 Lennard-Jones, Sir John (1949) *Proc.Roy.Soc.* **A198**,1,14
- 14 Lennard-Jones, J.E. (1931) *Proc.Camb.Phil.Soc.* **27**,469
- 15 Hall, G.G. and Lennard-Jones, Sir John (1950) *Proc.Roy.Soc.* **A202**,155
- 16 Mott, N.F. (1955) *Biograph.Mem.Roy.Soc.* **1**,175

THE FEYNMAN PATH INTEGRAL FORMALISM: ATOMIC AND MOLECULAR ELECTRONIC STRUCTURE

HORACIO GRINBERG

Departamento de Física, Facultad de Ciencias Exactas y Naturales, Universidad de Buenos Aires, (1428) Buenos Aires, Republica Argentina.

JULIO MARAÑÓN

Departamento de Física, Facultad de Ciencias Exactas, Universidad Nacional de La Plata, C.C. No 67, (1900) La Plata, República Argentina.

I. Introduction

II. Mathematical Outline

A. General Remarks

B. The Feynman Path Integral

C. Elementary Physical Systems

a. Harmonic Oscillator

b. Density matrix of fermionic states from coherent states via functional integral

III. Path Integral Theory of the Hydrogen Atom

A. General Remarks

B. Theory of the Hydrogenic Oscillator in \mathbb{R}^4

C. Justification of the KS Transformation

IV. General Treatment of Many Electron Systems Through the Feynman Path Integral Representation

A. Path Integral Approach to a Finite Many-Body Problem

- B. Partition Function of the Hückel Model
- C. Application of the Path Integral to the Quantum Fluctuations of the Ground State
- D. Presence of an External Field
- V. Path Integral Formulation of Roothaan's Equations
 - A. Preliminary Considerations and Closure Relations
 - B. The Projected Generating Functional
- VI. Feynman Path Integral Representation of Field Operators and Memory Superoperators in a Liouville Space
 - A. Preliminary Remarks
 - B. Theoretical Background
 - C. Feynman Representation of Memory Superoperators: Physical Interpretation
 - D. Feynman Path Integral Representation of Field Operators
 - E. Application to a Non-Interacting Many-Boson System
 - F. Final Remarks
- VII. Conclusions
- Acknowledgments
- References

I INTRODUCTION

Three classes of approximation methods are commonly employed in many body quantum mechanical problems. *Perturbation techniques* produce series expansions for quantities of interest in powers of a variable which specifies the departure of the given problem from an exactly soluble case. *Variational methods* produce the best estimate out of a given class of trial solutions. In the *Semiclassical approximation* the expressions for wave functions, energy levels, phase shifts, scattering cross sections, etc are derived in which analytic forms are correct in the limiting case where Planck's (reduced) constant \hbar is small in comparison with the action functions occurring in the corresponding classical problem.

This review will deal with the application to atomic and molecular systems of a particular semiclassical approximation, the *Feynman path* (or *functional*) *integral* approach [1] that constitutes the most appropriate tool to work in this scenario.

The original Feynman's path integral formalism was in the framework of classical least-action mechanical principle. The formalism was later extended to quantum mechanics [2] and quantum-field theoretic regime [3]. The problems involved in the precise nature of this transition are well known. It is the requirement of the correspondence principle that the laws of quantum theory must be formulated in such a way that in the limiting case, when many quanta are involved, these laws should go over into those of the corresponding classical theory. The usual interpretation of the correspondence principle is to regard classical theory as the limit of

quantum theory as \hbar goes to zero. This interpretation has led to the belief that deterministic (Hamilton's or Newton's) classical mechanics is indeed the classical limit of Schrödinger's wave mechanics.

In fact, the formulation of quantum theory draws heavily on classical notions, and it is natural that this is so. The various representations of quantum theory - such as the x - or the p -representation of quantum mechanics - are connected with the diagonalization of one or another operator, the physical significance of which is presumed to be known from a classical context. While classically both x and p are needed to specify a system, the Heisenberg uncertainty relation precludes simultaneous specification of both variables, and we are familiar with quantum representations that use only half the classical Cauchy data. Nevertheless, various phase-space representations, such as that proposed by Wigner [4] and Weyl [5], and developed by Moyal [6], employ functions of phase-space variables x and p in their quantum formulations. The price paid for this particular kind of generalization is the inability to specify states of the system that are sharp in both x and p in violation of the uncertainty relation. Once this kind of limitation is understood and accepted, it is no more difficult to use such quantum descriptions, and indeed sometimes it is of considerable conceptual and practical value. In particular, alternative formulations often lend themselves to new and unconventional approximation schemes, which may have applications for a wide variety of problems.

The relation of classical and quantum theories, and the use of semiclassical, or WKB, approximations in quantum problems are, in fact, topics which have

pervaded diverse branches of theoretical chemistry, examples being provided by the calculation of proton tunneling probabilities for the Löwdin model of mutagenesis [7], as well as the investigation of the semiclassical limit of Feynman path integral in order to determine the classical trajectories which contribute to tunneling processes [8,9].

From a methodological point of view, the path integral approach serves as a unifying entity among apparently disconnected disciplines. In recent years Feynman's path integral formulation of quantum mechanics [2], statistical mechanics [10] and quantum field theory [11] has proven to be a surprisingly powerful method in a large variety of problems ranging from nuclear physics [12,13], atomic and molecular physics [14-22], polymer physics [23-25], solid state physics [26,27] and stochastic processes [28] to quantum gravity [29].

Today path integrals play an ever increasing role in providing solutions to problems not so accessible by other methods. Thus, no other approach has been able to match the success of Feynman's treatment of the polaron problem [30].

To facilitate the discussion in this review it will suffice to imagine a functional to be a function of infinitely many variables which are labelled by a continuous index.

The systematic development of the functional calculus began with Volterra [31]. In his work various limiting processes of the analysis of functions, such as continuity and differentiability, were appropriately transcribed to the functional regime. Perhaps the most significant contribution made by Volterra was a general method for handling functional operations. This consists

in approximating a functional with a function of N variables. The results thus obtained depend on N , which in the end is allowed to go to infinity. An example of such a procedure is the well known technique for solving Fredholm's integral equation.

Functional integration as a means for solving partial differential equations of stochastic nature was introduced by Wiener [32], who succeeded in obtaining the fundamental solution (propagator) of the diffusion equation.

For the record of the early history, we should mention that Kirkwood [33] speculated that integration of special functionals in a Wiener sense, could be applied to quantum physics in connection with the evaluation of the statistical sum. As it is well known, this technique became of prime importance in the theory of the Brownian motion [34] as well as in the early development of quantum theory of fields [35].

The wave function of the path integral method has been compared with that deduced from microscopic Green's function approach [2]. In the formulation of the path-integral theory, the wave function is expressed in terms of the kernel of an integral equation. This kernel (the propagator) is a "macroscopic" function related to the result of superposition of microquantum states through the path integral principle. This is the reason why the path integral method can be developed to study quantum systems in an approximate way.

Thus, a careful treatment of the path integral using Feynman's time lattice subdivision process [36] shows that an appropriate formulation of the path integral theory leads to an alternative way [18,19] of handling such problems as those arising in molecular

quantum mechanics associated with the use of propagators or Green's functions [37-49] and based on the so-called second quantized hamiltonians.

In fact, propagators were introduced in molecular quantum mechanics about 20 years ago [50-52]. However, they were used quite extensively in other areas of physics before that [1,53-56].

In the first step of the path integral theory, the wave function is expressed in terms of the kernel of an integral equation

$$\psi(x_1, t_1) = \int_{-\infty}^{\infty} K(x_1, t_1; x_2, t_2) \psi(x_2, t_2) dx_2 \quad (I.1)$$

i.e., the total amplitude to arrive to the space-time point (x_1, t_1) [$\psi(x_1, t_1)$] is the sum, or integral, over all possible values of x_2 of the total amplitude to arrive to the space-point (x_2, t_2) [$\psi(x_2, t_2)$] multiplied by the amplitude to go from (x_2, t_2) to (x_1, t_1) , that is, $K(x_1, t_1; x_2, t_2)$. In the second step this kernel is written as an infinite series of the amplitude function $\phi(x(t_b, t_a))$ contributing between the end points t_b and t_a ,

$$K(a, b) = \sum \phi(x(t_b, t_a)), \text{ overall all paths } a \rightarrow b \quad (I.2)$$

where $\phi(x(t_b, t_a))$ is the amplitude contributed from each path. In the third step this amplitude is expressed as

an algebraic function of the Lagrangian,

$$\phi(x(t_b, t_a)) = \text{const} \exp \left\{ (i/\hbar) S(x(t_b, t_a)) \right\} \quad (1.3)$$

with the action function given by

$$S(x(t_b, t_a)) = \int_{t_a}^{t_b} L(\vec{x}, \dot{\vec{x}}, t) dt \quad (1.4)$$

L being the Lagrangian of the system and x and \dot{x} represent $\vec{x}_1, \vec{x}_2, \dots$ and $\dot{\vec{x}}_1, \dot{\vec{x}}_2, \dots$, respectively.

This review is organized as follows. Section II discusses the Feynman path integral and its application to elementary systems. Thus, in view of its importance in the treatment of the Feynman path integral of the hydrogen atom in four dimensions, we give the derivation of the propagator for the one-dimensional harmonic oscillator within the context of the Feynman path integral. The second example we deal with is a many Fermion particle system, which provides a good example of how the divergencies can be eliminated from the functional integral.

Section III deals with the theory of the hydrogenic oscillator in four dimensions. Following the work of Duru and Kleinert [14] we discuss the hydrogen-oscillator connection in the framework of the unified view of symmetry which emerges in such a treatment.

In Section IV, the Feynman path integral is used to

show the equivalence between a finite many-body problem for a non-relativistic molecular system of N electrons and N one-dimensional Ising models. The idea of quantum fluctuations of the ground state is discussed, a link is established with bifurcation and catastrophe theory and a connection with vacuum state fluctuations is investigated.

Section V is devoted to the generating functional of the molecular orbital theory. We show that the Roothaan's equations are easily obtained when this object is projected onto a subspace of atomic orbitals and the saddle-point approximation to the corresponding effective action is explicitly considered.

In Section VI the Feynman path integral representation for memory superoperators is investigated. A physical interpretation of evolution superoperators in a Liouville space is given and shown to be closely related to Feynman representation of quantum mechanics.

Finally, in Section VII we give the general conclusions.

II. MATHEMATICAL OUTLINE

A. General Remarks

In 1932 Dirac [57], with his paper on the role of Lagrangian mechanics in quantum theory, laid the foundation stone of what was destined to become, in the hands of Feynman, the third formulation of non-relativistic quantum mechanics [1]. Indeed, it was Feynman who began the building of the theory and raised the subject to the rank of a new discipline. The essential idea of this formulation is the concept of a probability amplitude with which every classical trajectory connects two points a and b of the space-time. It should be pointed out that, as far as these trajectories contribute with the same weight of probabilities, the sum over all of these possible paths results in the transition probability amplitudes between these two points.

By associating the idea of propagator or Green function of the Schrödinger equation, a formal definition of the path integral will be given and a detailed description of this methodology as applied to an harmonic oscillator will be presented. More details about the standard formulation of the path integral in terms of the classical action and the corresponding Lagrangian can be found in Refs. [58,59]. To close this Section we shall deal with functional integrals for Fermi systems utilizing a complete system of states, that are closely related with coherent states, and incorporate the necessary algebra of fermions.

B. The Feynman Path Integral

We are now entering fully into the regime of

quantum mechanics. In the present section, we shall construct a path integral giving the propagator of the Schrödinger equation in the case of a time-independent Hamiltonian.

As is well known, the propagator of the Schrödinger equation for a system contains all quantum mechanical information about the system. Thus, it would seem appropriate to begin with considerations as to how the propagator arises and telling us at the same time what thing this propagator is. Equations leading to the propagator are, in general, formulated in terms of the Lagrangian function; however it has been found more useful to work in the Hamiltonian representation and we shall develop our theory in this particular representation.

Let us consider a system with hamiltonian

$$H = -\hbar^2/(2m) \partial^2/\partial \vec{x}^2 + U(\vec{x}) \quad (II.1)$$

The problem we are faced with here is to find the evolution in time of a wavefunction, which at a given time (say $t = 0$) is given through $\psi_0(\vec{x})$. The answer to the problem is obtained by solving the Schrödinger equation:

$$[i \hbar \partial/\partial t - H] \psi(\vec{x}, t) = 0 \quad (II.2)$$

with the initial condition

$$\psi(\vec{x}, 0) = \psi_0(\vec{x}) \quad (II.3)$$

In terms of the evolution operator, $\exp[-(i/\hbar)H t]$, the solution is given by:

$$\psi(\vec{x}, t) = \exp [-(i/\hbar) H t] \psi_0(\vec{x}) \quad (\text{II.4})$$

This clearly satisfies the Schrödinger equation together with the appropriate initial condition (II.3).

In Eq.(II.4), the evolution operator acts locally on the initial wavefunction, which it transforms in time, so that it obeys the Schrödinger equation. If we wish now to disengage the process of propagation from the particular content of the wavefunction we rewrite (II.4) as follows:

$$\begin{aligned} \psi(\vec{x}, t) &= \int \exp [-(i/\hbar) H t] \delta(\vec{x} - \vec{x}') \psi_0(\vec{x}') d\vec{x}' \\ &= \int K(\vec{x}, t | \vec{x}', 0) \psi_0(\vec{x}') d\vec{x}' \end{aligned} \quad (\text{II.5})$$

The kernel

$$K(\vec{x}, t | \vec{x}', 0) = \exp [-(i/\hbar) H t] \delta(\vec{x} - \vec{x}') \quad (\text{II.6})$$

is the propagator in coordinate representation. It supplies the wavefunction at time t (not necessarily later) from the information carried by the wave-function at $t = 0$.

Assuming a discrete spectrum, we can write

$$\delta(\vec{x} - \vec{x}') = \sum_k \langle \vec{x} | \vec{k} \rangle \langle \vec{k} | \vec{x}' \rangle = \langle \vec{x} | \vec{x}' \rangle \quad (\text{II.7})$$

$$\delta(\vec{x} - \vec{x}') = \sum_{\vec{k}} \langle \vec{x} | \vec{k} \rangle \langle \vec{k} | \vec{x}' \rangle = \langle \vec{x} | \vec{x}' \rangle \quad (II.7)$$

where all $\langle \vec{x} | \vec{k} \rangle$ form a complete set of wavefunctions, (II.6) can take the form:

$$\begin{aligned} K(\vec{x}, t | \vec{x}', 0) &= \exp [-(i/\hbar) H t] \langle \vec{x} | \vec{x}' \rangle \\ &= \langle \vec{x} | \exp [-(i/\hbar) H t] | \vec{x}' \rangle \end{aligned} \quad (II.8)$$

Now, one way to obtain an explicit expression for the propagator is to operate as follows:

$$K = [1 - (i/\hbar) H t + 1/2! (-i/\hbar)^2 H^2 t^2 + \dots] \delta(\vec{x} - \vec{x}') \quad (II.9)$$

This is an additive procedure based on a series expansion of the evolution operator.

Another way to go about it is via a multiplicative process based on a product expansion of the evolution operator as follows:

$$\begin{aligned} K &= [1 - (i/\hbar) H t/N] [1 - (i/\hbar) H t/N] \\ &\dots [1 - (i/\hbar) H t/N] \delta(\vec{x} - \vec{x}') \end{aligned} \quad (II.10)$$

If we take the limit as $N \rightarrow \infty$ we have the required

propagator, since:

$$\lim_{N \rightarrow \infty} (1 - (i/\hbar) H \Delta t/N)^N = \exp [-(i/\hbar) H \Delta t] \quad (II.11)$$

The multiplicative procedure is the one employed in path integral constructions.

Next, before we go any further, notice that by adding a term of $O((\Delta t)^2)$, ($\Delta t = t/N$) to any one of the factors $(1 - i/\hbar H \Delta t)$ in (II.10) the limit of the product as $N \rightarrow \infty$ is not affected. So we can obtain our propagator as a limiting case of the matrix element:

$$\langle \vec{x} | (1 - (i/\hbar) H \Delta t) (1 - (i/\hbar) H \Delta t) \dots (1 - (i/\hbar) H \Delta t) | \vec{x}' \rangle \quad (II.12)$$

Inserting complete sets of wavefunctions between the various operators we have

$$K_N(\vec{x} \Delta t | \vec{x}' 0) = \int \langle \vec{x} | 1 - (i/\hbar) H \Delta t | \vec{x}_{N-1} \rangle$$

$$\langle \vec{x}_{N-1} | 1 - (i/\hbar) H \Delta t | \vec{x}_{N-2} \rangle \dots$$

$$\langle \vec{x}_2 | 1 - (i/\hbar) H \Delta t | \vec{x}_1 \rangle \langle \vec{x}_1 | 1 - (i/\hbar) H \Delta t | \vec{x}' \rangle$$

$$dx_1 \, dx_2 \, \dots dx_{N-1} \quad (II.13)$$

We have in (II.13) N short-time propagators of the form:

$$\langle \vec{x}_{j+1} | 1 - (i/\hbar) H \Delta t | \vec{x}_j \rangle = (1 - (i/\hbar) H \Delta t) \delta(\vec{x}_{j+1} - \vec{x}_j) \quad (II.14)$$

but $(N - 1)$ 3D integrations.

To obtain the form of the Feynman path integral we employ the plane wave decomposition of the identity transformation, i.e.,

$$\delta(\vec{x}_{j+1} - \vec{x}_j) = 1/(2\pi)^3 \int d\vec{k} \exp [i \vec{k} \cdot (\vec{x}_{j+1} - \vec{x}_j)] \quad (II.15)$$

The decomposition is done using essentially the eigenfunctions of the kinetic energy operator.

Putting the Hamiltonian (II.1) into (II.14), we have with the aid of (II.15) an approximate expression for the short-time propagator, as:

$$\begin{aligned}
& \langle \vec{x}_{j+1} | 1 - (i/\hbar) [-\hbar^2/(2m) \partial^2/\partial \vec{x}_{j+1}^2 + U(\vec{x}_{j+1})] \Delta t | \vec{x}_j \rangle \\
&= 1/(2\pi)^3 \int d\vec{k} \langle 1 - [i \hbar k^2/(2m) + (i/\hbar) U_j(\vec{x})] \Delta t \rangle \\
&\quad \exp [i \vec{k} \cdot (\vec{x}_{j+1} - \vec{x}_j)] \quad (II.16)
\end{aligned}$$

Notice that on the r.h.s. of (II.16) \vec{x}_{j+1} in $U(\vec{x}_{j+1})$ was replaced by \vec{x}_j on account of the δ -function accompanying it.

As pointed out earlier we can add to the short-time operators of (II.16) any terms of order higher than Δt , without this affecting the limit. So, we can replace in (II.16) the term in the angular brackets by an exponential, which has the same expansion to order Δt , i.e. $\langle \vec{x}_{j+1} | 1 - (i/\hbar) H \Delta t | \vec{x}_j \rangle$ is replaced by

$$\begin{aligned}
& 1/(2\pi)^3 \int d\vec{k} \exp [-i \hbar k^2/(2m) \Delta t - i/\hbar U(\vec{x}_j) \Delta t] \\
& \exp [i \vec{k} \cdot (\vec{x}_{j+1} - \vec{x}_j)] = [m/(2 \pi i \hbar \Delta t)]^{3/2} \\
& \exp (i/\hbar [m/2 ((\vec{x}_{j+1} - \vec{x}_j)/\Delta t)^2 - U(\vec{x}_j)] \Delta t) \quad (II.17)
\end{aligned}$$

Making the replacements (II.17) in (II.13) we have for the approximate propagator the expression

$$\begin{aligned}
K_N'(\vec{x} \ t | \vec{x}' \ 0) &= \int \exp \left[\frac{1}{\hbar} \left(m/2 \right) [(\vec{x}_{j+1} - \vec{x}_j)/\Delta t]^2 \right. \\
&\quad \left. - U(\vec{x}_j) \Delta t \right] [m/(2 \pi i \hbar \Delta t)]^{3/2} \\
&\quad \prod_{j=1}^{N-1} [m/(2 \pi i \hbar \Delta t)]^{3/2} d\vec{x}_j \quad (II.18)
\end{aligned}$$

with: $\vec{x}_0 = \vec{x}'$, $\vec{x}_N = \vec{x}$.

Notice that in Eq.(II.18) we have the Lagrangian (in discrete form) of our problem revealed.

The product accompanying the exponential on the r.h.s. of (II.18) is the path differential $\mathbb{D} [\vec{x}_1, \vec{x}_2, \vec{x}_3, \dots, \vec{x}_{N-1}]$. It contains the right normalizing factors (measure of integration) for obtaining the propagator, through the multiple process of integration in the limit of infinite sub-division of the interval $[0, t]$. In other words, in the limit as $N \rightarrow \infty$, the sequence $[K_N]$ goes to the required propagator.

$$K_N'(\vec{x} \ t | \vec{x}' \ 0) \rightarrow K(\vec{x} \ t | \vec{x}' \ 0)$$

The above method of path integral construction is essentially Hamiltonian based, and the steps (II.10)-(II.16) originated from Abe [60].

In the limit of infinite refinement of the partitions of the time interval $[0, t]$ we make use of a

notation, naturally emanating from (II.16), and indicating the multiple integrations (integration over paths). We have

$$K(\vec{x}(t) | \vec{x}'(0)) =$$

$$\int \exp \left\{ i/\hbar \int_0^t [m/2 \dot{\vec{x}}^2(\tau) - U(\vec{x}(\tau))] d\tau \right\} D[\vec{x}(\tau)] \quad (\text{II.19})$$

with $\vec{x}(0) = \vec{x}'$, $\vec{x}(t) = \vec{x}$ and where

$$D[\vec{x}(\tau)] =$$

$$[m/(2\pi i \hbar d\tau)]^{3/2} \prod_{0 < \tau < t} [m/(2\pi i \hbar d\tau)]^{3/2} d\vec{x}(\tau) \quad (\text{II.20})$$

However, a word of caution is more than in order here. Expression (II.19) may mislead (especially when vector potentials are involved) to a sequential form, from which although it can be reproduced for smooth (differentiable) paths in the limit of infinite refinement of $[0, t]$, it may fail as a functional integral to lead to the correct propagator. The difficulty arises from contribution made by the discontinuous paths. The 1-dimensional motion analogue of (II.32) is an $(N-1)$ -fold integral for which the range of each of its variables, $\vec{x}_1, \vec{x}_2, \dots, \vec{x}_{N-1}$ extends from $-\infty$ to $+\infty$. These variables take their values independently of

each other. Let us then freeze one particular set of these values and see what picture we reach. We get a set of points each of which lies on a different axis of the set of axes $\vec{x}_0, \vec{x}_1, \dots, \vec{x}_{N-1}, \vec{x}_N$. If we connect these points by a continuous curve we get an idea of the continuous paths entering the process of multiple integration. Actually, this is somewhat illusory, for the continuous paths are not by any means the only paths involved in the integration process; for imagine a sequence of denser and denser partitions of $[0, t]$, which implies that any two consecutive axes are separated from each other by a smaller and smaller distance, tending to zero. Now, since the variables of integration take any values from $-\infty$ to $+\infty$ (which are represented by points on the various axes), this means that the representative points on two consecutive axes (which tend to coalesce) can be separated by an appreciable distance. This sort of situation in the limit of infinite subdivision of our interval produces a broken path. In fact our integration involves all imaginable paths which cross only once each of the axes $x(\tau)$.

It has now become evident that the propagator $K(\vec{x}_t | \vec{x}'_0)$, from time 0 to time t , can be found from knowledge of the propagators $K(\vec{x}_\tau | \vec{x}'_0)$ and $K(\vec{x}_t | \vec{x}_\tau)$, from time 0 to time τ and from τ to t , respectively, by summing over all the intermediate positions \vec{x}_τ at time τ as in the formula:

$$K(\vec{x}_t | \vec{x}'_0) = \int K(\vec{x}_t | \vec{x}_\tau) K(\vec{x}_\tau | \vec{x}'_0) d\vec{x}_\tau \quad (\text{II.21})$$

This is the markovian property of the propagator,

characteristic of the formation of quantal amplitudes through all possible intermediate stages linked by a given time.

In the above construction of the path integral the Hamiltonian was taken to be time-independent. When the Hamiltonian is time dependent, $H(\tau) \neq H(\tau')$ at time τ does not commute with the Hamiltonian $H(\tau')$ at another τ' . The non-commutativity of the Hamiltonian produces a complication and one requires Dyson's time-ordering operator \mathbb{T} for obtaining the evolution $U(t|t')$ from time t' to time t :

$$U(t|t') = \mathbb{T} \exp \left[-i/\hbar \int_{t'}^t H(\tau) d\tau \right] \quad (\text{II.22})$$

The required propagator $K(\vec{x} \ t | \ \vec{x}' \ 0)$ from the space-time point (\vec{x}', t') to the space-time point (\vec{x}, t) is given by

$$K(\vec{x} \ t | \ \vec{x}' \ 0) = \langle \vec{x} \ | U(t|t') \ | \ \vec{x}' \rangle \quad (\text{II.23})$$

However, it is one thing writing down the evolution operator with formal use of the time-ordering operator and another thing obtaining, via a path integral, its configuration representation, the propagator. What we really need is an (approximate) form of the evolution operator suitable for path integral constructions. The way to proceed is via the infinitesimal generators of the evolution operator.

Let us now consider a fine partition, P_N , which for simplicity we take to be isomeric. Then we form the time ordered product, $U(t|t')$, of the various infinitesimal generators $[1 - i H(\tau_j) \Delta t/\hbar]$ as follows:

$$\begin{aligned}
 U_N(t|t') &= \\
 [1 - (i/\hbar) H(t) \Delta t] \dots [1 - (i/\hbar) H(\tau_2) \Delta t] \\
 [1 - (i/\hbar) H(\tau_1) \Delta t]
 \end{aligned}
 \tag{II.24}$$

The evolution operator $U(t|t')$ associated with the time dependent Hamiltonian $H(x,t)$ is obtained from $U_N(t|t')$ by passing to the limit of infinite refinement of the interval $[t',t]$ since:

(i) $U(t|t') \rightarrow 1$ as $t \rightarrow t'$ and (ii) $U(t|t')$ satisfies the (operator) Schrödinger equation.

(i) is easily seen, while (ii) can be obtained by considering the time interval $[t', t + \Delta t]$ and the associated sequence of ordered product, $U_{N+1}(t + \Delta t|t')$ approximating the evolution operator in the extended interval. We have:

$$U_{N+1}(t + \Delta t | t') = (1 - i/\hbar H(\vec{x}, t + \Delta t) \Delta t) U_N(t|t')
 \tag{II.25}$$

which can be written as follows:

$$i\hbar/\Delta t [U_{N+1}(t + \Delta t | t') - U_N(t | t')] = H(t + \Delta t) U_N(t | t') \quad (II.26)$$

We now take the limit as $N \rightarrow \infty$ (or $\Delta t = (t - t')/N \rightarrow 0$) and find

$$i\hbar \partial/\partial t U(t | t') = H(t) U(t | t') \quad (II.27)$$

which tells us that $U(t | t')$ produced from (II.24) through the process of infinite refinement of the interval $[t', t]$ obeys the Schrödinger equation.

Furthermore, as before, it can be seen that by adding to the various infinitesimal generators of (II.24) any quantity of $O((\Delta t)^2)$, these will not affect the limiting value of the operator $U(t | t')$, for they will only produce an additional operator with limiting value zero. This is very important since it also applies to the matrix elements of these operators, and the rest of the story regarding the construction of our path integral follows the lines of the time-independent case.

In fact our path integral for the propagator can be taken to be

$$K(\vec{x} \ t | \vec{x}' \ t') =$$

$$\lim_{\Delta t \rightarrow 0} \int \left[\prod_{r=0}^{N-1} \langle \vec{x}_{r+1} | 1 - (i/\hbar) H(\tau_{r+1}) \Delta t | \vec{x}_r \rangle \right] \prod_{r=1}^{N-1} d\vec{x}_r \quad (II.28)$$

with the end conditions $\vec{x}_0 = \vec{x}'$ and $\vec{x}_N = \vec{x}$.

Eventually (II.28) in the case of a time dependent Hamiltonian with a scalar potential leads again to formula (II.18) for the approximate propagator, but this time with $U(\vec{x}_j)$ replaced by $U(\vec{x}_j, \tau_j)$. Also in the expression (II.19) for the propagator we have the replacement of $U(\vec{x}(\tau))$ by $U(\vec{x}(\tau), \tau)$ i.e. the Lagrangian of the problem appears in the phase again.

C. Elementary Physical Systems

In view of its crucial importance in the treatment of the Feynman path integral of the non-relativistic hydrogen atom, we give the derivation of the propagator for the one-dimensional harmonic oscillator. This is a one-particle system and provides a good example of how to get such object. This technique will be extended to a many particle propagator, from which the density matrix for a fermionic system will be obtained. This constitutes a natural way to connect the methodology of second quantization with the functional integral or path integral.

a. The harmonic oscillator

For an harmonic oscillator the Lagrangian is

$$L = m/2 (\dot{x}^2 - \omega^2 x^2) \quad (II.29)$$

and the classical action is given by [1]

$$S_{cl} = m \omega / (2 \sin \omega T) [(x_a^2 + x_b^2) \cos \omega T - 2 x_a x_b] \quad (II.30)$$

where $T = t_b - t_a$. According to the method for evaluation of Gaussian integrals [1] the propagator can be written in the form

$$K(b,a) = F(T) \exp \{ i m \omega / (2 \hbar \sin \omega T) [$$

$$(x_a^2 + x_b^2) \cos \omega T - 2 x_a x_b] \} \quad (II.31)$$

The remaining function $F(T)$ depends upon the time interval only and is written [1]

$$F(T) = \int_0^0 \left\{ \exp \left[- i / \hbar \int_0^t m/2 (\dot{y}^2 - \omega^2 y^2) dt \right] \right\} D y(t) \quad (II.32)$$

where the integration limits come from the fact that the paths must both reach the same end points $y(t_a) = y(t_b) = 0$, i.e., all paths $y(t)$ start from and return to the

point $y = 0$. We shall solve this at least to within a factor independent of ω , by a method which illustrates a particular way of handling path integrals. Since all paths $y(t)$ go from 0 at $t = 0$ to 0 at $t = T$, such paths can be written as a Fourier sine series with a fundamental period of T . Thus

$$y(t) = \sum_n a_n \sin(n \pi t/T) \quad (\text{II.33})$$

It is possible then to consider the paths as functions of the coefficients a_n instead of functions of y at any particular value of t . This is a linear transformation whose jacobian J is a constant, obviously independent of ω , m , and \hbar .

Of course, it is possible to evaluate this jacobian J directly. However, here we shall avoid the evaluation of J by collecting all factors which are independent of ω (including J) into a single constant factor. We can always recover the correct factor at the end, since we know the value for $\omega = 0$, $F(T) = [m/(2 \pi i \hbar T)]^{1/2}$ (a free particle).

The integral for the action can be written in terms of the Fourier series of Eq.(II.33). Thus the kinetic-energy term becomes

$$\begin{aligned}
\int_0^T \dot{y}^2 dt &= \sum_n \sum_m (n \pi/T) (m \pi/T) a_n a_m \\
&\quad \int_0^T \cos (n \pi t/T) \cos (m \pi t/T) dt \\
&= (1/2) T \sum_n (n \pi/T)^2 a_n^2 \quad (11.34)
\end{aligned}$$

and similarly the potential-energy term is

$$\int_0^T y^2 dt = (1/2) T \sum_n a_n^2 \quad (11.35)$$

On the assumption that the time T is divided into discrete steps of length ε so that there are only a finite number N of coefficients a_n , the path integral becomes

$$\begin{aligned}
F(T) &= J \int_{-\infty}^{\infty} \int_{-\infty}^{\infty} \dots \int_{-\infty}^{\infty} \left\{ \exp \left\{ T/2 \sum_{n=1}^N i m/(2 \hbar) \right. \right. \\
&\quad \left. \left. \left[(n \pi/T)^2 - \omega^2 \right] a_n^2 \right\} \right\} da_1/A da_2/A \dots da_N/A \quad (11.36)
\end{aligned}$$

where, in the present case, the normalizing factor A is

$$A = (2 \pi i \hbar \epsilon / m)^{1/2} \quad (11.37)$$

Since the exponent in Eq.(11.36) can be separated into factors, the integral over each coefficient a_n can be done separately. The result of one such integration is

$$\begin{aligned} & \int_{-\infty}^{\infty} \exp \left[(T/2) i m / (2 \hbar) \left[n^2 \pi^2 / T^2 - \omega^2 \right] a_n^2 \right] da_n / A \\ &= (2 N)^{1/2} / T \left[n^2 \pi^2 / T^2 - \omega^2 \right]^{-1/2} \end{aligned} \quad (11.38)$$

where $T/\epsilon = N$ was used. Thus, the path integral is proportional to

$$\begin{aligned} & \prod_{n=1}^N (n^2 \pi^2 / T^2 - \omega^2)^{-1/2} \\ &= \prod_{n=1}^N (n^2 \pi^2 / T^2)^{-1/2} \prod_{n=1}^N [1 - \omega^2 T^2 / (n^2 \pi^2)]^{-1/2} \end{aligned} \quad (11.39)$$

The first product does not depend on ω and combines with the jacobian and other factors (e.g. $(2N)^{1/2}/T$)

into a single constant. The second factor has the limit $[(\sin \omega T)/(\omega T)]^{-1/2}$ as $N \rightarrow \infty$, that is, as $\epsilon \rightarrow 0$. Thus

$$F(T) = C [\sin \omega T / (\omega T)]^{-1/2} \quad (\text{II.40})$$

where C is independent of ω . But for $\omega = 0$ our integral is that for a free particle, for which it can be shown that

$$F(T) = [m / (2 \pi i \hbar T)]^{1/2} \quad (\text{II.41})$$

Hence for the harmonic oscillator we have

$$F(T) = [m \omega / (2 \pi i \hbar \sin \omega T)]^{1/2} \quad (\text{II.42})$$

and the complete solution is obtained as

$$K(b,a) = [m \omega / (2 \pi i \hbar \sin \omega T)]^{1/2} \exp \left\{ i m \omega / (2 \hbar \sin \omega T) \left[(x_a^2 + x_b^2) \cos \omega T - 2 x_a x_b \right] \right\} \quad (\text{II.43})$$

By keeping track of all the constants it is found that the Jacobian J satisfies the condition

$$J(2N)^{1/2} \pi^{-N} \prod_{n=1}^N (1/n) \rightarrow 1 \quad \text{as } N \rightarrow \infty \quad (\text{II.44})$$

b. Density matrix of fermionic systems from coherent states via functional integral

Functional integrals have been widely employed for the study of both the dynamical and the statistical properties of quantum systems. Functional integrals for second quantized Hamiltonians have been devised for boson systems [35c,61-63] but as Matthews and Salam [35d] pointed out, the functional integrals for Bose systems can be applied to Fermi systems with the use of quaternions. For applications to many-body expansions see refs. [64-66].

In what follows, use is made of functional integrals in order to construct a propagator, from which the matrix density of interacting fermions is obtained. Our procedure is based on the use of the complete system of coherent states.

We wish to produce a functional integral giving the propagator associated with a given Hamiltonian, H , in terms of a complete set of states $|\gamma\rangle$. We make use of a generalization of the formula (II.8)

$$\begin{aligned}
 & \langle \vec{\gamma} | T \exp \left[-(i/\hbar) \int_{t'}^t H(\tau) d\tau \right] | \vec{\gamma}' \rangle \\
 &= \lim \int \left[\prod_{r=0}^{N-1} \langle \vec{\gamma}^{(r+1)} | 1 - i/\hbar H(\tau_r) \Delta\tau_r \right. \\
 & \quad \left. + O((\Delta\tau)^2) | \vec{\gamma}^{(r)} \rangle \right] \prod_{r=0}^{N-1} d\vec{\gamma}^{(r)} \quad (II.45)
 \end{aligned}$$

with $\vec{\gamma}^{(0)} = \vec{\gamma}'$, $\vec{\gamma}^{(N)} = \vec{\gamma}$ and $\max(\Delta\tau_r) \rightarrow 0$.

The time interval $[t', t]$ is partitioned as usual by

points τ_r with $\tau_0 = t'$, $\tau_N = t$; $\Delta\tau_r = \tau_{r+1} - \tau_r$. \mathcal{T} signifies the time ordering operator; $d\vec{\gamma}$ is the product of differentials of the components of $\vec{\gamma}$ in the case of rectilinear variables, and this is the case we are dealing with.

The r.h.s. of Eq.(II.45) is essentially our functional integral. It is quite general and accomodates first and second quantized Hamiltonians, irrespective of the statistics obeyed by the system. Thus, we consider a Fermi system for which its particles can go into n channels and introduce the following n -channel state:

$$\begin{aligned}
 | \gamma_n \dots \gamma_2 \gamma_1 \rangle = & \pi^{-n/2} \exp \left[-1/2 \sum_{j=1}^n |\gamma_j|^2 \right] \\
 & \left[1 + \sum_{j=1}^n \gamma_j c_j^+ + \sum_{j>l=1}^n \gamma_j \gamma_l c_j^+ c_l^+ \right. \\
 & + \sum_{j>l>k=1}^n \gamma_j \gamma_l \gamma_k c_j^+ c_l^+ c_k^+ + \dots \\
 & \left. + \gamma_n \dots \gamma_2 \gamma_1 c_n^+ \dots c_2^+ c_1^+ \right] |0\rangle
 \end{aligned} \tag{II.46}$$

where the γ_j 's are complex numbers (labelling the state), $|0\rangle$ is the vacuum state, and c_j^+ is the fermion creation operator for the channel j .

The state (II.46) contains all possible independent 0,1,2,...,n fermion states; each once. Thus, the 2-fermion states for $n=3$ are taken to be: $c_2^+ c_1^+ |0\rangle$, $c_3^+ c_1^+ |0\rangle$, $c_3^+ c_2^+ |0\rangle$. Any permutation of their operators

will generate dependent states. As is well known, these states are orthogonal between themselves and all states with the lower or higher number of particles.

The bra-form of the state (II.46) is written in terms of the annihilation operators c_j and the complex conjugates $\bar{\gamma}_j$ of γ_j as:

$$\begin{aligned} \langle \gamma_1 \gamma_2 \dots \gamma_n | &= \pi^{-n/2} \exp \left[-1/2 \sum_{j=1}^n |\gamma_j|^2 \right] \\ \langle 0 | &\left[1 + \sum_{j=1}^n \bar{\gamma}_j c_j + \sum_{j>1}^n \bar{\gamma}_1 \bar{\gamma}_j c_1 c_j \right. \\ &+ \left. \sum_{j>1}^n \bar{\gamma}_k \bar{\gamma}_1 \bar{\gamma}_j c_k c_1 c_j + \bar{\gamma}_1 \bar{\gamma}_2 \dots \bar{\gamma}_n c_1 c_2 \dots c_n \right] \end{aligned} \quad (\text{II.47})$$

The totality of the states $|\gamma_n \dots \gamma_2 \gamma_1\rangle$ forms a complete set in the sense

$$\int |\gamma_n \dots \gamma_2 \gamma_1\rangle \langle \gamma_1 \gamma_2 \dots \gamma_n| \prod_{j=1}^n d^2 \gamma_j = 1 \quad (\text{II.48})$$

$d^2 \gamma$ means: $d(\text{Re } \gamma) d(\text{Im } \gamma)$.

For establishing (II.48) one needs repeated use of the integral

$$\int \pi^{-1} \exp \left[- |\gamma|^2 \right] \left\{ \begin{array}{c} 1 \\ |\gamma|^2 \\ \gamma, \bar{\gamma} \end{array} \right\} d^2 \gamma = \left\{ \begin{array}{c} 1 \\ 1 \\ 0,0 \end{array} \right\} \quad (\text{II.49})$$

and the completeness of independent $0,1,2,\dots,n$ fermion states produced through the action of combinations of products of creation operators on the vacuum state, as in (II.46).

The essentials of functional integration with our states can be shown in their entirety even in the simplest case with a Hamiltonian of the form $H = \sum \epsilon_j c_j^+ c_j$. In fact, from the technical point of view, the multi-channel case with interaction adds nothing more than similar manipulations of the same kind. However, we will use a Hamiltonian involving interaction, i.e.,

$$H_1 = \sum_{j=1}^3 \epsilon_j c_j^+ c_j + \sum_{j>l=1}^3 v_{jl} c_j^+ c_l^+ c_l c_j \quad (\text{II.50})$$

We wish to evaluate the propagator:

$$\langle \gamma_1 \gamma_2 \gamma_3 | \exp (-i H_1 t) | \gamma_3' \gamma_2' \gamma_1' \rangle$$

$$= \lim_{\Delta t \rightarrow 0} \int \left[\prod_{r=0}^{N-1} \langle \gamma_1^{(r+1)} \gamma_2^{(r+1)} \gamma_3^{(r+1)} | 1 - i H_1 \Delta t | \right]$$

$$\gamma_3^{(r)} \gamma_2^{(r)} \gamma_1^{(r)} \rangle \Big] \prod_{r=1}^{N-1} d^2 \gamma_1^{(r)} d^2 \gamma_2^{(r)} d^2 \gamma_3^{(r)} \quad (II.51)$$

with $\vec{\gamma}^{(0)} = \gamma'$, $\vec{\gamma}_N = \vec{\gamma}$.

In Eq.(II.51) the superscript, r , labels the complex variables associated with the point of partition $t_r = r \Delta t$ ($\Delta t = t/N$). Furthermore, for simplicity, we have absorbed in the t Planck's constant \hbar , i.e., our t is (time/\hbar) .

To do the evaluation in Eq.(II.51) we just need the matrix element:

$$\begin{aligned} & \langle \gamma_1^{(1)} \gamma_2^{(1)} \gamma_3^{(1)} | 1 - i H_1 \Delta t | \gamma_3' \gamma_2' \gamma_1' \rangle \\ &= \pi^{-3} \exp \left[-1/2 \sum_{j=1}^3 (|\gamma_j^{(1)}|^2 + |\gamma_j'|^2) \right] \left[1 + \sum_{j=1}^3 A_j \bar{\gamma}_j^{(1)} \gamma_j' \right. \\ &+ \sum_{j>l=1}^3 A_{jl} \bar{\gamma}_j^{(1)} \gamma_l' + A_{123} \bar{\gamma}_1^{(1)} \gamma_1' \bar{\gamma}_2^{(1)} \gamma_2' \bar{\gamma}_3^{(1)} \gamma_3' \Big] \end{aligned} \quad (II.52)$$

where:

$$A_j = 1 - i \epsilon_j \Delta t, \quad A_{jl} = 1 - i (\epsilon_j + \epsilon_l + V_{jl}) \Delta t$$

and

$$A_{123} = 1 - i (\varepsilon_1 + \varepsilon_2 + \varepsilon_3 + V_{12} + V_{13} + V_{23}) \Delta t \quad (II.53)$$

It is apparent from (II.52) that all creation and annihilation operators involved in the states $|\vec{\gamma}'\rangle$ or $\langle\vec{\gamma}|$ disappear when matrix elements are evaluated and, more importantly, the ordering of complex variables $\vec{\gamma}$ is of no consequence.

Next we perform the integral

$$\begin{aligned} & \int \langle \gamma_1^{(2)} \gamma_2^{(2)} \gamma_3^{(2)} | 1 - i H_1 \Delta t | \gamma_3^{(1)} \gamma_2^{(1)} \gamma_1^{(1)} \rangle \\ & \langle \gamma_1^{(1)} \gamma_2^{(1)} \gamma_3^{(1)} | 1 - i H_1 \Delta t | \gamma_3' \gamma_2' \gamma_1' \rangle \prod_{j=1}^3 d^2 \gamma_j^{(1)} \\ & = \pi^{-3} \exp \left[-1/2 \sum_{j=1}^3 (|\gamma_j^{(2)}|^2 + |\gamma_j'|^2) \right] \\ & \left[1 + \sum_{j=1}^3 A_j^2 \bar{\gamma}_j^{(2)} \gamma_j' + \sum_{j>l=1}^3 A_{jl}^2 \bar{\gamma}_j^{(2)} \gamma_j' \bar{\gamma}_l^{(2)} \gamma_l' \right. \\ & \left. + A_{123}^2 \bar{\gamma}_1^{(2)} \gamma_1' \bar{\gamma}_2^{(2)} \gamma_2' \bar{\gamma}_3^{(2)} \gamma_3' \right] \quad (II.54) \end{aligned}$$

The integrations are extremely simple and involve

repeated use of formula (II.49). It is clear from (II.54) that by folding two consecutive short-time propagators the resulting (approximate) propagator, corresponding to time $2 \Delta t$, has the same form, but with the quantities A_j , A_{jl} , A_{123} squared. The complete folding of the short-time propagators corresponding to finite time, t , leads to the same form, but with the various A 's raised to the power of N .

In the limit as $N \rightarrow \infty$ (i.e., $\Delta t \rightarrow 0$) these quantities [see Eq.(II.53)] become:

$$A_j^N \rightarrow \exp [-i \varepsilon_j t] , \quad A_{jl}^N \rightarrow \exp [-i (\varepsilon_j + \varepsilon_l + V_{jl})t]$$

$$A_{123}^N \rightarrow \exp [-i (\varepsilon_1 + \varepsilon_2 + \varepsilon_3 + V_{12} + V_{13} + V_{23})t]$$

So, it thus follows from Eq.(II.48), that the required propagator takes the form

$$\langle r_1 r_2 r_3 | \exp (-i H_1 t) | r_3' r_2' r_1' \rangle$$

$$= \pi^{-3} \exp \left[-\frac{1}{2} \sum_{j=1}^3 (|r_j|^2 + |r_j'|^2) \right]$$

$$\begin{aligned}
& \left\{ 1 + \sum_{j=1}^3 \exp \left(- i \varepsilon_j t \right) \bar{\gamma}_j \gamma_j' \right. \\
& + \sum_{j>1=1}^3 \exp \left[- i \left(\varepsilon_j + \varepsilon_1 + v_{j1} \right) t \right] \bar{\gamma}_j \gamma_j' \bar{\gamma}_1 \gamma_1' \\
& + \exp \left[- i \left(\varepsilon_1 + \varepsilon_2 + \varepsilon_3 + v_{12} + v_{13} + v_{23} \right) t \right] \\
& \left. \bar{\gamma}_1 \gamma_1' \bar{\gamma}_2 \gamma_2' \bar{\gamma}_3 \gamma_3' \right\} \quad (II.55)
\end{aligned}$$

from which we get for the expectation value of the density operator of the three fermion interacting system in the coherent state representation the expression

$$\begin{aligned}
\langle \rho(\gamma; \gamma') \rangle &= \pi^{-3} \exp \left[- 1/2 \sum_{j=1}^3 \left(|\gamma_j|^2 + |\gamma_j'|^2 \right) \right] \\
& \left\{ 1 + \sum_{j=1}^3 \bar{\gamma}_j \gamma_j' \right. \\
& + \sum_{j>1=1}^3 \bar{\gamma}_j \gamma_j' \bar{\gamma}_1 \gamma_1' + \bar{\gamma}_1 \gamma_1' \bar{\gamma}_2 \gamma_2' \bar{\gamma}_3 \gamma_3' \left. \right\} \quad (II.56)
\end{aligned}$$

The propagator (II.56) associated with the second

quantized Hamiltonian (II.50) is exact, and incorporates the Fermi-Dirac statistics. The various terms in (II.56) are (separately) symmetric with respect any exchange of a pair of indices. This enables one to remove restrictions on the indices in the sums and introduce appropriate factorials and δ 's of Kronecker, although this might not be helpful in an actual evaluation. Nevertheless, it helps to shorten the analytic expressions for more general cases, e.g., when use is made of a two body second quantized Hamiltonian involving n states. In this case the expressions for the various matrix elements required to evaluate the propagator are rather complicated. Recurrence relations for these matrix elements can be obtained from the anticommutation relations [67].

As a final remark it should be pointed out that replacement of complex variables in the boson functional integral with anticommuting complex variables (quaternions) would produce the corresponding functional integral for the fermion propagator [35c]. However, functional integrals with quaternions are good for obtaining relations, but not so easy for handling direct evaluations.

III. PATH INTEGRAL THEORY OF THE HYDROGEN ATOM

A. General Remarks

Path integrals are of special interest with respect to bound states, because one has to deal with infinitely many classical paths whose constructive interference leads to resonances, alias bound states. These can be in momentum space much better understood on the basis of classical trajectories for the following reasons. A particle with a given negative energy E has only a limited domain in position space that is available for its classical motion. On the other hand, all of momentum space is classically accessible, provided the attractive potential has a singularity of the Coulomb type. All we need are the classical trajectories and the first-order fluctuations around them. No effort is made to estimate the importance of the large fluctuations, because their effect vanishes in the limit of small Planck's quantum \hbar . It is natural to use the classical motion as a starting point in order to find an approximate solution for Schrodinger's equation. This idea was implicit in the "old quantum mechanics" of Bohr and Sommerfeld, and was made explicit in the WKB approximation.

In fact, approximate analytic expressions for single electron wave functions of bound states in atoms or simple molecules are provided by the phase-integral approximation, sometimes called the WKB method. In particular, this approximation was applied to the Coulomb potential in momentum space, in which the location of poles on the negative axis gives the Bohr formula for bound-state energies, and the residues of the approximate Green's function were shown to yield all the exact wave functions for the bound states of the

hydrogen atom [68].

On the other hand, it is well known that only Gaussian path integrals can easily be computed. The hydrogen atom does not belong to this kind of problem and the calculation of the density matrix involving the Coulomb potential is a formidable task. Nevertheless, this has been carried out with success within Feynman's path integral formalism, in which the eigenvalues and eigenfunctions of the hydrogen atom are calculated in a closed form by transforming the Coulomb three-dimensional problem into one in four dimensions [14-16,69]. This procedure is justified as the degeneracy of bound states of the nonrelativistic hydrogen atom is known to be linked with its rotational invariance in four-dimensional Euclidean space. It was recognized that the momentum representation is most convenient for realizing this connection, an approach which has been used to obtain an explicit construction for Green's function of this problem [70]. A semiclassical method of evaluating the path integral for the hydrogen atom was also proposed [71], in which the calculation is performed in configuration space with the Langer modification of the angular momentum [72]. More recently, the Feynman path integral for the Coulomb potential was calculated exactly by reducing it to a gaussian form by means of a transformation formula for a class of non-linear space-time transformations in the radial path integral [73].

B. Theory of the Hydrogenic Oscillator in \mathbb{R}^4

Among the various procedures leading to an appropriate kernel for the hydrogen atom, that of Duru et al. [14,69] in combination with the

$$K(\mathbf{r}_a, \mathbf{r}_b; \tau) = \int \mathbb{D}[\mathbf{r}] \exp \left[i \int_0^\tau L(\mathbf{r}, \dot{\mathbf{r}}) dt \right] \quad (\text{III.1})$$

in combination with the KS transformation made it possible to transform the non-relativistic hydrogen atom into a four-dimensional isotropic harmonic oscillator. In what follows we will consider analytical details of such a transformation, leading to a kernel which has residues that are the product of four one-dimensional harmonic oscillator wave functions. Then the well known expansion of the kernel of an isotropic harmonic oscillator [Eq.(II.43)] will be used to generate the hydrogenic wave functions Ψ_{nlm} as various combinations of the product of one-dimensional oscillator wave functions. Complete analytical details, as well as a discussion of the unified view of symmetry which emerges in such a treatment, were given by Grinberg et al. [16]. Also, the use of the KS transformation as applied to the Coulomb potential was justified [17,75] by connecting the homogenous space with the quotient space within the Feynman quantization formalism. It should be emphasized that the $\mathbb{R}^3 \rightarrow \mathbb{R}^4$ hydrogen-oscillator connection is of paramount importance in the study of atomic systems subjected to electric and/or magnetic fields. In this respect, the problem of a hydrogenlike atom in an electric field or a strong magnetic field can be transformed, by means of the KS transformation, into the problem of a four-dimensional isotropic oscillator presenting anharmonicity of degree 4 or 6, respectively [76]. Therefore, many calculations arising in the Zeeman

and Stark effects for the hydrogen atom may be conducted in the oscillator representation. It is thus desirable to have the wave functions for the corresponding four-dimensional oscillator.

The theory of the hydrogenic oscillator in \mathbb{R}^4 proceeds as follows. We start by writing Feynman's formula for Green's function involving the Coulomb potential; it reads

$$K(x_b, t_b; x_a, t_a) = \int \mathbb{D}^3[x] \frac{\mathbb{D}^3[p]}{(2\pi)^3} \exp \left[i \int_{t_a}^{t_b} dt \left[p \dot{x} - p^2/(2m) + e^2/r \right] \right] \quad (\text{III.2})$$

and is not readily integrable due to the $1/r$ potential. Duru and Kleinert [14] parametrize the paths in terms of a new auxiliary "time"

$$s(t) = \int^t d\tau \, 1/r(\tau) \quad (\text{III.3})$$

If this connection is enforced via a Dirac- δ function, the propagator $K(x_b, t_b; x_a, t_a)$ can be cast in the form

$$K(x_b, t_b; x_a, t_a) = \int dE/(2\pi) \exp [-iE(t_b - t_a)] K(x_b, x_a; E) \quad (\text{III.4})$$

where the energy propagator is given by ($\dot{r} = d/ds$)

$$K(x_b, x_a; E) = \int_{s_a}^{\infty} ds_b \exp [i e^2 (s_b - s_a)] r_b$$

$$\int \mathbb{D}^3[x] \frac{\mathbb{D}^3[p]}{(2\pi)^3} \exp \left[i \int_{s_a}^{s_b} ds \left[p \cdot \dot{x} - r \cdot p^2 / (2m) + E r \right] \right]$$

(III.5)

where $s_a = s(t_a)$, $s_b = s(t_b)$, and use has been made of the Fourier decomposition of the δ function.

After multiplying expression (III.4) by a dummy path integral involving a new completely arbitrary pair of canonical coordinates (x_4, p_4) [14,16,17], the path integral in Eq.(III.5) is brought to the four-dimensional form

$$\int_{-\infty}^{\infty} d(x_4)_b \int \mathbb{D}^4[x] \frac{\mathbb{D}^4[p]}{(2\pi)^4}$$

$$\exp \left[i \int_{s_a}^{s_b} ds \left(p \cdot \dot{x} - r \cdot p^2 / (2m) + E r \right) \right]$$

(III.6)

On introducing a fourth coordinate and momentum components, it is possible to get six generators of the angular momentum L_{ij} ($i, j=1,2,3,4$). These six generators L_{ij} obey the same commutation relations as (L_x, L_y, L_z) and therefore constitute the generalization of the three generators L from three to four dimensions. The group

that they generate can be shown to be the proper rotation group in four dimensions $O(4)$ [77]. This evidently does not represent a geometrical symmetry of the hydrogen atom, since the fourth components x_4 and p_4 are fictitious and cannot be identified with dynamical variables [78]. It turns out that the constants of the motion of the hydrogen atom in this space are the angular momentum L and the Runge-Lenz-Pauli vector [79]. These operators satisfy the commutation relations of the Lie algebra that corresponds to a symmetry transformation of the $O(4)$ group [80].

We now introduce a canonical change of variables through the KS transformation [74] from (x, p) to (u, p_u) such that

$$r = u = [x^2(s)]^{1/2} \quad (\text{III-7})$$

and construct a map from \mathbb{R}^4 into physical space \mathbb{R}^3 . The 4×4 linear orthonormal matrix $A(u)$ performing such a transformation is well known [14,16,75,81]. The space is mapped onto $\mathbb{R}^3 \ni (x_1, x_2, x_3)$ by A with the annihilation condition $dx_4 = 0$, i.e., x_4 is a cyclic coordinate of the system. In momentum space $p = (p_1, p_2, p_3) \in \mathbb{R}^3$ and $p_u \in \mathbb{R}^4$, where p_4 is a constant of the motion [16]. The Laplacian operator in this particular four-dimensional Riemann subspace becomes

$$4 r p^2 = p_u^2 = - \nabla_4^2 \quad (\text{III-8})$$

an equation which is useful for expressing the energy propagator $K(x_b, x_a; E)$ in the (u, p_u) space.

Although as yet there exists no rigorous mathematical definition of integration over paths, there is still a precise enough formulation of the method

introduced by Feynman which consists in defining the path integral as a limit of finite dimensional integration. Introducing the Jacobian J of the linear transformations $x = A(u) u$ and $p = A(u) p_u$ [14,16]:

$$J(x/u) = 16 r^2 \quad \text{in } r \text{ space} \quad (\text{III.9a})$$

$$J(p/p_u) = (16 r^2)^{-1} \quad \text{in } p \text{ space} \quad (\text{III.9b})$$

together with Eqs.(III.7) and (III.8), the path integral (III.6) is transformed to

$$1/(16 r_b) \int_{-\infty}^{\infty} d(x_4)_b / r_b \int_{x_a, (x_4)_a}^{x_b, (x_4)_b} \mathbb{D}^4[u] \mathbb{D}^4[p_u] / (2\pi)^4 \\ \exp \left[i \int_{s_a}^{s_b} ds \left(p_u u' - p_u^2 / (2\mu) - \mu^2 \omega^2 u^2 / 2 \right) \right] \quad (\text{III.10})$$

where $\mu = 4 m$ and $\omega^2 = -E/(2 m)$ and is recognized, apart from the integral over $d(x_4)_b / r_b$, to be the Green function of an isotropic harmonic oscillator in four dimensions .

When the KS transform is expressed in the quaternionic polar (or Euler-angle) coordinates (r, θ, φ) through an auxiliary angle α , defined on \mathbb{R}^4 through

$$u = r^{1/2} \begin{pmatrix} \sin 1/2 \theta \cos 1/2 (\alpha + \varphi) \\ \sin 1/2 \theta \sin 1/2 (\alpha + \varphi) \\ \cos 1/2 \theta \cos 1/2 (\alpha - \varphi) \\ \cos 1/2 \theta \sin 1/2 (\alpha - \varphi) \end{pmatrix} \quad (\text{III.11})$$

the integral $\int_{-\infty}^{\infty} d(x_4)_b / r_b$ can be written [14,16]

$$\int_{-\infty}^{\infty} d(x_4)_b / r_b = \int_0^{4\pi} d\alpha_b \sum_{\alpha_b \rightarrow \alpha_b + 4n\pi}, \quad n = \pm 1, \pm 2, \pm 3, \dots \quad (\text{III.12})$$

where the sum is part of the Green's function of the harmonic oscillator (as always if cyclic variables are used) [82]. Thus Eq.(III.10) can be written

$$1/(16 r_b) \int_0^{4\pi} d\alpha_b F^4(T) \exp \left[-\pi F^2(T) [(u_a^2 + u_b^2) \cos \omega T - 2 u_a u_b] \right], \quad (\text{III.13})$$

where $T = (s_b - s_a)$ and $F(T)$ is the usual fluctuation factor of the one-dimensional oscillator [Eq.(II.42)].

In order to relate the propagator $K(x_b, x_a; E)$ with the harmonic oscillator wave functions we perform the spectral decomposition of the integrand of Eq.(III.13) and symmetrize it in u_b (since $\alpha_b \rightarrow \alpha_b + 2\pi$ corresponds to $u_b \rightarrow -u_b$ and expand, for $E < 0$ as

$$\sum_{n_1=0}^{\infty} \exp \left[-i \omega \left[\sum_{i=1}^4 n_i + 2 \right] T \right] \Phi_{n_1 n_2 n_3 n_4}(u_b) \Phi_{n_1 n_2 n_3 n_4}^*(u_a) \quad (\text{III.14})$$

where

$$\Phi_{n_1 n_2 n_3 n_4}(u) = \prod_{i=1}^4 \phi_{n_i}(u_i) \quad (\text{III.15})$$

and the $\phi_{n_i}(u_i)$ ($i=1,2,3,4$) are the one-dimensional harmonic oscillator wave functions, i.e., they constitute the basis functions in a four-dimensional Riemann space. The n_i are subjected to the constraint

$$\sum_{i=1}^4 n_i = 2(n-1) = 0, 2, 4, \dots \quad (\text{III.16})$$

Finally, inserting (III.14) in the propagator (III.5), and after some rather involved analysis, leads to

$$K(x_b, x_a; E) = -m/p_o^2 \sum_{n=0}^{\infty} i(1 - \nu/n)^{-1} \int_0^{2\pi} d\alpha_b \left[(p_o/8n)^{1/2} \Phi_{n_1 n_2 n_3 n_4}(u_b) \right] \left[(p_o/8n)^{1/2} \Phi_{n_1 n_2 n_3 n_4}^*(u_a) \right] \quad (\text{III.17})$$

where the variables ν and p are abbreviated symbols for $\nu = e^2/2\omega = [-m e^4/(2 E)]^{1/2}$ and $p_0 = (-2 m E)^{1/2}$. The sum in Eq.(III.17) explicitly displays the bound state poles at

$$E_n = - m e^4/(2 n^2), \quad n = 1, 2, 3, \dots, \quad (\text{III.18})$$

with the residues being the wave functions in unconventional quantum numbers. In this connection, it should be pointed out that it is rather remarkable that almost all quantum numbers can be interpreted as invariants of certain groups. In fact, the KS transformation is closely connected to the $SU(2) \otimes SU(2)$ symmetry of the Kepler motion which exhibits the dynamical symmetry $SO(4)$. Clearly, there is a nice isomorphism between the two groups [83].

In three-dimensional space, the Schrödinger equation for the hydrogen atom is separable in spherical polar and parabolic coordinates. While its separability in the former is related to the spherical symmetry of the central Coulomb potential, its separability in the latter is attributed to the "hidden" symmetry which is responsible for the degeneracy peculiar to the potential.

We now use the four-dimensional results given above in order to evaluate the atomic orbitals of the non-relativistic hydrogen atom. This will be performed through the residues of the first order poles of the propagator (III.17) in combination with the KS transform in polar coordinates [Eq.(III.11)]. This makes possible to reduce the dynamical symmetry of the hydrogen atom described by the $O(4)$ generators to the geometrical symmetry of $O(3)$ [81,84,85]. In order to proceed, the

kernel describing the motion of an isotropic harmonic oscillator [Eq.(II.43)] is expanded in exponential functions of time multiplied by products of energy eigenfunctions

$$F(T) \exp \left[-\pi F^2(T) \left(u_a^2 + u_b^2 \right) \cos \omega T - 2 u_a u_b \right] \\ = \sum_{j=0}^{\infty} \exp (-E_j T) \phi_j(u_b) \phi_j^*(u_a) \quad (\text{III.19})$$

On expanding the left-hand side of this equation in successive powers of $\exp (i \omega T)$, the different one-dimensional oscillator eigenfunctions can be obtained [1]. Taking into account the constraint (III.16), it can easily be seen that when $n = 1$, the only combination of the n_i is $n_1 = 0$ ($i = 1,2,3,4$). Therefore from the residue of the propagator (III.17), the wave function of the lowest energy level of the hydrogen atom becomes

$$\Psi_{100} = (2 \pi)^{1/2} (p_0/8)^{1/2} \phi_{0000} \quad (\text{III.20a})$$

When $n = 2$, there exist different combinations of the n_i obeying the constraint (III.16), so that the hydrogenic wave functions ψ_{nlm} can be expressed as various combinations of the functions $\phi_{n_1 n_2 n_3 n_4}(u)$ given in Eq.(III.15). The first few cases are given below:

$$\Psi_{200} = (2\pi)^{1/2} (p_o/16)^{1/2} [\Phi_{2000} + \Phi_{0200} + \Phi_{0020} + \Phi_{0002}] \quad (\text{III.20b})$$

$$\Psi_{211} = (2\pi)^{1/2} (p_o/16)^{1/2} [\Phi_{1010} + \Phi_{0101}] \quad (\text{III.20c})$$

$$\Psi_{210} = (2\pi)^{1/2} (p_o/16)^{1/2} [\Phi_{0010} + \Phi_{1001}] \quad (\text{III.20d})$$

$$\Psi_{21-1} = (2\pi)^{1/2} (p_o/16)^{1/2} [\Phi_{2000} + \Phi_{0200} - \Phi_{0020} - \Phi_{0002}] \quad (\text{III.20e})$$

Similar results have been obtained by Chen [84] in the study of the Stark effect of the hydrogen atom. On using the one-dimensional oscillator eigenfunctions generated by expansion (III.19) together with the KS transform, the different hydrogenic atomic orbitals are easily generated [16].

It should be emphasized that the problem of the expansion of an \mathbb{R}^3 hydrogen wave function in terms of \mathbb{R}^4 oscillator wave functions was recently studied in a systematic way [86,87], in which passage formulas from oscillator to hydrogen wave functions were obtained in various cases resulting from the combination of several coordinate systems.

Moreover, on using the $SO(2,1)$ algebra generators and through the study of the N-dimensional Schrödinger equation, the equivalence between the hydrogen atom and the isotropic harmonic oscillator was established [88]. Finally, it was recently reported that the realization of a stereographic projection of the coordinates of an isotropic four-dimensional harmonic oscillator on two

orthogonal unit hyperboloids in a six-dimensional space is a new form of geometrizing the Coulomb field, that is, the homomorphism between $SO(4,2)$ and $SU(4,2)$ was explicitly demonstrated [89].

C. Justification of the KS Transformation

In general, a Hamiltonian path integral is not invariant under a nonlinear canonical transformation [90,91]. Therefore it is important to see if the KS transformation performed in each short-time integral would give rise to the desired global change of variables without bringing up any additional effect.

In view of its possible application to the helium atom we now make a series of topological considerations to justify the KS transformation as applied to the Coulomb potential. Ringwood and Devreese [92] considered this problem as the motion on the quotient space of a conformally flat manifold. We now make some further methodological comments on this interesting question, by connecting the homogeneous space with the quotient space within the Feynman quantization formalism. To this end, let \mathcal{L} be the classical Lagrangian

$$\mathcal{L} = 1/8 \dot{x}_i \dot{x}_i + e^2/r \quad (\text{III.21})$$

where the mass is taken as $1/4$. We now apply the KS transformation in polar coordinates [14,16,75] and obtain the Lagrangian in \mathbb{R}^4 (Roman indices run from 1 to 3 and Greek indices run from 1 to 4),

$$\mathcal{L} = 1/2 g^{\alpha\beta} \dot{u}_\alpha \dot{u}_\beta + e^2/u^2 \quad (\text{III.22})$$

where $g^{\alpha\beta}$ is the metric tensor in \mathbb{R}^4 and the metric is

$$ds^2 = \epsilon^{\alpha\beta} du_\alpha du_\beta \quad (\text{III.23})$$

for all points of the space; i.e., it is the metric of a conformally flat Riemannian space. The scalar curvature R is $-18 u^4$ so that the Lagrangian takes the scalar form

$$\mathbb{L} = 1/2 \epsilon^{\alpha\beta} \dot{u}_\alpha \dot{u}_\beta + e^2 (-R/18)^{1/2} \quad (\text{III.24})$$

R is constant for all points of the doubly connected space M since it is isotropic and homogeneous [93] and by definition its metric (III.23) is constant in all of its points. We find that Eq.(III.24) is the classical Lagrangian of a free particle which moves on an isotropic and homogeneous Riemannian space of metric $\epsilon^{\alpha\beta}$ [75].

The "short time" (quasiclassical) propagator of the Schrödinger equation in this Riemann space is

$$K(u_b, t_b; u_a, t_a) = N \int D^4[u] \exp \left[i \int_{t_a}^{t_b} \mathbb{L}_{\text{eff}} dt \right] \quad (\text{III.25})$$

where N is a normalization constant and \mathbb{L}_{eff} is the effective Lagrangian [90]

$$\begin{aligned} \mathbb{L}_{\text{eff}} = \mathbb{L} - \left\{ 1/8 R + 1/8 \left[\epsilon^{\alpha\beta} \partial_\beta \Gamma_{\alpha\gamma}^\delta - \epsilon^{\beta\gamma} \Gamma_{\beta\gamma}^\alpha \Gamma_{\alpha\delta}^\delta \right. \right. \\ \left. \left. - \epsilon^{\alpha\beta} \Gamma_{\alpha\delta}^\gamma \Gamma_{\beta\gamma}^\delta \right] \right\} \end{aligned} \quad (\text{III.26})$$

where $\Gamma_{\alpha\beta}^\gamma$ are the three-index Christoffel symbols. Since the homogeneous space is a conformally Riemannian space, Eq.(III.26) reduces to

$$L_{\text{eff}} = 1/2 \, \xi^{\alpha\beta} \dot{u}_\alpha \dot{u}_\beta - V_{\text{eff}} \quad (\text{III.27})$$

and V_{eff} is given by

$$V_{\text{eff}} = -e^2(-R/18) + R/8 \quad (\text{III.28})$$

In fact, R is a constant which in Eq.(III.25) introduces a phase as the only additional physical effect. On using Eqs.(III.25) and (III.27) together with the Fourier transform of the energy propagator [Eq.(III.4)], we are led to

$$K(u_b, u_a; E) = M \int \mathbb{D}^4[u] \mathbb{D}^4[p_u] / (2\pi)^4 \exp \left[i \int_{t_a}^{t_b} dt [(p_u)_\alpha \dot{u}_\alpha - 1/2 \, \xi^{\alpha\beta} (p_u)_\alpha (p_u)_\beta + E u^2] \right] \quad (\text{III.29})$$

where $M = N \exp [i e^2 (s_b - s_a)]$. In order to get the propagator in the homogeneous space we use the integral transform (III.3) and arrive at

$$K(u_b, u_a; E) = M \int \mathbb{D}^4[u] \mathbb{D}^4[p_u] / (2\pi)^4 \exp \left[i \int_{s_a}^{s_b} ds \left[p_u u' - 1/2 \, p_u^2 - 1/2 \, \omega^2 u^2 \right] \right] \quad (\text{III.30})$$

This is the propagator in the doubly connected space M . Increasing the value of the auxiliary angle α_b [Eq.(III.12)] in 4π one generates the Lie group of continuous rotations $SO(3)$, where the manifold of the

group is the universal covering space \bar{M} of the space M [75]. Following Dowker [94] the connection of the homogeneous space M with the quotient space $\bar{M}/SO(3)$ enables us to calculate the propagator of the Coulomb problem in the physical space \mathbb{R}^3 . Thus

$$\begin{aligned} K(x_b, x_a; E) \bar{M}/H &= \int_{SO(3)} K(u_b, u_a; E) \bar{M} \, d\alpha \\ &= \int_{-\infty}^{\infty} K(u_b, u_a; E) \bar{M} \, d\alpha \end{aligned} \quad (\text{III.31})$$

where the simply connected space \bar{M} is defined by the map $\bar{M} \rightarrow M = \bar{M}/H$ and H is a properly discontinuous discrete group of isometries of \bar{M} without fixed points.

The integral $\int_{-\infty}^{\infty} d\alpha$ can be written in the form

$$2 \int_0^{2\pi} d\alpha_b \quad \alpha_b \rightarrow \alpha_b + 4n\pi \quad (\text{III.32})$$

because the end points are homotopically equivalent; i.e., the K S transformation realizes a mapping from \mathbb{R}^4 in \mathbb{R}^3 , so that all the $\alpha_b + 4n\pi$ correspond to the same extreme x_b in \mathbb{R}^3 . Thus, developing the integrand of Eq.(III.31) for $E < 0$, the expansion (III.14) is obtained. As it has been shown [95,96] the strict equivalence between the Shrödinger equation and the Feynman path integral in a Riemann space together with the justification of the KS transform in the path integral formulation of the hydrogen atom gives an alternative proof of the results of Chen [84].

Finally, the singular character of the Lagrangian

$$L = p_u \dot{u} - 1/2 p_u^2 + e^2/u^2 = 1/2 p_u^2 + e^2/u \quad (\text{III.33})$$

with the constraint [see Eq.(III.3)]

$$t_b - t_a - \int_{s_a}^{s_b} ds \, r(s) = 0 \quad (\text{III.34})$$

is a matter of deep concern in the path integral formalism. In particular, the Lagrangian (III.33) becomes a constrained Lagrangian in \mathbb{R}^4 if the annihilation condition $dx_4 = 0$ is imposed [16]. On using the Dirac's theory [97] it is possible to transform such Lagrangian in that of a four-dimensional isotropic harmonic oscillator

$$L = p_u \dot{u} - 1/2 p_u^2 + E u + e \quad (\text{III.35})$$

performing the quantification of the corresponding constrained Hamiltonian [98].

It should be pointed out that the KS transformation is a generalization of the Levi-Civita transformation [99], which is a conformal mapping of \mathbb{R}^2 onto \mathbb{R}^2 [100]. Its generalization requires to use two complex variables in a four-dimensional Riemann space. Thus, the bilinear condition, implicit in the annihilation constraint $dx_4=0$, [16,75] has to be imposed in order that (x_4, p_4) become simultaneously zero. By means of this artifice it is possible to recover the problem in the physical space \mathbb{R}^3 .

A final point to be considered concerns to the topological meaning of this annihilation condition. The set of points in \mathbb{R}^4 which are in correspondence, through the KS transformation, with a given point in \mathbb{R}^3 constitute a "fibre". In this particular case these

fibres are circumferences contained in planes passing through the origin of coordinates of the \mathbb{R}^4 space. Therefore, topologically, the covering space \tilde{M} is a bundle, i.e., a fibred space and H is the group of the bundle. Together with the base space M and the mapping $\tilde{M} \rightarrow M$, H and M make up a fibre bundle. In short, through the KS transformation every trajectory $x(t)$ in \mathbb{R}^3 is mapped onto curves which, by virtue of the condition $dx_4 = 0$, are orthogonal to the fibres. Consequently, according to (III.31), the quotient space $M = \tilde{M}/H$ enables to "sum" (i.e., integrate) the different contributions of the propagator over all fibres through the Lie group H . It should be pointed out that the topological equivalence between the hydrogenic system and the free-particle system has recently been established [101] by a homeomorphic embedding of \mathbb{R}^3 into \mathbb{R}^4 .

IV. GENERAL TREATMENT OF MANY ELECTRON SYSTEMS THROUGH THE FEYNMAN PATH INTEGRAL REPRESENTATION

A. Path-Integral Approach to a Finite Many-Body Problem

Feynman's path-integral formulation of quantum mechanics reveals a deep connection between classical statistical mechanics and quantum theory. Indeed in an imaginary-time formalism, the Feynman integral is mathematically equivalent to a partition function. Now we will construct the Feynman path integral of a non-relativistic N-electron system for a one-dimensional problem. In particular we will be concerned with the formalism developed for field theories (which can be illustrated in the context of non-relativistic quantum mechanics) in order to get more insight into the chemical bonding within the context of the Hückel model [102].

We begin with the Lagrangian for a one-dimensional molecular system having N electrons

$$L = \sum_{\alpha=1}^N \left[\frac{1}{2} \dot{x}_{\alpha}^2 - V(x_{\alpha}) \right] - \sum_{\beta < \alpha} U(x_{\alpha}, x_{\beta}) \quad (\text{IV.1})$$

where $m = 1$ was taken; $V(x_{\alpha})$ is the potential energy of electron α and $U(x_{\alpha}, x_{\beta})$ is the electron-electron repulsion energy. The value of $V(x_{\alpha})$ is independent of the position of the N-1 remaining electrons. From now on Greek indices stand for electrons or molecular orbitals and Roman indices stand for sites or atomic orbitals.

We apply Feynman's formulation of quantum mechanics and consider the amplitude for an electron to propagate between the space-time points (x_a, t_a) and (x_b, t_b) . According to Sect.II the amplitude for this transition

is postulated to be [1]

$$\begin{aligned}
 Z &= Z(x_a, t_a; x_b, t_b) = \langle x_b | \exp [-(i/\hbar) H (t_b - t_a)] | x_a \rangle \\
 &= \int_{-\infty}^{\infty} D[x] \exp \{(i/\hbar) S[x]\} \quad (IV.2)
 \end{aligned}$$

where $D[x]$ is the Feynman path differential measure [Eq.(II.35)] and $S[x]$ is the Minkowski-space action for a particular path. The first form, $\langle x_b | \exp [-iH (t_b - t_a)/\hbar] | x_a \rangle$ [Eq.(II.23)], is the usual quantum mechanical expression for the propagator of a particle moving under the influence of a Hamiltonian H . The second form for $Z(x_b, t_b; x_a, t_a)$ is the path integral formulation [Eq.(II.34)].

On performing the Wick rotation [3]

$$t = -i\tau \quad (IV.3)$$

(t is real time) so as to realize the adequate analytic continuation, we get the euclidean action for discrete time slices

$$\begin{aligned}
 S[x] &= \varepsilon \sum_{i=1}^{N-1} \left\{ \frac{1}{2} \left[(x_{i+1} - x_i)/\varepsilon \right]^2 + V \frac{1}{2} (x_{i+1} + x_i) \right\} \\
 &\quad (IV.4)
 \end{aligned}$$

where the time axis was made discrete by introducing a time lattice $\varepsilon = t_{i+1} - t_i$, i.e., the integral (IV.2) was discretized using a space-time lattice of $N-1$ sites [36,103]. The integration measure of the euclidean path integral given in Eq.(IV.2) is now well defined and is given by

$$Z(N) = B \int_{-\infty}^{\infty} \prod_{i=1}^{N-1} dx_i \exp \left\{ -(1/\hbar) S[x_i] \right\} \quad (\text{IV.5})$$

where $B = (2\pi\hbar^2\Delta T)^{-1/2}$, with $\Delta T = t_b - t_a$.

Before continuing, we note that Eqs.(IV.4) and (IV.5) constitute a one-dimensional statistical-mechanical problem. We have a one-dimensional lattice whose sites are labeled with the index i . On each site there is a variable x_i which takes on values between $-\infty$ and ∞ . The action couples nearest-neighbor variables x_i and x_{i+1} . The integral $\int \prod dx_i$ implies a summation over all paths $x(t)$, which start at x_a at time t_a and end at x_b at time t_b . Each path $x(t)$ is weighted by a phase factor determined by the classical action S associated with this path. Thus, Eq.(IV.5) is identical to the partition function for a one-dimensional Ising model.

We now return to the evaluation of the integrals in Eq.(IV.5) and organize our analysis in an enlightening fashion by writing [36]

$$Z(N) = B \int_{-\infty}^{\infty} \prod_{i=1}^{N-1} dx_i \hat{T}(x_{i+1}, x_i) \quad (\text{IV.6})$$

since the action only couples nearest neighbor lattice variables x_i . \hat{T} is the matrix element of an operator - the transfer matrix - and is given by

$$\hat{T}(x_{i+1}, x_i) = \exp \left\{ -(1/\hbar) [(x_{i+1} - x_i)^2 / (2\epsilon)] \right\}$$

$$+ V(1/2(x_{i+1} + x_i)) \epsilon] \rangle \quad (\text{IV.7})$$

The equivalence of the path integral with the Hamiltonian approach to quantum mechanics can be established through this operator [36]. We now set up a space of one-electron states by expanding the eigenket $|\psi_\alpha\rangle \equiv |\alpha\rangle$ satisfying

$$H|\alpha\rangle = E_\alpha|\alpha\rangle \quad (\text{IV.8})$$

as a linear combination of atomic orbitals

$$|\phi_i(x_i)\rangle \equiv |\phi_i\rangle$$

$$|\alpha\rangle = \sum_{i=1}^N c_{\alpha i} |\phi_i\rangle \quad (\text{IV.9})$$

Then the spectral decomposition of the partition function in the site representation becomes

$$Z_{\text{rs}}(N) = \sum_{\alpha=1}^N \exp(-E_\alpha K/\hbar) \langle \phi_r | \alpha \rangle \langle \alpha | \phi_s \rangle \quad (\text{IV.10})$$

where K is a positive number. Thus, at large K the leading term in Eq.(IV.10) gives us the energy and wavefunction of the lowest-lying energy eigenstate.

Clearly, \hat{T} is the usual time evolution operator of quantum mechanics (imaginary time) evaluated over the interval ϵ . Using \hat{T} , a useful expression for $Z(N)$ can be obtained as

$$\begin{aligned}
Z(N) &= B \int_{-\infty}^{\infty} \prod_{i=1}^{N-1} d\phi_i \langle \phi_{i+1} | \hat{T} | \phi_i \rangle \\
&= B \int_{-\infty}^{\infty} \langle \phi_b | \hat{T} | \phi_{N-1} \rangle d\phi_{N-1} \langle \phi_{N-1} | \hat{T} | \phi_{N-2} \rangle d\phi_{N-2} \\
&\quad \langle \phi_{N-2} | \hat{T} | \phi_{N-3} \rangle \dots \langle \phi_2 | \hat{T} | \phi_1 \rangle d\phi_1 \langle \phi_1 | \hat{T} | \phi_a \rangle \\
&= B \langle \phi_b | \hat{T}^N | \phi_a \rangle
\end{aligned} \tag{IV.11}$$

where $N-1$ is the number of τ slices between τ_a and τ_b and use of the completeness condition

$$1 = \int d\phi |\phi\rangle \langle \phi| \tag{IV.12}$$

has been made. If we impose periodic boundary conditions ($x_b = x_a$) and sum over all possible initial positions of the electron, Eq.(IV.11) is replaced by the more familiar result

$$Z(N) = B \text{Tr } \hat{T}^N \tag{IV.13}$$

where the trace is over the physical Hilbert space. We now express the Hamiltonian in terms of the evolution operator for an infinitesimal step in time (short-time propagator); it was shown to be [36]

$$\hat{T} = \exp \{-(\varepsilon/\hbar) [H + O(\varepsilon)]\} \tag{IV.14}$$

Therefore, choosing $\tau' - \tau = \varepsilon$ to be infinitesimal so

that this interval consists of just one slice we have

$$Z_{rs}(N) = \langle x_r | \exp [-(\epsilon/\hbar) H] | x_s \rangle \quad (\text{IV.15})$$

The Hamiltonian in the site representation reads

$$H = \sum_s |\phi_s\rangle H_{ss} \langle\phi_s| + \sum_{\langle s,r \rangle}' |\phi_r\rangle H_{rs} \langle\phi_s| \quad (\text{IV.16})$$

where $\langle s,r \rangle$ are site indices coupling the nearest neighbors. The diagonal part is

$$H_{ss} = \langle\phi_s| \dot{x}^2/2 + V(x) |\phi_s\rangle \quad (\text{IV.17})$$

We restrict the present treatment to molecules consisting of the same kind of atoms. Therefore H_{rs} becomes a constant.

$$H_{rs} = \langle\phi_r| \dot{x}^2/2 + V(x) |\phi_s\rangle \quad (\text{IV.18})$$

and the second summation in Eq.(IV.16) becomes simply $(\beta = H_{rs})$

$$H = \beta \sum_{\langle s,r \rangle}' |\phi_s\rangle \langle\phi_r| \quad (\text{IV.19})$$

which is recognized to be the Hamiltonian of a continuum Ising model with no external field [104].

We now extend this result to an N -electron non-relativistic molecular system and characterize the wavefunction by a configuration specified by one-electron wavefunctions ψ_α . As long as the fermionic character is concerned we may select the antisymmetric component of the Hartree product in order to fulfill the Pauli exclusion principle automatically, which (except

for a constant factor) transforms the wavefunction into a Slater determinant, i.e.,

$$|\Psi\rangle = |N!|^{-1/2} \sum_{\{P\}} \delta_P P[\psi_1(1) \dots \psi_\alpha(\alpha) \dots \psi_N(N)] \quad (\text{IV.20})$$

where $\delta_P = (-1)^P$ (P , parity of the permutation) and the sum extends over all possible permutations. $\psi_\alpha(\alpha)$ ($\alpha = 1, 2, \dots, N$) are one-electron wavefunctions which can be expanded in terms of an orthonormal basis of atomic orbitals [Eq.(IV.9)].

The expression of the partition functional $Q(N)$ for N electrons can be written as [18]

$$Q(N) = B^N \int_{-\infty}^{\infty} \dots \int_{-\infty}^{\infty} \prod_{i=1}^{N-1} dx_i \exp \left\{ -(\epsilon/\hbar) \sum_{i=1}^{N-1} S[x_{i+1}, x_i] \right\} \quad (\text{IV.21})$$

where $x_i = \{x_i^{(1)}, x_i^{(2)}, \dots, x_i^{(\alpha)}, \dots, x_i^{(N)}\}$ represents the set of coordinates associated with the N electrons in the intermediate site i and $\prod dx_i$ is the volume element for all the coordinates. The action is given by

$$S(x_{i+1}, x_i) = \epsilon \left[1/2 [(x_{i+1} - x_i)/\epsilon]^2 + V(1/2 (x_{i+1} + x_i)) + \sum_{\alpha < \beta} U(x_i^\alpha, x_i^\beta) \right] \quad (\text{IV.22})$$

The exponential factor of Eq.(IV.21) can be written as the direct product of two matrices, \hat{T} and \hat{U} :

$$\hat{P} = \hat{T} \otimes \hat{U} \quad (IV.23)$$

where \hat{T} is the one-electron transfer matrix [Eq.(IV.7)]. Thus, the partition function $Q(N)$ for N electrons can be written as

$$Q(N) = B^N \int_{-\infty}^{\infty} \dots \int_{-\infty}^{\infty} \prod_{\alpha, \beta}^{N-1} dx_1^{\alpha} \hat{P}(x_{1+1}^{\alpha}, x_1^{\beta}) \quad (IV.24)$$

In order to write the \hat{P} matrix in the representation of the $\{\phi_i(x_i)\}$, we compute the matrix elements in the Slater determinant basis and get

$$\begin{aligned} \langle \Psi | \hat{P} | \Psi \rangle &= \langle \Psi | \exp \{ -(\varepsilon/\hbar) [H + O(\varepsilon)] \} | \Psi \rangle \\ &= \left\langle \sum_{\{P\}} \delta_{\{P\}} \left[\psi_1(1) \dots \psi_{\alpha}(\alpha) \dots \psi_N(N) \right] \middle| \exp \{ -(\varepsilon/\hbar) [H + O(\varepsilon)] \} \right. \\ &\quad \left. | P \left[\psi_1(1) \dots \psi_{\alpha}(\alpha) \dots \psi_N(N) \right] \right\rangle \end{aligned}$$

Therefore

$$\begin{aligned} &\left\langle \sum_{\{P\}} \delta_{\{P\}} \left[\psi_1(1) \dots \psi_{\alpha}(\alpha) \dots \psi_N(N) \right] \middle| H + O(\varepsilon) \right. \\ &\quad \left. | P \left[\psi_1(1) \dots \psi_{\alpha}(\alpha) \dots \psi_N(N) \right] \right\rangle \\ &= 2 \sum_{\alpha} \langle \psi_{\alpha} | h_{\alpha} | \psi_{\alpha} \rangle + \sum_{\alpha, \beta} \langle \psi_{\alpha} \psi_{\beta} | U(x_{1+1}^{\alpha}, x_1^{\beta}) [| \psi_{\alpha} \psi_{\beta} \rangle \\ &\quad - | \psi_{\beta} \psi_{\alpha} \rangle] \end{aligned} \quad (IV.25)$$

where h_{α} is the monoelectronic operator

$$h_{\alpha} = 1/2 \hbar^2 \nabla_{\alpha}^2 - \sum_{c=1}^N Z_c / r_{\alpha c} \quad (\text{IV.26})$$

and the bielectronic term of Eq.(IV.25) can be written as

$$\sum_{\langle \alpha, \beta \rangle} \langle \psi_{\alpha} \psi_{\beta} | U(x_{1+1}^{\alpha}, x_1^{\beta}) [| \psi_{\alpha} \psi_{\beta} \rangle - | \psi_{\beta} \psi_{\alpha} \rangle] \\ = \sum_{\langle \alpha, \beta \rangle} (2 J_{\alpha \beta} - K_{\alpha \beta}) = \sum_{\langle \alpha, \beta \rangle} G_{\alpha \beta} \quad (\text{IV.27})$$

In Eq.(IV.25) the integrations over the spins were performed according to the usual prescription and the $N/2$ lowest-energy orbitals are supposed to be doubly occupied. In Eq.(IV.27) $J_{\alpha\beta}$ and $K_{\alpha\beta}$ are the molecular coulombic and exchange integrals, respectively.

According to Eq.(IV.9), the molecular orbitals ψ_{α} can be expanded in the orthonormal basis set $\{\phi_1(x_1)\}$ where $\phi_1(x_1) = \{\phi_1(1), \phi_1(2), \dots, \phi_1(\alpha), \dots, \phi_1(N)\}$; taking into consideration Eqs.(IV.25) and (IV.27), $Q(N)$ can be written as

$$Q(N) = B^N \int_{-\infty}^{\infty} \dots \int_{-\infty}^{\infty} \prod_{i=1}^{N-1} d\phi_i \langle \phi_b | \hat{P} | \phi_{N-1} \rangle \\ \langle \phi_{N-1} | \hat{P} | \phi_{N-2} \rangle \dots \langle \phi_1 | \hat{P} | \phi_a \rangle \quad (\text{IV.28})$$

On applying periodic toroidal boundary conditions ($\phi_a = \phi_b$) [105] Eq.(IV.28) can be cast in the form

$$Q(N) = B^N \int_{-\infty}^{\infty} \prod_{i=1}^{N-1} d\phi_i \langle \phi_N | \hat{P}^N | \phi_1 \rangle = B^N \text{Tr } \hat{P}^N \quad (\text{IV.29})$$

which corresponds to the canonical partition function of a many-body system (identical particles) obeying Fermi-Dirac statistics.

The Hamiltonian in the representation of the basis set $\{\phi_i(x_i)\}$ can be written, according to Eq.(IV.25) in the form

$$H = \sum_j |\phi_j\rangle H_{jj} \langle \phi_j| + \sum_{\langle i,j \rangle} |\phi_i\rangle H_{ij} \langle \phi_j| + \sum_{\langle i,j,i',j' \rangle} |\phi_i \phi_j\rangle G_{ij,i',j'} [\langle \phi_{i'} \phi_{j'} | - \langle \phi_j \phi_{i'} |] \quad (\text{IV.30})$$

where H_{ij} and H_{jj} have the same meaning as in the mono-electronic problem. Since $G_{ij,i',j'} = G = \text{a constant}$ for the Hückel model, Eq.(IV.30) becomes (taking $H_{jj} = G = 0$)

$$H = \beta \sum_{\langle i,j \rangle} |\phi_i\rangle \langle \phi_j| \quad (\text{IV.31})$$

where the summations are carried out, as usual, only for the nearest neighbors. This result is analogous to that of a bidimensional continuum Ising model [3,104].

As long as G was taken to vanish, the N -electron transfer matrix \hat{P} can be written as

$$\hat{P} = A \hat{T} \quad (\text{IV.32})$$

where A is a constant which can be absorbed in the normalization of the path integral. Then $Q(N)$ becomes

$$\begin{aligned} Q(N) &= (AB)^N \int \dots \int_{-\infty}^{\infty} \prod_{\alpha=1}^N \prod_{i=1}^{N-1} dx_i^{(\alpha)} \langle \phi_b^{(\alpha)} | \hat{T}^N | \phi_a^{(\alpha)} \rangle \\ &= (AB)^N \prod_{\alpha=1}^N \langle \phi_b^{(\alpha)} | \hat{T}^N | \phi_a^{(\alpha)} \rangle = (AB)^N \prod_{\alpha=1}^N Z^{(\alpha)}(N) \end{aligned} \quad (\text{IV.33})$$

This result suggests that through the euclidean path integral we can represent a non-relativistic N -electron quantum system as a statistical-mechanics problem of N one-dimensional Ising models in a space-time lattice of N sites.

B. Partition Function of the Hückel Model

The purpose of this Section is to get the partition function of the Hückel model via the saddle-point approximation of the Gaussian integrals appearing in the path integral [19]. The present formalism constitutes an alternative method to those given previously using the Green's function [38] and Dyson equation [105] to get self-energies and reactivity indices.

In the site representation ψ_{α} can be written as $\psi_{\alpha}(x_1)$; since we are dealing with one-electron wave functions the index α can be dropped and the MO may be expressed as ψ_1 .

When the Hamiltonian in the MO's basis is expressed in terms of the evolution operator \hat{T} [Eq.(IV.14)] for an infinitesimal step in time [19] and the continuum Ising

model is used to evaluate the multiple integrals, the partition function in Eq.(IV.11) can be rewritten in the alternative form

$$Z(N) = B \int \prod_{i=1}^{N-1} d\psi_i d\psi_{i+1}^* W[\psi_i, \psi_{i+1}^*] \exp \{-(\varepsilon/\hbar) H(\psi_i, \psi_{i+1}^*)\} \quad (\text{IV.34})$$

where the weight function $W[\psi_i, \psi_{i+1}^*]$ is a Dirac δ function; as long as the Euclidean version (imaginary time) for the action is being considered, the δ function can, in fact be represented by its Gaussian approximation [106]; thus, $W[\psi_i, \psi_{i+1}^*]$ becomes

$$W[\psi_i, \psi_{i+1}^*] = \exp \{-(\varepsilon/\hbar) \lambda |\psi_i\rangle \langle \psi_{i+1}| \} \quad (\lambda \text{ real parameter}) \quad (\text{IV.35})$$

Therefore, an effective Hamiltonian, functional of ψ, ψ^* , can be defined in the form

$$H_{\text{eff}}(\psi, \psi^*) = H(\psi, \psi^*) + \lambda \sum_{i,j} |\psi_i\rangle \langle \psi_j| \quad (\text{IV.36})$$

which clearly represents a constrained Hamiltonian. In fact, the values that a particular MO takes on in each of the sites form a finite subset $\{\psi_i\}$ that fulfills the normalization condition

$$\langle \psi_i | \psi_j \rangle = \begin{cases} 1 & \text{if } i = j \\ > 0, < 1 & \text{if } i \neq j \end{cases} \quad (\text{IV.37})$$

On expanding the MO's in the atomic orbitals basis, Eq.(IV.34) becomes

$$Z(N) = B \int \prod_{i=1}^{N-1} dc_i dc_{i+1}^* \phi_i \phi_{i+1}^* \exp \left\{ - (\varepsilon/\hbar) H_{\text{eff}}(c_i, c_{i+1}^*) \right\} \quad (\text{IV.38})$$

where c_i are the expansion coefficients and $H_{\text{eff}}(c, c^*)$ is given by (S_{ij} are the overlap matrix elements)

$$H_{\text{eff}}(c, c^*) = \sum_i c_i c_i^* H_{ii} + \sum_{\langle i, j \rangle} c_i c_j^* H_{ij} + \lambda \sum_{\langle i, j \rangle} c_i c_j^* S_{ij} \quad (\text{IV.39})$$

Application of the saddle-point approximation to the integrals appearing in Eq.(IV.33), i.e., variation of H_{eff} with respect to c and c^* leads to [19]

$$\delta H_{\text{eff}}(c, c^*) / \delta c_j^* = \sum_i c_i (H_{ij} + \lambda S_{ij}) \quad (\text{IV.40})$$

from which the secular equations for confined systems based in the Dirac variational principle [95] of the constrained system are obtained. As a generalization of the above results, we point out that the Potts model [107] can be used as an alternative method instead of the Ising model for the evaluation of the partition function for a molecular system. In addition, explicitly introducing the electronic repulsion operator of Eq.(IV.1) and expanding each atomic orbital in terms of

contracted Gaussians, the exchange term can be incorporated in the formalism, thus leading to a bidimensional problem in which the partition function of an ab initio SCF method can be evaluated.

We now describe a non-linear formulation of the Hückel model by using the gaussian approximation introduced by Wilson [108] in an Ising model. As a consequence of the application of the saddle-point approximation to the multiple integrals of the partition function $Q(N)$, Eq.(IV.33), a set of non-linear equations will be generated [20a]. We start with Eq.(IV.34) and write the weight function $W[\psi, \psi^*]$ in the form

$$W[\psi, \psi^*] = \exp \left\{ (\epsilon/\hbar) u' \left[\sum_{i,j} |\psi_i\rangle \langle \psi_j| - 1 \right] \right\} \quad (\text{IV.41})$$

where u' is a positive quantity. Eq. (IV.41) can be considered as the gaussian approximation describing the quantum fluctuations in a molecular system via molecular orbital theory. This incorporation of the quantum fluctuations leads, within the context of this theory, to a proper description of phenomena such as the dynamical behavior of the double hydrogen bonding of nucleic bases as well as the resonance of annulenes, which could be interpreted in fact, as quantum fluctuations of the ground state of the molecule [109,110]. To this end the exponential factor of Eq.(IV.41) is approximated in the form [20a]

$$u' \left[\sum_{i,j} |\psi_i\rangle \langle \psi_j| - 1 \right]^2 \simeq (1/2) b \sum_{i,j} |\psi_i\rangle \langle \psi_j|$$

$$- u' \left[\sum_{\langle i, j \rangle} |\psi_i\rangle \langle \psi_j| \right] \quad (\text{IV.42})$$

where $b = -4 u'$, allows the partition function (IV.34) to be rewritten in the form

$$Z(N) = B \prod_{i=1}^{N-1} \int d\psi_i d\psi_{i+1}^* \exp \left\{ -(\mathcal{E}/\hbar) H_{\text{eff}}[\psi, \psi^*] \right\} \quad (\text{IV.43})$$

where $H_{\text{eff}}[\psi, \psi^*]$, the effective Hamiltonian, is given by [20a]

$$H_{\text{eff}}[\psi, \psi^*] = L \sum_i |\psi_i\rangle \langle \psi_i| + (K + (1/2) b) \sum_{\langle i, j \rangle} |\psi_i\rangle \langle \psi_j| \\ - u' \left[\sum_{\langle i, j \rangle} |\psi_i\rangle \langle \psi_j| \right]^2 \quad (\text{IV.44})$$

where L and K are respectively the diagonal and off-diagonal matrix elements of H in the molecular orbital site representation. In order to proceed further we follow the algebraic derivation of Wilson and Kogut [108] and directly arrive to

$$H_{\text{eff}}[\psi, \psi^*] = K \left\{ \sum_i (|\psi_{i+1}\rangle - |\psi_i\rangle) (\langle \psi_{i+1}| - \langle \psi_i|) \right. \\ \left. - R \sum_{\langle i, j \rangle} |\psi_i\rangle \langle \psi_j| + u \left[\sum_{\langle i, j \rangle} |\psi_i\rangle \langle \psi_j| \right]^2 \right\} \quad (\text{IV.45})$$

with $R = b/(2K) - L$ and $u = u'/K$. Expansion of the MO's ψ in the atomic orbital basis $\{\phi\}$, leads to

$$\begin{aligned}
H_{\text{eff}}[c, c^*] = & K \sum_{\langle i, j \rangle} c_i c_j^* + (1/2) b - L \sum_{\langle i, j \rangle} c_i c_j^* S_{ij} \\
& - 2 u' \left\{ \sum_{\langle i, j \rangle} (c_i c_j^*)^2 + \sum_{\langle i, j \rangle} \sum_{\langle i', j' \rangle} (c_i c_j^*) (c_{i'} c_{j'}^*) \right\} S_{ij}
\end{aligned}
\quad (\text{IV.46})$$

By applying the saddle-point approximation to the integrals of each partition function $Z^{(\alpha)}(N)$ in Eq.(IV.33) a set of N saddle-point equations and their adjoints is obtained [20]

$$\begin{aligned}
\partial H_{\text{eff}}[C(\alpha), C^*(\alpha)] / \partial C_i(\alpha) = & K \sum_j C_j^*(\alpha) \\
& + [E(\alpha) - L] \sum_j C_j^*(\alpha) S_{ij} - 2 u' \left\{ \sum_j [C_i(\alpha) C_j^*(\alpha)] C_j^*(\alpha) \right. \\
& \left. + 2 \sum_{\langle i', j' \rangle} [C_{i'}(\alpha) C_{j'}^*(\alpha)] C_{j'}^*(\alpha) \right\}
\end{aligned}
\quad (\text{IV.47})$$

where $E(\alpha) = b/2$ is the energy of the MO $\psi(\alpha)$. The set of equations (IV.47) and its adjoint, represents the non-linear secular equations of the Hückel model. When $u' = 0$ in Eq.(IV.47) and its adjoint, we are led to the secular equations of the classical Hückel model [102]. Further, the sign of the coefficients u' of the saddle-point equations (IV.47) correspond to these two possibilities: (i) $u' < 0$, corresponds to a single minimum energy; (ii) $u' > 0$, on the other hand, corresponds to a double minimum energy. The second situation allows to rationalize from this novel point of view, the dynamical behaviour of phenomena involving

double well potentials such as the double hydrogen bonding in nucleic basis and the resonance phenomenon in aromatic systems. In what follows we discuss the connection of this phenomenon with quantum fluctuations in molecules [109].

C. Application of the Path Integral to the Quantum Fluctuations of the Ground State

In recent years there has been a remarkable surge of interest in non-linear wave equations, particularly those which possess travelling solitary-wave solutions. The localized, particle-like nature of solitary waves has spurred their use in quantum field theory [110], condensed matter theory [111] and engineering applications [112], to mention a few. Most of the relatively few known analytic solitary wave solutions are to non-linear wave equations for a real scalar field in one space and one time dimension, with notable exceptions [113]. We now will discuss two phenomena closely related to this subject, namely the resonance phenomenon in molecules [109] and the double hydrogen bonding in nucleic bases [114]. To this end a link with bifurcation and catastrophe theory [115,116] will be established.

Bifurcation and catastrophe theory has led to a wide of applications of the elementary theory to many branches of science [115a,116]. The modelling of the treatment of hyperthyroidism [116], for example, is typical of applications in the biological science, where the model is a hypothesis, an aid to understanding the phenomenon, enabling data to be fitted, and leading to conjectures which may then be tested experimentally. In particular, the theory of bifurcation and catastrophe is

useful in describing phenomena where continuously changing causes give rise to discontinuous effects. As such, it would seem to be an appropriate tool to discuss double well potentials in molecular systems from a non-conventional point of view.

To describe the above mentioned link we write the multielectronic wave function of a n -electron system as a classical complex field

$$\psi(x,t) = U(x,t) \exp (i \phi(x,t)) \quad (\text{IV.48})$$

and the double well potential as a complex-valued expression with a self-interaction term involving a $(\psi \psi^*)^2$ potential (charged potential describing the behavior of particle and anti-particle)

$$V(\psi, \psi^*) = -1/4 (\psi \psi^*)^2 + a/2 (\psi \psi^*) + b (\psi + \psi^*) \quad (\text{IV.49})$$

where a and b are constants.

We now adhere to the mechanical model of the Zeeman's catastrophe machine [115,116] and take the derivative of Eq.(IV.48) with respect to ψ and ψ^* to get

$$\partial V(\psi, \psi^*) / \partial \psi = -1/2 (\psi \psi^*) \psi^* + a/2 \psi^* + b \quad (\text{IV.50})$$

and a similar equation involving ψ^* . The graph of $\partial V / \partial \psi = 0$ generates a smooth folded surface whose folds project down onto the bifurcation set. Thus, $\partial V / \partial \psi = 0$ defines a cusp catastrophe surface; a and b in Eq.(IV. 49) can therefore be considered as the axis of a plane over which the catastrophe map is projected.

The corresponding equation of motion is obtained by application of the Hamilton variational principle to the

classical action. The Lagrangian is taken as [117,118]

$$L(\psi, \psi^*) = 1/2 |\psi_t|^2 - 1/2 |\psi_x|^2 + A/2 |\psi|^2 - B/4 |\psi|^4 \quad (IV.51)$$

A and B being positive constants. This model was first introduced as a mathematical convenience in the description of charge-density waves in crystals [111].

The potential implicit in the non-linear Lagrangian (IV.51) must be compared to the phenomenological potential (IV. 48) in order to characterize the cusp catastrophe surface. In the present case, the discriminant $D (= a^3/2)$ of the cubic equation $\partial V/\partial \psi = 0$ is less than zero, i.e., the roots are real and distinct. In the map of cusp catastrophe [117] the single minimum bifurcates into two minima of stable equilibrium of less energy. If $D = 0$, then $a = 0$, i.e., this situation corresponds to that of the cusp point, there exists no maximum nor minimum. If $D > 0$, then $a > 0$, and therefore the proposed potential (IV.48) does not represent a double well.

The non-linear equation generated by the Lagrangian (IV.51)

$$i \partial \psi / \partial t + \partial^2 \psi / \partial x^2 + \lambda |\psi|^2 \psi = 0 \quad (IV.52)$$

where $\lambda > 0$ possesses soliton solutions [119] and may be regarded as the non-linear Schrödinger equation for a system of fermions in one space dimension. This suggests that ψ describes the motion of a solitary wave connecting those two minima through tunnel effect. From this point of view, it is concluded that phenomena

involving double well potentials such as the resonance in annulenes as well as the double hydrogen bonding in nucleic basis can be considered as a cusp catastrophe, i.e., as the motion of a soliton in a bistable potential, and therefore a proper description of such phenomena consequently should require the calculation of the tunnel effect of the soliton.

Expansion of the stationary solutions of Eq.(IV.52) in a basis of atomic orbitals leads to a set of coupled non-linear equations of the Gaussian Hückel model, Eq.(IV.47). This approach allows an effective theoretical calculation of resonance integrals in annulenes to be performed [120]. The asymptotic expression of such parameter, when the number of atoms is allowed to tend to infinity, was easily derived and the qualitative behavior of the variation of these integrals as a function of the number of atoms N was found to be similar to that observed for the ration $\mu/(E/N)$, where μ is the chemical potential.

It should also be pointed out that the potential energy term inherent in the Lagrangian (IV.46) describes a quantum fluctuation of the ground state and therefore can be thought of in the present case as representing two equivalent ground states, thus leading to a close analogy with what occurs in quantum field theory. In fact, since the phenomenological potential (IV.48) can formally be made to coincide with the potential describing the vacuum fluctuation, a correspondence can be established between the ground state and the vacuum state. Using Coleman's terminology [121] this is precisely the fate of the false vacuum. In the light of this analogy the Goldstone bosons of the spontaneous symmetry breaking (Cooper pairs, i.e., the π electrons

pairs) are absorbed by the self interaction term of Eq.(IV.48) (Higgs fields) generating a mass particle (soliton) which oscillates between those two ground states.

The present approach follows the increasing interest in problems involving structural (in)stability [122] and symmetry breaking [123]. This is closely connected to synergetics [124] where links can be established between critical phenomena and bifurcation theory.

Finally, it should be pointed out that the realization of a non-linear Hartree-Fock model should be the appropriate mean to deal with such problems as chemical bonding [125], resonance and hydrogen bonding phenomena (ground state quantum fluctuations) as well as phase transitions [126].

D. Presence of an External Field

The formalism developed in IV.b enables one to study some particular ground-state properties which are obtained or measured only in the presence of an external magnetic field. For closed-shell systems, such properties include the diamagnetic susceptibility and its anisotropy, and the magnetic resonance frequencies of protons and C-13. To undertake this study, it is necessary to obtain the modified secular equations in the presence of an external magnetic field.

Neglecting the electronic repulsion the modified molecular Lagrangian L' reads

$$L' = \sum_{\alpha=1}^N \left\{ 1/2 \left[\dot{\mathbf{x}}_{\alpha}^2 + (e/c) \dot{\mathbf{x}}_{\alpha} \cdot \mathbf{A}_{\alpha} \right]^2 - V(\mathbf{x}_{\alpha}) \right\} \quad (\text{IV.53})$$

where $\vec{x} + (e/c) \vec{A}$ represents the new velocity of the electron in the magnetic field \vec{H} with vector potential \vec{A} , i.e., $\vec{H} = \nabla \times \vec{A}$. In an external magnetic field, it is required that the MO's be gauge invariant. Thus, the modified atomic orbitals can be written as [127]

$$\phi'_i = \exp \{-i [e/(\hbar c)] \vec{A} \cdot \vec{r}\} \phi_i \quad (\text{IV.54})$$

where r is the point at which \vec{A} is evaluated. With this choice of the atomic orbitals, the modified Lagrangian (IV.53) is effectively invariant under a change of gauge. Therefore, the modified effective Hamiltonian (IV.36) becomes

$$H'_{\text{eff}}(\psi, \psi^*) = \sum_{\langle r, s \rangle} |\psi'_r\rangle H'_{rs} \langle \psi'_s| + \lambda \sum_{\langle r, s \rangle} |\psi'_r\rangle \langle \psi'_s| \quad (\text{IV.55})$$

where the ψ'_r are the gauge-invariant MO's and the modified matrix elements H'_{rs} and S'_{rs} are given by

$$H'_{rs} = \int \exp \left\{ i [e/(\hbar c)] (\vec{A}_r - \vec{A}_s) \cdot \vec{r} \right\} \phi_s^* \left\{ \frac{1}{2} \left[\vec{x} + (e/c) (\vec{A} - \vec{A}_r) \right]^2 + v \right\} \phi_r \, d\tau \quad (\text{IV.56})$$

$$S'_{rs} = \int \exp \left\{ i [e/(\hbar c)] (\vec{A}_r - \vec{A}_s) \cdot \vec{r} \right\} \phi_r^* \phi_s \, d\tau \quad (\text{IV.57})$$

where \vec{A}_s is the vector potential at the center of atom s and $(\vec{A} - \vec{A}_r)$ is a local vector potential independent of choice of origin. Thus, the average magnetization at the site i

$$M_1 = 1/Q'(N) \partial Q'(N) / \partial H_1 |_{H=0} \quad (IV.58)$$

as well as the magnetic susceptibility

$$\chi(H) = \partial M / \partial H \quad (IV.59)$$

can be calculated if the propagator (IV.33) modified in the prescence of an external magnetic field is known, which leads to an explicit account of phase transitions and critical phenomena [3]. Thus, the path integral formalism appears here as a practical tool for the evaluation of thermodynamic and magnetic properties in molecular systems.

V. PATH INTEGRAL FORMULATION OF ROOHTHAAN'S EQUATIONS

A. Preliminary Considerations and Closure Relations

Application of the saddle-point approximation [3,105] leads to a time-dependent mean-field theory in which coordinates, momenta, equations of motion, and quantization conditions are specified by the underlying effective Hamiltonian. Thus, the functional integral provides a bridge between the quantum many-body propagator and the time-dependent Hartree-Fock. In the saddle-point approximation, the propagator between two Slater determinants is dominated by the exponential of a time-dependent Hartree-Fock solution.

The Feynman path integral of a molecular system was recently obtained [21,22] through the generation of a overcomplete set of vectors $\langle \Psi |$ using Klauder's continuous representation theory [128]. A further use of the saddle-point approximation of the generating

functional of the molecular system, was shown to yield the Hartree-Fock equations.

As long as the Klauder's theory demands the existence of a continuous global symmetry and since Ψ is invariant with respect to a phase transformation, we can write (α is a constant phase)

$$\Psi'(N) = \exp(i\alpha) \Psi(N) \quad (V.1)$$

where N is the number of electrons of the molecular system. Therefore, the elements of the overcomplete set $(\langle \Psi |)$ are the elements of a "gauge" group $U(1)$ similar to the gauge of the electrodynamics. Thus, $\Psi(N)$ is parametrized by a Slater determinant. In what follows we intend to obtain the decomposition of the unit operator in an atomic orbital representation. This is an essential step towards building up the many body quantum mechanical path integral with constraints. Indeed, the secret of the use of the path integral in quantum mechanics lies in the introduction of the constraints via unit decomposition in a Hilbert space. Thus, we bosonize the MO's Ψ using the LCAO mapping

$$\Psi_{\alpha} = \sum_{j=1}^M C_j(\alpha) \phi_j \quad (V.2)$$

Therefore, the overlap matrix of Ψ_{α} can be written as a function of the set (ϕ) ,

$$\int_{\nu} \Psi_{\alpha} \Psi_{\beta}^{*} d\nu = \bar{C}(\alpha) \cdot \Lambda \cdot \bar{C}^{*}(\beta) = \delta_{\alpha\beta} \quad (V.3)$$

in which $d\nu$ is the volume element and $\bar{C}(\beta)$ and $\bar{C}^{*}(\alpha)$ are the column and row vector, respectively, of the matrix $C(\alpha) = [C_{ij}(\alpha)]$. The matrix Λ is the atomic overlap

matrix, where the matrix elements are given by $\Lambda_{ij} = \langle \phi_i | \phi_j \rangle$.

It follows from Eqs.(V.2) and (V.3) that we can obtain an expression for the product of the differential forms

$$d\Psi_\alpha = \sum_{j=1}^M \phi_j dC_j(\alpha) \quad (V.4)$$

as follows:

$$d\Psi_\alpha^* d\Psi_\beta = \sum_{j,k} dC_j^*(\alpha) d\Lambda_{jk} dC_k(\beta) = \sum_{j,k} da_{jk}(\alpha,\beta) = dA(\alpha,\beta) \quad (V.5)$$

where A is a (M x M) matrix. The overlap matrix elements in the molecular basis are explicitly given by

$$\begin{aligned} \int \psi^*(\alpha) \psi(\beta) dW &= \sum_{i,j}^M C_i^*(\alpha) \Lambda_{ij}(\alpha,\beta) C_j(\beta) \\ &= \sum_{i,j}^M a_{ij}(\alpha,\beta) = \delta_{\alpha\beta} \end{aligned} \quad (V.6)$$

where $\Lambda_{ij}(\alpha,\beta)$ are overlap matrix elements in the atomic basis.

Now, the closure relation for the $\langle D |$ vectors is

$$\int |D\rangle \langle D| d\mu [D^*, D] = 1 \quad (V.7)$$

where the measure $d\mu [D, D^*]$ with the condition (V.3) can be written as

$$d\mu [D, D^*] = \prod_{\alpha,\beta}^N d\Psi_\alpha d\Psi_\beta^* \cdot \delta \left[\int \Psi_\alpha \Psi_\beta^* d\nu - \delta_{\alpha\beta} \right] \quad (V.8)$$

which fulfills the phase invariance [see Eq.(V.1)]

[21,128]. In the atomic orbitals subspace the measure $d\mu [D, D^*]$ reads

$$d\mu [D, D^*] = \prod_{\alpha, \beta}^N dA(\alpha, \beta) \cdot \delta \left[\sum_{i,j}^M a_{ij}(\alpha, \beta) - \delta_{\alpha\beta} \right] \quad (V.9)$$

Then, upon using the above results, the closure relation (V.7) becomes

$$\int \prod_{\alpha, \beta}^N dA(\alpha, \beta) \cdot \delta \left[\sum_{i,j}^M a_{ij}(\alpha, \beta) - \delta_{\alpha\beta} \right] |D\rangle \langle D| = 1 \quad (V.10)$$

B. The Projected Generating Functional

The quantum mechanical evolution operator $\exp [-iH(t_j - t_i)]$ between the initial time t_i and the final time t_j , enables us to define, through its matrix elements defined on the overcomplete set $\langle D|$, an expression of the generating functional

$$Z(N) = \langle D_f | \exp [-iH(t_f - t_i)] | D_i \rangle \quad (V.11)$$

Now, following the standard procedure for constructing the path integral, we first factorize the evolution operator as done in Sect.(II). Thus, on setting $\tau = (t_f - t_i)/Q$, Eq.(V.11) can be written as

$$Z(N) = \prod_{q=1}^Q \langle D_f | D_Q \rangle \langle D_Q | \exp (-i\tau H) | D_{Q-1} \rangle \dots \langle D_{Q-1} | \exp (-i\tau H) | D_{Q-2} \rangle \dots \langle D_1 | D_i \rangle \quad (V.12)$$

Notice that in Eq.(V.12) a typical matrix element appears, $\langle D_Q | \exp (-i\tau H) | D_{Q-1} \rangle$, which may be

approximated in first order as

$$\begin{aligned} \langle D_Q | \exp(-i\tau H) | D_{Q-1} \rangle &= \langle D_Q | (1 - i\tau H + O(\tau^2)) | D_{Q-1} \rangle \\ &\cong \langle D_Q | D_{Q-1} \rangle \exp \left[-i\tau \frac{\langle D_Q | H | D_{Q-1} \rangle}{\langle D_Q | D_{Q-1} \rangle} \right] \end{aligned} \quad (V.13)$$

Use of the Klauder's continuous representation theory [128] shows that, in the short time interval τ , the inner product $\langle D_Q | D_{Q-1} \rangle$ is

$$\langle D_Q | D_{Q-1} \rangle < 1 \quad (V.14)$$

therefore, the matrix elements (V.13) read

$$\langle D_Q | e^{-i\tau H} | D_{Q-1} \rangle \cong e^{-i\tau \langle D_Q | H | D_{Q-1} \rangle} \quad (V.15)$$

the normalization constant implicit in Eq. (V.14) being absorbed in the normalization of the Slater determinant D_Q .

The constraint condition implicit in the Dirac δ function of Eq.(V.10) can be expressed through the Fourier transform of the identity

$$\delta(x) = \frac{1}{(2\pi)M^2} \int dE e^{iEx} \quad (V.16)$$

Upon insertion of the closure relation (V.10) between each factor of the $Z(N)$, substituting the expression of the matrix elements of the molecular Hamiltonian into $Z(N)$, using the expression (V.16) of the Dirac δ function, and after taking the limits $\tau \rightarrow 0$, $Q \rightarrow \infty$ in the expression (V.12), we are finally led,

after straightforward algebra, to the following useful form for $Z(N)$:

$$Z(N) = \int \frac{D[A]}{(2\pi)^{M^2}} \int dE \quad e^{iS_{\text{eff}}[\phi^*, \phi, A, E]} \quad (\text{V.17})$$

where the functional measure of the path integral (V.17) is given by

$$D[A] = \lim_{\substack{Q \rightarrow \infty \\ \tau \rightarrow 0}} \prod_1^Q \prod_{\alpha, \beta}^N dA_1^{(\alpha, \beta)} \langle D_f | D_Q \rangle \langle D_1 | D_1 \rangle. \quad (\text{V.18})$$

while the effective action S_{eff} reads

$$S_{\text{eff}}[\phi^*, \phi, A, E] = S[\phi^*, \phi, A] - \sum_{\alpha, \beta}^N E^{(\alpha, \beta)} \sum_{i, j}^M a_{ij}^{(\alpha, \beta)} \quad (\text{V.19})$$

and thus the functional $S[\phi^*, \phi, A]$ takes the form

$$\begin{aligned} S[\phi^*, \phi, A] = & \int_{t_i}^{t_f} dt \left\{ 2 \sum_i^M R_{ii} \langle K_\alpha \rangle_i \right. \\ & + \left[\sum_{ij, i'j'} R_{ij} R_{i'j'} \langle U_{\alpha, \beta} \rangle_{ij, i'j'} \right. \\ & \left. \left. - \sum_{ij, i'j'} R_{ij} R_{i'j'} \langle U_{\alpha, \beta} \rangle_{ij, j'i'} \right] \right\} \quad (\text{V.20}) \end{aligned}$$

with

$$R_{ij} = \sum_{\alpha}^N G_i^*(\alpha) G_j(\alpha)$$

Use of the Fock matrix F allows the functional $S[\phi^*, \phi, A]$ to be written in the compact form [129]

$$F = K + G \quad (V.21)$$

where K is the kinetic energy and electron-nuclei attraction term and G is the electron-electron repulsion energy. Thus, $S[\phi^*, \phi, A]$ becomes

$$S[\phi^*, \phi, A] = \int_{t_1}^{t_f} dt \left\{ \sum_{\alpha, \beta}^N \bar{G}^*(\alpha) F_{\beta} G(\alpha) \right\} \quad (V.22)$$

so that the effective action can finally be rewritten as

$$S_{\text{eff}}[\phi^*, \phi, A, E] = \int_{t_1}^{t_f} dt \left\{ \sum_{\alpha, \beta}^N \bar{G}^*(\alpha) F_{\beta} \bar{G}(\alpha) \right\} - \sum_{\alpha, \beta}^N \bar{G}^*(\alpha) \wedge \bar{G}(\beta) E(\alpha, \beta) \quad (V.23)$$

It is observed that the generating functional $Z(N)$ can be interpreted as a partition functional describing the dynamical behaviour of the $(N \times M)$ pseudobosonic particles constrained to move in the manifold of the complex phase space, where $G(\alpha)$ and $G^*(\alpha)$ are canonical coordinates. Noticeably, the motion constraint is given by the second term of the expression (V.23), where it can be given a topological interpretation, similar to that found in gauge field theory. Consequently, we could use the partition functional $Z(N)$ to study the molecular electronic behavior in an external field, for example environment (e.g., solvation) effects.

It should be noticed that as long as the bosonic Feynman path integral does not have the Grassman algebra

difficulties arising when the molecular orbitals ψ_α possess the status of the fermionic fields [128], the generating functional $Z(N)$ can be obtained in the present case rather straightforwardly.

Now, we are going to generate equations of motion of the electronic molecular system. Therefore, applying the saddle-point approximation (stationary phase approximation) to the multiple integrals of the $Z(N)$ propagator, Eq.(V.17), the semiclassical equations of motion result:

$$\frac{\partial S_{\text{eff}}}{\partial \bar{G}^*(\alpha)} = 2 \sum_{\alpha}^N \left\{ F \bar{G}(\alpha) - \sum_{\beta}^N \Lambda E(\alpha, \beta) \bar{G}(\beta) \right\} = 0 \quad (\text{V.24a})$$

$$\frac{\partial S_{\text{eff}}}{\partial \bar{G}(\alpha)} = 2 \sum_{\alpha}^N \left\{ F^+ \bar{G}^*(\alpha) - \sum_{\beta}^N \Lambda^+ E(\alpha, \beta) \bar{G}^*(\beta) \right\} = 0 \quad (\text{V.24b})$$

which are recognized to be the Roothaan's equations [130].

The importance of this formulation lies in the fact that the path integral is a nice mathematical tool for saddle-point expansion when the motion becomes semiclassical. In this sense, the correlation energy can be calculated through the saddle-point expansion around the saddle-point energy [130].

The path integral formalism has an important advantage with respect to others; namely, that by Gaussian approximation of the path integral, it can easily be extended to the nonlinear molecular orbital theory, and so it can be use the full mathematical power of the nonlinear field theory for studying the molecular quantum fluctuations [109] or for developing the Gaussian Hückel Model [20].

VI FEYNMAN PATH INTEGRAL REPRESENTATION OF FIELD OPERATORS AND MEMORY SUPEROPERATORS IN A LIOUVILLE SPACE

A. Preliminary Remarks

In this Section we extend the Feynman path integral approach to the operator space in which useful information on the time development of field operators for both fermionic and bosonic systems may be extracted. This dynamical behavior was clearly analysed (within the non-relativistic theory) for the density matrix [131] by means of memory superoperators. An extension of this treatment to fermionic field operators allowed to get a compact expression for the Green function in a Liouville space within the regime of the interaction picture [132]. More recently, a U-matrix theory in quantum mechanics has been developed into a workable approach based on Dyson's formulation [133] in which the wavefunction is written in terms of the U-matrix within the regime of the interaction picture [134]. It was claimed that in the special case when the unperturbed Hamiltonian and the Lagrangian commute, the wavefunction can be reduced to the form identical to that obtained from the path integral method and a comparison of the path integral theory and this U-matrix theory can be made [135].

Here we establish a link between memory superoperators [136] and the quantum analog of the classical action in operator space of a many particle interacting system. This will allow to generate a Feynman superpropagator in a Liouvillian space. Because one needs to specify essentially the action, this formalism will be potentially powerful in handling those

physical situations where Hamiltonian or Lagrangian cannot be written down explicitly [137]. Such a situation arises, for example, in a reduced description of a many particle system and is reflected through a memory term in the reduced action.

B. Theoretical Background

We consider a many particle interacting system described by a second quantized Hamiltonian written as $H = H_0 + H'$ where H_0 is a one-particle operator and H' contains the many body effects, i.e.,

$$H_0 = \int d\xi \int d\xi' \psi^\dagger(\xi, t) H_0(\xi|\xi') \psi(\xi', t) \quad (\text{VI.1a})$$

$$H' = 1/2! \int d\xi_1 \int d\xi_2 \int d\xi_1' \int d\xi_2' \psi^\dagger(\xi_1, t) \psi^\dagger(\xi_2, t)$$

$$H_1'(\xi_1 \xi_2 |\xi_1' \xi_2') \psi(\xi_2', t) \psi(\xi_1', t) + \dots \quad (\text{VI.1b})$$

Here ξ denotes the full set of coordinates (space and spin) of a particle; $H_0(\xi|\xi')$, $H_1'(\xi_1 \xi_2 |\xi_1' \xi_2')$, are the kernels of the one-, two-.....particle Schrödinger operators H_0 , H_1' , respectively, and $\psi^\dagger(\xi, t)$ and $\psi(\xi, t)$ are the time dependent field operators in the Heisenberg picture representation satisfying the proper commutation relations i.e.,

$$\begin{aligned} [\psi(\xi, t), \psi(\xi', t)]_{\pm} &= [\psi^\dagger(\xi, t), \psi^\dagger(\xi', t)]_{\pm} \\ &= [\psi^\dagger(\xi, t), \psi(\xi', t)]_{\pm} - \delta(\xi - \xi') = 0 \end{aligned} \quad (\text{VI.2})$$

Associated with these operators are the corresponding commutation superoperators $\hat{\mathcal{O}}_0 = [H_0, 1_-$ and $\hat{\mathcal{O}}' = [H', 1_-$,

whose sum $\hat{O} = \hat{O}_0 + \hat{O}' \equiv [H, 1_-]$, is the generator of motion for the field operators $\psi^\dagger(\xi, t)$, $\psi(\xi, t)$ [132]. As seen, \hat{O}_0 , \hat{O}' and \hat{O} are Liouville type superoperators, i.e., (linear hermitian) operators that act in the Hilbert space of operators rather than the space of states [136]. In this Liouvillian superoperator space the equation of motion of the interaction picture field operator is given by [132] ($\hbar = 1$)

$$i \partial/\partial t \psi_I(\xi, t) = - \hat{U}(t) \psi_I(\xi, t) \quad (\text{VI.3})$$

where $\hat{U}(t) = [U(t), 1_-]$ denotes the evolution superoperator associated with the interaction picture hamiltonian operator $U(t) = \exp(-i\hat{O}_0 t) H'$.

The superoperator $\hat{U}(t)$ is the generator of the motion group \hat{G} whose elements

$$\hat{G}(t, t') = \mathbb{F} \exp \left[i \int_{t'}^t ds \hat{U}(s) \right] \quad (\text{VI.4})$$

(defined in terms of the Dyson [133] time-ordering or chronological superoperator \mathbb{F}) exhibit well known group properties and propagate the field operator $\psi(\xi, t)$ according to the prescription

$$\psi_I(\xi, t) = \hat{G}(t, t') \psi_I(\xi, t') \quad (\text{VI.5})$$

Introduction of the mutually orthogonal projection superoperators P and $Q = 1 - P$ and defining the group of time-dependent superoperators \hat{U}_{RS} , $\hat{G}_S(t, s)$ in the manner

$$\hat{U}_{RS}(t) = R \hat{U}(t) S; \quad R, S = P, Q \quad (VI.6)$$

$$\hat{G}_S(t, s) = S F \exp \left[i \int_s^t ds_1 \hat{U}_{SS}(s_1) \right] S \quad (VI.7)$$

it is found that the solution of the differential equation (VI.3) for the two orthogonal complements of the field operator $\psi_P(\xi, t) = P \psi_1(\xi, t)$ and $\psi_Q(\xi, t) = Q \psi_1(\xi, t)$ can be expressed in the form

$$\begin{aligned} \psi_P(\xi, t) \\ = \hat{G}_P(t, t') \left[\hat{M}_{PQP}(t, t') \psi_P(\xi, t') + \hat{N}_{PQ}(t, t') \psi_Q(\xi, t') \right] \end{aligned} \quad (VI.8)$$

where it can be verified that the memory superoperator $\hat{M}_{PQP}(t, t')$ must satisfy the Volterra integral equation (here written for an arbitrary pair of complementary projections R and S)

$$\hat{M}_{SRS}(t, t') = \hat{S} - \int_{t'}^t ds \hat{W}_{SRS}(t, s, t') \hat{M}_{SRS}(s, t') \quad (9a)$$

and the $\hat{N}_{PQ}(t, t')$ coefficient of $\psi_Q(\xi, t')$ in Eq.(VI.8) is connected to $\hat{M}_{PQP}(t, t')$ through the expression

$$\hat{N}_{PQ}(t, t') = \int_{t'}^t ds \hat{B}_{PQ}(t', s) \hat{M}_{QPQ}(s, t') \quad (VI.9b)$$

whose kernels

$$\hat{W}_{SRS}(t, s, t') \equiv \left[\int_s^t ds' \hat{B}_{SR}(t', s') \right] \hat{B}_{RS}(t', s) \quad (VI.10)$$

involve superoperators

$$\hat{B}_{SR}(t,s) \equiv \hat{G}_S(t,s) \hat{U}_{SR}(s) \hat{G}_R(s,t) \quad (VI.11)$$

which couple the R- and S- subspaces at the common instant of time t. This coupling proceeds by propagation through R- space backward in time from t to s, a subsequent direct coupling between the two subspaces mediated by $\hat{U}_{SR}(s)$ and a final forward propagation through S-space from s to t. The kernel $\hat{M}_{SRS}(t,s,t')$ defined by Eq.(10) couples the S- and R-spaces at time t' through motions forward to s and back again to t'. The integral of $\hat{B}_{SR}(t',s')$ from $s' = s$ to $s' = t$ then recouples to S-space the dynamic information which has been accumulated in R-space during the interval.

The equations for the memory superoperators (\hat{M}_{SRS} and \hat{N}_{SR}) can be solved formally by iteration. Thus, using the Dysons' U matrix theory [134,135] and introducing a Dyson-like superoperator to order both the limit of integration and pairs of arguments of the integrand factors \hat{M}_{SRS} appearing in Eq.(VI.9a), it follows from this equation after some rather involved analysis [131,132] that

$$\hat{M}_{SRS}(t,t') = S M^C(t,t') S \quad (VI.12)$$

and

$$\int_{t'}^t ds \hat{B}_{RS}(t',s) \hat{M}_{SRS}(s,t') = R \hat{M}^S(t,t') S \quad (VI.13)$$

wherein

$$\begin{aligned}
& \hat{M}^C(t, t') \\
&= \sum_{n \geq 0} (-)^n \int_{t'}^t ds_1 \int_{t'}^{s_1} ds_2 \dots \int_{t'}^{s_{2n-1}} ds_{2n} \hat{B}(t', s_1) \\
&\quad \hat{B}(t', s_2) \dots \hat{B}(t', s_{2n}) = F \cos \left[\int_{t'}^t ds \hat{B}(t', s) \right]
\end{aligned}
\tag{VI.14}$$

and

$$\begin{aligned}
& \hat{M}^S(t, t') \\
&= \sum_{n \geq 0} (-)^n \int_{t'}^t ds_1 \int_{t'}^{s_1} ds_2 \dots \int_{t'}^{s_{2n}} ds_{2n+1} \hat{B}(t', s_1) \\
&\quad \hat{B}(t', s_2) \dots \hat{B}(t', s_{2n+1}) = F \sin \left[\int_{t'}^t ds \hat{B}(t', s) \right]
\end{aligned}
\tag{VI.15}$$

in which $\hat{B}(t', s)$ stands for the hermitian superoperator

$$\hat{B}(t, s) \equiv \hat{B}_{PQ}(t, s) + \hat{B}_{QP}(t, s)
\tag{VI.16}$$

Without going into mathematical details, the result, relevant to our discussion, is that in the Heisenberg picture representation in a Liouville space, quantum field operators, as given by Eq.(VI.8), evolve in time according to the prescription

$$\psi(\xi, t)$$

$$= \exp(i \hat{\Phi}_0 t) \hat{G}_D(t, t') \hat{G}_C(t, t') \exp(-i \hat{\Phi}_0 t') \psi(\xi, t') \quad (VI.17)$$

where $\hat{G}_D(t, t')$ and $\hat{G}_C(t, t')$ are the (operator subspaces) decoupling (D) and coupling (C) group superoperators [131,132] in the Zwanzig-Feshbach projection space technique [138,139] as follows

$$\begin{aligned} \hat{G}_D(t, t') &= \hat{G}_P(t, t') + \hat{G}_Q(t, t') \\ &= \mathbb{F} \exp \left[i \int_{t'}^t ds (\hat{U}_{PP}(s) + \hat{U}_{QQ}(s)) \right] \end{aligned} \quad (VI.18)$$

$$\begin{aligned} \hat{G}_C(t, t') &= \hat{M}^C(t, t') + i \hat{M}^S(t, t') \\ &= \mathbb{F} \exp \left[i \int_{t'}^t ds \hat{B}(t', s) \right] \end{aligned} \quad (VI.19)$$

C. Feynman Representation of Memory Superoperators: Physical Interpretation

The formal solution of the Heisenberg equation of motion in a Liouville space [136] [see Eq.(VI.3)]

$$i \partial/\partial t \psi(\xi, t) = - \hat{\Phi} \psi(\xi, t) \quad (VI.20)$$

can be written in this operator space in the form

$$\psi(\xi, t) = \exp \left[2i \hat{\Phi}_0(t-t') - i \int_{t'}^t \hat{\mathbb{L}}(\xi, \dot{\xi}; u) du \right] \psi(\xi, t') \quad (\text{VI.21})$$

where $\hat{\mathbb{L}}$ is the superlagrangian operator in the Liouville space, i.e., $\hat{\mathbb{L}} = \hat{\Phi}_0 - \hat{\Phi}' \equiv [L, \dots]_+$, such that

$$\hat{S} = \int_{t'}^t \hat{\mathbb{L}}(\xi, \dot{\xi}; u) du, \quad \hat{S} \equiv \hat{S}[\Gamma(t, t')] \quad (\text{VI.22})$$

and Γ stands for the paths in the operator space.

The exponential of the superoperator appearing in Eq.(21) can be decoupled as follows

$$\begin{aligned} & \exp \left[2i \hat{\Phi}_0(t-t') - i \int_{t'}^t \hat{\mathbb{L}}(\xi, \dot{\xi}; u) du \right] \\ &= \exp [2i \hat{\Phi}_0(t-t')] \exp \left[-i \int_{t'}^t \hat{\mathbb{L}}(\xi, \dot{\xi}; u) du \right] \hat{Z}(t, \tau) \end{aligned} \quad (\text{VI.23})$$

where $\hat{Z}(t, \tau)$ satisfies the operator equation [134,135]

$$\hat{Z}(t, \tau) = \exp \left[\int_0^\tau \hat{\zeta}(z) dz \right] + \sum_{n=2}^{\infty} 1/n! \sum_{r=0}^{n-2} (r+1)! \left[\int_0^\tau \hat{\zeta}(z) dz \right]^{n-r-2} \hat{P}_r(\tau, 0) \quad (\text{VI.24})$$

with $\hat{\zeta}(z)$ given by

$$\hat{\zeta}(z) = - \sum_{\nu=1}^{\infty} z^\nu / \nu! \left[\int_{t'}^t 2 \hat{\phi}_0 du, \hat{S}[\Gamma(t, t')] \right]_\nu \quad (\text{VI.25})$$

and

$$\hat{P}_r(\tau, 0) = \sum_{\alpha=0}^r \int_0^\tau dz_1 \hat{\zeta}(z_1) \int_0^{z_1} dz_2 \hat{\zeta}(z_2) \dots \int_0^{z_\alpha} dz_{\alpha+1} \left\{ \int_0^{z_{\alpha+1}} dz \left[\hat{\zeta}(z), \hat{\zeta}(z_{\alpha+1}) \right] \right\} \hat{Y}_{r-\alpha}(z_{\alpha+1}, 0) \quad (\text{VI.26})$$

$[A, B]_\nu$ stands for the iterated commutator,

$$[A, B]_\nu = [A, [A, [\dots, [A, B]] \dots]] \quad (\text{VI.27})$$

i.e., there are ν commutator terms in each term of the expansion (VI.25). In Eq.(VI.26) $\hat{Y}_n(\tau, 0)$ satisfies the recurrence relation [135]

$$\begin{aligned}
\hat{Y}_n(\tau, 0) &= \int_0^\tau d\tau_1 \hat{\zeta}(\tau_1) \int_0^{\tau_1} d\tau_2 \hat{\zeta}(\tau_2) \dots \int_0^{\tau_{n-1}} d\tau_n \hat{\zeta}(\tau_n) \\
&= \int_0^\tau dz \hat{\zeta}(z) \hat{Y}_{n-1}(z, 0), \quad \hat{Y}_0(z, 0) = \hat{0} \quad (VI.28)
\end{aligned}$$

where $\hat{0}$ is the identity superoperator.

It follows from Eqs.(VI.21) and (VI.23) that

$$\begin{aligned}
\psi(\xi, t) &= \exp \{ 2i \hat{\Phi}_0(t - t') \} \exp \{ -i \hat{\mathcal{S}}[\Gamma(t, t')] \} \\
&\quad [\hat{0} + \hat{\Xi}(t, \tau)] \psi(\xi, t') \quad (VI.29)
\end{aligned}$$

where $\hat{Z}(t, \tau)$ in Eq.(VI.23) has been written as $[\hat{0} + \hat{\Xi}(t, \tau)]$. The two terms in Eq.(VI.29) account for the time evolution of ψ at the phase space points ξ . The first term is closely related to the usual path integral wavefunctions [1,2] because it is seen to be modulated by the superphase $\exp(-i \hat{\mathcal{S}})$; the second term in Eq.(VI.29) arises from the noncommutability property of the operators H_0 and L [135,137]. A comparison of Eqs.(VI.17) and (VI.29) allows us to get a physical interpretation of the product of decoupling and coupling group superoperators

$$\begin{aligned}
&\exp(i \hat{\Phi}_0 t) \hat{G}_D(t, t') \hat{G}_C(t, t') \exp(-i \hat{\Phi}_0 t') \\
&= \exp \{ 2i \hat{\Phi}_0(t - t') \} \exp \{ -i \hat{\mathcal{S}}[\Gamma(t, t')] \} [\hat{0} + \hat{\Xi}(t, \tau)] \quad (VI.30)
\end{aligned}$$

This expression may be considered as the Feynman's superphase representation of memory superoperators. It should be noted that Eq.(VI.29) is not a standard Feynman path integral representation. In fact, we are dealing with time evolution only, i.e., no space propagation is involved. This implies that the superaction \hat{S} as defined in Eq.(VI.22) must not be interpreted as classical paths but rather as an action superoperator from which a Feynman path integral in operator space could be constructed. An action as a path in the operator space may be characterized as a way of implementing this kind of evolution scheme, and will be discussed elsewhere in a rigorous manner.

D. Feynman Path Integral Representation of Field Operators

To get the counterpart of the Feynman path integral formulation for quantum field operators as a quantum mechanical analog of the state function, we write the field operator as a homogeneous Fredholm integral equation of the second kind

$$\psi(\xi, t) = - \int \psi(\xi', t) d^3\xi', \quad (\text{VI.31})$$

where $\psi(\xi', t)$ may be considered as the phase space contribution for the field operator $\psi(\xi, t)$, namely a Huygens-like principle.

The solution of Eq.(VI.31) is arbitrary and hence, for the present purposes is only a useful way of expressing the field operator. Thus, introduction of the formal solution of Heisenberg's equation of motion (VI.20) into Eq.(VI.31) leads to

$$\psi(\xi, t) = - \int \exp \left[i \int_{t'}^t \hat{\phi} du \right] \psi(\xi', t') d^3\xi', \quad (\text{VI.32})$$

and using the same procedure as that followed to express the time evolution of ψ in the operator space we get

$$\psi_{\Gamma}(\xi, t) = - \int \exp \{ 2 i \hat{\phi}_0(t - t') \} \exp \{ - i \hat{S}_{\Gamma} \} [\hat{\Pi} + \hat{\Xi}(t, \tau)] \psi(\xi', t') d^3\xi', \quad (\text{VI.33})$$

As long as a particular choice of Γ is necessary for the evaluation of \hat{S} , $\psi_{\Gamma}(\xi, t)$ can be considered as the field operator on the Γ path in operator space. In the time evolution equation for ψ [Eq.(VI.21)] it is needed only one path for describing it; in fact, no propagation in space coordinates is required. So ψ_{Γ} may be interpreted as a projection on the possible paths between t and t' , and therefore the quantum field operator may be considered as a sum over all those projections, i.e.,

$$\begin{aligned} \psi(\xi, t) &= \sum_{\{\Gamma\}} \psi_{\Gamma}(\xi, t) = - \int \exp \{ 2 i \hat{\phi}_0(t - t') \} \\ &\sum_{\{\Gamma\}} \exp \{ - i \hat{S}_{\Gamma} \} [\hat{\Pi} + \hat{\Xi}(t, \tau)] \psi(\xi', t') d^3\xi', \end{aligned} \quad (\text{VI.34})$$

From this equation the Feynman path integral is recognized as

$$\sum_{\{\Gamma\}} \exp \{-i \hat{S}_{\Gamma}\} [\hat{U} + \hat{\Xi}(t, \tau)] \quad (\text{VI.35})$$

Thus, the field operator $\psi(\xi, t)$ satisfies the integral equation

$$\psi(\xi, t) = \int \hat{K}(\xi, t | \xi', t') \psi(\xi', t') d^3\xi', \quad (\text{VI.36})$$

Eq.(VI.36) represents the Feynman path integral formulation for quantum field operators, being \hat{K} the Feynman superpropagator, defined as

$$\hat{K}(\xi, t | \xi', t') = - \exp \{ 2i \hat{\Phi}_0(t - t') \} \sum_{\{\Gamma\}} \exp \{-i \hat{S}_{\Gamma}\} [\hat{U} + \hat{\Xi}(t, \tau)] \quad (\text{VI.37})$$

This equation again takes into account the noncommutability of the operators H_0 and L by means of $\hat{\Xi}(t, \tau)$.

On introducing Eq.(VI.36) into Heisenberg equation of motion [Eq.(VI.20)] it is easily verified that the differential equation for the superpropagator is

$$\left[i \partial/\partial t + \hat{\Phi} + \hat{U} \right] \hat{K}(\xi, t | \xi', t')$$

$$= \delta(\xi - \xi') \exp \left[-i \int_{t'}^t \hat{\Phi} du \right] \quad (\text{VI.38})$$

E. Application to a Non-Interacting Many-Boson System

In this sub-section we shall develop functional integrals, within the formalism of superoperators for second quantized hamiltonians with Bose operators.

For the purpose of developing our functional integrals we consider a many boson system and use the discrete form of H_0 . It follows from Eq.(VI.1a) that it reads

$$H_0 = \sum_k \epsilon_k a_k^+ a_k \quad (\text{VI.39})$$

where the ϵ_k 's are the one-particle energies and a_k^+ and a_k are the creation and annihilation boson like operators.

In order to proceed we need the superpropagator representation [Eq.(VI.37)] in the original form as given by Eq.(VI.32). Thus we write

$$\hat{K}(\xi, t | \xi', t') = \exp \left[i \int_{t'}^t \hat{\Phi}_0 du \right] \quad (\text{VI.40})$$

This equation may be written in terms of the short time approach as

$$\begin{aligned} \hat{K}(\xi, t | \xi', t') \equiv \hat{K} &= \exp(i \hat{\Phi}_0 \delta t_1) \exp(i \hat{\Phi}_0 \delta t_2) \\ &\dots \exp(i \hat{\Phi}_0 \delta t_N) \end{aligned} \quad (\text{VI.41})$$

where $\delta t_i \equiv \delta t = t/N$ ($i=1, \dots, N$), with N the short time

partition.

For obtaining expressions which could be handled in an easy way we introduce an operator space which will be the carrier space for the superoperator object. In the limit of no interaction this space is chosen to be

$$\mathfrak{S} = \{ a_k, a_l^+ ; k, l = 1, \dots, \infty \} \quad (\text{VI.42})$$

This set spans the one particle operator space and supports the closure relation

$$\hat{1} = \sum_m |a_m\rangle \langle a_m| \quad (\text{VI.43})$$

with the associated binary product operation

$$\langle X|Y \rangle = [Y, X^+]_- \quad (\text{VI.44})$$

Thus, the carrier space is metrized by

$$\langle a_l|a_k \rangle = [a_l; a_k^+]_- = \delta_{lk} \quad (\text{VI.45})$$

and the matrix elements for \hat{K} in the short time approach become

$$\begin{aligned}
 \langle a_1 | \hat{K} | a_k \rangle &= \sum_{i_1} \dots \sum_{i_N} \langle a_1 | \exp(i \hat{\Phi}_0 \delta t) | a_{i_1} \rangle \\
 &\langle a_{i_1} | \exp(i \hat{\Phi}_0 \delta t) | a_{i_2} \rangle \dots \langle a_{i_N} | \exp(i \hat{\Phi}_0 \delta t) | a_k \rangle
 \end{aligned}
 \tag{VI.46}$$

where the closure relation (VI.43) has been introduced between each exponential function in Eq.(VI.41). This procedure is analogous to that implicit in the summation over paths [Eq.(VI.37)].

Realizing that each a_l is an eigenelement of $\hat{\Phi}_0$ with eigenvalues $n_l \epsilon_l$ (where n_l is the corresponding occupation number associated to the l -th energy level), and allowing N to tend to infinity to get the exact propagator, yields

$$\langle a_i | \hat{K} | a_k \rangle = \exp(i n_k \epsilon_k t) \delta_{ik}
 \tag{VI.47}$$

Note that \hat{K} is diagonal in the operator basis set \mathcal{B} . Physically the matrix element (VI.47) is the projection of the \hat{K} superoperator onto the one particle operator space.

On performing the Wick's rotation [140] (β is the inverse of the absolute temperature and t is imaginary time)

$$i t = - \beta
 \tag{VI.48}$$

so as to realize the adequate analytic continuation into the Feynman superpropagator \hat{K} [Eq.(VI.40)], straightforwardly yields the thermodynamic matrix

elements

$$(a_i | \hat{K} a_k) = \exp(-\beta n_k \varepsilon_k) \delta_{ik} \quad (\text{VI.49})$$

which are the unnormalized one-particle density matrix elements. Thus, normalizing Eq.(VI.49) and noting that $\hat{K} = \hat{\rho}_1$ (one-particle density matrix superoperator) leads to

$$\text{Tr}(\hat{\rho}_1) = \sum_{\langle R_i \rangle} (a_i | \hat{\rho}_1 a_i)_{\langle R_i \rangle} = \sum_{n_i=0}^{\infty} \exp(-\beta n_i \varepsilon_i) \quad (\text{VI.50})$$

which is recognized to be the bosonic partition function for the one-state distribution. $\langle R_i \rangle$ stands for the accessible one particle configurations which are compatible with the i -th energy level [141]

We finally get, for the density superoperator matrix elements, the expression

$$(a_i | \hat{\rho}_1 a_k) = \frac{\exp(-\beta n_k \varepsilon_k) \delta_{ik}}{\sum_{n_k=0}^{\infty} \exp(-\beta n_k \varepsilon_k)} \quad (\text{VI.51})$$

Defining the number operator in the k -th energy level in the usual form

$$N_k = a_k^+ a_k \quad (\text{VI.52})$$

and its associated superoperator

$$\hat{N}_k = [N_k; 1_- \quad (VI.53)$$

allows to evaluate the mean occupation number for the k -th level as

$$\langle N_k \rangle \equiv \text{Tr}(\hat{\rho}_1 \hat{N}_k) \equiv \bar{n}_k = \sum_{\langle R_l \rangle} \sum_{\langle R_l \rangle} (a_1 | \hat{\rho}_1 a_1) (a_1 | \hat{N}_k a_1) \quad (VI.54a)$$

or equivalently

$$\bar{n}_k = \frac{\sum_{n_1=0}^{\infty} \sum_{\langle R_l \rangle} \exp(-\beta n_1 \varepsilon_1) (a_1 | \hat{N}_k a_1) \delta_{1l}}{\sum_{n_1=0}^{\infty} \exp(-\beta n_1 \varepsilon_1)} \quad (VI.54b)$$

Thus, using

$$(a_1 | \hat{N}_k a_1) = n_k a_1 \delta_{1k} \delta_{1l} \quad (VI.55)$$

we get immediately

$$\bar{n}_k = \frac{\sum_{n_k=0}^{\infty} n_k \exp(-\beta n_k \varepsilon_k)}{\sum_{n_k=0}^{\infty} \exp(-\beta n_k \varepsilon_k)} \quad (VI.56)$$

which after a little algebra leads to

$$\bar{n}_k = \frac{1}{\exp(\beta \varepsilon_k) - 1} \quad (VI.57)$$

which is the expected formulae of the Planck's distribution law.

F. Final Remarks

Quantum time evolution for field operators are useful for describing not only equilibrium processes but also non-equilibrium evolutions. In fact, there exists a close relation with Green functions expressed as propagators in operator space [132,136] and the reduced density functions which are the essential tools for evaluation of such properties. The Feynman path formulation for field operators leads us to state some interesting conclusions. As we have shown, the Feynman path representation of memory superoperators shows that the evolution depends on the whole history of the process, i.e., the evolution is non-instantaneous; in fact, the Feynman path integral representation includes the history of the process by means of the action superoperator. The resultant superpropagator contains all the information about the system, it being a sum of contributions from all paths; thus, the quantum superposition is already manifest in the present formulation. Finally, it should be stressed that since in an imaginary time formalism the Feynman path integral is mathematically equivalent to a partition function [18,19], the present formalism should appear as a practical tool for the evaluation of magnetic and thermodynamic properties of many-body systems.

VII. CONCLUSIONS

In this review we have shown that a beautiful and powerful mathematical framework for the understanding of the properties of physical systems having large or infinite number of degrees of freedom is provided by path integral formulations of the many-body problem.

The path integral for the Green's function involving the Coulomb potential in combination with the KS transformation (that corresponds to the Hopf fibration $S^3/S^1 = S^2$) was used in the derivation of the connection between the \mathbb{R}^5 hydrogen atom and the \mathbb{R}^8 harmonic [87]. It should be emphasized that the KS and Levi-Civita transformations, used to regularize the three- and two-dimensional Kepler problem respectively, were recently generalized to the n-dimensional case [142]. Thus, while the technique we have described is specific to the hydrogen atom, its success lends encouragement that a possible extension can be developed to describe correlation effects. This appears probable since the helium results [143] demonstrate implicitly the existence of new quantum numbers for a united atom limit classification of the molecular hydrogen spectrum.

The formalism described in Section II was used to show the equivalence between a finite many-body problem for a non-relativistic molecular system of N electron and N one-dimensional Ising models. This allowed us to get the propagator of the Hückel model through the Feynman path integral formulation. The corresponding secular equations were generated via the saddle-point approximation of the gaussian integrals appearing in the path integral. Also, application of this approximation to the corresponding effective action was shown to lead

to the Roothaan equations.

In the path integral approach one writes an exact expression for a quantum observable in terms of a functional integral over a field containing all the degrees of freedom. Then, by application of the saddle-point approximation, a time-dependent mean-field theory is obtained in which coordinates, momenta, equations of motion, and quantization conditions are specified by the underlying effective Hamiltonian. Thus, the functional integral provides a bridge between the quantum many-body propagator and the time dependent Hartree-Fock theory. In the saddle-point approximation, the propagator between two Slater determinants is dominated by the exponential of a time-dependent Hartree-Fock solution.

The emphasis of the path integral formalism is a quantum mechanical generalization of the time-dependent Hartree-Fock theory, which is addressed as many-body corrections. This formalism at least offers the potential of extending the quantum theory of many-body notion beyond the state obtained with conventional techniques. Certainly, recent achievements using mean field models lend credence to this promise [12,13].

It should also be emphasized that enormous strides have been achieved in the last several years in the simulation of quantum systems [144]. The examples that we have discussed indicate the versatile way in which path integrals methods can be used to study interesting and difficult problems. One major advantage of path integral simulations of quantum systems is the insight gained by examining the details of the quantum paths. It is hoped that examination of the details will provide a sound basis for analytical treatment of some of these

problems. Despite explosion in activity, much remains to be accomplished, even in the simulations of the equilibrium properties of quantum systems. For example, efficient ways to reduce systematically the number of beads for highly quantum mechanical systems are needed. More importantly, reliable and practical methods are needed to treat systems in which the exchange contribution to the partition function is significant. The needed tools include methods for treating systems with fermionic degrees of freedom, thereby providing a natural framework to treat chemical bonding [145]. Finally, a practical way to obtain real time dynamics for interacting quantum systems is still lacking. Despite some signs of hope, this is still an open problem, and progress in this area is sorely needed. Some of the problems outlined here give the reader a perspective on how path integral methods can be used to address problems in fields ranging from particle physics to biological sciences.

ACKNOWLEDGMENTS. The authors are grateful to the Consejo Nacional de Investigaciones Científicas y Técnicas (CONICET), Republica Argentina, for continued support of this research program and to the Facultad de Ciencias Exactas y Naturales, Universidad de Buenos Aires and Universidad Nacional de La Plata for facilities provided at their respective Departments of Physics during the course of this work.

The authors wish to express their gratitude to Professor Per-Olov Löwdin for his kind invitation to write this review and for his interest and encouragement during the evolving manuscript.

REFERENCES

- [1] a) R. P. Feynman, Rev. Mod. Phys. 20, 367 (1948).
b) R. P. Feynman and A. R. Hibbs, Quantum Mechanics and Path Integrals, McGraw-Hill, New York, 1965.
- [2] L. S. Schulman, Techniques and Applications of Path Integration, Wiley, New York, 1981.
- [3] D. J. Amit, Field Theory, The Renormalization Group and Critical Phenomena, McGraw-Hill, New York, 1978.
- [4] E. Wigner, Phys. Rev., 40, 749 (1932)
- [5] H. Weyl, The Theory of Groups and Quantum Mechanics, Dover, New York, p.14, 1931.
- [6] J. E. Moyal, Proc. Cambr. Phil. Soc., 45, 99 (1949).
- [7] P.-O. Löwdin, Adv. Quantum Chem., 2, 213 (1965).
- [8] K. F. Freed, J. Chem. Phys., 6, 692 (1972).
- [9] W. Miller, J. Chem. Phys., 54, 5386 (1971).
- [10] R. P. Feynman, Statistical Mechanics, Reading, Mass W. A. Benjamin, 1972.
- [11] T. D. Lee, Particle Physics and Introduction to Field Theory, Contemporary Concepts in Physics, Vol.1, Revised and updated First Edition, Science Press (Beijing), Columbia University, harwood academic publishers.
- [12] J. W. Negele, Rev. Mod. Phys., 54, 913 (1982).
- [13] J. W. Negele, Physics Today, April, 24 (1985).
- [14] I. H. Duru and H. Kleinert, Phys. Lett., 84B, 185 (1979); Fortschr. Phys., 30, 401 (1982).
- [15] a) R. Ho and A. Inomata, Phys. Rev. Lett., 48, 231 (1982);
b) A. Inomata, Phys. Lett. A 101, 253 (1984).
- [16] H. Grinberg, J. Marañón, and H. Vucetich, J. Chem. Phys., 78, 839 (1983).

- [17] H. Grinberg, J. Marañón, and H. Vucetich, *Int. J. Quantum Chem.*, XXIII, 379 (1983).
- [18] H. Grinberg and J. Marañón, *Phys. Lett.*, 94A, 275 (1983).
- [19] J. Marañón and H. Grinberg, *J. Chem. Phys.*, 81, 4537 (1984).
- [20] J. Marañón, *Phys. Lett.*, 103A, 116 (1984).
- [21] a) J. Marañón, *Phys. Lett.*, 104A, 459 (1984).
b) J. Marañón and J. L. Pousa, *Phys. Rev.*, 36A, 5530 (1987).
- [22] J. Marañón, *Int. J. Quantum Chem.*, Vol. XXXIII, 491 (1988).
- [23] a) S. F. Edwards and K. F. Freed, *J. Phys.* 3C, 739 (1970);
b) K. F. Freed, *J. Chem. Phys.*, 54, 1453 (1971);
c) S. F. Edwards and J. W. Grant, *J. Phys.* 6A, 1169 (1973).
- [24] F. W. Wiegel, *Introduction to Path-Integral Methods in Physics and Polymer Science*, World Scientific, Singapore, 1986.
- [25] K. F. Freed, *Renormalization Group Theory of Macromolecules*, Wiley, New York, 1987.
- [26] K. K. Thornber and R. P. Feynman, *Phys. Rev.*, 1B, 4099 (1970).
- [27] K. K. Thornber, *Phys. Rev.*, 3B, 1929 (1971).
- [28] M. C. Gutzwiller, in *Path Integrals and their Applications in Quantum, Statistical, and Solid State Physics*, eds. G. J. Papadopoulos and J. T. Devreese, Plenum Press, New York and London, 1978.
- [29] S. Hawking, *The Path Integral Approach to Quantum Gravity*, in *General Relativity - an Einstein Centenary Survey*, eds. S. Hawking and W. Israel,

- Cambridge, Univ. Press, London, 1979.
- [30] R. P. Feynman, *Phys. Rev.*, **97**, 660 (1955).
- [31] V. Volterra, *Theory of Functionals and of Integral and Integrodifferential Equations*, Blackie and Son, London and Glasgow, 1930.
- [32] a) N. Wiener, *J. Math. Phys. Mass. Inst. Techn.* **2**, 131 (1923);
b) N. Wiener, *Proc. Lond. Math. Soc.*, **22**, 454 (1924).
- [33] J. Kirkwood, *Phys. Rev.*, **44**, 31 (1933).
- [34] a) S. Chandrasekhar, *Rev. Mod. Phys.*, **15**, 1 (1943);
b) G. J. Papadopoulos, *J. Phys.*, **6A**, 1479 (1973).
- [35] a) N. N. Bogoliubov, *Dok.* **99**, 225 (1954);
b) K. Zymanzik, *Z. Naturforsch* **9A**, 409 (1954);
c) P. T. Matthews and A. Salam, *Nuovo Cim.*, **2**, 120 (1955);
d) K. O. Friedrichs and H. N. Shapiro, *Proc. Nat. Acad. Sci. (U.S.)*, **43**, 336 (1957);
e) J. Schwinger, *Phys. Rev.* **115**, 721 (1959);
f) I. E. Segal, *J. Math. Phys.*, **1**, 468 (1960);
g) S. F. Edwards, *Analysis in Function Space*, p.31 and p.167, eds. W. T. Martin and I. Segal, MIT Press Cambr. Mass., 1964;
h) J. Tarski, *Lectures in Theoretical Physics*, X-A p.443, eds. A. D. Barut and W. E. Brittin, Gordon and Breach, N. Y., 1968.
- [36] J. B. Kogut, *Rev. Mod. Phys.*, **51**, 659 (1979).
- [37] Y. Gsanak, H. S. Taylor, and R. Yaris, *Adv. Atom. Molec. Phys.*, **7**, 287 (1971).
- [38] J. Linderberg and Y. Öhrn, *Propagators in Quantum Chemistry*, Academic Press, London, 1973.
- [39] P. Jorgensen, *Annu. Rev. Phys. Chem.*, **26**, 359 (1975).

- [40] Y. Öhrn, *Proceedings from the Second International Congress on Quantum Chemistry*, ed. B. Pullman, Reidel, Boston, 1976.
- [41] J. Simons, *Ann. Rev. Phys. Chem.*, 28, 1 (1977).
- [42] L. S. Gederbaum and W. Domcke, *Adv. Chem. Phys.*, 36, 205 (1977).
- [43] Y. Öhrn and G. Born, *Adv. Quantum Chem.*, 13, 1 (1981).
- [44] O. Goscinski and B. Pickup, *Mol. Phys.*, 26, 1013 (1973).
- [45] Aa. E. Hansen and T. D. Bouman, *Adv. Chem. Phys.*, 44, 545 (1980).
- [46] M. F. Herman, K. F. Freed, and D. L. Yeager, *Adv. Chem. Phys.*, 48, 1 (1981).
- [47] W. Von Niessen, J. Schirmer, and L. S. Gederbaum, *Comput. Phys. Rep.*, 1, 57 (1984).
- [48] J. Oddershede, P. Jorgensen, and D. L. Yeager, *Comput. Phys. Rep.*, 2, 33 (1984).
- [49] J. Oddershede, *Adv. Chem. Phys.*, 69, 201 (1987), Part II.
- [50] M. A. Ball and A. D. McLachlan, *Mol. Phys.*, 7, 501 (1964).
- [51] A. D. McLachlan and M. A. Ball, *Rev. Mod. Phys.*, 36, 84 (1964).
- [52] J. Linderberg and Y. Öhrn, *Proc. Roy.*, 285A, 445 (1965).
- [53] J. Lindhard, *K. Danske Vidensk. Selsk., Mat. Fys. Meddr.*, 28, No 8 (1954).
- [54] R. Kubo, *J. Phys. Soc. Japan*, 12, 570 (1959).
- [55] D. N. Zubarev, *Usp. Fiz. Nauk.*, 71, 71 (1960); *Sov. Phys. Usp. (Eng. Transl.)*, 3, 320 (1960).
- [56] L. Heding and S. Lundquist, *Solid State Phys*, 23, 1 (1969).

- [57] P. A. M. Dirac, *Selected Paper on Quantum Electrodynamics*, p.312, ed.: J. Schwinger, Dover Publ. Inc. N. Y., 1958.
- [58] J. W. Negele and H. Orland, "Quantum Many-Particle Systems", Addison-Wesley, 1988.
- [59] G. Parisi, "Statistical Field Theory", Addison Wesley, 1988.
- [60] R. Abé, *Busseiron Kenk-yu* 79, 101 (1954).
- [61] J. R. Klauder, *Ann. Phys.*, N. Y., 11, 123 (1960).
- [62] S. S. Schweber, *J. Math. Phys.*, 3, 831 (1962).
- [63] A. Gasher, P. Lurié, and M. Revzen, *J. Math. Phys.*, 9, 1312 (1969).
- [64] J. Hubbard, *Phys. Rev. L* 3, 77 (1959).
- [65] S. F. Edwards and D. Sherrington, *Proc. Phys. Soc.*, 90, 3 (1967).
- [66] D. Sherrington, *J. Phys. C*, 4, 402 (1971).
- [67] H. Grinberg and J. Marañón, *J. Molec. Struct. (THEOCHEM)*, in press.
- [68] M. C. Gutzwiller, *J. Math. Phys.*, 8, 1979 (1967).
- [69] I. H. Duru and E. Keyman, *Current ICTP IC/80/129*, preprint, Miramare, Trieste (1980).
- [70] J. Schwinger, *J. Math. Phys.*, 5, 1606 (1964).
- [71] G. G. Gerry and A. Inomata, *Phys. Lett. A*, 84, 172 (1981).
- [72] R. E. Langer, *Phys. Rev.*, 51, 669 (1937).
- [73] F. Steiner, *Phys. Lett. A*, 106, 363 (1984).
- [74] P. Kustaanheimo and E. Stiefel, *J. Reine Angew. Math.*, 218, 204 (1965).
- [75] H. Grinberg, J. Marañón, and H. Vucetich, *Z. Phys. C*, 20, 147 (1983).
- [76] M. Kibler and T. Négadi, *Lett. Nuovo Cimento* 39, 319 (1984).
- [77] C. D. H. Chisholm, *Group Theoretical Techniques*

in Quantum Chemistry (Academic, New York, 1976)

- [78] a) V. Fock, Z. Phys., 98, 145 (1935);
- b) V. Bargmann, Z. Phys., 99, 576 (1936);
- c) M. Bander and G. Itzykson, Rev. Mod. Phys., 38, 330, 346 (1966).
- [79] a) C. Runge, Vectoranalysis (Hirzel, Leipzig, (1919), Vol. 1, p. 70;
- b) W. Lenz, Z. Phys., 24, 197 (1924);
- c) W. Pauli, Z. Phys., 36, 336 (1926).
- d) J. G. F. Belinfante and B. Kolman, A Survey of Lie Groups and Lie Algebras with Applications and Computational Methods, Society for Industrial and Applied Mathematics, 1972.
- [80] B. G. Adams, J. Čizek and J. Paldus., Adv. Quantum Chem., Vol.19(1988) p. 1.
- [81] A. Barut, G. K. E. Schneider, and R. Wilson, J. Math. Phys., 20, 2244 (1979).
- [82] a) V. P. Popov, CERN preprint TH 2424 (1977);
- b) V. P. Popov, Functional Integrals in Quantum Field Theory and Statistical Physics (Atomizdat, Moscow, 1976);
- c) H. Kleinert, Fortschr. Phys., 26, 565 (1978).
- d) H. Kleinert, Collective Field Theory of Superliquid ^3He , Berlin preprint FUB-HEP 14/78, extended version of Erice Lecture Note, Z. Zichichi, Ed., 1978.
- [83] F. Ravndal and T. Toyoda, Nucl. Phys. B, 3, 312 (1967).
- [84] A. C. Chen, Phys. Rev. A, 22, 333 (1980).
- [85] J. Linderberg, Int. J. Quantum Chem., 19, 237 (1981).
- [86] A. C. Chen and M. Kibler, Phys. Rev. A 31, 3960 (1985).

- [87] M. Kibler, A. Ronveaux, and T. Négadi, *J. Math. Phys.*, 27, 1541 (1986).
- [88] J. Cizek and J. Paldus, *Int. J. Quantum Chem.*, XII, 875 (1977).
- [89] A. C. Chen, *Phys. Rev. A*, 23, 1655 (1981).
- [90] M. S. Marinov, *Phys. Rep.*, 60, 26 (1980).
- [91] W. Langguth and A. Inomata, *J. Math. Phys.*, 20, 499 (1979).
- [92] G. A. Ringwood and J. T. Devreese, *J. Math. Phys.*, 21, 1390 (1980).
- [93] L. D. Landau and E. M. Lifshitz, *The Classical Theory of Fields* (Addison-Wesley, Reading, MA, 1951), Vol. II.
- [94] J. S. Dowker, *J. Phys. A*, 5, 936 (1972).
- [95] J. S. Dowker, *J. Phys. A*, 9, 1256 (1974).
- [96] G. Ringwood, *J. Phys. A*, 9, 1253 (1976).
- [97] P. A. M. Dirac, *Lectures on Quantum Mechanics* (Belfer Graduate School of Science, Yeshiva University, New York 1964).
- [98] H. Grinberg, J. Marañón, and H. Vucetich, *J. Math. Phys.*, 25, 2648 (1984).
- [99] E. L. Stiefel, G. Scheifele, *Linear and Regular Celestial Mechanics, Grundlehren der Mathematischen Wissenschaften Bd, 174*, Berlin, Heidelberg, New York, Springer 1971.
- [100] A. Inomata, *Phys. Lett. A*, 387 (1982).
- [101] A. C. Chen, *Phys. Rev. A*, 26, 669 (1982).
- [102] L. Salem, *The molecular orbital theory of conjugated systems*, Benjamin, Reading, MA, 1969.
- [103] M. Creutz and B. Freedman, *Ann. Phys.*, 132, 427 (1981).
- [104] K. Huang, *Statistical Mechanics*, Wiley, New York, 1963.

- [105] K. Nishikawa, M. Yamamoto, and S. Aono, J. Chem. Phys. 78, 5031 (1983).
- [106] T. H. Berlin and M. Kac, Phys. Rev., 86, 821 (1952).
- [107] F. Y. Wu, Rev. Mod. Phys., 54, 235 (1982).
- [108] K. G. Wilson and J. Kogut, Phys. Rep., 12, 75 (1974).
- [109] J. Marañón and H. Grinberg, J. Molec. Struct. (THEOCHEM), 120, 181 (1985).
- [110] R. Rajaraman, Phys. Rep., 21C, 229 (1975).
- [111] a) M. J. Rice, A. R. Bishop, J. A. Krumhansl and S. E. Trullinger, Phys. Rev. Lett., 36, 432(1976);
b) Kazumi Maki and Pradeep Kumar, Phys. Rev., B14, 118 (1976);
c) J. A. Krumhansl and J. R. Schrieffer, Phys. Rev., B11, 3535 (1975).
- [112] K. Nakajima, Y. Sawada and Y. Onodera, J. Appl. Phys., 46, 5272 (1975).
- [113] F. Calogero and A. Degasperis, Lett. Nuovo Cim., 16, 425 (1976).
- [114] H. Grinberg, A. L. Capparelli, A. Spina, J. Marañón, and O. M. Sorarrain, J. Phys. Chem., 85, 2751 (1981), and references therein.
- [115] a) T. Poston and I. N. Stewart, Catastrophe Theory and its Applications, Pitman, London, 1978;
b) I. N. Stewart, Catastrophe Theory in Physics, Rep. Prog. Phys., 45, 185 (1982).
- [116] E. C. Zeeman, Lectures on Catastrophe Theory, with Applications to Biology and the Social Sciences, Summer School on Dynamical Systems, International Centre for Theoretical Physics, Trieste, 1983.
- [117] S. Sarker, S. E. Trullinger and A. R. B. Bishop,

- Phys. Lett., 59A, 255 (1976).
- [118] M. F. Augusteijn and E. Breitenberger, *Physica*, 6D, 321 (1983).
- [119] Y. Nogami and G. S. Warke, *Phys. Lett.*, 59A, 251 (1976).
- [120] J. Marañón and H. Grinberg, *J. Molec. Struct. (THEOCHEM)*, 166, 119 (1988).
- [121] S. Coleman, in *The Uses of Instantons, Lectures delivered at the 1977 International School of Subnuclear Physics*, Ettore Majorana.
- [122] W. Guttinger and H. Eikemeier (Ed.), *Structural Stability in Physics*, Berlin: Springer, 1979.
- [123] H. Haken, *Cooperative Phenomena*, H. Haken and M. Wagner (Eds.), Berlin: Springer, 1973.
- [124] a) H. Haken, *Rev. Mod. Phys.*, 47, 67 (1975);
b) H. Haken, *Synergetics an Introduction: Nonequilibrium Phase Transitions and Self-Organization in Physics, Chemistry and Biology*, Berlin: Springer, 1978.
- [125] A. M. F. Gomes and S. Canuto, *J. Phys.*, B15, 1307 (1982).
- [126] a) D. Chandler and P. G. Wolynes, *J. Chem. Phys.*, 74, 4078 (1981);
b) K. S. Scheweizer, R. M. Stratt, D. Chandler, and P. G. Wolynes, *ibid.*, 75, 1347 (1981).
- [127] F. London, *J. Phys. Rad.* 8, 397 (1937).
- [128] Klauder, *J. Math. Phys.*, 4, 1055, 1058 (1963).
- [129] C. G. J. Roothaan, *Rev. Mod. Phys.*, 23, 69 (1951).
- [130] J. Marañón, unpublished results.
- [131] a) R. E. Turner and J. S. Dahler, *J. Phys.*, 13B, 161 (1980);
b) R. E. Turner, J. S. Dahler and R. F. Snider, *Can. J. Phys.*, 60, 1371 (1982).

- [132] H. Grinberg, International Centre for Theoretical Physics, Miramare, Trieste, preprint IC/83/172.
- [133] F. J. Dyson, Phys. Rev., 75, 1736 (1949).
- [134] C. Lam and P. C. W. Fung, Phys. Rev. 27A, 1760 (1983).
- [135] P. C. W. Fung and C. C. Lam, Phys. Rev. 29A, 2364 (1984).
- [136] P. O. Löwdin, Int. J. Quantum Chem., S16, 485 (1982).
- [137] R. C. Boichicchio and H. Grinberg, Phys. Rev.A, in press.
- [138] a) R. Zwanzig, J. Chem. Phys. 33, 1338 (1960);
b) R. Zwanzig, Physica, 30, 1109 (1964).
- [139] H. Feshbach, Ann. Phys. N. Y., 19, 287 (1982).
- [140] a) A. L. Fetter and J. D. Walecka, Quantum Theory of Many Particle Systems, McGraw-Hill Book Co., N. Y., 1966;
b) L. P. Kadanoff and G. Baym, Quantum Statistical Mechanics, W. A. Benjamin Inc., N. Y., 1962.
- [141] F. Reif, Fundamentals of Statistical and Thermal Physics, McGraw-Hill Kogakusha Ltd., Tokio, 1965 (Chap. 9).
- [142] B. Cordani, J. Phys. 22A, 2441 (1989).
- [143] O. Sinanoglu and D. R. Herrick, Chem. Phys. Lett., 31, 373 (1975).
- [144] B. J. Berne and D. Thirumalai, Ann. Rev. Phys. Chem., 37, 401 (1986).
- [145] S. R. White, J. W. Wilkins and K. G. Wilson, Phys. Rev. Lett., 56, 412 (1986).

**TRANSITION METAL CLUSTERS:
ELECTRONIC STRUCTURE AND INTERACTION
WITH HYDROGEN AND OXIDES**

D.E. Ellis, J. Guo and H.-P. Cheng

*Department of Physics and Astronomy
and Materials Research Center
Northwestern University
Evanston, IL 60208*

J.J. Low

*UOP Research Center
Des Plaines, IL 60017*

1. INTRODUCTION

The structure and reactivity of transition metal (TM) clusters is interesting both from the point of view of intermetallic bonding and from the aspect of interaction with external ligands. The internal structure and external bonding of metal clusters differ sufficiently from an isolated TM atom or the bulk metal to merit intensive experimental and theoretical attention. A great deal of research has focussed on metal clusters in both inorganic (1) and organometallic (2) chemistry. Metal clusters play an important role in enzymatic reaction centers (3) and the photographic process (4). The design of more efficient and selective

catalysts, which are often supported metal clusters, is an important part of the petroleum refining and chemical industries (5).

Here we report results for clusters of Ni and Pt. First we discuss the rearrangement of bonds during approaches of a rigid probe hydrogen molecule to a Ni_4 tetrahedron. A topological analysis of charge density in Ni_4 and Ni_4H_2 reveals changes in metal-metal bonds during the approaches. Metal clusters are often reduced by hydrogen during preparation; the present work is intended to lead to an understanding of how hydrogen affects the structure of such clusters. Next we discuss the progress we have made in using theory to interpret X-ray absorption near edge spectra (XANES) of Pt clusters. In both XANES and molecular beam experiments it is clearly helpful to use theory to provide the structural data which are not directly observable. Finally, we discuss the progress we have made in modelling H atom chemisorption on a small Pt cluster and a Pt atom adsorbed on $\gamma\text{-Al}_2\text{O}_3$. The metal-metal oxide interface has important consequences for the stability and chemistry of ceramics (6) and catalysts (5). These calculations represent important first steps in modelling metal-metal oxide interfaces. The relative simplicity of the local spin density (LSD) single-particle theory (7) allows one to construct a number of observable properties for comparison with experiment. These properties include (but are not limited to):

1. Charge and Spin Densities
2. Density of States
3. Cohesive Energies
4. Photoelectron Spectra
5. X-Ray Absorption Spectra
6. Infra-Red Vibrational Spectra
7. Effective Potentials for Dynamics

The charge and spin densities, cohesive energy and related properties follow directly from the electronic ground state in LSD theory. Spectroscopic properties such as (2), (4) and (5) depend upon an interpretation of single-particle orbital structure. The calculation of these properties involves use of transition states (8) or similar extensions of the theory. This aspect of LSD theory is still very much in a state of development, but we shall only require the most simple applications. The particular method used in the present work is the discrete-variational (DV-

X α) scheme, in which the self-consistent orbitals are expanded in a basis of numerical atomic functions. This approach, and the underlying self-consistent-field formalism has been discussed extensively in the literature (7,9-11). Here we only wish to comment on variational features with respect to

1. Orbital Expansions
2. Potential Expansions.

The degree of completeness of the orbital expansion used in Hartree-Fock (HF) and LSD calculations is the result of a compromise between available computer resources and the size of the problem. For convenience, we choose the number of variationally treated electrons, N as a measure of problem size. The number of two-electron integrals increases as N^4 for HF, and the number of Hamiltonian matrix elements increases as N^2 for LSD. Since for an efficient basis set one expects to employ more than twice as many functions as electrons for an expansion of acceptable quality, it is easy to see why most work has been done on diatomics and very small clusters.

The use of "frozen-core" approximations and effective core potentials reduces the variational space to manageable dimensions. However, a great part of the "art" of variational calculations remains in the process of basis selection, sometimes called basis optimization. The DV-X α scheme accomplishes the basis optimization through an iteration procedure. The effective atomic configuration as measured by Mulliken orbital populations, is used to generate new atomic orbitals until internal consistency is obtained (10). One can obtain additional degrees of freedom by placing the atom in a potential well to increase the number of bound states. Alternatively, as in the Linear Muffin Tin Orbital (LMTO) and Scattered Wave methods, the spherically averaged self-consistent-field (SCF) potential can be used to generate radial functions centered at nuclear sites. We match the SCF potential to a harmonic potential at a convenient radius R_v so that for $r_v > R_v$, the radial functions are rapidly decaying harmonic oscillator solutions in our implementation (12).

The quality of the potential expansion in general is as important as the choice of exchange-correlation potential, and often more so. The so-called Self-Consistent-Charge (SCC) scheme employed in many DV-X α applications uses a Mulliken atomic orbital analysis of the SCF eigenvectors to produce an overlapping spherical atom approximation to density and Coulomb potential.

The simple SCC potential retains an interpretation of the molecular potential in terms of contributing atomic configurations. This potential is sufficiently accurate for many purposes. We employ the Self-Consistent-Multipolar (SCM) approximation based on a least squares fit to the density, when greater accuracy is required; e.g., in describing energetics of covalent bonding (11). This approximation allows the number of radial and angular degrees of freedom at each nuclear site to increase until the desired degree of precision is attained. This increased precision leads to increased computation time. In the TM cluster calculations presented below the SCC potential was used, with the simple Kohn-Sham-Slater exchange potential (scaling constant $\alpha = 0.7$). Charge and spin density maps show that nonspherical terms play a very small role (see below) in the structure of clusters like Ni_4 or Pt_{13} . Description of an incoming molecule interacting with the cluster is more problematical. We shall continue to use the SCC potential in data presented here for H_2Ni_4 and $\text{Pt:Al}_2\text{O}_3$ for the sake of simplicity. However, the omitted multipolar terms in the potential may have important consequences.

2. Ni_4 AND H_2Ni_4

2.1. Ni_4

We have previously studied several planar Ni_n ($n=2,3,4,7$) clusters with surface simulation in mind(12). In this paper we concentrate on the Ni_4 cluster of T_d symmetry and its interaction with a probe H_2 molecule. As in Ref. 12, we find that basis iteration within the SCC approximation can increase the cohesive energy appreciably. Using the optimized basis functions from Ref. 12, we find the binding energy per atom of 2.0 eV at the equilibrium Ni-Ni bond length $R_e = 4.36$ a.u. for the Ni_4 (T_d) cluster, which is more stable than the planar Ni_4 (D_{4h}) cluster presented in Ref. 12. These values can be compared with the experimental bulk cohesive energy of 4.44 eV/atom and bond length 4.71 a.u. and the dimer binding energy of 1.0 eV/atom(13). Here we simply note that HF yields planar Ni_4 more stable than tetrahedral, with binding energies typically

30% of our LD values(14). The cluster is ferromagnetic with a moment of $0.50 \mu_B/\text{atom}$. The SCC analysis yields an effective atomic charge (spin) configuration $3d^{8.93(0.59)}4s^{0.85(-0.06)}4p^{0.22(-0.03)}$, which can be compared with the HF values $3d^{8.88}4s^{0.93}4p^{0.19}$.

The $3d4s4p$ partial spin density of states at the equilibrium point are plotted in Fig. 1. We see that the center of the majority $3d$ spin states of all atoms lies about 1.6 eV below the Fermi level; the d -bands have width of 3 eV. The $3d$ exchange splitting is ~ 0.4 eV. The lowest $4s$ states begin 4 to 6 eV below the Fermi level, and have about 0.4 eV exchange splittings. The splitting of $4p$ states is less than 0.1 eV.

The topological charge density analysis of Bader et al.(15) can give some further understanding of the Ni_4 bonding. Although well established as a technique of analysis for organic and light atom molecules, little has been known heretofore about topological atom(TA) properties of transition metal clusters.

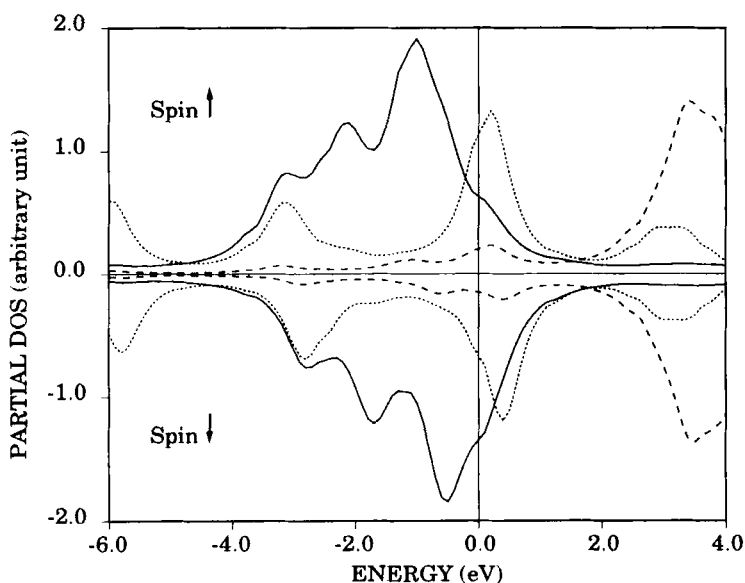


Figure 1. Partial spin densities of states for $Ni_4(Td)$ cluster at equilibrium point. The Fermi energy of -1.55 eV is chosen as the origin of energy scale. The solid, dotted and dashed curves are for $3d$, $4s$ and $4p$ states, respectively.

Thus Bader and MacDougall have developed quantitative correlations between chemical bond properties of molecules like CH_4 , CH_3F and CH_3Li and characteristics of the critical points(16). They have further emphasized the importance of $\nabla^2\rho$ as an indicator of local compression or expansion of electronic density and its relevance for predicting the initial directions of complex formation. Wiberg et al. extended this analysis to a large series of hydrocarbons, extracting empirical correlations to bond order and exploring TA transferability(17).

Since bonding mechanisms of TM clusters are very much open to discussion, even "pretty pictures" resulting from TA analyses are indeed helpful to provide a perspective on these systems. We shall see that more work is needed to make the TA analysis more satisfactory; what we have done here is to uncover and discuss this problem.

We use the following terms in this analysis:

1. A topological atom (TA) is a subsystem bounded by surfaces with surface normal \hat{n} satisfying

$$\hat{n} \cdot \nabla\rho = 0. \quad (1)$$

where ρ is the charge density. Bader has shown that TAs separately satisfy a Virial Theorem on their contribution to the total energy(15).

2. Critical points (CP) satisfy the condition $\nabla\rho = 0$. We characterize CPs by the indices (a,b). Here \underline{a} is the number of nonzero curvatures at the CP and \underline{b} is the sum of their signs.
3. A bond path or atomic interaction line is a line defined by two and only two gradient paths that originate at a (3,-1) CP each of which terminates at a neighboring (3,-3) CP (usually at a nucleus). A bond path(BP) connects atoms sharing a common surface.
4. The asymmetry of the charge distribution in a plane perpendicular to the bond path may be appreciated considering the ratio $\eta=\lambda_1/\lambda_2-1$ of the two negative curvatures ($\lambda_1<\lambda_2<0$) of ρ at the (3,-1) CP. The η quantity, called ellipticity of the bond, gives a measure of the deviation of the charge distribution from cylindrical symmetry.

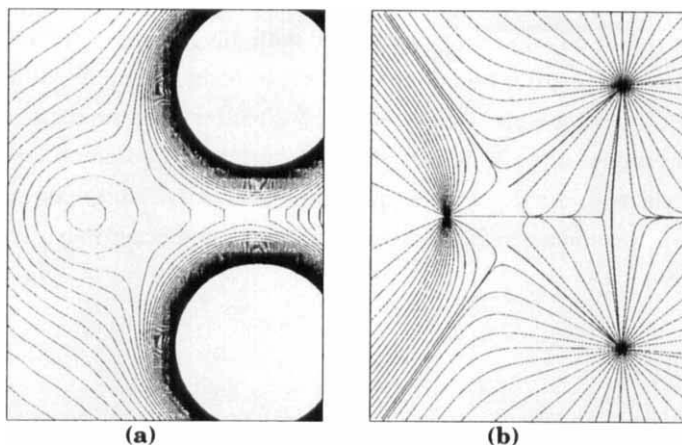


Figure 2. Charge density contours (a) and density gradient field (b) for tetrahedral Ni_4 cluster. Symmetry plane contains two atoms and bisects a perpendicular Ni-Ni bond. Contour interval is 0.002 a.u.

Figure 2 contains a ρ contour map and a $\nabla\rho$ map for Ni_4 in a symmetry plane containing two atoms, at the nearest neighbor distance of 4.68 a.u. This cluster serves as a reference for the following study of its interaction with a probe H_2 molecule. From Fig. 2, one can see the buildup of charge along the Ni-Ni interatomic axis, and a transverse cut through an equivalent bond between atoms above and below the plane in the conventional map. A curved bond path appears in the $\nabla\rho$ map (we shall loosely call this construction a "bond" in the following) connecting the pair of atoms lying in the plane. There are six such equivalent bonds in tetrahedral Ni_4 . Topological analysis of the charge density for Li and Na clusters has suggested the presence of non-nuclear attractors (19). However, the three dimensional tetrahedral Ni_4 cluster displays no such remarkable features. Bearing in mind that the gradient field of an isolated atom is radial and extends to infinity, we can see also distortions suffered by the atom in forming the cluster. The transverse cut containing a (3,-1) CP at the middle of a bond forms part of the interatomic surface. In addition to the (3,-1) bond CP, we find a (3,+3) nonbonding CP at the center of the cluster, and four equivalent (3,+1) nonbonding CP near the cluster faces. Thus, while the total density can be modelled well by a superposition of spherical "pseudo-atoms" or "proto-atoms", the topological atoms of a TM cluster are far from spherical. Although this

theory can define the presence or absence of a bond path, it does not satisfactorily define a bond energy associated with this feature. After examining density maps for numerous transition metal clusters, including Ni_n $2 \leq n \leq 7$ (12) and Pt_n $2 \leq n \leq 7$ (present work) among others, one realizes that the classical nearly free electron model of bulk metals with a spherical d^m core and uniform sp conduction electron density applies quite well in the description of even very small clusters. Of course, in exterior regions the density decays in typical atomic fashion.

2.2. H_2Ni_4

We explored "covalent" interactions of Ni_4 by bringing a rigid H_2 probe molecule "end-on" into a tetrahedral face of Ni_4 . This geometry corresponds to the three-fold "pocket" site on a $\text{Ni}(111)$ surface. The corresponding "bridge" and "atop" sites were studied as well, but we will focus mostly on the pocket site here. The chemisorption of C_2H_2 on a $\text{Ni}(111)$ surface using an embedded Ni_3 cluster has been previously presented(12). In this paper, both Ni-Ni and H-H distances are kept at 4.68 a.u. and 1.75 a.u., respectively. These values are chosen with modelling adsorption of H_2 on $\text{Ni}(111)$ surface in mind, but have little to do with the observed dissociation of H_2 upon Ni surfaces. We only varied the distance h of the nearest H atom from the face and wish to concentrate on the response of the charge density of the Ni_4 cluster upon the approach of the rigid probe H_2 molecule, which is modeled by a minimal 1s numerical basis.

This highly restricted face approach path results in a local minimum in energy at $h = 0$, with one H atom in the face. This geometry is more than 1 eV "uphill" from the separated fragments. It is interesting to see, and possibly important to understand how bond paths form and break as the cluster-ligand fragments are assembled. Figures 3 and 4 provide two snapshots of ρ , $\nabla\rho$ structure and BP evolution along the threefold chemisorption path.

Figure 3 displays ρ and $\nabla\rho$ maps for H_2Ni_4 in the same orientation as given previously, with $h = 2.5$ a.u. While most features of the H_2 and Ni_4 fragments at $h \gg 1$ appear clearly, the buildup of overlap charge between H1 and the nearest Ni is also visible, and an H1-Ni bond path has formed. Some encroachment of the H1 region onto the transverse Ni-Ni bond is evident.

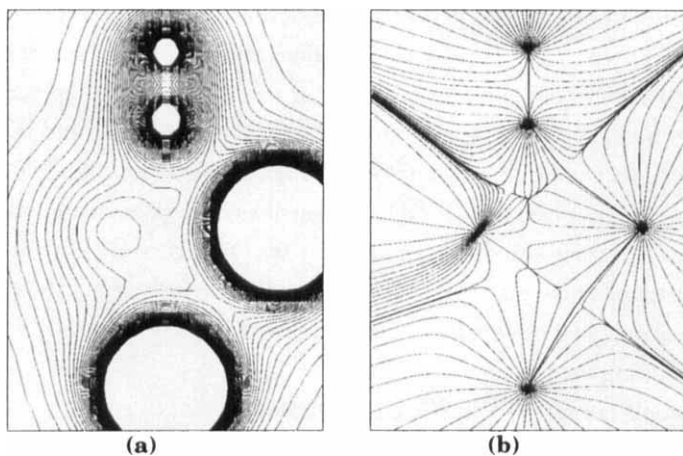


Figure 3. Density contours (a) and gradient field (b) for H_2Ni_4 : H_2 approaching tetrahedral face, with the nearest atom H1 2.48 a.u. above the face. Units and orientation as in Fig. 2.

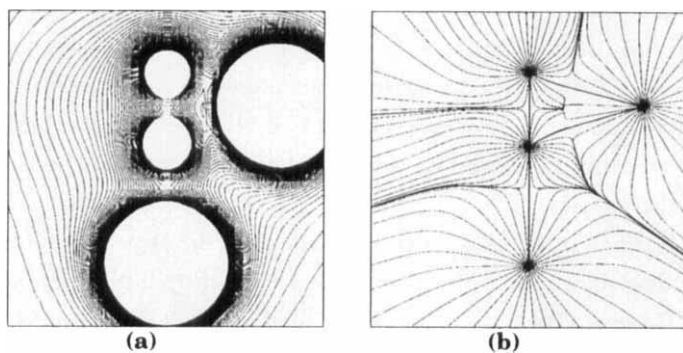


Figure 4. Density contours (a) and gradient field (b) for H_2Ni_4 : H_2 approaching a face, with H1 at the center. Units and orientation as in Fig. 2.

When H1 reaches the face ($h = 0$), three equivalent bond paths form between H1 and each of the nearby Ni atoms. In addition a bond path has formed between H1 and the remaining (apical) Ni; all Ni-Ni bond paths have disappeared. It would be very interesting to allow the system to relax to

minimum energy in this ($h = 0$) geometry and observe the reformation of Ni-Ni bonds. Finally, when H1 is pushed into the center of the cluster (Fig. 4) (repulsive by 1.5 eV) both H atoms are more or less symmetrically placed with respect to the face, and additional bond paths form between H2 and the three facial Ni atoms. As can be seen by comparing Figs. 3 and 4, considerable charge transfer $\text{Ni} \rightarrow \text{H}$ takes place and Ni-Ni bond densities have been disrupted.

The bridge-bonding site of C_{2v} symmetry was treated similarly with H-H and Ni-Ni distances held fixed. For the "end-on" approach of H_2 the binding energy curve is everywhere repulsive, and there exist three types of Ni-Ni BP:

1. 1-2, forming the bridge
2. 3-4, atoms not involved in the edge attacked by H_2
3. 1-3, 1-4, 2-3, 2-4, each involving one atom of the bridge.

For an H-bridge distance of 1.2 a.u., BP 1-2 has been broken while BP 3-4 is essentially unaltered. There have formed BP H-1 and H-2 between the hydrogen and nearest neighbor Ni atoms. When H1 reaches the middle of the bridge, the BP structure has not changed but the density and curvature associated with H-1 and H-2 have strongly increased. When H1 reaches the center and H2 is approximately in the middle of the bridge, all Ni-Ni BP are broken and the repulsive energy is 9.4 eV. The strong repulsion found for this geometry and the absence of BP formation between H1 and two Ni atoms on the bridge are remarkable, since this path could be considered a precursor to an H-absorbed + H-bridge bonded species.

The atop-bonding path of C_{3v} symmetry lies along the same (111) line as the pocket-bonding path, this time directly approaching a Ni vertex of the tetrahedron. There is a local minimum in the binding energy of -0.9 eV relative to infinite separation, at a distance $R(\text{H-Ni}) = 3.5$ a.u. The Ni-Ni BP are of two types:

1. 1-2, 1-3, 1-4, connecting the apical Ni with basal plane atoms
2. 2-3, 2-4, 3-4, among basal plane atoms.

An H-Ni BP forms very easily even for $R \geq 5.9$ a.u. and remains the sole H-Ni topological feature throughout the approach, even to very short distances. The Ni-Ni BP structure remains stable, although CP quantitative values change considerably (see Table I) as charge is transferred onto H and into the H-Ni bond region.

Table I. The values of charge density, Laplacian and ellipticity at the (3,-1) CP of Ni-Ni and Ni-H and H-H bond for the approach of a rigid H₂ to a Ni₄ tetrahedron. All values are in atomic units; negative binding energies (BE) indicate repulsion with respect to energy at infinite separation of H₂ and Ni₄ molecules ($h \gg 1$).

Cases	H-H			Ni-Ni			Ni-H		
	ρ	$\nabla^2\rho$	η	ρ	$\nabla^2\rho$	η	ρ	$\nabla^2\rho$	η
Large Separation $h \gg 1$	0.122	-0.291	0.00	0.049	0.095	0.15			
Face Approach ^a									
(1)	0.127	-0.249	0.00	0.051	0.087	0.23	0.048	0.086	0.23
				0.051	0.087	0.14			
(2)	0.140	-0.072	0.00				0.134	0.355	0.03
							0.055	0.129	0.00
(3)	0.151	-0.021	0.00				0.117	0.325	0.54
							0.114	0.355	0.89
							0.115	0.268	0.00
Bridge Approach ^b									
(1)	0.132	-0.161	0.05	0.051	0.089	0.23	0.136	0.326	0.03
				0.051	0.084	0.11			
(2)	0.153	-0.084	0.26	0.050	0.102	2.17	0.206	0.440	0.04
				0.051	0.086	0.03	0.050	0.104	11.50
(3)	0.160	0.025	0.29				0.207	0.413	0.06
							0.113	0.275	0.02
Atop Approach ^c									
(1)	0.121	-0.289	0.00	0.050	0.088	0.21	0.004	0.008	0.00
				0.050	0.087	0.21			
(2)	0.125	-0.260	0.00	0.049	0.091	0.22	0.085	0.174	0.00
				0.050	0.086	0.21			
(3)	0.138	-0.187	0.00	0.048	0.094	0.35	0.447	-1.98	0.00
				0.051	0.084	0.24			

(a) For face approach: (1) H1 is 2.48 above the face with BE of -0.6 eV; (2) H1 on the face with BE of -1.0 eV; (3) H1 is 0.95 below (on the center) with BE of -1.4 eV.

(b) For bridge approach: (1) H1 is 1.2 a.u. above the edge with BE of -1.3 eV; (2) H1 is on the edge with BE of -2.6 eV; (3) H1 is 1.66 a.u. below (on the center) with BE of -9.4 eV.

(c) For atop approach: (1) H1 is 5.90 above the vertex with BE of -1.3 eV; (2) H1 is 2.90 above with BE of -1.0 eV; (3) H1 is 1.70 above with BE of -8.4 eV.

In the cases where there exist more than one different Ni-Ni and/or Ni-H bond, they are listed in the order of distance from the most distant H atom (H2).

Table II. The values of charge density and Laplacian at the (3,+1) and (3,+3) CP of the Ni tetrahedron. Same conventions as Table I.

Systems	(3,+3)CP		(3,+1)CP	
	ρ	$\nabla^2\rho$	ρ	$\nabla^2\rho$
Free Ni ₄	0.043	0.039	0.043	0.060
Face (1)	0.045	0.034	0.045	0.042
Bridge (1)	0.044	0.037	0.045	0.044
Atop (1)	0.044	0.035	0.044	0.045
Atop (2)	0.044	0.034	0.044	0.042
Atop (3)	0.044	0.032	0.045	0.038

Numerical data given in Table I show charge density, Laplacian and bond ellipticity at all the (3,-1) critical points in nine configurations studied along with the configuration with infinite separation of the two rigid H₂ and Ni₄. Although these values do not correlate directly with any experiment, perhaps like Mulliken populations, their variation with geometry and composition may be of interpretative value. These parameters have been previously correlated with bond strength, site of chemical activity, and directionality of the chemical bond⁽¹⁵⁻¹⁷⁾ and thus may be of interest for future comparisons.

From Table I, we see that charge density ρ and $\nabla^2\rho$ at H-H (3,-1) CP increase as the H₂ approach and enter the Ni₄ cluster in all three configurations. The value of $\nabla^2\rho$ even changes sign at case (3) of the edge approach. The increase in $\nabla^2\rho$ is due to the depletion of ρ along the H-H bond path. The charge distribution on the cross section of H-H bond has cylindrical symmetry except in the edge approach as measured by the ellipticity η .

The ρ and $\nabla^2\rho$ at Ni-Ni (3,-1) CPs changes within the range of $\pm 5\%$ and $\pm 10\%$, respectively. The change in η is most remarkable at case (2) of the edge approach. The values at Ni-H (3,-1) CPs vary over a wide range because of the variation in the H-Ni bond length. We note that $\nabla^2\rho$ changes sign at case (3) of the vertex approach; and two anormal cases of sign change in $\nabla^2\rho$ are much

more repulsive in energy than the remaining cases. Further study in the correlation of these values and kinetic energy density with the binding energy of the system will be presented elsewhere (18).

In addition to the (3,-1) bond CP already discussed, the (3,+3) and (3,+1) nonbonding CPs, which are present in the free Ni_4 cluster, disappear at the two distances (2) and (3) listed in Table I for both the face and edge approaches. They are presented in the remaining five geometries listed in Table I. Parameters of these additional CPs are given in Table II. We see that upon the H_2 approach ρ increases by ~ 0.002 a.u. and $\nabla^2\rho$ decreases at the (3,+3) and (3,+1) CPs.

In all the H_2Ni_4 configurations investigated, with H-Ni distance ≤ 6 a.u., we found that the Ni magnetic moment totally disappeared due to the interaction with the H atoms. This quenching of TM magnetism by chemisorbed atoms and molecules has been found in many previous calculations.

2.3. Toward a Bond Energy

In order to gain a better and more quantitative understanding of the processes of bond formation and disruption it is desirable to carry out a volume-partitioned analysis of contributions to the cohesive energy. Within the TA formalism, the expression

$$(\hbar^2/4m) \nabla^2\rho(r) = 2G(r) + V(r) \quad (2)$$

is used to link the Laplacian to a kinetic energy density G and a potential energy density V . Using independently calculated $G(r)$, for example, from HF orbitals, the energy $E(\Omega)$ associated with topological atoms has been determined (15-17). Orbital-by-orbital analysis of binding energy contributions offers another valuable technique, which has been exploited within HF and LD theory(20-21). Within LSD theory it is straightforward to devise an energy density function $\rho_E(r)$ whose integral yields the total energy. In turn, the cohesive energy can be partitioned into arbitrary volumes $\{\Omega_i\}$ satisfying

$$E_{\text{coh}} = \sum_i \int_{\Omega_i} \rho_{\text{coh}}(r) d^3r. \quad (3)$$

This approach has been used to describe defect structures in TM oxides (22), and will be equally applicable in the present case. A major unanswered question is: which volume partitioning will give the best insights? On one hand we have the possibility of using the topological atoms to define $\{\Omega_i\}$; on the other hand we may prefer the idea of nearly spherical pseudo-atoms connected by bond-regions. Some further numerical experiments on the Ni-H system have been undertaken to explore different partitionings. It will clearly be necessary to examine a larger portion of the interacting fragment potential surface before drawing conclusions about the relative strength of TM-TM and TM-H bonds, the effective TM valency versus cluster geometry, and related questions. Nevertheless, we believe the LSD results obtained to date help to illuminate this problem area and point the way for highly specific bonding studies by Generalized Valence Bond and other more rigorous methods which are too time- consuming to be used for surveys.

3. PLATINUM CLUSTERS

Since platinum in catalysts is typically in the form of small metal clusters on a metal oxide support a better understanding of its electronic structure when in contact with reactants and the support is vital to obtain improved performance and to develop less costly alternatives. Therefore, we have embarked on a effort to model Pt clusters supported on $\gamma\text{-Al}_2\text{O}_3$. This effort has thus far involved calculations on naked Pt clusters, H atoms on Pt_4 and Pt atoms chemisorbed on $\gamma\text{-Al}_2\text{O}_3$. These calculations have been used to model the relative energetics of isomers of several Pt clusters and their X-ray Absorption Near Edge Spectra.

3.1. Naked Clusters and XANES

At first sight one would suppose that Pt, with its $5d^9 6s^1$ ground configuration, requires a full relativistic treatment. Indeed there are indications, particularly for the dimer, that relativistic effects on the electronic structure are of great importance in determining bond lengths and cohesive energies. However, there are also many cases, including neighboring ($5d^{10} 6s^1$) Au_6 complexes (23) and even actinide compounds(24) where relativistic effects are

of a distinctly secondary nature relative to general features of the electronic density and level structure.

We used the moment-polarized Dirac-Slater fully relativistic scheme (25) to explore some aspects of the level structure and charge density of Pt_n , $n = 2, 3, 4$. Aside from the expected contraction in R_e and increase ($>100\%$!) in cohesive energy for Pt_2 , we also observe a decrease in 5d occupancy with accompanying increase in 6s occupation. Single particle properties of small Pt clusters and Pt-ligand complexes have been discussed in the relativistic multiple-scattering LD model by Yang(26). The indirect shielding effects which modify the s-d balance in the valence shell in comparison with nonrelativistic theory can have consequences for the interaction with ligands, which need to be explored in detail.

Here we wish to discuss briefly nonrelativistic studies on Pt_n , $n = 2, 4$ (T_d), 9 (bcc structure), 13 (fcc structure), 24 (core of $Pt_{24}(CO)_{22}$ (μ_2-CO) $_8^{2-}$ dianion). As in the isoelectronic Ni species, the small clusters are found to carry a magnetic moment; e.g. $0.25 \mu_B/\text{atom}$ for Pt_4 . The interaction with a ligand, such as H, rapidly quenches the magnetic moment as we also found in H_2Ni_4 . The SCC calculations give an effective atomic configuration which shows a

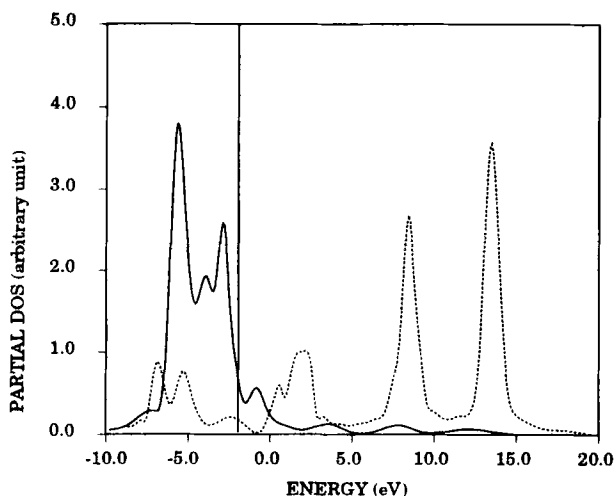


Figure 5. Partial densities of states for central atom of Pt_{13} cluster: solid curve is 5d, and dashed curve is 6sp.

declining 5d population and increasing 6sp "conduction electron" population with increasing particle size: thus $\text{Pt}_2(d^{9.87}) > \text{Pt}_3(d^{9.53}) > \text{Pt}_4(d^{9.43})$.

The central atom partial densities of states (DOS) for Pt_{13} shown in Fig. 5 reveal at a glance the s-d hybridization typical of the 5d metals. The 6sp states have a tail extending across the Fermi energy into the occupied "d-band" region; the 5d density has a corresponding tail extending above E_F . The t_{2g} - e_g crystal field splitting dominates the central atom DOS; admixture with other metal states leads to a band width of ~ 10 eV.

X-ray near edge absorption spectra (XANES) provides a powerful probe of unoccupied state structure which can be interpreted to learn much about the atomic configuration and effects of the local environment. For example, the use of synchrotron light sources and high resolution spectrometers reveal considerable differences in the Pt L_I , L_{II} and L_{III} spectra of bulk metal, small particles, and carbonyl compounds (27). If we consider the simplest single particle picture, with dipole allowed transitions dominating, the absorption cross-section appears as

$$\sigma_i(\omega, \hat{e}) \sim \omega \sum_f |\langle \Psi_f | \hat{e} \cdot \mathbf{r} | \Psi_i \rangle|^2 \delta(\epsilon_i - \epsilon_f + \hbar\omega) \quad (4)$$

Here Ψ_i is the Pt 2s (L_I), $2p_{1/2}$ (L_{II}) or $2p_{3/2}$ (L_{III}) initial state, Ψ_f are all possible final states satisfying energy conservation, and (ω, \hat{e}) are energy and polarization of the photon respectively (28). With localized core levels as initial states, selection rules allow one to determine various details; such as:

1. Pre-edge features result from bound \rightarrow bound transitions to a subset of available states. Such lines are typically narrow and sensitive to covalent mixing with neighboring atoms.
2. The intense main peak near the continuum onset ("white line") can be identified; e.g., $L_{III} 2p_{3/2} \rightarrow 5d$ (partially empty). The area can be correlated with the occupancy of the band, and the width depends upon interaction with neighbors.
3. Modulation of cross-section above the edge is due to back scattering of the outgoing photoelectrons from neighboring potentials. This structure results from both single and multiple-scattering events which are very

structure sensitive (29-41) merging eventually with the higher energy EXAFS region.

We show synthesized data for Pt_n $n = 2, 4, 9, 13, 24$ using the Multiple Scattering (MS- $X\alpha$) method to generate the continuum final states in Fig. 6. One can see the structure sensitivity of XANES in this data. The free Pt atom cross-section, as shown, consists of transitions into the 5d hole state, followed by a step and nearly featureless structure. We show only bound \rightarrow continuum transitions in the cluster data presented. We used the same potential (from the central atom of Pt_{13}) for every scattering site to ensure that only effects of geometrical structure are seen. The XANES from only a single atom of each cluster are presented. When the data are superimposed on the atomic absorption one really sees a modulation of the cross-section which preserves the total area.

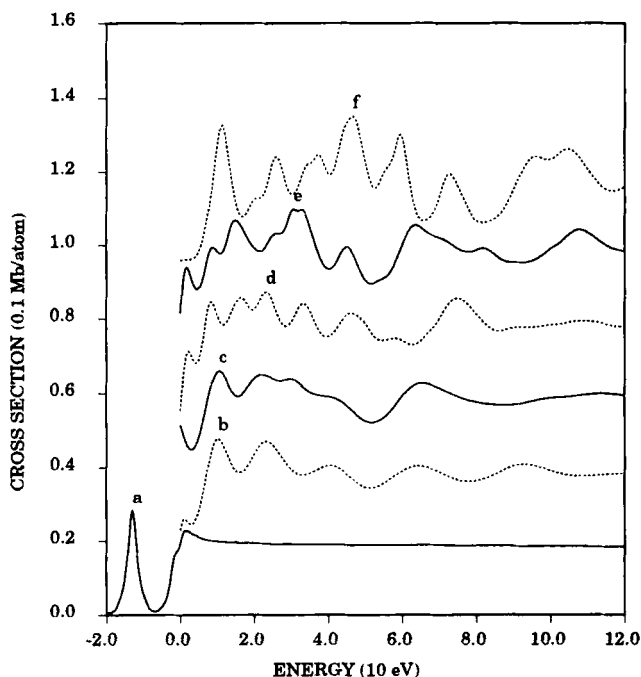


Figure 6. Pt L_{III} -edge absorption cross-section for (a) atom, (b) Pt_2 , (c) $Pt_4(T_d)$, (d) $Pt_9(O_h)$, (e) $Pt_{13}(O_h)$, (f) $Pt_{24}(C_{2v})$. Bound-bound transitions shown only for the atom. Identical scattering potentials used in (b-e) to emphasize modulation due to geometrical structure. Curves are offset by 0.2 Mb for easy viewing.

The metal-metal oxide interface contains several inequivalent metal sites which contribute simultaneously to the experimental XANES. Resolving the signatures of different sites involves subtracting of a reference background and fitting theory and experiment by a common parametrization scheme. Details of this approach and applications to metal oxide compounds have been presented elsewhere(32). A model which can resolve and analyze XANES to the limits set by experimental resolution requires the detailed analysis of Pt-based model systems such as PtO, PtCl₄ and HPt_n to establish their characteristic XANES features.

3.2. Interatomic Potentials

It is possible to prepare mass-separated Pt_n fluxes with modern molecular beam techniques and to examine their interactions with gas phase species or on surfaces (42). However, it is difficult to determine the geometric configuration of these particles, since the mass flux is presently too weak for diffraction measurements. Investigation of significant portions of the interatomic potential energy surface by purely quantum mechanical methods (including LSD) becomes prohibitively slow and costly for clusters containing more than 5 atoms. Semiempirical approaches and classical dynamical methods using potentials consistent with both experiment and available quantum data offer attractive possibilities for generating plausible geometries for metal clusters and cluster-ligand systems.

We have been considering methods for generating approximate cohesive energy expansions of the form(43)

$$E_{\text{coh}} = \sum_i E_i^{(1)} + \sum_{i<j} E_{ij}^{(2)} + \sum_{i<j<k} E_{ijk}^{(3)} + \dots \quad (5)$$

with 1-, 2-, 3-body contributions determined by fitting to LSD theoretical data. A reasonable starting point is to generate a fit to a reference system such as Pt₂, and to use the resulting two-body potential $E_{ij}^{(2)}$ as a starting point for analysis of Pt_n, $n > 2$. One can equally well start from the equilateral triangle Pt₃ or the tetrahedral Pt₄, and in fact a survey of various geometries of Pt_n shows that the

optimized 2-body potential from Pt_4 is superior in the sense that

$$|\Delta E| = |E_{\text{coh}} - \sum E_{ij}^{(2)}| \quad (6)$$

has reasonably small values for all clusters studied. By comparing $E_{ij}^{(2)}$ for $n = 2, 3, 4$ one can see how "many-body" effects lead to an evolution in the effective pair potential with increasing particle size. It would be very desirable to extend this comparison to $n = 6, 9, 13, 19$ to observe the approach to bulk values.

The most traditional approach to treating the "correction" energy ΔE would be to ignore the 1-body terms $E_i^{(1)}$ and to attempt a fit to $E_{ijk}^{(3)}$ and possibly higher order interactions, in terms of interparticle co-ordinates.(44) This is quite feasible for a small particle; for example in the isosceles triangle Pt_3 with $E^{(2)}$ optimized to $n = 3$, ΔE is a simple repulsive curve for $r < R_e$ and essentially zero for $r > R_e$. Again, for the square geometry of Pt_4 with $E^{(2)}$ optimized to $n = 4$, ΔE is a monotonic curve showing attraction for $r < R_e$ and weak repulsion at larger distances. While any particular case can be rather easily parameterized, there does not emerge any obvious generalization which can be carried forward into more complex deformations and large cluster sizes(45).

The idea of an average molecular-field approach is exploited in the semiempirical Embedded Atom Method (EAM)(46). Instead of contending with the co-ordinate complexity of $E_{ijk}^{(3)}$, etc. the EAM considers the single particle energy terms $E_i^{(1)}$ as a functional of the local charge density:

$$E_{\text{coh}} \approx \sum_i F(\rho_i) + \sum_{i < j} E_{ij}^{(2)}. \quad (7)$$

Here $F(\rho_i)$ is the embedding energy of the atom at position R_i with host charge density $\rho_i = \rho_h(R_i)$. In conjunction with classical molecular dynamics (MD) calculations, the EAM has been successfully used to study bulk metals, surfaces and defect structures.

In general, the pair potential $E^{(2)}(r)$ and embedding function $F(\rho)$ have been determined (nonuniquely) by fits to experimental data. There are rarely sufficient experimental data for systems of interest, so theoretical data are needed to provide an alternative input. Jellium-model LSD theory provides a general picture of the form of $F(\rho)$, and LSD calculations on clusters can give quantitative values (45,47). The EAM-MD calculations on bulk, surface,

overlayer and defect Ni and Ni-Fe systems using similarly derived $E^{(2)}$ and F potentials give a reasonably good account of experimental properties including cohesion and lattice constant (45). Similar calculations on relative energies and conformation of free Pt_n particles are needed to determine whether the LSD-EAM-MD scheme has sufficient predictive power to be used in interpreting molecular beam data.

As a step in this direction we present in Fig.7 a binding energy curve for Pt_2 , calculated in the relativistic Dirac-Slater model. As discussed at the beginning of this section, the primary relativistic effect on the Pt atom and, as we shown in Table III, on the dimer is a transfer of electrons $d \rightarrow s$ due to the increased binding of the 6s level. since the 6s electron is spatially more extended than 5d, the Pt-Pt interaction is enhanced relative to the nonrelativistic case. The resulting increase in binding energy, from 0.8 to 5.8 eV, and decrease in equilibrium length, from 5.4 to 4.4 a.u. is striking. A detailed analysis of important contributions to the well-known relativistic bond contribution, involving for example changes in orbital kinetic energy, has been given by Snijders et al. (48) in the context of a self-consistent perturbative DV- $X\alpha$ approach. Their results for Au_2 are consistent with our present findings for Pt_2 , which were made by direct solution of the Dirac equation.

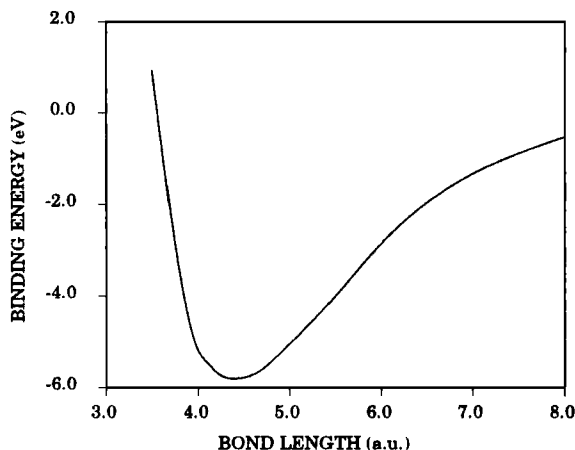


Figure 7. Binding energy curve for Pt_2 calculated in the relativistic Dirac-Slater model.

Table III. Relativistic effect on Pt_2 atomic orbital populations, at equilibrium distance.

Nonrelativistic $R_e = 5.4$ a.u.		Relativistic $R_e = 4.4$ a.u.	
5d	9.79	5d _{3/2}	3.85
		5d _{5/2}	4.76
6s	0.21	6s _{1/2}	1.13
6p	0.00	6p _{1/2}	0.09
		6p _{3/2}	0.18

In previous work, we have noted that $E_{\text{coh}}(R)$ curves for nonrelativistic models of Pt_2 , Pt_3 and Pt_4 become progressively more consistent with bulk properties. It seems likely that the Pt-Pt bonding interactions which drive the depletion of 5d states and population of 6sp states produces an atomic configuration more in harmony with the relativistic orbital structure. This prediction needs to be verified by full scale calculations.

Another point of interest concerns contributions of core orbitals to cohesion. Snijders et al. have pointed out the importance of core orbital relaxation, as part of the self-consistent iteration process – a contribution generally ignored in discussions of relativistic bonding vs. nonrelativistic models. We have observed that exclusion of 5s orbitals from the variational space results in an increase of R_e by 0.3 a.u. and a decrease in E_b by 0.8 eV. This does not indicate a 5s bonding interaction; it indicates the importance of intra-atomic relaxation mechanisms in determining molecular structure.

4. Pt-SUPPORT AND Pt-H INTERACTIONS

4.1. γ -Alumina Support

γ - Al_2O_3 has a poorly defined surface structure. Surface defects and the presence of reactive groups such as OH^- play a major role in mediating reactions on a surface containing dispersed Pt particles. The oxidation state and valency of Pt atoms constituting the particle may vary, depending upon the local environment and upon the particle-support interaction. These and other more detailed electronic structure properties have to be determined in order to understand basic reaction steps. (49,50)

A model of the γ - Al_2O_3 [110] surface was constructed using electrostatic techniques to select minimum energy configurations. The interatomic potential chosen was that of a simple electrostatic model with Al^{3+} and O^{2-} point ions. The structure utilized for detailed LSD electronic structure calculations has an open triangular network of oxygen anions in the top layer; Al cations form the second layer, with every third lattice site vacant. There are 130 ions in the periodic unit cell generated by the electrostatic energy minimization. A single Pt atom was allowed to interact with this surface (51), forming a cluster $\text{PtAl}_5\text{O}_7^+$. The remainder of the host lattice was included by Ewald summation of ionic potentials. There are at least three interesting sites for Pt occupancy on this surface:

1. Atop, directly above any oxygen.
2. Pocket, 3-fold coordination to O, with an Al directly below.
3. Empty pocket, as in (2), with empty site below.

We find in all cases studied that Pt is a charge donor, transferring a few tenths of an electron to the lattice from the 6s shell as measured by Mulliken populations. The partial densities of states (DOS) shown in Fig. 8 for the atop case reveal a 5d structure broadened to ~6 eV by interaction, primarily with the nearest-neighbor oxygen. A 6sp tail extending into the occupied states region is found, similar to the hybridization seen in Pt_n clusters. Here as in other self-consistent calculations on metal oxides, the anion is found with fewer electrons than indicated by formal valency, with net charge ~-1.6 e. It is also clear from the Al DOS that Al 3sp mixing into the "oxygen" valence band plays a significant role

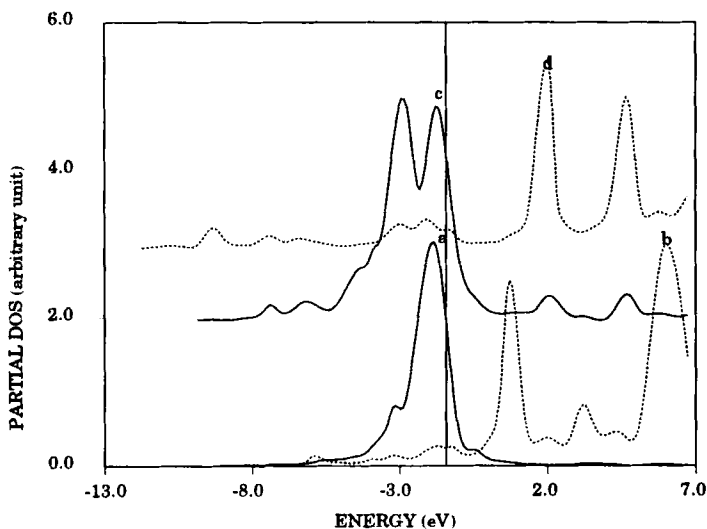
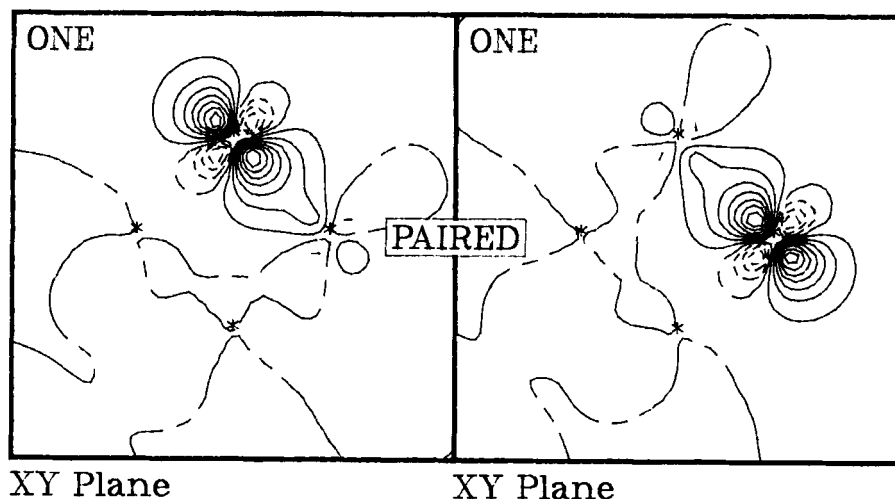


Figure 8. Partial densities of states for Pt atom on γ - Al_2O_3 : (a) Pt 5d, (b) Pt 6spd, (c) nearest neighbor O 2sp, (d) Al 3sp.

in stabilizing the lattice. Further, the presence of Al structure overlapping the Pt 5d band shows that although Pt and Al are somewhat spatially separated in this case, conditions for resonant charge transfer are satisfied.

4.2. A Valency Model for Platinum

In this section we discuss the interaction of hydrogen with Pt_4 particles, with the intention of gaining a clearer physical idea of the fundamental metal-ligand interaction. Calculations were made on the isolated Pt_4 system by the *ab initio* Generalized Valence Bond (GVB) method to develop a localized orbital picture of the ground state of the 'unperturbed' metal. A survey of the low lying states of Pt_4 revealed two different types of metal-metal bonds. The ground state forms a square with a Pt-Pt distance of 2.58 Å. The GVB orbitals in Fig. 9 show that the Pt-Pt bonds are constructed from overlapping Pt sd hybrid orbitals. The four two-electron two-center (2e-2c) bonds tie up all the unpaired electrons in the d^9s^1 ground state of four Pt atoms. This results in a closed shell singlet.

Figure 9. GVB orbitals for Pt_4 .

Pt 's d^9s^1 ground state is isolobal to methylene when a d orbital other than d_{z^2} is singly occupied. Thus, the square planar ground state of Pt_4 is isolobal to cyclobutane. Hoffmann's isolobal analogy between the bonding in organic molecules and metal clusters has led us to label the bonding in Pt_4 ground state as covalent (52). Covalent metal-metal bonds form by overlapping sd hybrids analogous to the overlapping sp hybrids in the carbon-carbon bonds of organic molecules.

A manifold of excited states appear about 10 kcal/mol above the covalent ground state. The optimum geometry of the lowest state in this manifold is a planar rhombus with Pt-Pt distances of 2.78 Å (± 0.2 Å) and Pt-Pt-Pt angles of $60^\circ(\pm 2)$. Fig. 10 shows the GVB orbitals for the metal-metal bonds in this state. These bonds consist of electrons localized on edges between atoms. Four one-electron two-center (1e-2c) bonds tie up all the s electrons in Pt_4 . The d electrons remain nonbonding in these states. Various couplings of the d^9 shells give rise to the observed manifold of excited states. The lowest state in this manifold is a singlet state with singly occupied d_{z^2} orbitals on each Pt atom oriented perpendicular to plane defined by the Pt_4 rhombus. The bonds in these excited states are similar to those observed by McAdon and Goddard in Li , Na and Ag clusters (53) and by Goodgame and Goddard in Ni_4 (54). McAdon and Goddard

have shown that this type of bonding is typical of metallic systems. Therefore we will refer to these states as metallic.

The ground state of a metal cluster predicted by an *ab initio* method depends on many factors including relativistic effects, electron correlation and the size of basis set used. We believe that the bonding in metal clusters will be represented by either covalent or metallic bonding. An example of metallic bonding can be found in $\text{Pt}_4(\text{CO})_5(\text{PMe}_2\text{Ph})_5$. Two X-ray crystal structures of the cluster complex show a bent rhombus or butterfly structure with an average Pt-Pt distances of 2.76 Å (orthorhombic) (55) and 2.735 Å (monoclinic) (56). The differences between the theoretical and experimental structures are most likely due to the influence of ligands on the cluster. An example of covalent bonding can be found in $\text{Pt}_4(\text{O}_2\text{CCH}_3)_8$. This complex is approximately square with average Pt-Pt distances of (2.495 Å) (57). The oxidation state of the Pt atoms in this complex is different than in our theoretical model. However, it does represent a case of Pt-Pt covalent bonds which have substantial amounts of d character. Therefore, it represents a valid comparison to the Pt-Pt bonds in the covalent state of Pt_4 .

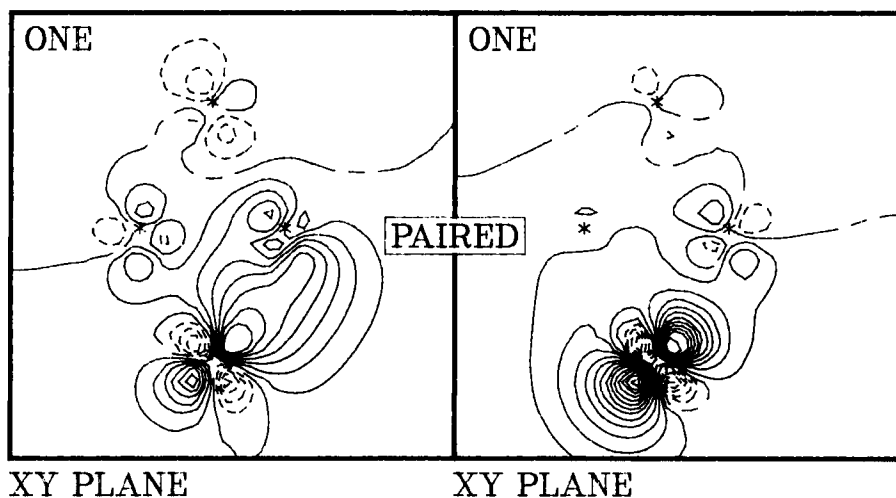


Figure 10. GVB orbitals for metal-metal bonds in Pt_4 .

We have used the relativistic effective core potential and double-zeta basis of Noel and Hay (58) which includes the contraction of the core electrons due to mass-velocity and Darwin effects. The results obtained with CAS-SCF calculations (59) in which there were 8 electrons in an active space spanned by 8 orbitals [CAS-SCF (8/8)] orbitals. This CAS-SCF (8/8) wave function will dissociate to four $^3D(s^1d^9)$ Pt atoms. The inclusion of polarization functions should improve the description of bonds involving d orbitals. Adding these functions to our basis set should favor the covalent state of Pt_4 . Therefore f functions should not change our predicted ordering of states. The electrons in the active space of the CAS-SCF correspond to the singly occupied orbitals of the $^3D(s^1d^9)$ state of four Pt atoms at the dissociated limit. The remaining valence electrons of Pt are in doubly occupied d orbitals which are left at the Hartree-Fock level. The splitting between the low lying $^3D(s^1d^9)$, $^3F(s^2d^8)$, and $^1S(d^{10})$ states change as one increases electron correlation from the HF level, HF correctly predicts a $^3D(s^1d^9)$ ground state for Pt (60). The Pt atoms in all of the low lying states of Pt_4 have predominately $^3D(s^1d^9)$ character. Thus the CAS-SCF wave function should be a qualitatively correct description of Pt_4 .

On the basis of these results we have proposed a valence model for platinum, which should be able to explain the metal:hydrogen ratios in molecular beam data. In the case of Pt_4 the four singly occupied d orbitals and four 1c-1e bonds are predicted to be able to bind up to eight hydrogen atoms. At the same time Pt is predicted to retain its d^9s^1 configuration.

As described below, we have tested our proposed Pt cluster valency model with Local Density Functional (LDF) calculations on various Pt_4H_x ($x=1,2,4,6,8$) complexes. The LDF method was chosen because of its relative efficiency and rapidity of calculation, permitting a survey of a larger number of clusters and geometries than would be possible with *ab initio* methods. We have calculated equilibrium geometries for a hydrogen atom at the 4-fold bridge, 2-fold bridge and on-top sites of the Pt_4 cluster. The 4-fold bridge site is the preferred site found for hydrogen atom chemisorption. We used geometric parameters derived from the Pt_4H studies to create geometries for isomers of Pt_4H_2 , Pt_4H_4 , Pt_4H_6 , Pt_4H_8 , and Pt_4H_{10} . Hydrogen prefers the 2-fold and 4-fold geometries over the on-top sites in these isomers. Although binding energies are typically overestimated by the LDF, the calculated geometries and relative

energetics appear to be qualitatively correct. An H to Pt ratio of higher than 2 to 1 is predicted as energetically unfavored. This ratio has been observed in molecular beam experiments by Riley (61) and predicted by our cluster valency model.

4.3. Local Density Functional Scheme

We used the discrete variational local density functional (DV- $X\alpha$) method (7-12) in this study. The single particle LD orbitals were expanded in a near minimal basis of numerical atomic orbitals (LCAO), and the potential was treated in the Self-Consistent-Charge (SCC) approximation. The SCC scheme approximates the true cluster charge density by overlapping spherical densities, to achieve rapid solution of the Poisson equation. The limited expansion bases for orbitals and potential place limits on the accuracy of the calculated binding energies, which are appropriate for preliminary surveys. We have found this approach efficient at evaluating the total energy of Pt_4H_n clusters, giving we believe sufficient relative accuracy to test the valency model.

The LDF approach treats the ground state electron density as the fundamental variable, and single particle orbitals are merely used as "computational aids" in generating the kinetic energy. Thus, it is not possible to make rigorous comparisons between *ab initio* orbitals such as those derived from GVB theory. Therefore, the localized orbital model information about bonding in metal clusters we have extracted from valence bond methods is not directly available in LDF calculations. However, we have found that a Mulliken population analysis of the DV electron densities for Pt_4 is in qualitative agreement with our valency model. The projection of the LDF density on an LCAO set is obviously arbitrary, as are all population analyses. However, the use of an LD Pt atom as the reference state here makes good physical sense.

4.4. Results For The Naked Pt_4 Cluster

Table IV contains a comparison of the electron densities from the LDF and GVB wave functions. This comparison highlights the biases of each of the methods:

1. The neglect of relativistic effects in the LDF calculations favors Pt atom configurations with larger d orbital populations. This leads to larger d orbital populations than the GVB wave function which does include core relativistic potential effects.
2. The GVB wavefunction neglects some of the electron correlation in Pt₄, and these neglected terms contain a large fraction of the cohesive energy. Thus, the GVB wave function underestimates the cohesive energy by a substantial amount.
3. Although the LDF method includes an averaged treatment of electron correlation, the approximate form of the potential leads to an overestimate of the cohesive energy.

In spite of these errors, it does appear that the geometries and relative energetics of various isomers are accurate enough to predict trends in hydrogen chemisorption on Pt clusters.

Table IV. Comparison of the GVB and LDF Wave Functions of Pt₄

Parameter	R _{Pt-Pt} Å	θ _{Pt-Pt-Pt} degrees	Mulliken Population				Binding Energy (kcal/mol)
			5p	5d	6s	6p	
LDF	2.77 ^a	90,90	6.0	9.30	0.63	0.07	46.6
Covalent GVB ^b	2.58	90,90	6.0	9.03	0.95	0.02	55.0
Metallic GVB ^{b,c}	2.79	60.4,119.6	6.0	8.88	1.18	0.14	44.1
			6.0	8.90	0.50	0.40	

^a The Pt₄ fragment's geometry was frozen at the nearest neighbor distance from bulk Pt.

^b The Pt-Pt bond distance and Pt-Pt-Pt angles were optimized.

^c Six 5p electrons are included in the Pt relativistic effective potential. Populations of two inequivalent Pt atoms are given.

Our analysis of the LDF calculations focuses on the changes in the d orbital occupation. Since the d orbital occupation decreases in the covalent to metallic excitation, we will use this parameter to follow the conversion of Pt_4 from its covalent ground state to an excited metallic state during the chemisorption of hydrogen.

4.5. Hydrogen Atom Chemisorption

We have completed geometry optimizations for hydrogen atoms chemisorbed at the 4-fold bridge, 2-fold bridge and on-top sites of a Pt_4 cluster. The geometry of each cluster is shown in Fig. 11. We froze the geometry of the Pt_4 fragment at a square planar geometry with Pt-Pt distances of 2.775 Å. Table V contains the optimized geometry parameters for these sites.

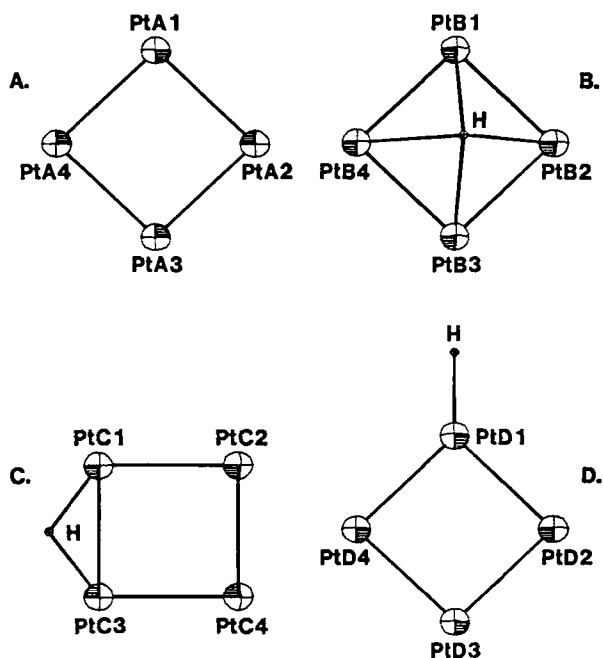


Figure 11. The geometry of the Pt_4 and Pt_4H clusters.

Table V. Optimized Binding Energy Parameters for Hydrogen Atom Chemisorbed on Pt₄

Parameter	R _e	D _e	ω
(units)	Å	(kcal/mol)	(cm ⁻¹)
on-top	1.72	80	1908
2-fold bridge	1.02	101	1768
4-fold bridge	0.72	114	1124

R_e: the equilibrium distance of the H atom from each site;

D_e: bond energy at equilibrium;

ω: the vibrational frequency derived from the curvature of the potential well at equilibrium.

Mulliken populations for each isomer are shown in Table VI. The following changes occur in the Pt populations as the coordination number of the hydrogen atom increases:

1. The d orbital occupation for atoms bonded to hydrogen increases
2. The negative charge on the hydrogen atom remains constant
3. The Pt s and p orbital occupations decrease.

It appears from these trends that the excitation required to chemisorb H on Pt₄ is localized on Pt atoms adjacent to the H atom. The constant charge on the hydrogen indicates that the cluster excitation is about the same for the whole Pt₄ fragment in each of H atom cluster complexes. However, the excitation is larger for Pt atoms involved in lower coordination sites.

Table VI. Local Density Mulliken Populations for Pt_4 and Pt_4H

Complex	Atom (see Fig.11)	Pt	Orbital Populations				H Atom
		Charge	5p	5d	6s	6p	Charge
$\text{Pt}_4\text{H}(\text{on top})$	PtD1	+0.08	5.99	9.11	0.70	0.13	-0.17
	PtD2	+0.04	6.00	9.27	0.63	0.07	
	PtD3	+0.02	6.00	9.29	0.62	0.07	
$\text{Pt}_4\text{H}(\text{2-fold})$	PtC1	+0.08	5.99	9.30	0.55	0.07	-0.16
	PtC2	-0.01	6.00	9.39	0.54	0.08	
$\text{Pt}_4\text{H}(\text{4-fold})$	PtB1	+0.04	5.99	9.40	0.50	0.07	-0.16
Pt_4	PtA1	0.0	6.00	9.30	0.63	0.07	

4.6. Hydrogen Saturation: Pt_4H_x ($x=2,4,6,8,10$)

In order to follow changes in electronic structure which occur when additional H_2 is brought to a small Pt cluster we have examined several isomers of Pt_4H_2 , Pt_4H_4 , Pt_4H_6 , and Pt_4H_{10} . The Pt-H distances were chosen to be the same as those optimized in Pt_4H . These geometries are shown in Figs. 12 and 13. Table VII contains the LDF binding energies of these structures along with Mulliken populations.

Table VIII contains the relative energetics calculated by the LDF method for Pt_4H_x isomers. We show here the energetics for each addition of H_2 . Addition of H_2 to Pt_4 , Pt_4H_2 and Pt_4H_4 is downhill energetically, while addition of H_2 to Pt_4H_8 is uphill. These energetics are both consistent with our valency model and the results of Riley's molecular beam experiments.

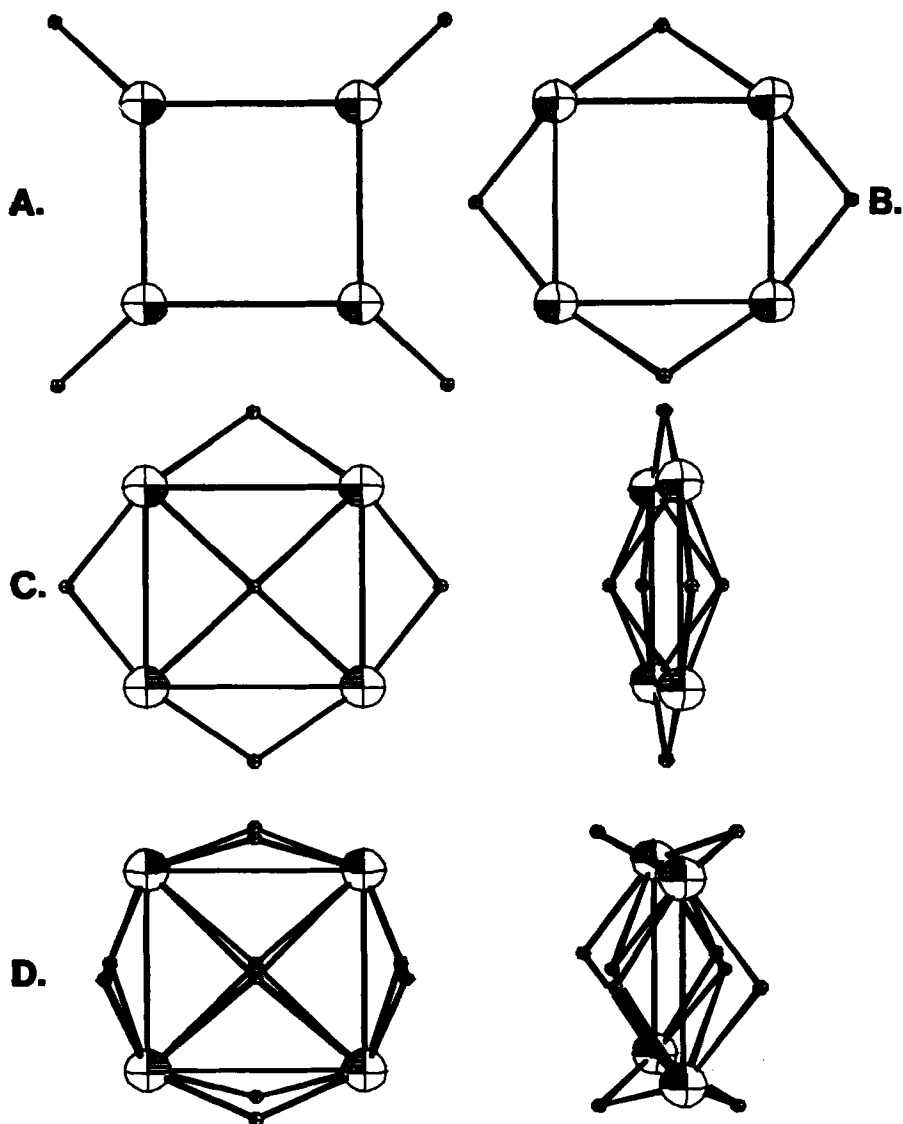


Figure 12. The geometry of the Pt_4H_x ($x=4,6,10$) clusters.

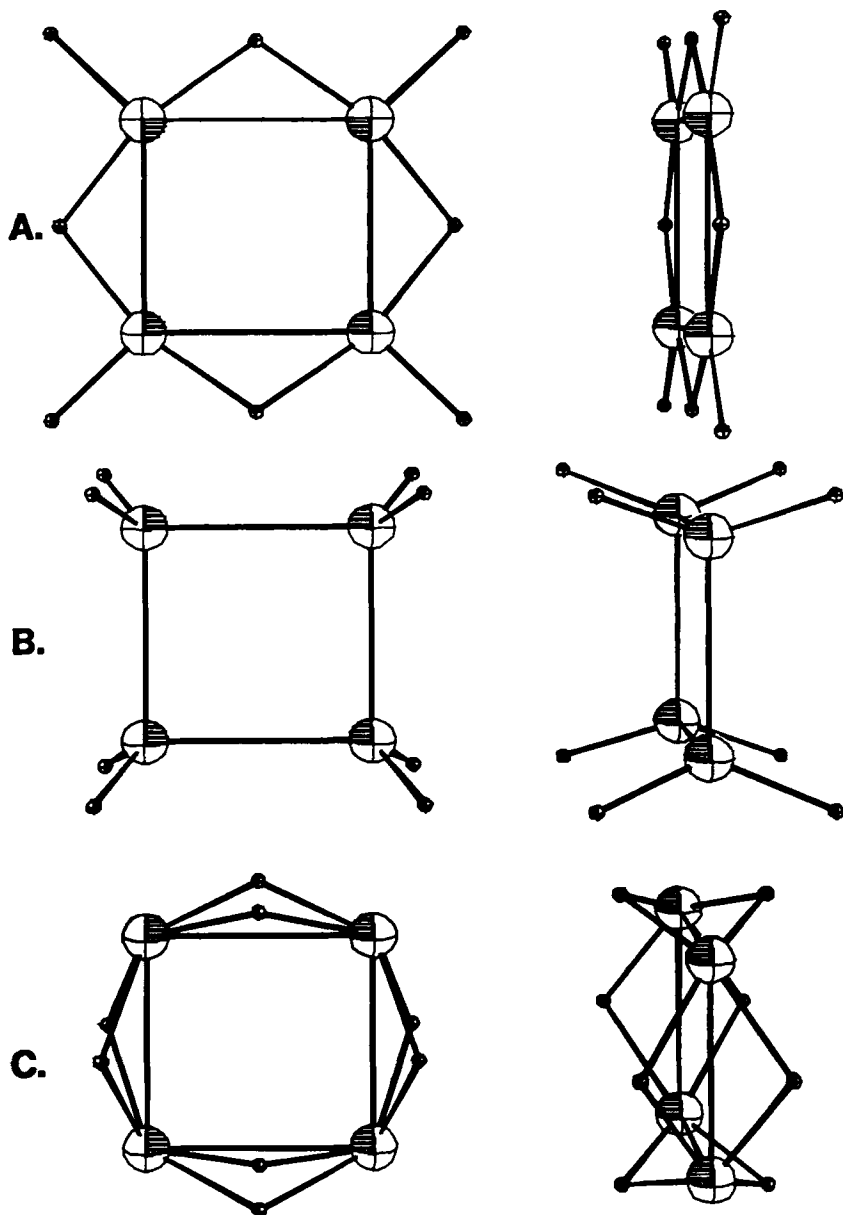


Figure 13. The geometry of the Pt_4H_8 clusters.

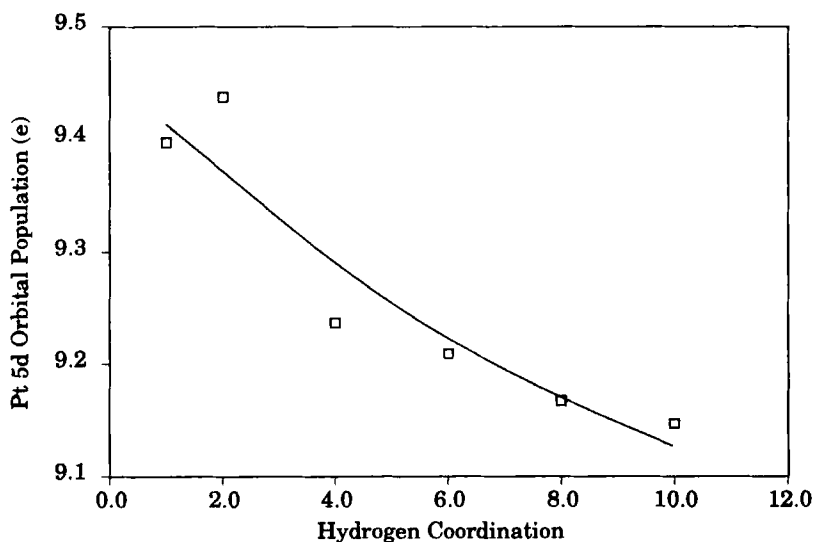
Table VII. Mulliken Populations and Binding Energies in Pt_4H_x Complexes

Complex	Pt	Pt Orbital Pop.				H Atom Binding Energy	
	Charge	5p	5d	6s	6p	Charge	Hartrees
<hr/>							
Pt₄H₂							
2-fold site see figure 12b	0.08	5.99	9.37	0.48	0.07	-0.17	1.0215
4-fold site see figure 12c	0.07	5.99	9.44	0.43	0.07	-0.13	1.0300
Pt₄H₄							
1-fold site see figure 12a	0.11	5.99	9.13	0.64	0.12	-0.11	1.1127
2-fold site see figure 12b	0.23	5.98	9.24	0.45	0.07	-0.23	1.2832
Pt₄H₆							
four 2-fold and two 4-fold sites see figure 12c	0.38	5.98	9.21	0.37	0.06	-0.32 ^a -0.12 ^b	1.5170
Pt₄H₈							
1-fold site see figure 13b	0.22	5.98	9.02	0.61	0.17	-0.11	1.6052
planar isomer see figure 13a	0.36	5.98	9.10	0.52	0.05	-0.30 ^a -0.07 ^c	1.6820
2-fold site see figure 13c	0.46	5.97	9.17	0.30	0.11	-0.23	1.7290
Pt₄H₁₀							
eight 2-fold and two 4-fold sites see figure 13e	0.52	5.96	9.15	0.24	0.12	0.05 ^a -0.28 ^b	1.9002

a) charge at 2-fold site; b) charge at 4-fold site; c) charge at 1 fold site.

Table VIII. Relative Energetics of Pt_4H_x Complexes

Species	Binding Energies (Hartrees)	Relative Energetics (kcal/mol)
$\text{Pt}_4 + 5\text{H}_2$	1.6709	0.0
$\text{Pt}_4\text{H}_2 + 4\text{H}_2$	1.7730	-64.0
$\text{Pt}_4\text{H}_4 + 3\text{H}_2$	1.8404	-106.3
$\text{Pt}_4\text{H}_6 + 2\text{H}_2$	1.8885	-136.5
$\text{Pt}_4\text{H}_8 + \text{H}_2$	2.1005	-269.5
Pt_4H_{10}	1.9002	-143.9

Figure 14. The average Mulliken Pt 5d orbital population versus H coordination in Pt_4H_x .

We find that in the isomers studied thus far the 2-fold and 4-fold bridge sites are favored over the on-top site. The valency model predicts that Pt_4 will convert from a covalent state to a metallic state with a lower d orbital population during chemisorption of H_2 . In Fig. 14 we show the average Mulliken d orbital population versus H coordination. The d orbital occupations for the lowest energy structures of Pt_4H , Pt_4H_4 , Pt_4H_6 and Pt_4H_8 (9.40, 9.24, 9.21 and 9.17 electrons, respectively) decrease with increasing numbers of chemisorbed hydrogen. The valency model predicts that the Pt atoms are never promoted from d^9s^1 to d^8s^2 . The d occupations in these complexes, predicted by the LDF method, never drop below 9 electrons. Thus a qualitative analysis of the electron densities for LDF calculations on Pt_4H_n is consistent with our Pt cluster valency model. However the addition of a single hydrogen atom at the 4-fold site of the Pt_4 cluster actually increased the d orbital populations by 0.1 electrons. Although this result is inconsistent with our valency model, Mulliken populations depend upon basis set and cannot be used in any rigorous quantitative sense. A more valid analysis would involve relaxing the geometry of the Pt_4 fragment in these complexes. Since the Pt-Pt bond distances in the metallic state are predicted to be somewhat greater, verification of elongation of Pt-Pt bonds in Pt_4H_n would tend to confirm our valency model. Such relaxation calculations are beyond the scope of the present work, but should be undertaken as a next step in modelling the chemisorption on Pt clusters.

5. CONCLUSION

The self-consistent local spin density theory has been used to explore several aspects of transition metal clusters. The electronic structure and geometry of Ni_n and Pt_n free particles calculated by LSD methods provides at least a reasonable starting point for more intensive and specifically correlated wavefunction approaches. We have tried to emphasize that a continuum of methods ranging from classical molecular dynamics to highly accurate quantum studies of interelectronic correlation need to be applied to these particles in order

to extract the geometries, single particle spectra and many- body cohesive properties being measured presently.

The interaction of TM particles with supports and bonding interaction with ligands as simple as hydrogen provides models restricted enough to be amenable to computation by several methods, and close enough to reality, to be compared with experiment. Observations about the magnitude of charge transfer and delocalization of atomic orbitals by interaction with a model substrate may not be quantitatively accurate, but instead form an orientation for thinking about the dominant mechanisms and how they may be modified. Mass-selected gas phase data on clusters like H_mPt_n will play a crucial role in testing theoretical models and guiding development of more powerful computational techniques. For example, the saturation rule $m \leq 2n$ demands a straightforward explanation; it appears that presently available techniques are capable of answering such a question (61). Questions about distribution of particle size in a molecular beam of given temperature and pressure appear to be much more difficult, involving both dynamical (reaction rate) and bonding-energy information. We suggest that classical simulation schemes using potentials derived from quantum cluster calculations can be useful in this endeavor.

ACKNOWLEDGMENTS

This work was supported in part by the National Science Foundation (through the Northwestern University Materials Research Center, Grant No. DMR85-20280). We thank R.F.W. Bader and P.J. MacDougall for comments and suggestions, and for making available density analysis codes.

REFERENCES

1. Klabunde, K.J. Chemistry of Free Atoms and Particles; Academic: New York, New York, 1980; Moskovits, M. Metal Clusters; Wiley-Interscience: New York, 1986.

2. Collman, J.P., Hegedus, L.S. Principles and Applications of Organotransition Metal Chemistry; University Science Books: Mill Valley, CA, 1980.
3. Fersht, A. Enzyme Structure and Mechanism; 2nd edition, Freeman: New York, NY, 1985.
4. The Theory of the Photographic Process; James, T.H., Ed.; Macmillan: New York, NY, 1977.
5. Catalyst Design, Progress and Perspectives; Hegedus, L.L.; Wiley-Interscience: New York, NY, 1987.
6. Ceramic Containing Systems; Evans, A.G., Ed.; Noyes Publications: Park Ridge, NJ, 1986; Surfaces and Interfaces in Ceramics and Ceramic-Metal Systems; Pask, J.; Evans, A., Eds.; Plenum Press: New York, NY, 1981.
7. See for example, Local Density Approximations in Quantum Chemistry and Solid State Physics; edited by Dahl, J.P.; Avery, J.; Plenum: New York, NY, 1984.
8. Slater, J.C., The Self-Consistent-Field for Molecules and Solids; McGraw-Hill: New York, NY, 1974.
9. Baerends, E.J.; Ellis, D.E.; Ros P. Chem. Phys. 1973, 2, 41.
10. Rosén, A.; Ellis, D.E.; Adachi, H.; Averill, F.W. J. Chem. Phys. 1976, 65, 3629.
11. Delley, B.; Ellis, D.E. J. Chem. Phys. 1982, 76, 1949.
12. Ellis, D.E.; Guo, J.; Cheng, H.-P. J. Phys. Chem. 1988, 92, 3024.
13. Morse, M.D.; Hansen, G.P.; Langridge-Smith, P.R.R.; Zheng, L.-S.; Guesic, M.E.; Michalopoulos, D.L.; Smalley, R.E. J. Chem. Phys. 1984, 80, 5400.
14. Basch, H.; Newton, M.D.; Moskowitz, J.W. J. Chem. Phys. 1980, 73, 4492.
15. Bader, R.F.W. Acc. Chem. Res. 1985, 18, 9.; Acc. Chem. Res. 1975, 8, 34.
16. Bader, R.F.W.; MacDougall, P.J. J. Am. Chem. Soc. 1985, 107, 6788.
17. Wiberg, K.B.; Bader, R.F.W.; Lau, C.D.H. J. Am. Chem. Soc. 1987, 109, 985; 1987, 109, 1001.

18. Guo, J.; Ellis, D.E.; Bader, R.F.W.; MacDougall, P.J.; J. Cluster Science 1990, 1, 201.
19. Gatti, C.; Fantucci, P.; Pacchioni, G. Theor. Chim. Acta 1987, 72, 433; Cao, W.L.; Gatti, C.; MacDougall, P.J.; Bader, R.F.W. Chem. Phys. Lett. 1987, 141, 380.
20. Bauschlicher, C.W.; Bagus, P.S. J. Chem. Phys. 1984, 81, 5889; Post, D.; Baerends, E.J. Surf. Sci. 1981, 109, 167; J. Chem. Phys. 1983, 78, 5663; Surf. Sci. 1982, 110, 117.
21. Averill, F.W.; Painter, G.S. Phys. Rev. B 1986, 34, 2088.; Bader, R.F.W. in "The Force Concept in Chemistry", ed. Deb, B.M. (Van Nostrand, New York, 1981).
22. Ellis, D.E.; Lam, D.J. Physica B 1988, 150, 25.
23. Rösch, N.; Görling, A.; Ellis, D.E.; Schmidbauer, H. Angew. Chemie 1989 101, 1410.
24. Koelling, D.D.; Ellis, D.E.; Bartlett, R.J. J. Chem. Phys. 1976, 65, 3331.
25. Ellis, D.E. Hand book on Physics and Chemistry of Actinides, Freeman, A.J.; Lander, G.H., Ed; Elsevier Science Publishers, B.V., 1985, p 1.
26. Yang, C.Y. NATO Adv. Sci. Inst. Ser. Ser.B 1983, 87, P 335.
27. Robota, H.J., private communication
28. Dill, D.; Dehmer, J.L. J. Chem. Phys. 1974, 61, 692.
29. Chou, S.-H.; Guo, J.; Ellis, D.E. Phys. Rev. B 1986, 34, 12.
30. Bianconi, A.; Dell'Ariccia, M.; Durham, P.J.; Pendry, J.B. Phys. Rev. B 1982, 26, 6502; Bianconi, A.; In EXAFS and Near Edge Structure; Bianconi, A.; Incoccia, L.; Stipcich, S. Ed.; New York, 1983; p 118.
31. Dehmer, J.L.; Dill, D. J. Chem. Phys. 1976, 65, 5327.
32. Guo, J.; Ellis, D.E.; Alp, E.; Soderholm, L.; Shenoy, G.K. Phys. Rev. B 1989, 39, 6125.
33. Guo, J.; Ellis, D.E.; Goodman, G.L.; Alp, E.; Soderholm, L.; Shenoy, G.K. Phys. Rev. B 1990, 41, -.
34. Horsley, J.A. J. Chem. Phys. 1982, 76, 1451.; Horsley, J.A.; Stohr, J.; Koestner, R.J. J. Chem. Phys. 1985, 83, 3146.
35. Kutzler, F.W.; Ellis, D.E. Phys. Rev. B 1984, 29, 6890.
36. Kutzler, F.W.; Misemer, D.K.; Doniach, S.; Hodgson, K.O. Chem. Phys. Lett. 1982, 92, 626.

37. Kutzler, F.W.; Natoli, C.R.; Misemer, D.K.; Doniach, S.; Hodgson, K.O. J. Chem. Phys. 1980, **73**, 3274.
38. Natoli, C.R. In EXAFS and Near Edge Structure; Hodgson, K.O.; Hedman, B.; Penner-Hahn, J.E. Ed.; Springer Verlag: New York, 1984; p 38.
39. Natoli, C.R.; Kutzler, F.W.; Misemer, D.K.; Doniach, S. Phys. Rev. A 1980, **22**, 1104.
40. Norman, D.; Stohr, J.; Jaeger, R.; Durham, P.J.; Pendry, J.B. Phys. Rev. Lett. 1983, **51**, 2052.
41. Stohr, J.; Sette, F.; Johnson, A.L. Phys. Rev. Lett. 1984, **53**, 1684.
42. Parks, E.K.; Nieman, G.C.; Pobo, L.G.; Riley, S.J. J. Phys. Chem. 1987, **91**, 2671.
43. Landau, L.D.; Lifshitz, E.M. In Statistical Physics; Skyes, J.B.; Kearsley, M.J. Translators; Addison-Wesley Publishing Co., 1969; p 220
44. Chelikowsky, J.R. Phys. Rev. Lett. 1989, **62**, 292.
45. Cheng, H.-P. Ph.D. Thesis, Northwestern University, Evanston, IL, 1988; Cheng, H.-P and Ellis, D.E. Phys. Rev. B 1989, **39**, 12469.
46. Daw, M.S.; Baskes, M.I. Phys. Rev. B 1983, **29**, 6443.
47. Stott, M.J.; Zaremba, E. Phys. Rev. B 1980, **22**, 1564.
48. T. Ziegler, J.G. Snijders and E.J. Baerends, J. Chem. Phys. 1981, **74**, 1271.
49. Tauster, S.J. Acc. Chem. Res. 1987, **20**, 389.
50. Altman, E.I.; Gorte, R.J. J. Catal. 1988, **110**, 191.
51. Low, J.J.; Ellis, D.E. "Microstructure and Properties of Catalysts", Treacy, M.M.J.; Thomas, J.M.; White, J.M., Ed.; Materials Research Society: Pittsburgh, PA, 1988; p. 341.
52. Hoffmann, R. Angew. Chem. Int. Ed. Engl. 1982, **21**, 724-733.
53. McAdon, M.H.; Goddard III, W.A. J. Chem. Phys. 1988 **88**, 277; McAdon, M.H. Ph.D. Thesis, Cal. Tech. Pasadena, Ca. 1988
54. Goodgame, M.M. Ph.D. Thesis, Cal. Tech. Pasadena, CA., 1983.
55. Vranka, R.G.; Dahl, L.F.; Chin, P.; Chatt, J. J. Am. Chem. Soc. 1969 **91**, 1574.
56. Moor, P.; Pregosis, P.S.; Venanzi, L.M.; Welch, A.J. Inorg. Chem. Acta. 1984 **85**, 103.

57. Carrondo, M.A.A.F. de C.T.; Skapski, A.C. J. Chem. Soc., Chem. Commun. 1976, 410-411
58. Noell, J.O.; Hay, D.J. Inorg. Chem. 1982 21, 14-20.
59. Roos, B.O.; Taylor, P.R.; Siegbahn, P.E.M. Chem. Phys. 1980 48, 175.
60. Low, J.J.; Goddard III, W.A. J. Am. Chem. Soc. 1984 106, 6928.
61. Low, J.J.; Ellis, D.E.; Riley, S. Paper presented at the AIChE meeting, Denver, CO, August 23, 1988 (unpublished).

SOME ASPECTS OF THE
COUPLED CLUSTER BASED
POLARIZATION PROPAGATOR METHOD

Jan Geertsen
Steffen Eriksen
Jens Oddershede

Department of Chemistry
Odense University
DK-5230 Odense M
Denmark

TABLE OF CONTENTS

1. Introduction
 2. Spin-adapted coupled cluster equations
 3. Perturbative polarization propagator methods
 4. The coupled cluster polarization propagator approximation (CCPPA)
 5. Analysis of the coupled cluster polarization propagator method
 6. Numerical illustrations
 7. Conclusions
- Appendix A. Spin-adapted coupled cluster singles and doubles equations
Appendix B. Spin-adapted matrix elements of $A(3)$
Acknowledgment
References

1. INTRODUCTION

The concept of *pair interactions* has played a key role in molecular electronic structure calculations. When it was reconciled that the independent particle methods had to be improved by consideration of electronic correlation, the first methods considered were based on the notion that the pair interaction gave the most important contributions to the electronic correlation. Suffice it to mention the work of Sinanoglu /1,2/, Nesbet /3/, and Cizek /4,5/. The computational successes in recent years of the coupled electron pair approximations (CEPA) /6/ and the second order many body perturbation theory (MBPT (2)) /7/ are manifestations of the same idea.

It was realized rather early during the development of accurate electronic structure methods that it was important to include the pair interactions through high order in perturbation theory and the coupled cluster (CC) methods, originating in nuclear physics /8,9,10/, were introduced in quantum chemistry by Cizek /4/. These methods made it possible not just to sum pair interactions to infinite order but also to incorporate general N -body interactions to infinite order. Furthermore, CC methods are size extensive /11/, i.e. they scale with the size of the system, a desirable property that CC does not have in common with e.g. configuration interaction (CI) methods.

Coupled cluster methods have mainly been applied to the calculation of ground state properties such as total energies and electric and magnetic multipole moments. Only lately has there been some progress towards the calculation of excitation energies /12–16/ and very little is done for other excited state properties. It was therefore a logical step to try to use the coupled cluster wavefunction within the polarization propagator formalism /17/ to obtain excitation energies, transition probabilities, and response properties. This approach is the subject of the present review.

In propagator /18/ or response /19/ methods we determine excitation energies and transition probabilities from the eigenvalues and eigenvectors, respectively, of the inverse linear response function or polarization propagator. The propagator itself determines (frequency dependent) response pro-

perties. Normally, the polarization propagator is expressed in the so-called super operator formalism /20/ and approximate solutions to it are obtained (1) by truncating the operator manifold that we use to expand the excitation space and (2) by approximating the reference state. The reference state is the state with respect to which the polarization propagator is defined, that is, the state for which we are determining the response of the system to external perturbations. In nearly all applications the reference state has been chosen to be the ground state.

The approximate reference states that have been used so far in polarization propagator theory include MBPT /21,22/, multiconfigurational selfconsistent field (MCSCF) /23/, antisymmetrized geminal power (AGP) /24/, and CC /17,25/ wavefunctions. Due to the infinite nature of CC theory we have implemented the CC polarization propagator approximation (CCPPA) within the framework of the perturbative propagator methods as modifications of the second order polarization propagator approximation (SOPPA) where the polarization propagator is evaluated through second order in the fluctuation potential (the electron repulsion minus the Fock potential). Since SOPPA is based on an MBPT expansion of the reference state, the CCPPA method gives improved descriptions of spectral properties in cases where the MBPT expansion is slowly convergent. Examples from calculations on CH^+ will be used to demonstrate this point in Sec. 6. We analyze the extra diagram series that are introduced in the CCPPA method and we show that the most important extra terms appear already in third order in the fluctuation potential (Sec. 5.).

It is convenient to work in a spin-adapted formalism for the particle-hole excitation operators, thus obtaining directly singlet, triplet etc. excitation properties from the corresponding propagators. This implies that we would like to have the CC cluster amplitudes in a spin-adapted form. The next section describes how this is done.

2. SPIN-ADAPTED COUPLED CLUSTER EQUATIONS

The coupled cluster expansion of the exact ground state wavefunction uses the exponential ansatz /4,5,9–11,26/

$$\begin{aligned} |\psi_0\rangle &= e^T |\phi_0\rangle \\ &= (1 + T + \frac{1}{2!} T^2 + \dots) |\phi_0\rangle \end{aligned} \quad (1)$$

where the cluster operator, T , may be separated into one-body, two-body, etc. components

$$T = T_1 + T_2 + T_3 + \dots \quad (2)$$

A general method for deriving the explicit form of the CC equations was given by Cizek /4,5/. In the present work a spin-adapted version of the coupled cluster singles and doubles (CCSD) model is considered (see also ref. 27)

$$|\psi_{\text{CCSD}}\rangle = e^{T_1+T_2} |\phi_0\rangle \quad (3)$$

$$T_1 = \sum_{m\alpha} t_{\alpha}^m q^+(0,0)_{m\alpha} \quad (4)$$

$$T_2 = \frac{1}{4} \sum_{i=1}^2 \sum_{mn} t_{\alpha\beta}^{mn} [i] S^+ [i]_{m\alpha n\beta} \quad (5)$$

The operator $q^+(0,0)_{m\alpha}$ generates singly excited singlet states when working on the closed shell reference function, $|\phi_0\rangle$ (often the SCF solution)

$$q^+(0,0)_{m\alpha} = \frac{1}{\sqrt{2}} (a_{m+}^{\dagger} a_{\alpha+} + a_{m-}^{\dagger} a_{\alpha-}) \quad (6)$$

and $S^+[i]_{m\alpha n\beta}$ are the two normalized and linearly independent two-particle, two-hole (2p–2h) singlet excitation operators /28,29/.

$$S^+[1]_{m\alpha n\beta} = \frac{1}{2} [(1 + \delta_{mn})(1 + \delta_{\alpha\beta})]^{-\frac{1}{2}} \{a_{m+}^+ a_{\alpha+} a_{n-}^+ a_{\beta-} + a_{m-}^+ a_{\alpha-} a_{n+}^+ a_{\beta+} - a_{m+}^+ a_{\alpha-} a_{n-}^+ a_{\beta+} - a_{m-}^+ a_{\alpha+} a_{n+}^+ a_{\beta-}\} \quad (7)$$

$$S^+[2]_{m\alpha n\beta} = \frac{1}{2\sqrt{3}} (1 - \delta_{mn})(1 - \delta_{\alpha\beta}) \{2a_{m+} a_{\alpha+} a_{n+} a_{\beta+} + a_{m+} a_{\alpha+} a_{n-} a_{\beta-} + a_{m-} a_{\alpha-} a_{n+} a_{\beta+} + a_{m+} a_{\alpha-} a_{n-} a_{\beta+} + a_{m-} a_{\alpha+} a_{n+} a_{\beta-} + 2a_{m-} a_{\alpha-} a_{n-} a_{\beta-}\} \quad (8)$$

Indices α, β, \dots (m, n, \dots) denote occupied (unoccupied) Hartree-Fock (HF) spatial orbitals and the spin quantum numbers are given as the $+/-$ subscripts. The permutation symmetry of the two types of double excitation cluster amplitudes is

$$t_{\alpha\beta}^{mn}[1] = t_{\alpha\beta}^{nm}[1] = t_{\beta\alpha}^{mn}[1] = t_{\beta\alpha}^{nm}[1] \quad (9)$$

$$t_{\alpha\beta}^{mn}[2] = -t_{\alpha\beta}^{nm}[2] = -t_{\beta\alpha}^{mn}[2] = t_{\beta\alpha}^{nm}[2] \quad (10)$$

The CCSD energy is obtained by projecting the Schrödinger equation on the left by $\langle \emptyset_0 |$

$$\langle \emptyset_0 | (H - E_{\text{CCSD}}) | \psi_{\text{CCSD}} \rangle = 0 \quad (11)$$

or, since the hamiltonian has only one- and two-electron operators

$$\langle \emptyset_0 | (H - E_{\text{CCSD}}) (1 + T_1 + T_2 + \frac{1}{2}T_1^2) | \emptyset_0 \rangle = 0$$

In the case of HF (SCF) orbitals we then have

$$E_{\text{CCSD}} = E_{\text{HF}} + \frac{1}{2} \sum_{\substack{mn \\ \alpha\beta}} (m\alpha|n\beta) \{t_{\alpha\beta}^{mn}[1] + \sqrt{3} t_{\alpha\beta}^{mn}[2] + 2t_{\alpha}^m t_{\beta}^n - t_{\beta}^m t_{\alpha}^n\} \quad (12)$$

Similarly, the equation for determining the t_{α}^m and $t_{\alpha\beta}^{mn}[i]$ amplitudes may be obtained from

$$\langle \text{HF} | q(0,0)_{m\alpha} (H - E_{\text{CCSD}}) e^{T_1+T_2} | \text{HF} \rangle = 0 \quad (13a)$$

$$\langle \text{HF} | S[i]_{m\alpha n\beta} (H - E_{\text{CCSD}}) e^{T_1+T_2} | \text{HF} \rangle = 0 \quad ; \quad i = 1, 2 \quad (13b)$$

These equations are solved for CCSD in appendix A. However, in order to see the structure of the solution let us consider the resulting equations in the simpler case of CCD where T is approximated by T_2

$$|\psi_{\text{CCD}}\rangle = e^{T_2} |\text{HF}\rangle \quad (14)$$

The corresponding expressions for the energy and the amplitudes are easily obtained by simply putting $T_1 = 0$ in the CCSD equations (see Eq. (12) and appendix A)

$$E_{\text{CCD}} = E_{\text{HF}} + \frac{1}{2} \sum_{\substack{mn \\ \alpha\beta}} (m\alpha|n\beta) \{t_{\alpha\beta}^{mn}[1] + \sqrt{3} t_{\alpha\beta}^{mn}[2]\} \quad (15)$$

$$D_{\alpha\beta mn} t_{\alpha\beta}^{mn}[i] = \Delta_{\alpha\beta}^{mn}[i] + \Gamma_{\alpha\beta}^{mn}[i] + \Omega_{\alpha\beta}^{mn}[i] \quad ; \quad i = 1, 2 \quad (16)$$

where $D_{\alpha\beta mn}$ is the orbital energy difference

$$D_{\alpha\beta mn} = \epsilon_{\alpha} + \epsilon_{\beta} - \epsilon_m - \epsilon_n \quad (17)$$

and

$$\Delta_{\alpha\beta}^{mn}[i] = (2i - 1)^{\frac{1}{2}} \{ (m\alpha|n\beta) - (-1)^i (m\beta|n\alpha) \} \quad (18)$$

$$\begin{aligned} \Gamma_{\alpha\beta}^{mn}[i] = & (1 - \delta_{mn})^{i-1} \sum_{cd} (mc|nd) t_{\alpha\beta}^{cd}[i] \\ & + (1 - \delta_{\alpha\beta})^{i-1} \sum_{\mu\nu} (\mu\alpha|\nu\beta) t_{\mu\nu}^{mn}[i] \\ & - \sum_{\mu c} \left[(\mu\alpha|mc) t_{\beta\mu}^{nc}[i] - (-1)^i (\mu\alpha|nc) t_{\beta\mu}^{mc}[i] \right. \\ & + (\mu\beta|nc) t_{\alpha\mu}^{mc}[i] - (-1)^i (\mu\beta|mc) t_{\alpha\mu}^{nc}[i] \\ & + (2i - 1)^{\frac{1}{2}} \left[\frac{(-1)^i}{2} (\mu c|m\beta) \{ t_{\alpha\mu}^{nc}[1] + \sqrt{3} t_{\alpha\mu}^{nc}[2] \} \right. \\ & + \frac{(-1)^i}{2} (\mu c|n\alpha) \{ t_{\beta\mu}^{mc}[1] + \sqrt{3} t_{\beta\mu}^{mc}[2] \} \\ & - \frac{1}{2} (\mu c|m\alpha) \{ t_{\beta\mu}^{nc}[1] + \sqrt{3} t_{\beta\mu}^{nc}[2] \} \\ & \left. \left. - \frac{1}{2} (\mu c|n\beta) \{ t_{\alpha\mu}^{mc}[1] + \sqrt{3} t_{\alpha\mu}^{mc}[2] \} \right] \right] \quad (19) \end{aligned}$$

$$\begin{aligned} \Omega_{\alpha\beta}^{mn}[i] = & \frac{1}{2} \sum_{\substack{\mu\nu \\ cd}} (\mu c|\nu d) \left[(2i - 1)^{-\frac{1}{2}} t_{\alpha\beta}^{cd}[i] t_{\mu\nu}^{mn}[i] \right. \\ & + \{ (-1)^i P_{\alpha\beta} - 1 \} t_{\alpha\mu}^{mn}[i] \{ t_{\beta\nu}^{cd}[1] + \sqrt{3} t_{\beta\nu}^{cd}[2] \} \\ & + \frac{1}{2} \{ (-1)^i P_{mn} - 1 \} \left[2 t_{\alpha\beta}^{mc}[i] \{ t_{\mu\nu}^{nd}[1] + \sqrt{3} t_{\mu\nu}^{nd}[2] \} \right. \\ & + t_{\alpha\mu}^{md}[1] \{ (-1)^i (2i - 1)^{\frac{1}{2}} t_{\beta\nu}^{nc}[1] + (5 - 2i)^{\frac{1}{2}} t_{\beta\nu}^{nc}[2] \} \\ & + t_{\alpha\mu}^{md}[2] \{ (5 - 2i)^{\frac{1}{2}} t_{\beta\nu}^{nc}[1] + \left. \left. \left[\frac{5}{\sqrt{3}} \right]^{i-1} t_{\beta\nu}^{nc}[2] \} \right. \right. \\ & \left. \left. - (2i - 1)^{\frac{1}{2}} \{ t_{\alpha\mu}^{mc}[1] + \sqrt{3} t_{\alpha\mu}^{mc}[2] \} \{ t_{\beta\nu}^{nd}[1] + \sqrt{3} t_{\beta\nu}^{nd}[2] \} \right] \right] \quad (20) \end{aligned}$$

P_{kl} is a permutation operator: $P_{kl}f(k,l) = f(l,k)$. The CCD and CCSD equations are non-linear and may be solved iteratively. Setting initially all

amplitudes on the right hand side of Eq. (16) equal to zero, yields the two spin-adapted first order Rayleigh-Schrödinger (RS) correlation coefficients

$$t_{\alpha\beta}^{mn}[i]_1 = \frac{\Delta_{\alpha\beta}^{mn}[i]}{D_{\alpha\beta mn}} \equiv \kappa_{\alpha\beta}^{mn}[i] \quad ; \quad i = 1, 2 \quad (21)$$

and the second order correlation energy

$$E_2 = \frac{1}{2} \sum_{\substack{mn \\ \alpha\beta}} (m\alpha | n\beta) \{ \kappa_{\alpha\beta}^{mn}[1] + \sqrt{3} \kappa_{\alpha\beta}^{mn}[2] \} \quad (22)$$

The third order correlation energy, which has contributions only from double substitutions, is obtained in the following iteration if the quadratic term, $\Omega_{\alpha\beta}^{mn}[i]$ is neglected. Using $t_{\alpha\beta}^{mn}[i] = \kappa_{\alpha\beta}^{mn}[i]$ in $\Omega_{\alpha\beta}^{mn}[i]$ gives the quadruple contribution to the fourth order energy. The CCD result is given as the converged result of this procedure.

If $\Omega_{\alpha\beta}^{mn}[i]$ is neglected throughout the calculation, the method is equivalent to the infinite order RS perturbation theory (RSPT) restricted to biexcited configurations, D-MBPT (∞), also known as linearized CCD, LCCD /30,31/. This method often overestimates the ground state correlation energy.

In actual CCD calculations the individual terms contributing to $\Omega_{\alpha\beta}^{mn}[i]$ may be evaluated most efficiently using intermediate arrays. We express $\Omega_{\alpha\beta}^{mn}[i]$ as

$$\begin{aligned} \Omega_{\alpha\beta}^{mn}[i] = & \sum_{\mu\nu} S_{\mu\nu\alpha\beta}[i] t_{\mu\nu}^{mn}[i] + \{(-1)^i P_{\alpha\beta} - 1\} \sum_{\mu} T_{\mu\beta} t_{\alpha\mu}^{mn}[i] \\ & + \dots \end{aligned} \quad (23)$$

$$S_{\mu\nu\alpha\beta}[i] = \frac{1}{2} (2i-1)^{-\frac{1}{2}} \sum_{cd} (\mu c | \nu d) t_{\alpha\beta}^{cd}[i] \quad (24)$$

$$T_{\mu\beta} = \frac{1}{2} \sum_{\nu\gamma\delta} (\mu\gamma | \nu\delta) \{ t_{\beta\nu}^{\gamma\delta}[1] + \sqrt{3} t_{\beta\nu}^{\gamma\delta}[2] \} \quad (25)$$

where the "+" terms in Eq. (23) are all but the two first terms in Eq. (20). If we had expressed these terms in the same form as the two first terms we would have seen that the S and T arrays are the least time consuming quantities to compute. Restricting $\Omega_{\alpha\beta}^{mn}[i]$ only to include these two terms, which are often dominant, gives the approximate CCD method, ACCD or ACP-D45 /32,33/.

In MBPT the lowest order effect on the ground state energy of inclusion of single excitations appears in the fourth order. As the CCD model is correct to fourth order in the DQ-space, the leading term of CCSD corresponds to MBPT(4)-SDQ. Thus, CCSD may be viewed as the infinite order generalization of that model /34/. From these considerations it follows that if $|\phi_0\rangle$ is a HF function, T_1 is not expected to be very important. However, in the non-HF case T_1 can provide the dominant contribution to ground state the correlation energy /35/. Similar considerations hold for the CCPPA schemes and we do not expect to see any substantial effects of T_1 provided we use a HF-based theory.

3. PERTURBATIVE POLARIZATION PROPAGATOR METHODS

Due to the structural similarity between CCPPA /17/ and propagator methods based on an MBPT expansion of the reference state /21/, we will start by giving a brief review of the theory for perturbative polarization propagator methods.

The double-time retarded Green's function or linear response function /19,29/ is given as /36/

$$G(t, t') = -i\theta(t-t') \langle 0 | [a(t), b(t')] | 0 \rangle \quad (26)$$

where a, b are both number conserving operators in the Heisenberg representation

$$a(t) = \exp(i\hbar t) a(0) \exp(-i\hbar t) \quad (27)$$

$|0\rangle$ is the exact ground state and the Heaviside step function, $\theta(t)$ is defined as

$$\begin{aligned} t \geq 0: \theta(t) &= 1 \\ t < 0: \theta(t) &= 0 \end{aligned} \quad (28)$$

An energy dependent Green's function is obtained by taking the Fourier transform of $G(t, t')$ /37/

$$\langle\langle a; b \rangle\rangle_E = \int_{-\infty}^{\infty} d(t-t') G(t, t') \exp[iE(t-t')] \quad (29)$$

where we have used the fact that $G(t, t')$ only depends on the time difference $t-t'$. After integration the so-called spectral representation of the polarization propagator is obtained

$$\text{Re}\langle\langle a; b \rangle\rangle_E = \sum_n \left\{ \frac{\langle 0 | a | n \rangle \langle n | b | 0 \rangle}{E - E_n + E_0} - \frac{\langle 0 | b | n \rangle \langle n | a | 0 \rangle}{E + E_n - E_0} \right\} \quad (30)$$

where the summation extends over all excited states of the system. It is seen that the poles for the propagator are the excitation energies of the system. If we choose a, b both to be the electric dipole moment operator, r , the residues give the electric dipole transition moments.

An alternative expression for the polarization propagator (the equation of motion) is /38/

$$\langle\langle a; b \rangle\rangle_E = (a | \hat{\hbar}) (h | E \hat{I} - \hat{H} | \hat{\hbar})^{-1} (h | b) \quad (31)$$

where h is a complete operator manifold /39/ consisting of excitation, $\{q^+, q^+q^+, \dots\}$, and deexcitation, $\{q, qq, \dots\}$, components

$$\begin{aligned}
 h &= \{h_2, h_4, h_6, \dots\} \\
 h_2 &= \{q^+, q\} = \{a_m^+ a_\alpha, a_\alpha^+ a_m\} \\
 h_4 &= \{q^+q^+, qq\} = \{a_m^+ a_\alpha a_n^+ a_\beta, a_\beta^+ a_n a_\alpha^+ a_m\} \quad ; \quad m > n, \alpha > \beta \\
 &\dots \\
 &\dots
 \end{aligned} \tag{32}$$

The round parentheses label a superoperator /20/ binary product

$$(A|B) = \langle 0 | [A^+, B] | 0 \rangle, \tag{33}$$

\hat{I} and \hat{H} are the superoperator identity and hamiltonian, respectively

$$\hat{I}A = A$$

$$\hat{H}A = [H, A]$$

and \tilde{h} is the transposed (row) vector. Equation (31) is exact provided that h is the complete manifold and $|0\rangle$ is the exact reference state.

In perturbative polarization propagator approaches Eq. (31) is expanded to a given order in the fluctuation potential, U , that is, the total hamiltonian minus the Fock operator. To be more specific, in an n -th order approach $(a|\tilde{h})$, $(h|E\hat{I} - \hat{H}|\tilde{h})$ and $(h|b)$ are *all* computed through order n in U . Taking $|0\rangle = |HF\rangle$ and $h = h_2$ gives the consistent first order method /38/, also known as the random phase approximation (RPA) or time-dependent Hartree-Fock (TDHF). In a consistent second order theory, the second order polarization propagator approximation (SOPPA) /22,29/, it may be shown that it is only necessary to include h_2, h_4 and take $|0\rangle$ as

$$\begin{aligned}
|0\rangle &= |HF\rangle + |DE(1)\rangle + |SE(2)\rangle \\
&= \left\{ 1 + \frac{1}{4} \sum_{i=1,2} \sum_{\alpha\beta} \kappa_{\alpha\beta}^{mn}[i] S^+[i]_{m\alpha n\beta} + \sum_{m\alpha} \kappa_{\alpha}^m q^+(0,0)_{m\alpha} \right\} |HF\rangle \quad (34)
\end{aligned}$$

Here $\kappa_{\alpha\beta}^{mn}[i]$ and κ_{α}^m are the first order double excitation and second order single excitation RS correlation coefficients, respectively. $\kappa_{\alpha\beta}^{mn}[i]$, $S^+[i]_{m\alpha n\beta}$, and $q^+(0,0)_{m\alpha}$ are given by Eqs. (21), (7), (8), and (6), respectively, and

$$\begin{aligned}
\kappa_{\alpha}^m &= 2^{-\frac{1}{2}} (\epsilon_{\alpha} - \epsilon_m)^{-1} \left\{ \sum_{\substack{a,b \\ \pi}} (\pi a | mb) \{ \kappa_{\pi\alpha}^{ab}[1] + \sqrt{3} \kappa_{\pi\alpha}^{ab}[2] \} \right. \\
&\quad \left. - \sum_{\substack{a,b \\ \pi\delta}} (\pi a | \delta\alpha) \{ \kappa_{\pi\delta}^{am}[1] + \sqrt{3} \kappa_{\pi\delta}^{am}[2] \} \right\} \quad (35)
\end{aligned}$$

By inserting $|0\rangle$ and h in the equation of motion, Eq. (31), it may be shown /22/ that the SOPPA propagator can be expressed as

$$\begin{aligned}
\langle\langle a; b \rangle\rangle_E &= \{ t(a, E), \mp t(a, \mp E) \} P(E) \begin{bmatrix} \tilde{t}(b, E) \\ \mp \tilde{t}(b, \mp E) \end{bmatrix} \\
&\quad + (a | \tilde{q}^* \tilde{q}^+) [(EI-D)^{-1} \bullet (-EI-D)^{-1}] (q^* q^+ | b) \quad (36)
\end{aligned}$$

In the first term the minus signs in front of t , \tilde{t} , and E hold for symmetric operators a/b , whereas the plus signs are used for antisymmetric operators. The minus sign in the square bracket of the last term only applies when a and b are not both symmetric or antisymmetric /40/.

The matrices t , P are defined as

$$t(a, E) = (a | \tilde{q}^+) + (a | \tilde{q}^* \tilde{q}^+) (EI-D)^{-1} C \quad (37)$$

$$P(E) = \begin{bmatrix} ES-A-\tilde{C}(EI-D)^{-1}C & \tilde{B} \\ -B & -ES-A-\tilde{C}(-EI-D)^{-1}C \end{bmatrix}^{-1} \quad (38)$$

where

$$A = (q^+ | H | \tilde{q}^+) \quad (39)$$

$$B = (q | U | \tilde{q}^+) \quad (40)$$

$$C = (q^+ q^+ | U | \tilde{q}^+) \quad (41)$$

$$D = (q^+ q^+ | F | \tilde{q}^+ \tilde{q}^+) \quad (42)$$

$$S = (q^+ | \tilde{q}^+) \quad (43)$$

Explicit expressions for these matrix elements in the spin-adapted representation are given in Appendix C of ref. 29.

The particle-hole (p-h) dominated excitation energies are thus obtained as the eigenvalues of $P(E)^{-1}$ and the corresponding eigenvectors together with Eq. (37) determine the transition amplitudes.

In many cases SOPPA-based calculations are of satisfactory quality when compared with experiments and other calculations (see e.g. Table III of ref. 18 for a summary of SOPPA calculations). However, in some systems with low-lying excited states (for example CH^+ , Be, and BH) the perturbation series is slowly convergent, which means that third and higher order contributions could become important. The third order polarization propagator approximation has been described in the work of Oddershede and Jørgensen /21/ but so far this method has not been applied in direct calculations. In the present work we will study the effect of including the third order A-matrix in SOPPA since – as will be discussed in Sec. 5. – this term is expected to provide the dominant part of the third order corrections. The only terms contributing to the third order A-matrix are

$$A(3) = A'(3) + A''(3) + A'''(3) \quad (44)$$

where

$$A'(3) = \langle DE(1) | [q, [U, \tilde{q}^*]] | DE(1) \rangle \quad (45)$$

$$A''(3) = \langle SE(2) | [q, [U, \tilde{q}^*]] | HF \rangle + \langle HF | [q, [U, \tilde{q}^*]] | SE(2) \rangle \quad (46)$$

$$A'''(3) = \langle HF | [q, [U, \tilde{q}^*]] | DE(2) \rangle \quad (47)$$

Explicit expressions for the $A(3)$ matrices in the spin-adapted basis are given in Appendix B.

Another way of improving the convergence of the SOPPA method would be to include certain extra diagram series summed to infinite order (in addition to the ones inherent in RPA-like methods; see Sec. 5.). The coupled cluster method, which provides an infinite order extension of RS based methods, would provide a convenient way of doing so and the next chapter shows how we propose to do that.

4. THE COUPLED CLUSTER POLARIZATION PROPAGATOR APPROXIMATION (CCPPA)

In the coupled cluster polarization propagator method we use a coupled cluster rather than a Rayleigh–Schrödinger reference state, i.e.

$$|0\rangle = e^T |HF\rangle \quad (48)$$

In perturbative methods both the projection manifold and the reference state are uniquely determined once the order is specified; see Table I.

TABLE I. Reference state and projection manifold in perturbative propagator schemes.

Order	Method	$ 0\rangle$	h
1	RPA ^a , TDHF ^b , CHF ^c	$ HF\rangle$	h_2
	HRPA ^d	$ HF\rangle + DE(1)\rangle$	h_2
2	SOPPA ^e	$ HF\rangle + DE(1)\rangle + SE(2)\rangle$	$\{h_2, h_4\}$

^aRandom phase approximation.

^bTime-dependent Hartree-Fock.

^cCoupled Hartree-Fock.

^dHigher random phase approximation.

^eSecond order polarization propagator approximation.

However, because of the infinite nature of the reference state, Eq. (48), in the present scheme, it is not possible to truncate h using the order concept, but we may be guided by experience with perturbative approaches. It is well known that it is essential to keep a balance between the correlation incorporated by expanding $|0\rangle$ and h , respectively. For instance, the higher random phase approximation (HRPA), which includes some second terms but not all, often gives excitation energies which are too large and in many cases also inferior to the consistent first order approximation (RPA). Augmenting this method with the two-particle, two-hole (2p–2h) corrections (h_4) and $|SE(2)\rangle$ gives the consistent second order approach (SOPPA), which gives a much more balanced description of the spectrum and spectral properties. In the following we therefore consider a similar truncation of h , i.e.

$$h = \{h_2, h_4\} \quad (49)$$

which implies that the CC polarization propagator is determined by the same equations as in the SOPPA method, i.e. by Eqs. (36)–(43). The only difference is that when evaluating explicit expressions for the matrices

$(a|\tilde{q}^+)$, $(a|\tilde{q}^+\tilde{q}^+)$, A , appearing in Eqs. (36)–(43), we must use

$|0\rangle = e^T|HF\rangle$. As an example let us consider the S matrix in the CCD

case

$$\begin{aligned}
 S_{m\alpha, n\beta} &= \langle \text{HF} | \exp(T_2^+) [q_{m\alpha}, \tilde{q}_{n\beta}^*] \exp(T_2) | \text{HF} \rangle \\
 &= \sum_{k,l}^{\infty} (k!l!)^{-1} \langle \text{HF} | (T_2^+)^k [q_{m\alpha}, \tilde{q}_{n\beta}^*] T_2^l | \text{HF} \rangle \quad (50)
 \end{aligned}$$

Clearly, the expansion in T_2 does not terminate and a truncation at a certain power of the T_2 cluster amplitudes must be applied. A similar conclusion holds for the remaining matrices. However, a reasonable way to truncate the individual matrices would be to require that we *must obtain the SOPPA method when we use the first iteration of the cluster equations* (see Sec. 2.) in CCPPA.

As discussed in Sec. 2., the initial amplitudes $t_{\alpha\beta}^{mn}[1]_1$, $t_{\alpha\beta}^{mn}[2]_1$ are the two spin-adapted RSPT correlation coefficients. Thus, keeping terms up to and including second order in the fluctuation potential, U for the first iteration gives the following expressions for the propagator matrices at all levels of iterations of the CC method

$$A = \langle \text{HF} | [q, [H, \tilde{q}^*]] (1+T_2) | \text{HF} \rangle \quad (51)$$

$$B = \langle \text{HF} | (1+T_2^+) [q^*, [U, \tilde{q}^*]] | \text{HF} \rangle \quad (52)$$

$$C = \langle \text{HF} | [qq, [U, \tilde{q}^*]] | \text{HF} \rangle \quad (53)$$

$$D = \langle \text{HF} | [qq, [F, \tilde{q}^* \tilde{q}^*]] | \text{HF} \rangle \quad (54)$$

$$S = \langle \text{HF} | (1+T_2^+) [q, \tilde{q}^*] (1+T_2) | \text{HF} \rangle \quad (55)$$

$$(a|\tilde{q}^*) = \langle \text{HF} | (1+T_2^+) [a^*, \tilde{q}^*] (1+T_2) | \text{HF} \rangle \quad (56)$$

$$(a|\tilde{q}^+\tilde{q}^+) = \langle HF|T_2^+[a^*,\tilde{q}^+\tilde{q}^+]|HF\rangle \quad (57)$$

A computational scheme which uses these truncations with respect to the fully iterated amplitudes is referred to /17/ as the coupled cluster doubles polarization propagator approximation (CCDPPA) or, if the quadratic part, $\Omega_{\alpha\beta}^{mn}[i]$ in Eq. (16) is neglected, the linearized coupled cluster doubles polarization propagator approximation (LCCDPPA). This relation between SOPPA and the CC polarization propagator method means that we can express the CCPPA and the SOPPA matrix elements in the same form. The only change is that the RS correlation coefficients are replaced by the corresponding CC amplitudes. For example, the S matrix can then be written

$$S_{m\alpha,n\beta} = \delta_{mn}\delta_{\alpha\beta} - \frac{1}{2}\delta_{mn}\sum_{\substack{a,b \\ \pi}} (\beta a|\pi b)\{t_{\alpha\pi}^{ab}[1] + \sqrt{3}t_{\alpha\pi}^{ab}[2]\}/D_{\beta\pi ab} \\ - \frac{1}{2}\delta_{\alpha\beta}\sum_{\substack{a,b \\ \pi\delta}} (\beta a|\pi n)\{t_{\pi\delta}^{ma}[1] + \sqrt{3}t_{\pi\delta}^{ma}[2]\}/D_{\delta\pi an} \quad (58)$$

The same similarity holds for the A, B, $(a|\tilde{q}^+)$, and $(a|\tilde{q}^+\tilde{q}^+)$ matrices.

As long as only double substitutions are included in the CC method, the elements of $(a|\tilde{q}^+)$ are given as

$$(a|\tilde{q}^+_{m\alpha}) = 2^{\frac{1}{2}}a_{m\alpha} - 2^{-\frac{1}{2}}\sum_{\substack{a,b \\ \pi\delta}} (\delta a|\pi b)\{a_{m\delta}[t_{\alpha\pi}^{ab}[1] + \sqrt{3}t_{\alpha\pi}^{ab}[2]] \\ + a_{b\alpha}[t_{\pi\delta}^{ma}[1] + \sqrt{3}t_{\pi\delta}^{ma}[2]]\} \quad (59)$$

where $\{a_{kl}\}$ are one electron integrals in the molecular orbital representation

$$a_{kl} = \langle k | a | l \rangle \quad (60)$$

Let us now consider in a little more detail the structural relationship between the present coupled cluster approximation and the second order polarization propagator method. In the latter case the reference function includes effects of double excitations (first order) and single excitations (second order); see Table I. These single excitation effects are not accounted for in the present CCD scheme which uses

$$|0\rangle = \exp(T_2) |HF\rangle \quad (61)$$

However, as $|SE(2)\rangle$ makes no contribution to $P(E)$, the SOPPA and CCDPPA (LCCDPPA) excitation energies are the same in the initial cluster iteration.

The effect of the single excitation subspace only shows up in the transition matrix $(a|\tilde{q}^+)$

$$(a|\tilde{q}^+)_{SOPPA} = (a|\tilde{q}^+)_{DE} + (a|\tilde{q}^+)_{SE} \quad (62)$$

where the double excitation part is equal to the expression given by Eq. (59) after having replaced the cluster amplitudes by the corresponding RS correlation coefficients.

$(a|\tilde{q}^+)_{SE}$ is given as /22/

$$(a|\tilde{q}^+_{m\alpha})_{SE} = \sum_n \kappa_{\alpha}^n a_{mn} - \sum_{\beta} \kappa_{\beta}^m a_{\beta\alpha} \quad (63)$$

To make a structural analogue to the second order method also for transition probabilities and response properties, we consider an extended coupled cluster doubles polarization propagator approximation (E-CCDPPA), or the alternative linearized version (E-LCCDPPA), which includes the perturbation correction, $(a|\tilde{q}^+)_{SE}$ calculated as in Eq. (63), i.e. using RS

single excitation correlation coefficients.

Inclusion of T_1 in the reference state gives the CCSDPPA approach /25/ where the expressions for the matrix elements are analogous to those of E-CCDPPA. The only difference being that the second order RS correlation coefficients κ_α^m entering in Eq. (63) are replaced by t_α^m . Thus, the singles directly affect the transition matrix and modify the double excitation CC amplitudes.

Since correlation energies obtained from ACCD (Sec. 2.) are often very close to those of the full CCD method and since the ACCD iteration process is far less time-consuming than CCD, it was a logical step also to investigate the performance of the ACCD wavefunction as a reference state for the propagator /41/.

In Sec. 6. we give numerical comparisons between the perturbative and the CC polarization propagator methods presented in Sec. 3. and 4., but prior to this a diagrammatic order analysis of the method will be discussed.

5. ANALYSIS OF THE COUPLED CLUSTER POLARIZATION PROPAGATOR METHOD

By replacing $\kappa_{\alpha\beta}^{mn}$, κ_α^n with $t_{\alpha\beta}^{mn}$, t_α^n we effectively include additional series of diagrams summed to infinite orders. The first "new" diagrams, relative to SOPPA, appear in third order of perturbation theory. Exactly which diagrams we include can be seen by partitioning the principal propagator $P(E)$ (see Eqs. (36) and (38)). The particle-hole, particle-hole part is thus given as

$$P(E)_{ph,ph}^{-1} = ES - A - \tilde{C}(EI-D)^{-1}C - B(-ES - A - \tilde{C}(-EI-D)^{-1}C)^{-1}B \quad (64)$$

We can now identify the particle-hole self-energy diagrams by comparing with the complete diagrammatic analysis of the particle-hole self-energy $M(E)_{ph}$ of Paldus and Cizek /42/. This tells us to which order the particle-hole dominated excitation energies (but not transition moments and response properties) are determined. In fact, we need to consider

$$S^{-\frac{1}{2}} P_{ph,ph}^{-1} S^{-\frac{1}{2}} = E - M(E)_{ph} \quad (65)$$

to get the correct form of the self-energy, the definition of which follows from a comparison of Eqs. (64) and (65). Oddershede and Jørgensen /21/ have previously identified all contributions to $M(E)_{ph}$ through third order as obtained from the polarization propagator.

Since all four blocks of $P(E)^{-1}$ in Eq. (38) are computed through second order in the fluctuation potential at the SOPPA level, it follows that A, B, and S include terms up to second order and C and D are of order one and zero, respectively. We see from Eq. (64) that the second order B matrix, B(2), contributes to $P_{ph,ph}^{-1}$ in third and higher order, while A(2), C(1), and D(0) also give second order contributions to $M(E)_{ph}$. Proceeding to third order we may thus argue that, based on a diagrammatic analysis, the A(3) terms are more important than the B(3) terms as the latter matrix enters in fourth or higher orders in $M(E)_{ph}$. We have computed the three (see Eqs. (44)–(47)) A(3) terms for two cases where we know that we need to go beyond SOPPA in order to get a good description of the lowest excitation energies /17,25/. The results are given in Tables II and III. For Be (Table II) we used the [9s9p5d] basis set of Graham *et al.* /43/ for which the same authors also reported full CI calculations of several excitation energies. The quality of the basis set is so good that the full CI results (listed in Table II) differ by less than 0.04 eV from experiment for all the quoted excitations. For CH⁺ the calculations were performed using the 46 CGTO basis set of Larsson and Siegbahn /44/.

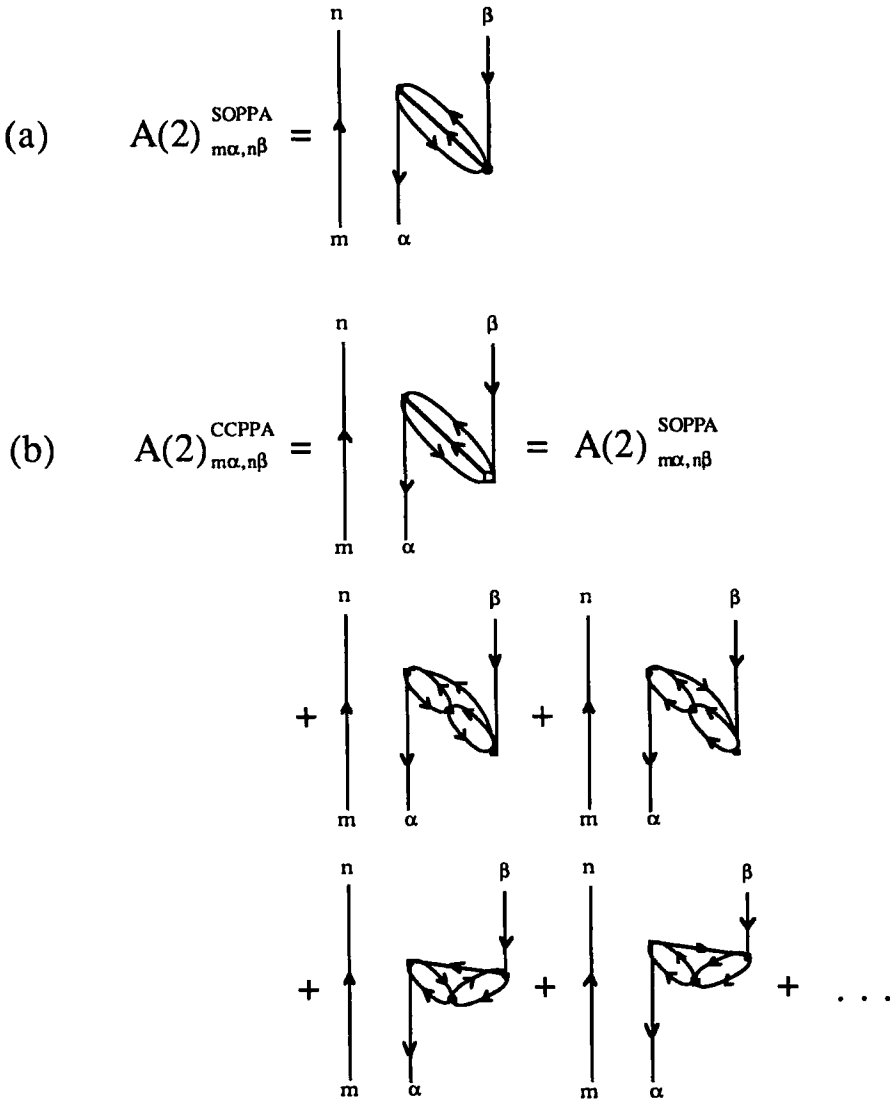
TABLE II. Excitation energies (in eV) from the ground state of Be atom.

Final state	SOPPA	SOPPA augmented by				CCDPPA	Full CI ^b
		A'(3)	A''(3)	A'''(3)	A(3) ^a		
2s2p; ¹ P	4.90	5.08	4.87	5.24	5.39	5.28	5.32
2s3s; ¹ S	6.47	6.56	6.40	6.73	6.75	6.87	6.77
2s3p; ¹ P	7.10	7.20	7.06	7.37	7.42	7.51	7.46
2s3d; ¹ D	7.39	7.47	7.33	7.64	7.66	7.79	8.03
2s4s; ¹ S	7.72	7.77	7.66	7.98	7.97	8.16	8.08
2s4p; ¹ P	7.95	8.00	7.89	8.20	8.20	8.38	8.30
2s4d; ¹ D	8.08	8.12	8.02	8.34	8.32	8.53	8.54
2s2p; ³ P	1.82	2.14	1.80	2.23	2.52	2.46	2.73
2s3s; ³ S	6.01	6.14	5.98	6.27	6.37	6.40	6.44
2s3p; ³ P	6.90	7.00	6.84	7.16	7.20	7.30	7.30
2s3d; ³ D	7.35	7.44	7.30	7.61	7.64	7.76	7.74
2s4s; ³ S	7.60	7.66	7.54	7.85	7.86	8.03	7.99
2s4p; ³ P	7.89	7.94	7.83	8.14	8.14	8.32	8.27
2s4d; ³ D	8.07	8.11	8.01	8.33	8.31	8.52	8.45

^aA(3) = A'(3) + A''(3) + A'''(3).

^bGraham *et al.* /43/ using the same basis set as the present study except for the exclusion of the s-component of the Cartesian d-functions in the full CI calculation.

The results in Tables II and III demonstrate that: (1) it is important to go beyond the SOPPA method for the two systems, (2) the A(3) matrix gives a large fraction of the difference between SOPPA and experiment/full CI, (3) the A''(3) matrix is only of minor importance ($\sim \pm 0.02$ eV), and (4) the A'(3) matrix gives a positive contribution to the excitation energy, the magnitude of which is about 1/2 to 1/3 of the *dominant* A'''(3) matrix. We see from Eq. (47) that A'''(3) is the lowest order new term added to SOPPA when performing a CCDPPA calculation. Diagrammatically this is illustrated in Fig. 1 where we give a representation of the A(2) matrix included in SOPPA (Fig. 1a), the "renormalized" A(2)^{CCPPA} matrix

Fig. 1


The Hugenholtz representation of half of the $A(2)$ matrix elements in (a) SOPPA and (b) in CCPPA. The coupled cluster double excitation amplitudes are represented by . The full $A(2)$ matrices are obtained by adding the particle-hole transformed counterparts of all the diagrams in the Figure.

TABLE III. Vertical excitation energies (in eV) from the ground state of the CH^+ ion^a.

Excitation	SOPPA	SOPPA augmented by				CCDPPA	Exp. ^c
		A'(3)	A''(3)	A'''(3)	A(3) ^b		
$X^1\Sigma^+ \rightarrow A^1\Pi$	2.54	2.81	2.56	2.97	3.25	3.05	3.07
$X^1\Sigma^+ \rightarrow ^3\Pi(1)$	inst. ^d	inst. ^d	inst. ^{d,e}	inst. ^{d,e}	0.82	1.01	—

^aAt the ground state equilibrium.

^b $A(3) = A'(3) + A''(3) + A'''(3)$.

^cBotterud *et al.* /45/.

^dInstability of the method for triplet excitations.

^eAddition of both $A''(3)$ and $A'''(3)$ to SOPPA removes the instability (0.80 eV).

where $\kappa_{\alpha\beta}^{mn}$ is replaced by $t_{\alpha\beta}^{mn}$ (Fig. 1b), and finally an iterated representation of the latter matrix element which shows that the first non-SOPPA parts of it are the $A'''(3)$ matrix elements (see e.g. Fig. 7 in Oddershede and Jørgensen /21/). Thus, the examples in Tables II and III indicate that $A(3)$ is the most important correction to the SOPPA method and that of the three different terms contributing to $A(3)$, the term which is included in the CCDPPA, i.e. $A'''(3)$, is the largest.

From the similarities of the CCDPPA and the *SOPPA augmented by* $A'''(3)$ excitation energies in Tables II and III we can see that $A'''(3)$ makes up a large fraction of the difference between SOPPA and CCDPPA. This is further illustrated in Table IV where we have considered a serial inclusion of the various matrices that form the difference between SOPPA and CCSDPPA. Including all CC corrections to the pure $A(2)$ matrix increases the excitation energies by approximately 0.5 eV, that is, an extra ~ 0.2 eV relative to what was obtained when the lowest order term alone, $A'''(3)$, was added. However, these extra positive contributions to the excitation energies are offset by small negative CC effects from the other matrices, primarily $S(2)^{\text{CC}}$, so that the overall effect is that CCSDPPA does not deviate much from just SOPPA augmented with $A'''(3)$. In agreement

TABLE IV. Excitation energies (in eV) from the ground state of the Be atom at various levels of approximations of coupled cluster singles and doubles polarization propagator theory.

Final state	SOPPA augmented by ^a		
	$A(2)^{CC}$	$A(2)^{CC};S(2)^{CC}$	$A(2)^{CC};S(2)^{CC};B(2)^{CC}$
2s2p; ¹ P	5.54	5.40	5.30 ^b
2s3s; ¹ S	6.94	6.88	6.89 ^b
2s3p; ¹ P	7.60	7.54	7.53 ^b
2s3d; ¹ D	7.86	7.81	7.81 ^b
2s4s; ¹ S	8.20	8.17	8.18 ^b
2s4p; ¹ P	8.43	8.40	8.40 ^b
2s4d; ¹ D	8.56	8.54	8.55 ^b
2s2p; ³ P	2.58	2.28	2.48 ^b
2s3s; ³ S	6.49	6.41	6.41 ^b
2s3p; ³ P	7.38	7.32	7.32 ^b
2s3d; ³ D	7.83	7.78	7.78 ^b
2s4s; ³ S	8.07	8.04	8.05 ^b
2s4p; ³ P	8.36	8.34	8.34 ^b
2s4d; ³ D	8.55	8.53	8.55 ^b

^aThe $A(2)^{CC}$, $S(2)^{CC}$, and $B(2)^{CC}$ matrices are obtained from the corresponding SOPPA second order matrices by replacing the first order Rayleigh-Schrödinger coefficients with the CC $t_{\alpha\beta}^{mn}$ coefficients from a CCSD calculation.

^bIdentical to the CCSD polarization propagator approximation (CCSDPPA).

with our expectations based on diagrammatic arguments we note that the extra correlation added to the $B(2)$ matrix by the CC approach has little effect on the excitation energies. However, it should be pointed out that this conclusion does not hold for the *lowest* excitation energies, in particular in the triplet case (cf. Tables III and IV).

As a last point we observe that it does not matter much for the exci-

tation energies whether we use CCSD $t_{\alpha\beta}^{mn}$ correlation coefficients (CCSDPPA in Table IV) or CCD $t_{\alpha\beta}^{mn}$ correlation coefficients (CCDPPA in Table II) in the coupled cluster polarization propagator approximations.

6. NUMERICAL ILLUSTRATIONS

Instead of giving a complete survey of all the properties that may advantageously be calculated using CCPPA we will illustrate the performance of the method for a range of properties for the molecule, the CH^+ ion, that was also the first example treated by the method /17/. The lowest singlet and triplet excitation energies have already been presented in Table III where it is seen that: (1) the SOPPA triplet instability is removed in CCPPA and (2) the CCPPA singlet result is in good agreement with experiment. Table V displays the convergency behavior of $\Delta\epsilon_S$ and $\Delta\epsilon_T$ for CH^+ in the LCCD case. It is interesting to note that the triplet instability

TABLE V. Convergence of the lowest singlet, $\Delta\epsilon_S$ and triplet, $\Delta\epsilon_T$ excitation energies in CH^+ (eV)^a.

Iteration no.	LCCD correlation energy	$\Delta\epsilon_S$	$\Delta\epsilon_T$
1 ^b	-0.09673	2.623	inst.
2	-0.11570	2.924	0.423
3	-0.12236	3.045	0.777
4	-0.12554	3.108	0.911
7	-0.12904	3.185	1.045
10	-0.12998	3.210	1.079
13	-0.13031	3.219	1.091
16	-0.13044	3.224	1.095
19	-0.13050	3.226	1.097
22	-0.13053	3.227	1.098
25	-0.13055	3.227	1.099
∞	-0.13056	3.228	1.099

^aLCCDPPA results using a [5s4p1d/3s1p] basis set /17/.

^bSecond order MBPT correlation energy and SOPPA singlet excitation energy (triplet instability).

is removed already in the second iteration. Clearly, it is not necessary to make the correlation energy converge to five decimal places to get acceptable converged excitation energies. This is essential since the CC iterative procedure is computationally the most expensive part of the calculation.

In Table VI the electronic transition moment and oscillator strengths for the $X^1\Sigma^+ \rightarrow A^1\Pi$ transition are reported. Compared with the effects seen on excitation energies only minor changes are observed for these properties when going from RPA, SOPPA to the more correlated CC approximations. For the radiative lifetime of the $A^1\Pi$ state, however, which depends on both excitation energies (to the third power) and the square of the transition moment, the CCPPA results are in much better agreement with experiment than those of the perturbative methods; see Table VII.

TABLE VI. The $X^1\Sigma^+ \rightarrow A^1\Pi$ transition moment (a.u.) and oscillator strength in CH^+ . Dipole length formalism^a.

	Transition moment ^b	Oscillator strength
RPA	0.2982	0.0115
SOPPA	0.2879	0.0103
LCCDPPA	0.2773	0.0120
E-LCCDPPA	0.2788	0.0121
CCDPPA	0.2798	0.0117
E-CCDPPA	0.2813	0.0119
Other work		
CI ^c		0.0147
CASSCF ^d	0.2691	0.0115

^aSame basis set as in Table III.

^bThe $\langle X^1\Sigma^+ | x | A^1\Pi_x \rangle$ component.

^cRef. 46.

^dRef. 44.

TABLE VII. Radiative lifetime (in ns) for the ground vibrational level of the $A^1\Pi$ state in CH^+ .

RPA	696
SOPPA	755
LCCDPPA	814
E-LCCDPPA	805
CCDPPA	799
E-CCDPPA	791
Experiment ^a	815±25
Other work	
CASSCF ^b	900
CASSCF, renormalized ^b	850

^aRef. 47.^bRef. 58.

The improvements obtained for CH^+ in the CC approaches mainly stem from the fact that excitations into the low-lying 1π orbital are much better described by the CC propagator methods. From Table VIII, which compares some of the most important correlation coefficients with the corresponding cluster amplitudes, it is seen that primarily the coefficients describing double excitations from 3σ into 1π are markedly different.

TABLE VIII. MBPT correlation coefficients and cluster amplitudes for some of the lowest double excitations in CH^+ .

Hole and particle indices		$\kappa_{\alpha\beta}^{mn}[1]^a$	$t_{\alpha\beta}^{mn}[1]^b$
$(1\sigma, 1\sigma)$	$(1\pi, 1\pi)$	-0.0014	-0.0009
$(1\sigma, 2\sigma)$	$(1\pi, 1\pi)$	-0.0028	-0.0026
$(1\sigma, 3\sigma)$	$(1\pi, 1\pi)$	-0.0016	-0.0010
$(2\sigma, 2\sigma)$	$(1\pi, 1\pi)$	-0.0894	-0.1362
$(2\sigma, 3\sigma)$	$(1\pi, 1\pi)$	-0.0438	-0.0865
$(3\sigma, 3\sigma)$	$(1\pi, 1\pi)$	-0.0755	-0.2068

^aUsed in SOPPA.^bUsed in CCPPA.

TABLE IX. List of CCPPA calculations.

System	GTO's	Reference state	Property ^a	Reference
CH ⁺	29,42	LCCD,CCD	$\Delta\epsilon, M, f, \tau$	Geertsen and Oddershede /17/
CH ⁺	42	LCCD,CCD	J_{AB}	Geertsen /49/
C ₂ H ₂	24	CCD	J_{AB}	Geertsen /49/
Be	66	CCD,CCSD	$\Delta\epsilon, f$	Geertsen <i>et al.</i> /25/
HF	72	CCD,CCSD	J_{AB}	Geertsen <i>et al.</i> /25/
CH ⁺	46	ACCD	$\Delta\epsilon, \tau$	Geertsen /41/
Be	66	ACCD	$\Delta\epsilon$	Geertsen /41/
HD	50-94	CCSD	$J_{AB}(R), J_{AB}(v, T), \Delta J$	Oddershede <i>et al.</i> /50/
Li ⁻	28-76	CCD,CCSD, CCSDT-1	$\alpha(0)$	Canuto <i>et al.</i> /51/
Li ⁻	46	CCSDT-1	$f, \text{photodetachment cross section}$	Canuto <i>et al.</i> /52/
BH	65	CCD,CCSD	$\Delta\epsilon(R), M(R), \tau, J_{AB}$	Scuseria <i>et al.</i> /53/
AlH	89	CCD,CCSD	$\Delta\epsilon, M(R), \tau, J_{AB}$	Scuseria <i>et al.</i> /53/
H ₂ O	44-101	CCSD	μ	Geertsen <i>et al.</i> /54/
ArH ⁺	71-93	CCSD	μ, g	Geertsen and Scuseria /55/
CH ₄	51-109	CCSD	$J_{AB}(R), J_{AB}(v, T), \Delta J$	Geertsen <i>et al.</i> /56/

TABLE IX (continued)

^aNotation for various properties

$\Delta\epsilon$	vertical excitation energy
M	transition moment
f	oscillator strength
τ	radiative lifetime
J_{AB}	nuclear spin-spin coupling constant
ΔJ	isotope shift of coupling constant
$\alpha(0)$	static polarizability
μ	dipole moment
g	rotational g factor

Symbols used in parentheses

R:	the property is calculated as a function of internuclear coordinates
v:	vibrational averaging
T:	temperature averaging

This observation suggests that it should be possible to 'freeze' some of the orbitals in the CC iteration process with only minor loss in accuracy on the computed excitation energies and response properties; and this has in fact been found to hold in direct calculations /48/.

In Table IX we give a complete compilation of papers in which we have applied the CCPPA method. Of particular computational importance is the work of Geertsen /41/ where it was shown that even with an ACCD reference state (where the most time-consuming terms in the CCD equations are neglected; see Sec. 2.), nearly all the CC effect is retained. This tells us that the so-called ACCDPPA should be an effective method for larger systems for which full CCSD calculations might not be possible.

Let us furthermore mention the work of Geertsen *et al.* /54/ where it was shown that also ground state average values like the electric dipole moment can be determined within the framework of propagators. In a test calculation for H₂O /54/ it was demonstrated that CCPPA works better than finite field MBPT (4)-SDQ and the analytic CCSD gradient method.

7. CONCLUSIONS

We have described a spin-adapted formulation of the CCSD method which is apt for subsequent use in the coupled cluster polarization propagator approximation (CCPPA). After a brief review of the perturbative polarization propagator methods (see e.g. Table I) we introduce the CCPPA method by requiring that when using the first iteration of the CC coefficients in the CCPPA method we obtain the second order polarization propagator approximation (SOPPA). We have thus maintained the same kind of relation between CCPPA and SOPPA as there exists between, for instance, MBPT (2) and CCD calculations of ground state correlation energies: in the first iteration of the coupled cluster method we get the MBPT-based solution.

We then continue to analyze the extra terms that the iterated CCPPA method introduces relative to SOPPA. Based on a diagrammatic representation (Fig. 1) we argue that the most important correlation contributions are expected to show up in the A matrix. A calculation of all the three third order contributions to A shows that the most important of these three terms, the $A'''(3)$ term, is in fact the one that is included in CCPPA. Furthermore, $A'''(3)$ gives most of the difference between SOPPA and CCPPA, thus demonstrating that terms beyond third order in A as well as corrections to the other propagator matrices (B and S) are not so important.

A few examples of CCPPA calculations, together with a complete summary of all applications of the method (Table IX), ends the review. These examples show that excitation energies are more affected by the extra correlation introduced by the CC method than are transition moments. We also demonstrate that the difference between CCPPA and SOPPA is due to an enhancement of the cluster amplitudes, $t_{\alpha\beta}^{mn}$, relative to RS correlation coefficients, $\kappa_{\alpha\beta}^{mn}$, for low-lying double excited states. This means that the perturbation expansion based on $t_{\alpha\beta}^{mn}$ (CCPPA) is much faster convergent than the one based on $\kappa_{\alpha\beta}^{mn}$ (SOPPA). We would hence

expect a considerable improvement of CCPPA over SOPPA for systems with low-lying excited states. Table IX contains several such cases (CH^+ , Be, Li^- , BH and AlH). However, even in some of the other cases (HD and CH_4 , for example) do we find a significant, but small effect of introducing a CC reference state.

Computationally, there is no difference in the propagator part of the calculation whether we do a SOPPA or a CCPPA calculation. In fact, it is very simple to change a SOPPA program into a CCPPA program. One only needs to replace $\kappa_{\alpha\beta}^{mn}$ with $t_{\alpha\beta}^{mn}$ (and perhaps κ_{α}^m with t_{α}^m). The rate determining step is the CC calculation. Here it is useful to note that the outcome of a CCPPA calculation is nearly the same whether we use cluster amplitudes from a full CCSD calculation or from the much simpler ACCD method /41/.

APPENDIX A. SPIN-ADAPTED COUPLED CLUSTER SINGLES AND DOUBLES EQUATIONS

The CCSD equations satisfied by single excitation amplitudes t_{α}^m can be obtained from Eq. (13a)

$$\langle \text{HF} | q(0,0)_{m\alpha} (H - E_{\text{CCSD}}) (1 + T_1 + T_2 + \frac{1}{2}T_1^2 + T_1T_2 + \frac{1}{3!}T_1^3) | \text{HF} \rangle = 0 \quad (\text{A1})$$

Using Eqs. (4), (5), and (12) we get

$$\begin{aligned} (E_{\alpha} - E_m) t_{\alpha}^m &= \sum_{\frac{a}{\pi}} \{ 2(m\alpha | \pi a) - (m\alpha | \pi \alpha) \} t_{\pi}^a \\ &+ \sum_{\frac{ab}{\pi}} (\pi a | mb) A_{\pi\alpha}^{ab} - \sum_{\frac{\alpha\delta}{\pi}} (\pi a | \delta\alpha) A_{\pi\delta}^{a\alpha} \\ &- \sum_{\frac{ab}{\pi\sigma}} (a\pi | b\sigma) \{ t_{\alpha}^a B_{\pi\sigma}^{mb} + t_{\pi}^m B_{\alpha\sigma}^{ab} \\ &+ t_{\sigma}^a C_{\alpha\pi}^{mb} [1] - 2t_{\sigma}^b C_{\alpha\pi}^{ma} [1] \} \end{aligned} \quad (\text{A2})$$

where

$$A_{rs}^{ab} = \sqrt{2} (C_{rs}^{ab} [1] + t_r^a t_s^b) \quad (\text{A3})$$

$$B_{rs}^{ab} = \frac{1}{2} (t_{rs}^{ab} [1] + \sqrt{3} t_{rs}^{ab} [2]) \quad (\text{A4})$$

$$C_{rs}^{ab} [i] = \sqrt{2i-1} (B_{rs}^{ab} - \frac{1}{2} t_s^a t_r^b) \quad ; \quad i = 1, 2 \quad (\text{A5})$$

Eq. (13b) gives the equations satisfied by $t_{\alpha\beta}^{mn}[i]$

$$\langle \text{HF} | S[i]_{\text{m}\alpha\text{n}\beta} (H - E_{\text{CCSD}}) (1 + T_1 + T_2 + \frac{1}{2}T_1^2 + T_1T_2 + \frac{1}{2}T_2^2 + \frac{1}{2}T_1^2T_2 + \frac{1}{3!}T_1^3 + \frac{1}{4!}T_1^4) | \text{HF} \rangle = 0 \quad ; \quad i = 1, 2 \quad (\text{A6})$$

or

$$D_{\alpha\beta\text{mn}} t_{\alpha\beta}^{\text{mn}}[i] = \Delta_{\alpha\beta}^{\text{mn}}[i] + \Phi_{\alpha\beta}^{\text{mn}}[i] + \Gamma_{\alpha\beta}^{\text{mn}}[i] + \Pi_{\alpha\beta}^{\text{mn}}[i] + \Omega_{\alpha\beta}^{\text{mn}}[i] \quad ; \quad i = 1, 2 \quad (\text{A7})$$

where $D_{\alpha\beta\text{mn}}$, $\Delta_{\alpha\beta}^{\text{mn}}[i]$ are given by Eqs. (17) and (18), respectively, and

$$\Phi_{\alpha\beta}^{\text{mn}}[i] = [1 + P(\text{mn})P(\alpha\beta)] \left\{ \sum_c E_{\text{n}\beta}^{\text{c}\text{m}} t_{\alpha}^{\text{c}} - \sum_{\mu} E_{\beta\mu}^{\text{m}\alpha} t_{\mu}^{\text{n}} \right\} \quad (\text{A8})$$

$$\begin{aligned} \Gamma_{\alpha\beta}^{\text{mn}}[i] = & (1 - \delta_{\text{mn}})^{i-1} \sum_{\text{cd}} (\text{mc} | \text{nd}) F_{\alpha\beta}^{\text{cd}}[i] \\ & + (1 - \delta_{\alpha\beta})^{i-1} \sum_{\mu\nu} (\mu\alpha | \nu\beta) F_{\mu\nu}^{\text{mn}}[i] \\ & - [1 + (-1)^{i+1} \{P(\alpha\beta) + P(\text{mn})\} + P(\alpha\beta)P(\text{mn})] \\ & \sum_{\mu\text{c}} \{ (\mu\beta | \text{nc}) G_{\alpha\mu}^{\text{mc}}[i] - (\mu\text{c} | \text{n}\beta) C_{\alpha\mu}^{\text{mc}}[i] \} \end{aligned} \quad (\text{A9})$$

$$\begin{aligned} \Pi_{\alpha\beta}^{\text{mn}}[i] = & [1 + (-1)^{i+1}P(\text{mn})] \sum_{\pi}^{ab} (a\pi | \text{nb}) \Pi_{\pi\alpha\beta}^{\text{amb}}[i] \\ & - [1 + (-1)^{i+1}P(\alpha\beta)] \sum_{\pi}^{a} (a\pi | \beta\sigma) I_{\pi\alpha\delta}^{\text{amb}}[i] \end{aligned} \quad (\text{A10})$$

$$\begin{aligned}
\Omega_{\alpha\beta}^{mn}[i] = & -[(1-\delta_{\alpha\beta})(1-\delta_{mn})]^{i-1} \sum_{\substack{\mu\nu \\ \text{cd}}} (\mu c | \nu d) \\
& \{ [1+(-1)^{i+1}P(\alpha\beta)] M_{\alpha\mu\beta\nu}^{mncd}[i] \\
& - L_{\alpha\beta\mu\nu}^{cdmn}[i] + [1+(-1)^{i+1}P(mn)] [M_{\alpha\beta\mu\nu}^{mncd}[i] \\
& - N_{\alpha\mu\beta\nu}^{mdnc}[i] - (2i-1)^{-\frac{1}{2}} C_{\alpha\mu}^{mc}[i] C_{\beta\nu}^{nd}[i]] \}
\end{aligned} \tag{A11}$$

The following definitions have been used

$$E_{rs}^{ab}[i] = \sqrt{i-1} \{ ab|rs \} - (-1)^i (ar|bs) \} \tag{A12}$$

$$F_{rs}^{ab}[i] = t_{rs}^{ab}[i] + \left(\frac{1}{2}\sqrt{2i-1}\right) \{ t_r^a t_s^b - (-1)^i t_r^b t_s^a \} \tag{A13}$$

$$G_{rs}^{ab}[i] = t_{rs}^{ab}[i] - \left(\frac{1}{2}\right) (-1)^i \sqrt{2i-1} t_s^a t_r^b \tag{A14}$$

$$H_{rsu}^{abc}[i] = \eta_{rsu}^{abc}[i] - t_r^b \gamma_{su}^{ac}[i] + [1 + (-1)^{i+1}P(su)] \rho_{sru}^{cba}[i] \tag{A15}$$

$$I_{rsu}^{abc}[i] = \tilde{\eta}_{rsu}^{abc}[i] - t_s^a \gamma_{ru}^{bc}[i] + [1 + (-1)^{i+1}P(bc)] \tilde{\rho}_{usr}^{bac}[i] \tag{A16}$$

$$\eta_{rsu}^{abc}[i] = \frac{1}{\sqrt{2}} [2 - P(ac)] t_r^a t_{su}^{bc}[i] \tag{A17}$$

$$\tilde{\eta}_{rsu}^{abc}[i] = \frac{1}{\sqrt{2}} [2 - P(ru)] t_r^a t_{su}^{bc}[i] \tag{A18}$$

$$\gamma_{rs}^{ab}[i] = \frac{1}{2\sqrt{2}} \{ 2t_{rs}^{ab}[i] + \frac{1}{3}\sqrt{2i-1} [1 + (-1)^{i+1}P(rs)] t_r^a t_s^b \} \tag{A19}$$

$$\rho_{rsu}^{abc}[i] = J_{rsu}^{abc}[i] - K_{rsu}^{cba}[i] \tag{A20}$$

$$\tilde{\rho}_{rsu}^{abc}[i] = J_{rsu}^{abc}[i] - K_{usr}^{abc}[i] \tag{A21}$$

$$J_{rsu}^{abc}[i] = \frac{(-1)^{i+1}}{2\sqrt{2}} \sqrt{2i-1} t_r^a [t_{su}^{bc}[1] - \sqrt{3} t_{su}^{bc}[2] - \frac{1}{3} t_s^b t_u^c] \quad (A22)$$

$$K_{rsu}^{abc}[i] = \frac{1}{2\sqrt{2}} t_r^a [2t_{su}^{bc}[i] + \frac{1}{3}\sqrt{2i-1} t_s^b t_u^c] \quad (A23)$$

$$L_{rsuv}^{abcd}[i] = \frac{1}{2} \left[\frac{1}{\sqrt{2i-1}} t_{rs}^{ab}[i] t_{uv}^{cd}[i] + \{t_{rs}^{ab}[i] t_u^c t_v^d + t_r^a t_s^b t_{uv}^{cd}[i]\} \right] \quad (A24)$$

$$M_{rsuv}^{abcd}[i] = \frac{1}{\sqrt{2}} t_{rs}^{ab}[i] A_{uv}^{cd} \quad (A25)$$

$$N_{rsuv}^{abcd}[i] = \frac{1}{4} \left[(-1)^{i-1} t_{rs}^{ab}[1] \{ \sqrt{2i-1} t_{uv}^{cd}[i] + (-1)^i 3^{(2-i)/2} t_{uv}^{cd}[2] \} \right. \\ \left. - t_{rs}^{ab}[2] \{ 3^{(2-i)/2} t_{uv}^{cd}[1] + \left(\frac{5}{\sqrt{3}} \right)^{i-1} t_{uv}^{cd}[2] \} \right. \\ \left. + 2 \{ t_{rs}^{ab}[i] t_v^c t_u^d + t_{uv}^{cd}[i] t_s^a t_r^b \} \right] \quad (A26)$$

APPENDIX B. SPIN-ADAPTED MATRIX ELEMENT OF A(3)

The third order A matrix elements are defined in Eqs. (45)–(47). Introducing the spin-adapted double excitation operators of Eqs. (7) and (8) in the singlet case and the corresponding three operators /29/ for singlet to triplet 2p–2h excitations we find that

$$A'(3)_{m\alpha, n\beta} =$$

$$\begin{aligned} & -\delta_{nm} \left[\frac{1}{4} \sum_{\pi\gamma\delta}^{\text{ab}} \{ (\beta\gamma | \pi\alpha) - 2(\beta\alpha | \pi\gamma) \} \{ \kappa_{\pi\delta}^{\text{ab}}[1] \kappa_{\gamma\delta}^{\text{ab}}[1]^* + \kappa_{\pi\delta}^{\text{ab}}[2] \kappa_{\gamma\delta}^{\text{ab}}[2]^* \} \right. \\ & + \frac{1}{4} \sum_{\pi\delta}^{\text{aqb}} \{ 2(\beta\alpha | qa) - (\beta a | q\alpha) \} \{ \kappa_{\pi\delta}^{\text{ab}}[1] \kappa_{\pi\delta}^{\text{qb}}[1]^* + \kappa_{\pi\delta}^{\text{ab}}[2] \kappa_{\pi\delta}^{\text{qb}}[2]^* \} \\ & + \frac{1}{4} \sum_{\pi\delta\gamma}^{\text{ab}} (\beta\delta | \gamma\pi) \{ \kappa_{\gamma\alpha}^{\text{ab}}[1] \kappa_{\pi\delta}^{\text{ab}}[1]^* + \kappa_{\gamma\alpha}^{\text{ab}}[2] \kappa_{\pi\delta}^{\text{ab}}[2]^* \} \\ & - \frac{1}{2} \sum_{\pi\delta}^{\text{abq}} (\beta\delta | aq) \{ \kappa_{\pi\alpha}^{\text{qb}}[1] \kappa_{\pi\delta}^{\text{ab}}[1]^* + \kappa_{\pi\alpha}^{\text{qb}}[2] \kappa_{\pi\delta}^{\text{ab}}[2]^* \} \\ & + \frac{1}{4} \sum_{\pi\delta}^{\text{abq}} (\beta q | a\pi) \{ \kappa_{\alpha\delta}^{\text{qb}}[1] + \sqrt{3} \kappa_{\alpha\delta}^{\text{qb}}[2] \}^* \{ \kappa_{\pi\delta}^{\text{ab}}[1] + \sqrt{3} \kappa_{\pi\delta}^{\text{ab}}[2] \}^* \} \\ & - \delta_{\alpha\beta} \left[\frac{1}{4} \sum_{\pi\delta}^{\text{abq}} \{ (qn | ma) - 2(mn | qa) \} \{ \kappa_{\pi\delta}^{\text{ab}}[1]^* \kappa_{\pi\delta}^{\text{qb}}[1] + \kappa_{\pi\delta}^{\text{ab}}[2]^* \kappa_{\pi\delta}^{\text{qb}}[2] \} \right. \\ & \left. + \frac{1}{4} \sum_{\pi\delta\gamma}^{\text{ab}} \{ 2(mn | \pi\gamma) - (\pi n | m\gamma) \} \{ \kappa_{\pi\delta}^{\text{ab}}[1]^* \kappa_{\gamma\delta}^{\text{ab}}[1] + \kappa_{\pi\delta}^{\text{ab}}[2]^* \kappa_{\gamma\delta}^{\text{ab}}[2] \} \right] \end{aligned}$$

$$\begin{aligned}
& + \frac{1}{4} \sum_{\substack{abq \\ \pi\delta}} (bn|aq) \{ \kappa_{\pi\delta}^{qm}[1] * \kappa_{\pi\delta}^{ab}[1] + \kappa_{\pi\delta}^{qm}[2] * \kappa_{\pi\delta}^{ab}[2] \} \\
& - \frac{1}{2} \sum_{\substack{ab\gamma \\ \pi\delta}} (bn|\gamma\pi) \{ \kappa_{\gamma\delta}^{am}[1] * \kappa_{\pi\delta}^{ab}[1] + \kappa_{\gamma\delta}^{am}[2] * \kappa_{\pi\delta}^{ab}[2] \} \\
& + \frac{1}{4} \sum_{\substack{ab\gamma \\ \pi\delta}} (\gamma n|a\pi) \{ \kappa_{\gamma\delta}^{mb}[1] + \sqrt{3} \kappa_{\gamma\delta}^{mb}[2] \} * \{ \kappa_{\pi\delta}^{ab}[1] + \sqrt{3} \kappa_{\pi\delta}^{ab}[2] \} \\
& + \frac{1}{4} \sum_{\substack{bg \\ \pi\delta}} [(\beta\alpha|qb) + (\beta b|q\alpha)] \kappa_{\pi\delta}^{mb}[1] \kappa_{\pi\delta}^{nq}[1] * \\
& + \frac{1}{4} \sum_{\substack{bg \\ \pi\delta}} [(\beta\alpha|qb) - (\beta b|q\alpha)] \kappa_{\pi\delta}^{mb}[2] \kappa_{\pi\delta}^{nq}[2] * \\
& - \frac{S}{2} \sum_{\substack{bg \\ \pi\delta}} [(\beta b|q\alpha) \{ \kappa_{\pi\delta}^{mb}[1] \kappa_{\pi\delta}^{nq}[1] * - \frac{1}{3} \kappa_{\pi\delta}^{mb}[2] \kappa_{\pi\delta}^{nq}[2] * \} \\
& - \frac{1}{2} \sum_{\substack{bg \\ \pi\delta}} (\beta\alpha|\pi\gamma) \{ \kappa_{\pi\delta}^{mb}[1] \kappa_{\gamma\delta}^{nb}[1] * + \kappa_{\pi\delta}^{mb}[2] \kappa_{\gamma\delta}^{nb}[2] * \} \\
& + \frac{1}{4} \sum_{\substack{bg \\ \pi\delta}} (\beta\gamma|\pi\alpha) \{ \kappa_{\pi\delta}^{mb}[1] + \frac{\sqrt{3}}{1-4S} \kappa_{\pi\delta}^{mb}[2] \} \{ \kappa_{\gamma\delta}^{ab}[1] + \frac{\sqrt{3}}{1-4S} \kappa_{\gamma\delta}^{nb}[2] \} * \\
& - \sum_{\substack{ab \\ \pi\delta}} \{ \frac{1-S}{2} (\beta b|m\alpha) - \frac{1}{4} (\beta\alpha|mb) \} \{ \kappa_{\pi\delta}^{ab}[1] \kappa_{\pi\delta}^{an}[1] * + \kappa_{\pi\delta}^{ab}[2] \kappa_{\pi\delta}^{an}[2] * \} \\
& - \sum_{\substack{ab \\ \pi\delta}} \{ \frac{1-S}{2} (m\pi|\beta n) - \frac{1}{4} (mn|\beta\pi) \} \{ \kappa_{\pi\delta}^{ab}[1] \kappa_{\alpha\delta}^{ab}[1] * + \kappa_{\pi\delta}^{ab}[2] \kappa_{\alpha\delta}^{ab}[2] * \}
\end{aligned}$$

$$\begin{aligned}
& -\frac{1}{4} \sum_{\substack{ab \\ \pi\gamma}} (\beta\gamma|mb) \{ \kappa_{\pi\alpha}^{ab}[1] + \frac{\sqrt{3}}{1-4S} \kappa_{\pi\alpha}^{ab}[2] \} \{ \kappa_{\gamma\pi}^{na}[1] + \frac{\sqrt{3}}{1-4S} \kappa_{\gamma\pi}^{na}[2] \}^* \\
& + \frac{1}{2} \sum_{\substack{ab \\ \pi\gamma}} (\beta b|m\gamma) \{ \kappa_{\pi\alpha}^{ab}[1] \kappa_{\gamma\pi}^{na}[1]^* + \kappa_{\pi\alpha}^{ab}[2] \kappa_{\gamma\pi}^{na}[2]^* \} \\
& - \frac{S}{2} \sum_{\substack{ab \\ \pi\gamma}} (\beta b|m\gamma) \{ \kappa_{\pi\alpha}^{ab}[1] - \frac{1}{\sqrt{3}} \kappa_{\pi\alpha}^{ab}[2] \} \{ \kappa_{\gamma\pi}^{na}[1] - \frac{1}{\sqrt{3}} \kappa_{\gamma\pi}^{na}[2] \}^* \\
& + \frac{1}{4} \sum_{\substack{ab \\ \gamma\delta}} [(mn|\delta\gamma) + (\delta n|m\gamma)] \kappa_{\alpha\delta}^{ab}[1]^* \kappa_{\beta\gamma}^{ab}[1] \\
& + \frac{1}{4} \sum_{\substack{ab \\ \gamma\delta}} [(mn|\delta\gamma) - (\delta n|m\gamma)] \kappa_{\alpha\delta}^{ab}[2]^* \kappa_{\beta\gamma}^{ab}[2] \\
& - \frac{S}{2} \sum_{\substack{ab \\ \gamma\delta}} (\delta n|m\gamma) \{ \kappa_{\alpha\delta}^{ab}[1]^* \kappa_{\beta\gamma}^{ab}[1] - \frac{1}{3} \kappa_{\alpha\delta}^{ab}[2]^* \kappa_{\beta\gamma}^{ab}[2] \} \\
& - \frac{1}{2} \sum_{\substack{ab \\ q\delta}} (mn|qa) \{ \kappa_{\alpha\delta}^{ab}[1]^* \kappa_{\beta\delta}^{qb}[1] + \kappa_{\alpha\delta}^{ab}[2]^* \kappa_{\beta\delta}^{qb}[2] \} \\
& + \frac{1}{4} \sum_{\substack{ab \\ q\delta}} (qn|ma) \{ \kappa_{\alpha\delta}^{ab}[1] + \frac{\sqrt{3}}{1-4S} \kappa_{\alpha\delta}^{ab}[2] \}^* \{ \kappa_{\beta\delta}^{qb}[1] + \frac{\sqrt{3}}{1-4S} \kappa_{\alpha\delta}^{ab}[2] \} \\
& - \sum_{\substack{ab \\ \pi\delta}} \{ \frac{1-S}{2} (\delta n|m\alpha) + \frac{1}{4} (mn|\delta\alpha) \} \{ \kappa_{\pi\delta}^{ab}[1]^* \kappa_{\pi\beta}^{ab}[1] + \kappa_{\pi\delta}^{ab}[2]^* \kappa_{\pi\beta}^{ab}[2] \} \\
& - \sum_{\substack{ab \\ \pi\delta}} \{ \frac{1-S}{2} (\alpha\alpha|\beta n) - \frac{1}{4} (\beta\alpha|an) \} \{ \kappa_{\pi\delta}^{ab}[1]^* \kappa_{\pi\delta}^{mb}[1] + \kappa_{\pi\delta}^{ab}[2]^* \kappa_{\pi\delta}^{mb}[2] \}
\end{aligned}$$

$$\begin{aligned}
& -\frac{1}{4} \sum_{\substack{a \\ \pi}} (q_n | \delta \alpha) \{ \kappa_{\pi \delta}^{am} [1] + \frac{\sqrt{3}}{1-4S} \kappa_{\pi \delta}^{am} [2] \}^* \{ \kappa_{\beta \pi}^{ga} [1] + \frac{\sqrt{3}}{1-4S} \kappa_{\beta \pi}^{ga} [2] \} \\
& + \frac{1}{2} \sum_{\substack{a \\ \pi}} (\delta n | q \alpha) \{ \kappa_{\pi \delta}^{am} [1] * \kappa_{\beta \pi}^{ga} [1] + \kappa_{\pi \delta}^{am} [2] * \kappa_{\beta \pi}^{ga} [2] \} \\
& - \frac{S}{2} \sum_{\substack{a \\ \pi}} (\delta n | q \alpha) \{ \kappa_{\pi \delta}^{am} [1] - \frac{1}{\sqrt{3}} \kappa_{\pi \delta}^{am} [2] \}^* \{ \kappa_{\beta \pi}^{ga} [1] - \frac{1}{\sqrt{3}} \kappa_{\beta \pi}^{ga} [2] \} \quad (B1)
\end{aligned}$$

where $S = 0, 1$ for singlet-to-singlet and singlet-to-triplet excitations, respectively. The RS correlation coefficients $\kappa_{\alpha\beta}^{mn}[i]$ are defined in Eq. (21).

The $A''(3)$ matrix involves the second order, singly excited states and can be expressed as

$$\begin{aligned}
A''(3)_{m\alpha, n\beta} = & -\frac{\sqrt{2}}{2} \delta_{nm} \sum_{a\pi} \{ [2(\beta\alpha | a\pi) - (\beta\pi | a\alpha)] \kappa_{\pi}^{a*} + [2(\beta\alpha | \pi a) - (\beta a | \pi\alpha)] \kappa_{\pi}^a \} \\
& -\frac{\sqrt{2}}{2} \delta_{\alpha\beta} \sum_{a\pi} \{ [(m\pi | an) - 2(mn | a\pi)] \kappa_{\pi}^{a*} + [(ma | \pi n) - 2(mn | \pi a)] \kappa_{\pi}^a \} \\
& -\sqrt{2}(1-S) \{ \sum_{\pi} [(\beta\pi | m\alpha) \kappa_{\pi}^{n*} + (\pi\alpha | \beta n) \kappa_{\pi}^m] \\
& - \sum_a [(m\alpha | an) \kappa_{\beta}^{a*} + (ma | \beta n) \kappa_{\alpha}^a] \}
\end{aligned}$$

$$-\frac{\sqrt{2}}{2} \left\{ \sum_a [(mn|a\alpha) \kappa_{\beta}^{a*} + (mn|\beta a) \kappa_{\alpha}^a] - \sum_{\pi} [(\beta\alpha|m\pi) \kappa_{\pi}^{n*} + (\beta\alpha|\pi n) \kappa_{\pi}^m] \right\} \quad (B2)$$

where κ_{α}^m is defined in Eq. (35).

The last third order matrix is given by the same expression as the $A(2)$ matrix (ref. 29, Eq. (C13)) *except that* whenever the $\kappa_{\alpha\beta}^{mn}[i]$ appears in the expression, it should be replaced by the second order doubly excited correlation coefficient

$$\begin{aligned} K_{\alpha\beta}^{mn}[i] = & [1 + \delta_{nm})(1 + \delta_{\alpha\beta})]^{-\frac{1}{2}} [(1 - \delta_{\alpha\beta})(1 - \delta_{nm})]^{i-1} (\epsilon_{\alpha} + \epsilon_{\beta} - \epsilon_n - \epsilon_m)^{-1*} \\ & * \left\{ \sum_{a\pi} [(2i-1)^{\frac{1}{2}} \left[\frac{1}{2} (\pi a|n\beta) \{ \kappa_{\alpha\pi}^{ma}[1] + \sqrt{3} \kappa_{\alpha\pi}^{ma}[2] \} \right. \right. \\ & - \frac{(-)^i}{2} (\pi a|n\alpha) \{ \kappa_{\beta\pi}^{ma}[1] + \sqrt{3} \kappa_{\beta\pi}^{ma}[2] \} \\ & - \frac{(-)^i}{2} (\pi a|m\beta) \{ \kappa_{\alpha\pi}^{na}[1] + \sqrt{3} \kappa_{\alpha\pi}^{na}[2] \} \\ & \left. \left. + \frac{1}{2} (\pi a|m\alpha) \{ \kappa_{\beta\pi}^{na}[1] + \sqrt{3} \kappa_{\beta\pi}^{na}[2] \} \right] \right\} \\ & - (\pi\beta|na) \kappa_{\alpha\pi}^{ma}[i] - (\pi\alpha|ma) \kappa_{\beta\pi}^{na}[i] \\ & + (-)^i \{ (\pi\beta|ma) \kappa_{\alpha\pi}^{na}[i] + (\pi\alpha|na) \kappa_{\beta\pi}^{ma}[i] \} \\ & + \sum_{ab} (ma|nb) \kappa_{\alpha\beta}^{ab}[i] + \sum_{\pi\delta} (\pi\alpha|\delta\beta) \kappa_{\pi\delta}^{mn}[i] \} \quad (B3) \end{aligned}$$

ACKNOWLEDGMENTS

The authors thank Poul Jørgensen for assistance in preparing Appendix B. This work was supported by a grant from the Danish Natural Science Research Council (Grant # 11-6844).

REFERENCES

1. Sinanoglu, O. (1962). *J. Chem. Phys.* **36**, 706 and 3198.
2. Sinanoglu, O. (1964). *Adv. Chem. Phys.* **6**, 315.
3. Nesbet, R. K. (1967). *Phys. Rev.* **156**, 99.
4. Cizek, J. (1966). *J. Chem. Phys.* **45**, 4256.
5. Cizek, J. (1969). *Adv. Chem. Phys.* **14**, 35.
6. Ahlrichs, R. (1983). In *Methods in Computational Molecular Physics* (G. H. F. Diercksen and S. Wilson, eds.), p. 209.
7. Simandiras, E. D., Amos, R. D., and Handy, N. C. (1987). *Chem. Phys.* **114**, 9; *Chem. Phys. Lett.* **133**, 324.
8. Hubbard, J. (1957). *Proc. Roy. Soc. A* **240**, 539.
9. Coester, F. (1958). *Nucl. Phys.* **7**, 421.
10. Coester, F., and Kümmel, H. (1960). *Nucl. Phys.* **17**, 477.
11. Bartlett, R. J. (1981). *Ann. Rev. Phys. Chem.* **32**, 359.
12. Nakatsuji, H., Ohta, K., and Hirao, K. (1981). *J. Chem. Phys.* **75**, 2952.
13. Takahashi, M., and Paldus, J. (1986). *J. Chem. Phys.* **85**, 1486.
14. Kaldor, U. (1986). *Intern. J. Quantum Chem. Symp.* **26**, 445.
15. Pal, S., Rittby, M., Bartlett, R. J., Sinha, D., and Mukherjee, D. (1988). *J. Chem. Phys.* **88**, 4357.
16. Geertsens, J., Rittby, M., and Bartlett, R. J. (1989). *Chem. Phys. Lett.* **164**, 57.
17. Geertsens, J., and Oddershede, J. (1986). *J. Chem. Phys.* **85**, 2112.
18. Oddershede, J. (1987). *Adv. Chem. Phys.* **69**, 201.
19. Olsen, J., and Jørgensen, P. (1985). *J. Chem. Phys.* **82**, 3235.

20. Pickup, B. T., and Goscinski, O. (1973). *Mol. Phys.* **26**, 149.
21. Oddershede, J., and Jørgensen, P. (1977). *J. Chem. Phys.* **66**, 1541.
22. Nielsen, E. S., Jørgensen, P., and Oddershede, J. (1980). *J. Chem. Phys.* **73**, 6238.
23. Yeager, D. L., and Jørgensen, P. (1979). *Chem. Phys. Lett.* **65**, 77.
24. Linderberg, J., and Öhrn, Y. (1977). *Intern. J. Quantum Chem.* **12**, 161.
25. Geertsen, J., Oddershede, J., and Scuseria, G. E. (1987). *Intern. J. Quantum Chem. Symp.* **21**, 475.
26. Kümmel, H. (1969). *Nucl. Phys.* **22**, 177.
27. Piecuch, P., and Paldus, J. (1989). *Intern. J. Quantum Chem.* **36**, 429.
28. Paldus, J., Adams, B. G., and Cizek, J. (1977). *Intern. J. Quantum Chem.* **11**, 813.
29. Oddershede, J., Jørgensen, P., and Yeager, D. L. (1984). *Compt. Phys. Rep.* **2**, 33.
30. Bartlett, R. J., and Shavitt, I. (1977). *Chem. Phys. Lett.* **50**, 190.
31. Bartlett, R. J., and Shavitt, I. (1978). *Chem. Phys. Lett.* **57**, 157.
32. Adams, B. G., Jankowski, K., and Paldus, J. (1979). *Chem. Phys. Lett.* **67**, 144.
33. Chiles, R. A., and Dykstra, C. E. (1981). *Chem. Phys. Lett.* **80**, 69.
34. Bartlett, R. J., and Purvis, G. D. (1978). *Physica Scripta* **21**, 255.
35. Laidig, W. D., Purvis, G. D., and Bartlett, R. J. (1982). *Intern. J. Quantum Chem. Symp.* **16**, 561.
36. Zubarev, D. N. (1960). *Usp. Fiz. Nauk.* **71**, 71; *Sov. Phys. Usp.* (Eng. Transl.) **3**, 320.
37. Linderberg, J., and Öhrn, Y. (1973). *Propagators in Quantum Chemistry*, Academic, London.
38. Jørgensen, P., and Simons, J. (1981). *Second Quantization-Based Methods in Quantum Chemistry*, Academic, New York.
39. Dalgaard, E. (1979). *Intern. J. Quantum Chem.* **15**, 169.
40. Sauer, S. P. A., Diercksen, G. H. F., and Oddershede, J. (1990) *Intern. J. Quantum Chem.*, in press.

41. Geertsen, J. (1988). *Intern. J. Quantum Chem. Symp.* **22**, 491.
42. Paldus, J., and Cizek, J. (1974). *J. Chem. Phys.* **60**, 149.
43. Graham, R. L., Yeager, D. L., Olsen, J. Jørgensen, P., Harrison, R., Zarrabian, S., and Bartlett, R. J. (1986). *J. Chem. Phys.* **85**, 6544.
44. Larsson, M., and Siegbahn, P. E. M. (1983). *Chem. Phys.* **76**, 175.
45. Botterud, I., Lofthus, A., and Veseth, L. (1973). *Physica Scripta* **8**, 218.
46. Yoshimine, M., Green, S., and Thaddeus, P. (1973). *Astrophys. J.* **183**, 899.
47. Mahan, B. M., and O'Keefe, A. (1981). *Astrophys. J.* **248**, 1209.
48. Geertsen, J. (unpublished results).
49. Geertsen, J. (1987). *Chem. Phys. Lett.* **134**, 401.
50. Oddershede, J., Geertsen, J., and Scuseria, G. E. (1988). *J. Phys. Chem.* **92**, 3056.
51. Canuto, S., Duch, W., Geertsen, J., Müller-Plathe, F., Oddershede, J., and Scuseria, G. E. (1988). *Chem. Phys. Lett.* **147**, 435.
52. Canuto, S., Geertsen, J., Müller-Plathe, F., and Gustavo, G. E. (1988). *J. Phys. B: At. Mol. Opt. Phys.* **21**, 3891.
53. Scuseria, G. E., Geertsen, J., and Oddershede, J. (1989). *J. Chem. Phys.* **90**, 2338.
54. Geertsen, J., Jensen, F., and Scuseria, G. E. (1989). *J. Chem. Phys.* **91**, 364.
55. Geertsen, J., and Scuseria, G. E. (1989). *J. Chem. Phys.* **90**, 6486.
56. Geertsen, J., Oddershede, J., Raynes, W. T., and Scuseria, G. E. (1990). *J. Magn. Reson.* (in press).

BOUNDS TO ATOMIC AND MOLECULAR ENERGY FUNCTIONALS

Shridhar R. Gadre

*Department of Chemistry, University of Poona
Pune - 411 007, India.*

Rajeev K. Pathak

*Department of Physics, University of Poona
Pune - 411 007, India.*

CONTENTS

1. Introduction
2. Survey of the Density Functional Theory
 - 2.1 The Hohenberg-Kohn Theorem
 - 2.2 N- and V-representability Concepts
 - 2.2.1. N-representability
 - 2.2.2. V-representability
 - 2.3 The Kohn-Sham Method
 - 2.4 Some Further Noteworthy Aspects of DFT
3. Bounds to Kinetic Energy Functionals
 - 3.1 Density Matrix Based Bounds to Kinetic Energy :
The March-Young Approach
 - 3.2 Density-Based Upper and Lower Bounds to Kinetic Energy
 - 3.3 Lower Bounds to the Weizsäcker Correction
 - 3.4 Information Theory and Kinetic Energy
 - 3.5 Kinetic Energy Anisotropies

- 3.6 Applications of the Constrained Search Procedure
- 3.7 Kinetic Energy and Pointwise Electron Densities
- 3.8 Interconnections between Kinetic and Potential Energies
- 4. Bounds to Electron Repulsion Energies
 - 4.1 Bounds to Direct Coulomb Energies
 - 4.2 Bounds to Indirect Coulomb Energies
 - 4.3 Bounds to Electron Repulsion Integrals over Gaussian Basis-Sets
- 5. Bounds to Total Electronic Energies for Coulomb Systems
 - 5.1 Stability of Negative Ions
 - 5.2 Nonbinding Theorems within Statistical Theories
 - 5.3 Inequalities for Number of Bound Eigenvalues for a Discrete Spectrum
 - 5.4 Stability of Matter
 - 5.5 Scaling Properties and Constrained Search Approach to Energy Functionals
 - 5.6 Density Functionals and Coulomb Systems
 - 5.7 Monotonicity of Molecular Electronic Energy in Nuclear Co-ordinates
 - 5.8 Other Miscellaneous Works
- 6. Concluding Remarks

1. INTRODUCTION

The advent of computers has accelerated the progress in quantum chemical computations of atomic and molecular wave functions and properties (see, for example, Szabo and Ostlund /1/ for a lucid and comprehensive introduction) at the Hartree-Fock (HF) and more sophisticated levels such as CI, MC-SCF, MBPT, Coupled-cluster, etc./2/. Vectorization and parallel-processing have indeed revolutionized the entire computational chemistry and physics scenario (see, for example Ostlund /3/; Clementi /4/). A quantum chemist is now able to perform highly accurate

calculations on reasonably large molecules. Less accurate SCF-level ab initio computations can easily be carried out even with the ubiquitous personal computer (see Colwell, Marshall, Amos and Handy/5/ for a description of their "MICROMOL" package). However, the inherently complex nature of the many-body problem demands a large CPU time as well as enormous secondary storage /6-8/. In particular, the Herculean task of evaluation of numerous electron repulsion integrals (ERI's) has aptly been described as "a long bottleneck" of quantum chemistry /8/. For example, with the use of N real basis functions at the primitive level, the number of ERI's denoted, in general, by

$$\langle ij|kl \rangle \equiv \int d^3r_1 d^3r_2 u_i^*(\mathbf{r}_1) u_j(\mathbf{r}_1) u_k^*(\mathbf{r}_2) u_l(\mathbf{r}_2) / r_{12} \quad (1)$$

turns out to be $(N^4 + 2N^3 + 3N^2 + 2N)/8$, for a simple Roothaan-HF-SCF calculation. Typically, $N \sim 10^3$ for a moderately large molecule, necessitates computation of a staggering number ($\sim 10^{11}$) of ERI's, barring molecular symmetries. Several works that have appeared in the literature (cf. Section 4 for further references) aim at the estimation of the magnitude of an ERI in a certain prescribed manner. A decision then is made whether the integral be completely ignored, or, computed with a 'differential accuracy criterion' /8/. However, strict boundedness (from above or from below) of a given ERI is not rigorously ensured, except as in a notable result due to Ahlrichs /9, 10/, valid strictly only for integrals involving s-type Gaussians. The estimation of the magnitude of the general ERI's carried out by Clementi /11/ in a rather heuristic spirit, though reasonable, is not based on a completely rigorous footing.

An attractive alternative to wavefunction-based calculations is proffered by the density-functional theory (DFT) which has hitherto been applied to a wide variety of atomic, molecular and solid-state problems. The crux of DFT is manifest in the elegant Hohenberg-Kohn/12/ theorem which proves that all ground-state properties of a many electron bound state problem are unique

functionals of its ground state electron density, $\rho(\mathbf{r})$, which is defined as $\rho(\mathbf{r}) = N \int d^3r_2 d^3r_3 \dots d^3r_N |\psi(\mathbf{r}, \mathbf{r}_2, \dots, \mathbf{r}_N)|^2$, ψ being the ground state wave function. In particular, the total electronic energy E , as a functional of ρ , within the Born-Oppenheimer approximation, emerges as

$$E[\rho] = \int d^3r \rho(\mathbf{r})v(\mathbf{r}) + F[\rho]. \quad (2)$$

Here, $v(\mathbf{r})$ is a one-body, multiplicative external potential, and $F[\rho]$, is the universal HK functional, which comprises of two parts : $T[\rho]$ and $U[\rho]$, the kinetic- and electron-repulsion energy functionals, respectively. The functional U has, for its ingredients, the 'direct', or the classical Coulomb part, $J[\rho]$, given by $J[\rho] \equiv \int d^3r_1 d^3r_2 \rho(\mathbf{r}_1)\rho(\mathbf{r}_2)/(2r_{12})$ and the indirect, or the exchange-correlation part $E_{xc}[\rho] = U[\rho] - J[\rho]$. The exchange-correlation energy, E_{xc} thus exclusively contains the quantal piece of U . A practical, orbital-based procedure for implementing density-functional calculations was realized with the inception of the Kohn and Sham (KS) /13/ method. Thus, all the ground state properties of an N -electron system are, in principle, derivable exclusively from its ground state electron-density $\rho(\mathbf{r})$, a far more tractable entity than $\psi(\mathbf{r}_1, \mathbf{r}_2, \dots, \mathbf{r}_N)$, the many-particle wave function. In spite of this very desirable attribute, DFT has a major problem that the exact form of the universal functional $F[\rho]$ is as yet unknown and may never be realized in the future. In fact, a serious drawback of DFT is that, while the exact forms of the kinetic energy and electron-repulsion energy functionals are all known within the wavefunction-based approach, their explicit forms as electron-density functionals are unknown as yet. In particular, the exact exchange-correlation energy density functional, in spite of several attempts towards its accurate representation, has thus far eluded an exact treatment.

Keeping in mind the above limitations, one may adopt the following strategy towards an affirmative end. If a physical quantity Q is explicitly unknown or is difficult to evaluate, a

rigorous estimate of the quantity may be provided by upper and lower bounds, say, U and L respectively, such that $L \leq Q \leq U$. These rigorous bounds are useful in practice only if they (i) closely bracket Q and (ii) can be readily computed. For certain situations, only the upper (or, lower) bounds may be derivable. The forms of known or unknown functionals may be imported from those of the corresponding bounds, if necessary, by suitably adjusting numerical constants in a semi-empirical manner. The quantity of interest may then be replaced by its bound (in the appropriate direction) within the variational machinery. Thus, the quest for unknown functionals is facilitated through the medium of inequalities. Such cases are indeed not rare in the literature on the quantum theory of atoms and molecules. In recent years, a variety of bounds to these functionals have become available (for prototype results see Lieb /14/, Hoffmann-Ostenhof and Hoffmann-Ostenhof/15/, Gadre et al./16/, Lieb and Oxford /17/; Sahni and Levy /18/ and Arteca and Mezey /19/). The purpose of this article is not only to provide a compendium of rigorous bounds to the energy functionals and their ingredients within the wavefunction- as well as density-based approaches; but also to reveal their salient physical and mathematical underpinnings. The present review-article is aimed at emphasizing significant density-based inequalities for atomic and molecular energy functionals. For the sake of completeness, a comparison will be made with the corresponding wavefunction-based results, wherever possible. Evidently, this will exclude studies on the standard variation /20/ and perturbation approaches. A general study of inequalities incorporating these as well as other related aspects is currently being undertaken in our laboratory. Here, we work within the time-independent, non-relativistic, extra-field-free domain. Hartree atomic units ($|e| = m_e = \hbar = 1$) are employed throughout this article (unless otherwise stated, where it would be solely for the purpose of consistency with the elaborate treatments in the literature).

The organization of the present work is as follows. In Section 2, the relevant developments of DFT are briefly outlined. An overview of this formalism is imminent keeping in mind our aim of reviewing rigorous inequalities for different electronic energy functionals. It should be noted here that the contents of this Section do not purport to be an exhaustive treatment of this topic : we discuss only significant results of broad general interest and those necessary for further development of rigorous inequalities. For a more complete treatment of DFT, one may consult excellent reviews and monographs such as those by Parr/21/, March and Lundqvist/22/, Dreizler and da Providencia/23/ and Parr and Yang /24/. In Section 3, we present density-based bounds to the kinetic energy functional and in Sections 4.1 and 4.2, those to the electron-electron repulsion energy functionals along with their classical and quantal ingredients. Section 4.3 expounds on the bounds to ERI's and electrostatic potentials evaluated by using Gaussian basis-sets. We connect these results to the density-based bounds given earlier in Section 4.1 and 4.2. Section 5 presents certain other significant and rigorous works on the total energy of atoms and molecules, including the remarkable study on the stability of matter by Lieb /14/ and that of Lieb and others on atomic and molecular negative ions /25-27/. A review of Lieb's /28/ rigorous results on DFT for Coulomb systems and the nonbinding theorems of Teller /29/ and Balázs/30/, is also presented. We now embark upon a review of the themes presented in this article with an introduction to DFT in the following Section.

2. SURVEY OF THE DENSITY FUNCTIONAL THEORY

The term "electron density" has been a part of the vocabulary of chemists for the description of molecular properties, reactivities, etc. for a long time. The seed of the concept of

employing the electron density as a basic variable for the description of an atomic or molecular system, existed in the literature since 1927 in the Thomas-Fermi (TF) statistical model for atoms /31-37/. However, only in 1964 did the Hohenberg-Kohn argument formally rank the electron-density as a fundamental entity.

2.1. The Hohenberg-Kohn Theorem

The Hohenberg-Kohn /12/ theorem, which is seminal to DFT, may be stated in its original form as follows : For the (nondegenerate) ground state (g.s.) of an arbitrary collection of electrons moving under the influence of a local external (binding) one-body potential $\hat{V} \equiv V = \sum_{i=1}^N v(\mathbf{r}_i)$ and their mutual repulsion, the electron density, ρ , is a unique functional of v and conversely. The proof of this epoch-making theorem now follows.

In the Hamiltonian $\hat{H} = \hat{T} + \hat{U} + \hat{V}$ for an N -electron system, the kinetic-energy operator \hat{T} and the electron-electron repulsion operator \hat{U} have universal operator structures. Hence, the external potential alone fixes the nondegenerate g.s. wave function whereby the density, $\rho(\mathbf{r})$ evidently becomes a functional of $v(\mathbf{r})$. The proof of what is intuitively a rather non-obvious converse follows by reductio ad absurdum.

Let, if possible, there exist two potentials, V and V' , differing by more than an additive constant and yielding the same g.s. $\rho(\mathbf{r})$. The ground state eigenfunctions of the respective Hamiltonians $\hat{H} = \hat{T} + \hat{U} + \hat{V}$ and $\hat{H}' = \hat{T} + \hat{U} + \hat{V}'$ are denoted by ψ and ψ' . Clearly, ψ and ψ' are linearly independent, for if they were identical (or, proportional), $\hat{H}\psi = E\psi$ and $\hat{H}'\psi = E'\psi$ would have led to $(\hat{H} - \hat{H}')\psi = (E - E')\psi$. Thus, except for the nodes of ψ (a set of zero measure), $V = V' + \text{const.}$, which is contrary to the hypothesis. The variational principle, in conjunction with the nondegeneracy of the g.s., leads to the strict inequalities

$$E = \langle \psi | \hat{H} | \psi \rangle < \langle \psi' | \hat{H} | \psi' \rangle = E' + \int d^3r \rho(\mathbf{r})(v(\mathbf{r}) - v'(\mathbf{r})) \quad \dots (3)$$

and

$$E' = \langle \psi' | \hat{H}' | \psi' \rangle < \langle \psi | \hat{H}' | \psi \rangle = E + \int d^3r \rho(\mathbf{r})(v'(\mathbf{r}) - v(\mathbf{r})). \quad \dots (4)$$

Addition of (3) and (4) leads clearly to a contradiction viz. $E + E' < E + E'$; thereby establishing the mapping $v(\mathbf{r}) \leftrightarrow \rho(\mathbf{r})$. The converse, by virtue of which the ground state electron density can unequivocally be looked upon as a signature of the system, forms an important part of the HK theorem. For example, to an X-ray crystallographer interested in the determination of electron densities, the following argument may be appealing: Given a full three-dimensional $\rho(\mathbf{r})$ map, locate the "cusps" at the respective nuclei to obtain the corresponding nuclear charges. These, along with their respective positions, fix the external potential. This argument was first given by Professor E.B. Wilson.

All the g.s. properties (and, in particular, the energy, E) become functionals of the corresponding $\rho(\mathbf{r})$ by the HK theorem. It was further established by HK that the functional $E_v[\rho]$ in fact attains a minimum w.r.t. arbitrary variations in the density, for the g.s. $\rho_{g.s.}(\mathbf{r})$, viz. one can establish the bounds

$$E_v[\rho] = \int d^3r \rho v + F[\rho] \\ \geq E_v[\rho_{g.s.}] \approx \int d^3r \rho_{g.s.} v + F[\rho_{g.s.}] \quad \dots (5)$$

Here, $F[\rho] = \langle \psi | \hat{T} + \hat{U} | \psi \rangle$ (for normalized ψ 's leading to a given V -representable (cf. Sec. 2.2.2) ρ) is termed the universal HK functional since it does not involve the external potential V whereas the operators \hat{T} and \hat{U} bear universal structures.

An extension of the HK theorem to degenerate g.s. has also been worked out. Parr et al. /38/ pointed out that only a minor

addition is necessary to generalize the HK theorem to cover degenerate g.s. as well. A proof to this effect has been explicitly presented by Katriel et al. /39/ and also by Englisch and Englisch/40/, which is outlined as follows: Let the manifolds of g.s. wave functions corresponding to V and V' be denoted by $\{\psi\}$ and $\{\psi'\}$ respectively. Clearly, these two sets are disjoint. Now, assume that for some $\psi \in \{\psi\}$ and $\psi' \in \{\psi'\}$ one has the same $\rho(r)$. Following HK, one obtains $E = \langle \psi | \hat{H} | \psi \rangle < \langle \psi' | \hat{H} | \psi' \rangle = E' + \int d^3r (v-v')\rho$. Likewise, $E' < E + \int d^3r (v'-v)\rho$; leading at once to a contradiction, thus establishing the HK theorem for the degenerate case as well.

As an initial orientation, HK applied their method to an ideal electron gas of almost constant, as well as slowly varying densities, leading to a functional- perturbation expansion of the total energy functional $E[\rho]$ (termed the "gradient expansion", representing, in a series, the deviations from the homogeneous density-case) that involves functionals incorporating gradients of the density to various orders. Adopting the form of the kinetic energy functional from the homogeneous electron gas case and dropping out the exchange-correlation part yields the well-known Thomas-Fermi energy functional as a limit. Consequently, the quasiclassical TF energy functional for an atom is given by

$$E_{TF}[\rho] = (3(3\pi^2)^{2/3}/10) \int d^3r \rho^{5/3} - Z \int d^3r \rho/r + J[\rho].$$

... (6)

Here, $J[\rho]$ denotes the classical Coulomb repulsion energy defined earlier. The minimization of $E_{TF}[\rho]$ in Eq.(6) w.r.t. the appropriately normalized electron density, ρ , yields the celebrated TF equation/31-35/. Simplicity and universality of the neutral-atomic properties are the forte of the TF theory.

Several refinements of this model may be found in the literature /34, 35, 41-43/, the most well-known being the Thomas-Fermi-Dirac(TFD) and Thomas-Fermi-Dirac-Weizsäcker (TFDW) models. The TFD functional incorporates an additional term (free electron

exchange) = $-(3(3/\pi)^{1/3}/4) \int d^3r \rho^{4/3}$; a further addition of the inhomogeneity term $T_w = \int d^3r (\nabla\rho)^2/(8\rho)$ leads to the TFDW model.

Thomas-Fermi and related theories are very interesting from a mathematical point of view, especially for a study /44-46/ of inequalities. That the TF theory becomes asymptotically (i.e. as $Z \rightarrow \infty$) exact, in the nonrelativistic limit, has been shown explicitly by Lieb and Simon /45/.

It may thus be seen in retrospect that the above statistical models employ rather simple yet explicit approximations to the ingredients of $F[\rho]$. For real atomic and molecular systems, however, it is difficult to represent $F[\rho]$ rigorously and universally. Several attempts have been made /23, 24/ to seek good approximations to $F[\rho]$ and this search still continues. A fair amount of success has been achieved in approximating $F[\rho]$ for atoms and molecules /47, 24/. For treatment of solids and surfaces, decent density-based approximations to the exchange-correlation functional are indeed indispensable (see Lang /48/ and references therein). Despite these practical successes, the exact explicit form of $F[\rho]$ has escaped the search. To sum up the scenario, we quote here Epstein and Rosenthal /49/ verbatim : "Since its discovery, the HK theorem has been a continued source of inspiration and interest. Nevertheless, it is probably fair to say that the theorem itself remains somewhat mysterious primarily because it remains an existence theorem only : one does not know how to write down explicit formulas for the various functionals of the density whose existence is guaranteed by the theorem". This fact, reflecting on unattainability of equalities, makes DFT a natural stage upon which inequalities play their role.

It may be noted that the original HK derivation tacitly assumes the existence of an antisymmetric N-particle wave function corresponding to a g.s. $\rho(\mathbf{r})$ for a given $v(\mathbf{r})$. Thus, the HK theorem naturally entails N- and V-representability conditions, with which we shall deal in the following subsection.

2.2. N- AND V- Representability Concepts

2.2.1. N-representability (NR)

A given (trial) density $\rho(\mathbf{r})$ is said to be N-representable if there exists at least one N-particle antisymmetric wave function leading to $\rho(\mathbf{r})$. The NR of electron density in fact forms a special case of the problem of NR of fermion density-matrices /50/. Only the necessary conditions for NR of density matrices are hitherto known : not the sufficient ones. Consequently, the general NR-problem remains unresolved. However, the constructions by Gilbert /51/ and Harriman /52/ show that all normalizable non-negative densities are indeed N-representable.

Gilbert /51/ devised an explicit geometrical construction to decompose a given $\rho(\mathbf{r}) \geq 0$ into a sum : $\rho(\mathbf{r}) = 2 \sum_j n_j f_j(\mathbf{r}) = \sum_j g_j(\mathbf{r})$ where $0 \leq n_j \leq 1$ and the f_j 's are real, non-negative functions normalized to unity. A set of functions $\phi_k(\mathbf{r})$, given by $\phi_k(\mathbf{r}) = \exp[i\omega_k(\mathbf{r})] f^{1/2}(\mathbf{r})$, with phase factors $\{\omega_k\}$ was then introduced. Subsequently, exploiting the flexibility offered by the problem, it was conjectured that these phase factors can always be selected so as to make the corresponding $\{\phi_k\}$ an orthonormal set.

Harriman /52/ concretely demonstrated Gilbert's construction for a one-dimensional density $\rho(x)$ normalized over $[a,b]$ by setting $f(x) = 2\pi \int_a^x \rho(y)dy$, so that the equidensity orbitals defined by $\phi_k(x) = (\rho(x))^{1/2} \exp(ik f(x))$ (for $k = 0, \pm 1, \pm 2, \dots$) form an orthonormal set. Further, a three - dimensional generalization of this construction was also proposed by Harriman. This synthesis of orbitals from a given density is of course, carried out a posteriori. Moreover, these orbitals are not eigenfunctions of a Fock-type operator, since energy minimization has not been alluded to, in this scheme. On the other hand, the atomic/molecular orbitals as visualized by quantum chemists are far from equidensity ones! However, an important application of the Harriman construction lies in the orbitals

being harnessed for obtaining rigorous bounds to the kinetic energy (cf. Sec. 3).

2.2.2. V-representability

A given trial density $\rho(\mathbf{r})$ is V-representable (VR) if there exists some multiplicative external potential $V_L = \sum_j v_L(\mathbf{r}_j)$, which has $\rho(\mathbf{r})$ for its g.s. density. General conditions for the V-representability of a given $\rho(\mathbf{r})$ are yet unknown. However, Levy /53/ circumvented this problem by an ingenious construction outlined below : Define a functional $Q[\rho]$ which searches over the set of antisymmetric wave functions $\{\psi_\rho\}$, all leading to ρ , and then delivers a minimum of $\langle \hat{T} + \hat{U} \rangle$ as

$$Q[\rho] = \min_{\psi_\rho} \left\{ \langle \psi_\rho | \hat{T} + \hat{U} | \psi_\rho \rangle \mid \psi_\rho \Rightarrow \rho \right\} . \quad (7)$$

This construction which closely resembles that used by Percus /54/ for non-interacting systems. For a vivid pictorial representation of the constrained search procedure see p. 59 of Parr and Yang /24/ : Note, however, that the problem of search over a non-denumerably infinite set of wave functions cannot be overcome in practice ! Levy further proved a rigorous bound, viz. $\int d^3r \, v \rho + Q[\rho] \geq E_{g.s.}$ where the equality is attained only when $\rho = \rho_{g.s.}$. This proof does not allude to V at all and thus makes redundant the VR of ρ ; and, is further not restricted to the non-degenerate ground states. Additionally, if ρ is VR, then the functional Q coincides with the Hohenberg-Kohn functional $F[\rho]$. An inequality for $F[\rho]$ is further obtained /24/ by restricting the choice of wave functions (leading to ρ) to a particular subspace S of the N -electron Hilbert-space, viz. $F[\rho] \leq \min \{ \langle \psi | \hat{T} + \hat{U} | \psi \rangle \mid \psi \Rightarrow \rho, \psi \in S \}$. Levy /55/ subsequently used this construction to obtain the following theorem regarding the "marriage", i.e. an exclusively bijective map, of ground state densities to the respective external potentials. Suppose that we are given g.s. densities $\rho_1, \rho_2, \dots, \rho_m$ corresponding to different inequivalent external

potentials v_1, v_2, \dots, v_m . Suppose further that we do not know their exact correspondence. The matching is achieved by minimization of

$$G_{1,2,\dots,m}^{\alpha,\beta,\dots,\mu} = \int d^3r [v_1 \rho_\alpha + v_2 \rho_\beta + \dots + v_m \rho_\mu] . \quad (8a)$$

The minimum is reached only when $\alpha = 1, \beta = 2, \dots, \mu = m$.

Otherwise, one has a strict inequality

$$G_{1,2,\dots,m}^{\alpha,\beta,\dots,\mu} > \int d^3r \left[\sum_{j=1}^m v_j \rho_j \right] . \quad (8b)$$

Thus, vide the Levy construction, the proof of HK-like theorem is no longer vitiated by non-VR of the trial densities.

Levy's elegant formulation of $Q[\rho]$, of course, has no more direct practical applications than those offered by the original HK functional, $F[\rho]$. However, this work has engendered several important formal studies such as the momentum-space DFT /56/; excited states /40,57/; scaling properties of the functionals involved /142/ as well as detailed investigations of the mathematical structure of functionals for Coulomb systems /28/.

Henderson /56/ transcribed the Levy construction to momentum space and established the inequality $G[\gamma] + \int d^3p \gamma(\mathbf{p}) \times p^2/2 \geq E_{g.s.}$ (equality iff $\gamma = \gamma_{g.s.}$). Here, $G[\gamma] = \text{Min} \langle \phi | \hat{U} + \hat{V} | \phi \rangle$ searches over all antisymmetric functions ϕ of the momentum variables leading to a given trial momentum density $\gamma(\mathbf{p})$. Note that unlike the Levy functional $Q[\rho]$, the functional $G[\gamma]$ is not universal since it inherently involves the external potential V , rendering direct \mathbf{p} -space calculations rather difficult. Smith *et al.* /58-60/ independently put forth the \mathbf{p} -space extension of the Levy construction. Only one direct, momentum-density-based model for atoms has so far been developed, by Pathak *et al.* /61/.

Levy /55/ further classified the general VR problem into four different types. The VR of HK is termed interacting wave function- or pure state (PS) VR. If ρ belongs to a g.s. wave function of some noninteracting $\hat{H} = \hat{T} + \hat{V}_{eff}$ (with $\hat{V}_{eff} =$

$\sum_i v_{\text{eff}}(\mathbf{r}_i)$), where v is not restricted to a Coulomb case, it is said to be noninteracting-PSVR. A density ρ could also be ensemble-VR of either interacting or noninteracting type. The Kohn-Sham (KS) theory /13/ assumes that reasonable densities are simultaneously interacting- as well as noninteracting-PSVR, as will be seen in Section 2.3. Levy /55/, with the help of a simple and convincing construction, clearly demonstrated that this need not always be the case. His argument may be outlined thus : Consider an ensemble $\{\psi_k\}$ of (degenerate) many-particle g.s. wave functions of a Hamiltonian \hat{H} , and introduce the density matrices $D^{(N)} = \sum_i d_i \psi_i(1', 2', \dots, N') \psi_i^*(1, 2, \dots, N)$; $0 \leq d_i \leq 1$ and $\sum_i d_i = 1$; $\rho(\mathbf{r}) = \sum_i d_i \rho_{ii}(\mathbf{r})$; $\rho_{ii}(\mathbf{r}) = \langle \psi_i | \hat{\rho}(\mathbf{r}) | \psi_i \rangle$ with $\hat{\rho}(\mathbf{r}) = \sum_i \delta(\mathbf{r} - \mathbf{r}_i)$. An elementary HK-like theorem dictates that ρ cannot belong to a g.s. wave function of any \hat{H}' which differs from \hat{H} by more than an additive constant. Thus, to rule out PSVR in this case, it only remains to be shown that there exist no constants such that $\rho(\mathbf{r}) = \sum_i \sum_j \langle a_i \psi_i | \hat{\rho}(\mathbf{r}) | a_j \psi_j \rangle$. This implies by the above expression for $\rho(\mathbf{r})$, the pointwise (i.e. for all \mathbf{r}) requirement that, $\sum_{i,j=1}^q (\delta_{ij} d_j - a_i^* a_j) \rho_{ij}(\mathbf{r}) = 0$ which will not, in general, lead to a solution (except for $q = 2$) for the a_i , barring some pathological linear dependencies. Thus, for example, the electron density for a noninteracting Ne^- ion written in terms of the core orbitals and the 3s, 3p and 3d orbitals (that are totally nine-fold degenerate) is far from pathological but is still not noninteracting PSVR.

Englisch and Englisch /40/ discussed the problem of non-VR densities in detail. Hohenberg and Kohn (1964) had believed that the complementary set of non-negative integrable densities contains, but only "pathological" examples. Englisch and Englisch, on the other hand, constructed several examples of non-VR densities some of which are (to quote them verbatim) 'trivial' but had not been pointed out earlier in the DF literature, e.g. (i) If $\rho(\mathbf{r})$ has zeros, it cannot be g.s. density of a one particle-system with a nodeless ground state. This

argument is also valid for more than one boson (but is not strictly valid for fermions). (ii) If $\rho(\mathbf{r})$ does not fall off at least exponentially, $\psi = \rho^{1/2}$ is an eigenvector of $\hat{H} = -\nabla^2/2 + (\nabla^2\psi/\psi)$ with the eigenvalue zero, leading to an unstable ground state.

Englisch and Englisch also presented some "nontrivial" examples of one-dimensional densities which are non-PSVR : $\rho(x) = \{a + b|x|^{(\varepsilon+1/2)}\}^2$, for instance, for small $|x|$, with $a, b > 0$ and $0 < \varepsilon < 1/2$. Their argument proceeds as follows : for an arbitrary ψ , the function $V - E = (\nabla^2\psi / (2\psi))$ can be singular at certain countable number of locations viz, the nodes of ψ . However, if there exists a test function $\phi \in L^2(\mathbb{R}^3)$ such that $\langle \phi | V | \phi \rangle$ is infinite, then the discontinuities in V occur over a set with a nonzero measure. The choice $\psi = \rho^{1/2}(x) \Rightarrow \psi' = d\psi/dx = \pm(\varepsilon + 1/2)b|x|^{\varepsilon-1/2} \in L^2(-1,1)$ leads to finite kinetic energy. Take a test function $\phi = 1$ over $(-1,1)$; then setting $E = 0$, gives rise to the inequality

$$\int_{-1}^1 dx \phi^2 V = \int_{-1}^1 dx \phi^2 (\psi''/\psi) \leq (c/(a+b)) \int_{-1}^1 dx |x|^{\varepsilon-3/2} \rightarrow -\infty \quad \dots (9)$$

[Here, note that $c = b(\varepsilon^2 - 1/4)^{-1} < 0$]. This unphysical result clearly indicates that $\rho^{1/2}(x)$ cannot be a ground state density corresponding to any V , thereby illustrating the existence of non- V -representable densities.

Katriel, Appelhoff and Davidson /39/ carried out numerical tests on V -representability of 'smooth' densities in one dimension and they found no indication of non-VR. More recently, Kohn /62/ showed that if $\rho(\mathbf{r})$ is a discrete density on a lattice (enclosed in a finite box) associated with a nondegenerate g.s. of an external potential, $v(\mathbf{r})$, then the density $\rho'(\mathbf{r}) = \rho(\mathbf{r}) + \mu \tilde{\rho}(\mathbf{r})$ is also VR. Here, $\tilde{\rho}(\mathbf{r})$ is an arbitrary density obeying $\int d^3r \tilde{\rho}(\mathbf{r}) = 0$ such that $\tilde{\rho}(\mathbf{r}) = 0$ at the boundary of the lattice, μ being a small constant. This study implies that the non-VR may not pose a serious problem for a class of well-behaved electron densities.

It may be reiterated that the problem of V-representability is an artefact of the density being used as a basic variable : the wave function - based treatments are free of this obstacle. In practical applications, however, V-representability is always tacitly assumed.

2.3. The Kohn-Sham (KS) Method

An important development was made by Kohn and Sham /13/ rendering the density-functional-theory, amenable to practical applications, describing actual, interacting many-particle systems. Kohn and Sham (KS) established that the density-based variational principle is operationally equivalent to solving Hartree- or Hartree-Fock like single-particle equations, viz. the KS equations. It is here that DFT makes its contact with a Schrödinger-like description. The KS theory thus makes it possible to establish a much warranted direct link with the orbital picture.

To accomplish the variational minimization, KS broke up the HK energy functional into the following ingredients :

$$E_v[\rho] = T_s[\rho] + J[\rho] + \int d^3r v_{\text{ext}}(\mathbf{r}) \rho(\mathbf{r}) + E_{\text{xc}}^{\text{KS}}[\rho] \quad \dots (10)$$

The first term on the r.h.s. is the noninteracting, "single-particle" kinetic energy functional, the second being the classical part of the interelectron repulsion. The third term represents the coupling with the external binding potential, while in the last one are buried the terms : the quantal part of electron repulsion, (U-J), (the usual exchange and correlation effects) and the 'missing' kinetic energy piece ($T - T_s$). The sum total of these two parts is termed the KS exchange-correlation energy functional, $E_{\text{xc}}^{\text{KS}}[\rho]$. The philosophy underlying the KS theory is as follows: The interacting many - electron system at hand is simulated by an equal number of noninteracting electrons

immersed in a field of a common effective one-body potential, $v_s(\mathbf{r})$; a theme analogous to the familiar concept of a self-consistent-field. The KS-theory leads to the following set of one-electron equations :

$$\left\{ -\nabla^2/2 + v_s(\mathbf{r}) \right\} \phi_i(\mathbf{r}) = \epsilon_i \phi_i(\mathbf{r}) \quad (i = 1, 2, \dots, N)$$

... (11)

with $T_s = \sum_{i=1}^N \langle \phi_i | -\nabla^2/2 | \phi_i \rangle$. The subscript "i" running from 1 to N labels the lowest lying energy levels ϵ_i . The orbitals $\phi_i(\mathbf{r})$ are called the KS-orbitals and the effective potential $v_s(\mathbf{r})$ is given by

$$v_s(\mathbf{r}) = v_{\text{ext}}(\mathbf{r}) + \int d^3r' \rho(\mathbf{r}')/|\mathbf{r}-\mathbf{r}'| + \delta E_{\text{xc}}^{\text{KS}}[\rho]/\delta \rho(\mathbf{r})$$

... (12)

The first two terms occur just like they do in the Hartree theory while the last one, the functional derivative of the KS exchange-correlation functional, represents purely quantal effects. Popular approximations to this term are indeed replete in the literature. Implicit in the derivation of KS equations is the assumption that an interacting, V-representable density is also noninteracting V-representable /63/. It must be noted that the Kohn-Sham orbitals, by themselves do not carry any physical meaning : but the sum of their squares does, as it simply yields the ground state density of the system. After solving the KS-equations self consistently, they yield, in principle, the highest occupied orbital energy ϵ_N (that has connections with the electronegativity) as well as the ionization potential, besides the density and the ground-state energy.

Hadjisavvas and Theophilou /64/ formulated a "rigorous" Kohn-Sham (KS) theory, in that, the V-representability was bypassed and the variables of the theory were N-particle single Slater-determinants, ψ_s , with finite kinetic energy, i.e. $\langle \psi_s | \hat{T} | \psi_s \rangle < \infty$ (For a discussion on the finiteness of the kinetic

energy, refer to Section 3). Defining appropriate functionals, this study formally enabled Hadjisavvas and Theophilou to construct the Kohn-Sham orbitals a priori through a variational principle. Even though the Hadjisavvas-Theophilou functional does not necessarily equal $\langle \psi | \hat{H} | \psi \rangle$ for an arbitrary Hilbert space ψ , the minima of these two functionals exactly coincide, thereby establishing a variational principle over the space of single Slater-determinants.

The X_α -scheme represents a method for a speedy implementation of atomic and molecular-structure calculations. The essence of this method is the approximation of the nonlocal HF exchange term by a local functional, viz. $-\alpha(3(3/\pi)^{1/3}/4) \int d^3r \rho^{4/3}(\mathbf{r})$. It was identified only in hindsight that the X_α -method is a realization of the KS-scheme employing a local exchange (-only) potential/65/. One of the early methods for a practical computation of α was proposed by Schwarz /66/. Slater /67/ observed that the Koopmans theorem is not obeyed within the X_α -approximation, and subsequently devised an ingenious method for computing ionization potentials, viz. the transition state method, which was put on a more formal footing by Janak /68/. Janak proved that $\partial E / \partial n_i = \epsilon_i$ within the KS-scheme in general, where the subscript "i" labels an occupied KS-orbital with occupancy n_i and orbital energy ϵ_i , irrespective of the choice of the KS-exchange-correlation potential. Using this theorem, one can readily derive an approximation to the ionization potential, I , which is given by the integral $\int_0^1 dn_i (\partial E / \partial n_i) = \epsilon_i(0.5)$, by the mid-point rule of numerical quadrature. Here, $\epsilon(0.5)$ denotes the energy of a half-occupied orbital. This procedure can be identified with the Slater transition-state scheme. Janak's theorem is applicable to any choice of the exchange-correlation functional. A multitude of exchange-correlation potentials have been used in the literature /23,69/. Gopinathan et al. /69/ formulated a scheme for computing the spin-dependent α -values for atoms. More recently, Gopinathan and co-workers /70-71/ have developed highly accurate KS-based

atomic models incorporating the Fermi- and Coulomb-hole considerations. It may be noted here that a formal treatment of spin-polarized DFT was proposed earlier by several researchers /72-74/. Perdew and Zunger /75/ for the first time, formally established that a fully occupied KS-spin-orbital, in general, does not satisfy the strict requirement

$$J[\rho_{i\sigma}] + E_{xc}[\rho_{i\sigma}, 0] = 0, \quad (13)$$

where i refers to the orbital-index and σ , to the spin-index, $\rho_{i\sigma}$ being the orbital spin-density. This prompted them to propose a self-interaction-correction [SIC] leading to the exact orbitalwise cancellation of the Coulomb- and exchange-correlation terms in Eq.(13). The modification does not conform to the KS-scheme in the strict sense, in that, the effective KS-potential now becomes orbital-dependent. Incidentally, an earlier study by Gopinathan et al. /69/ within the X_α -scheme, had also alluded to the self-interaction correction.

A notable contribution of DFT is towards consolidation and quantification of the often-used chemical terms such as electro-negativity /38,76/ and hardness/77/. Electronegativities of atoms within the X_α -theory were computed by Bartolotti, Gadre and Parr /76/. These authors employed the definition of electronegativity χ within DFT, proposed earlier by Parr et al. /38/ viz. $\chi = -\mu = -(\delta E/\delta \rho)_v$, where μ , the chemical potential, stems from the stationary property

$$\delta \left\{ E_v[\rho] - \mu \int d^3r \rho \right\} = 0. \quad (14)$$

For a further comprehensive review on electronegativity and hardness consult Sen and Jorgensen/78/and Parr and Yang/24/. In the works cited above, it has been implicitly assumed that the plot of electronic energy against the number of electrons for atomic systems is continuous. However, as argued by Perdew et al. /79/, it turns out that the E vs. N curve is continuous but piecewise linear, giving rise to derivative-discontinuities

precisely at integral number of electrons. The convexity of the E vs N curve for atoms was also postulated by Lieb /28/ from which emerges the inequality

$$E_v(N+1) + E_v(N-1) \geq 2 E_v(N) \quad (15)$$

Even though all known electronic systems seem to conform to inequality (15), no rigorous proof to this effect exists as yet. Incidentally, within the KS framework, the negative of the highest-occupied orbital-energy turns out to be the exact ionization potential /38,80/.

2.4. Some Further Noteworthy Aspects of DFT

From the above discussion, it is evident that the HK-type arguments are valid strictly only for the ground-state of a many-electron system. Formal extensions to excited states have also been developed /81,82,83,57/. It is noteworthy, however, that the much warranted practical applications to the theory of excited states of atoms and molecules are extremely scarce to date. The scaling properties of various energy-density-functionals were systematically studied for the first time by Szasz, Berrois-Pagan and McGinn /84/. It is well-known within the wave function domain /85-87/ that $T_\lambda = \lambda^2 T$ and $V_\lambda = \lambda V$ (for Coulombic systems). Here, λ denotes the uniform scaling factor of the electron co-ordinates; $T_\lambda = \langle \psi_\lambda | \hat{T} | \psi_\lambda \rangle$ and $V_\lambda = \langle \psi_\lambda | \hat{V} | \psi_\lambda \rangle$. Here, the original wave function $\psi(\mathbf{r}_1, \mathbf{r}_2, \dots, \mathbf{r}_N)$ has for its scaled version, $\psi_\lambda \equiv \lambda^{3N/2} \psi(\lambda \mathbf{r}_1, \lambda \mathbf{r}_2, \dots, \lambda \mathbf{r}_N)$. Of course, scaling arguments alone do not lead to unique forms of energy functionals but enable one to eliminate the functionals that do not satisfy the correct scaling requirements.

Inclusion of temperature in DFT /88/ leads to an HK-type theorem : The thermodynamic grand potential attains a minimum for the exact density matrix which is determined uniquely by the external potential /88/. More recently, Löwdin /89/ has discussed

some further thermodynamical inequalities. Unlike its thermodynamic counterpart, the extension of the HK theorem to a general class of time-dependent external potentials is not possible. However, minimal principles applicable to harmonically varying external potentials $v(\mathbf{r},t)$ were established by Peuckert /90/, Bartolotti /91/, and Deb and Ghosh /92/. A somewhat restricted extremal principle encompassing a far more wider domain of general external potentials, $v(\mathbf{r},t)$ has recently been presented by Runge and Gross /93/. Time- and temperature-dependent frameworks, however, fall outside the scope of the present review article.

In this Section, an attempt has been made to summarize important contributions to the density-functional-theory : we make no claim for its completeness. An account of only fundamentally significant contributions to DFT, along with those that have a direct bearing on further inequality-related developments has been given. In this light, we now focus our attention on the ingredients of the universal HK functional, $F[\rho]$. In particular, we discuss the kinetic energy and the electron-repulsion pieces incorporated in $F[\rho]$. In the following Section, we present an exhaustive discussion of rigorous bounds to kinetic energy treated as a functional of the wave function and separately, that of the one-electron density.

3. BOUNDS TO KINETIC ENERGY FUNCTIONALS

Within the conventional wavefunction-based approach, the kinetic energy T of a system bears an exact, known universal form: $T = \langle \psi | \sum_i -\nabla_i^2 / 2 | \psi \rangle$. On the contrary, the kinetic energy-density-functional does not enjoy such a privilege. This calls for a more detailed treatment of the kinetic-energy-density functional with which we begin this Section.

3.1. Density Matrix based Bounds to Kinetic Energy :

The March-Young /94/ Result

March and Young /94/ (MY) appear to be the first ones to have systematically studied the general variational methods based on the first-order reduced density matrix. For some earlier related works, consult Macke /95,96/. It may be further worth noting that the March-Young paper precedes the formal birth of the DFT, viz. the Hohenberg-Kohn work. We reproduce here the MY argument for the one-dimensional case. The basic idea in their treatment is to approximate the first-order density matrix, $\Gamma(x'|x)$ which obeys the normalization condition, viz. $\int_{-\infty}^{\infty} dx \Gamma(x|x) = N$, the number of particles, and also the idempotency condition, viz. $\int_{-\infty}^{\infty} dx'' \times \Gamma(x'|x'') \Gamma(x''|x) = \Gamma(x'|x)$. For example, consider the expression

$$\begin{aligned} \Gamma(x'|x) &= \left\{ (dy/dx)_x \cdot (dy/dx)_x \right\}^{1/2} \Gamma_0(y(x')|y(x)) \\ &\equiv (y_1'|y_1)^{1/2} \Gamma_0(y'|y) \end{aligned} \quad \dots (16)$$

where, y_i denotes $d^i y/dx^i$ for $i = 1, 2, 3$; Γ_0 refers to a density matrix for a known problem and Γ is the trial one to be used for energy minimization :

$$E = -(1/2) \int_{-\infty}^{\infty} dx \left[\partial^2 \Gamma(x'|x) / \partial x^2 \right]_{x'=x} + \int_{-\infty}^{\infty} dx \Gamma(x|x) v(x), \quad \dots (17)$$

$v(x)$ being a local potential. It can be readily verified that $\Gamma(x'|x)$ in Eq. (16) satisfies the normalization and idempotency requirements if Γ_0 does so. The final expression for E in terms of Γ_0 turns out to be, with the use of Eq. (16) and Eq. (17),

$$\begin{aligned} E &= -(1/2) \int_{-\infty}^{\infty} dx \left[(y_3'^2/2 - y_2'^2/(4y_1')) \Gamma_0 + 2y_1'y_2' \partial \Gamma_0 / \partial y \right. \\ &\quad \left. + y_1'^3 \partial^2 \Gamma_0 / \partial y^2 \right]_{x'=x} + \int_{-\infty}^{\infty} dx \Gamma_0(x|x) v(x) \quad \dots (18a) \end{aligned}$$

By employing $\Gamma_0(x'|x)$ generated by plane waves of the type

$\exp(2\pi i\nu x)$ for integral ν -values running from $-m$ through $+m$, for $N = 2m$ or $N = 2m + 1$ (m being an integer ≥ 0) viz. $\Gamma(x'|x) = \sin(N\pi(x'-x))/\sin(\pi(x'-x))$; one obtains, in terms of the electron density $\rho(x) = \Gamma(x|x)$,

$$\begin{aligned}
 E = & [\pi^2 (N^2-1)/(6N^2)] \int_{-\infty}^{\infty} dx \rho^3 + (1/8) \int_{-\infty}^{\infty} dx (d\rho/dx)^2/\rho \\
 & + \int_{-\infty}^{\infty} dx \rho(x) v(x). \quad \dots (18b)
 \end{aligned}$$

Now, consider the exact solution to the eigenvalue problem (with the potential $v(x)$) to be ψ and the corresponding density, ρ . Since the potential energy ingredient is identical, the ground state has a minimum kinetic energy, $T[\psi]$ leading to a rigorous bound

$$T[\psi] \leq (\pi^2/6)((N^2-1)/N^2) \int_{-\infty}^{\infty} dx \rho^3 + (1/8) \int_{-\infty}^{\infty} dx (d\rho/dx)^2/\rho. \quad \dots (19)$$

The second term in the above inequality represents the full Weizsäcker/97/ correction, in one dimension.

March and Young subsequently carried out a straightforward extension of this logic to three-dimensional problems with $\Gamma(\mathbf{r}'|\mathbf{r}) = [J(\mathbf{r}') J(\mathbf{r})]^{1/2} \Gamma_0(\mathbf{R}'|\mathbf{R})$ and J denoting the Jacobian of co-ordinate transformation from \mathbf{r} to $\mathbf{R}(\mathbf{r})$. However, as has been aptly pointed out by Lieb /98/ and Müller /99/ (as quoted by Siedentop /100/, the existence of transformation $\mathbf{R}(\mathbf{r})$ is not always guaranteed. A general conformal transformation from the three- N to three dimensional space is not always guaranteed. Γ_0 was chosen by MY to bear the form

$$\Gamma_0(\mathbf{r}'|\mathbf{r}) = \prod_{i=1}^3 \sin(K_i \pi (x'_i - x_i))/\sin(\pi(x'_i - x_i)), \quad (20)$$

suggested by their one-dimensional progressive wave case. Here, K_i 's are positive integers subject to $K_1 K_2 K_3 = N$. With this case, one obtains a bound

$$T[\psi] \leq (1/6)[K_1^2 + K_2^2 + K_3^2 - 3](\pi^2/N^{2/3}) \int d^3r \rho^{5/3} \\ + (1/8) \int d^3r (\nabla \rho)^2 / \rho \quad \dots (21)$$

Considering a set of plane waves given by $\psi_{\mathbf{k}_1} = \exp[2\pi i(\mathbf{k}_1 - \mathbf{g}) \cdot \mathbf{r}]$ where \mathbf{k}_1 has integer-valued components and \mathbf{g} , a constant vector, MY obtained, in their special "conformal" case, an upper bound to $T[\psi]$ as

$$T[\psi] \leq 2\pi^2 C_N \int d^3r \rho^{5/3} + (1/8) \int d^3r (\nabla \rho)^2 / \rho, \quad (22)$$

where constants C_N were determined by them numerically. The coefficient C_N varies rather slowly with N , e.g. $C_{10} = 0.2169$, $C_{27} = 0.2222$ and $C_{89} = 0.2314$.

The MY work indeed is a pioneering attempt resulting in density-based upper bounds to $T[\psi]$. As it precedes the HK work, it is not surprising that the V-representability problem of $\Gamma(\mathbf{r}|\mathbf{r}')$ was not even raised. It may be noted that both Müller /99/ and Lieb /28/ have pointed out that the result (22) needs restriction in the proof, and that the inequality (19) is valid for an arbitrary number of N particles only in one dimension.

3.2 Density-Based Upper and Lower Bounds to Kinetic Energy

Lieb /28/, in a general study of Coulomb systems (to be further detailed out in Section 5) summarized rigorous upper bounds for bosonic and fermionic kinetic energies, viz.

$$T[\psi] \leq T_w[\rho_\psi] \quad (\text{bosons}) \quad (23)$$

and

$$T[\psi] \leq 16\pi^2 N^2 T_w[\rho_\psi] \quad (\text{fermions}). \quad (24)$$

For bosons, set $\psi(\mathbf{r}_1, \mathbf{r}_2, \dots, \mathbf{r}_N) = \prod_{i=1}^N \rho^{1/2}(\mathbf{r}_i) / N^{1/2}$ (a Hartree-like product); each term contributing T_w/N , leading directly to the inequality (23). Further, with the help of a

general inequality due to the Hoffmann-Ostenhofs /15/, viz.

$$T[\psi] \geq T_w[\rho_\psi] , \quad (25)$$

one may notice that the inequality (23), in fact, turns out to be an equality for all bosonic systems, in that there exists a (Hartree-type) product wave function yielding $T[\psi] = T_w[\rho_\psi]$. Of course, an arbitrary ψ leading to a given ρ is not guaranteed to satisfy this equality.

For fermions, an orthonormal set

$$\phi_k(\mathbf{r}) = (\rho(\mathbf{r})/N)^{1/2} \exp(ik f(\mathbf{x})) \quad (26)$$

is generated with the prescription (cf. Harriman's /52/ work outlined in Section 2)

$$f(\mathbf{x}) = (2\pi/N) \int_{-\infty}^{\mathbf{x}} ds \int_{-\infty}^{\infty} dt \int_{-\infty}^{\infty} du \rho(s, t, u) . \quad (27)$$

One then obtains

$$N \int d^3r |\nabla \phi_k|^2 = \int d^3r (\nabla \rho^{1/2})^2 + (2\pi k/N)^2 \int_{-\infty}^{\infty} g^B(s) ds \quad \dots (28)$$

where $g^2(s)$ stands for $\int_{-\infty}^{\infty} \int_{-\infty}^{\infty} dt du \rho(s, t, u) = 2 \int_{-\infty}^s g(y) [dg(y)/dy] dy$. The desired result is obtained by noting that

$$dg^2/ds = 2 \int_{-\infty}^{\infty} \int_{-\infty}^{\infty} \rho^{1/2} (\partial r / \partial s) \nabla \rho^{1/2} dt du \quad (29)$$

which, in conjunction with the Cauchy-Schwarz inequality gives

$$\int_{-\infty}^{\infty} ds (dg/ds)^2 \leq \int d^3r (\nabla \rho^{1/2})^2 . \quad (30)$$

A subsequent use of the Cauchy-Schwarz inequality followed by some algebraic simplifications, together yield the desired result, viz. the inequality (24). This bound (24), due to Lieb is, however, rather weak in general. In particular, for a one-electron system, $T[\psi]$ must equal $T[\rho]$, but (24) grossly overestimates the kinetic energy.

Zumbach/101/ obtained a stricter upper bound for the kinetic energy of fermions, viz.

$$T[\psi] \leq \left\{ 1 + 45 (4\pi)^2 (N/q)^{2/3} / 5^{5/3} \right\} T_w[\rho_\psi] \quad , \quad (31)$$

q here being the number of spin states. Zumbach's construction is basically the same as that employed by Lieb, and the filling of orbitals is akin to the MY arguments, but the spin of the particles is taken into consideration explicitly. The constant accompanying unity in the numerical factor of the inequality (31) is obtained by inspection of the trend of the energy levels for a three-dimensional rigid box, with increasing N . However, it becomes tighter in comparison with (24) with progressively increasing N .

The subtle difference between the philosophies of MY on the one hand and that of Lieb and Zumbach on the other, may be noted here. In the MY approach the kinetic energy obtained from the energy-minimizing first-order density matrix $\Gamma(\mathbf{r}|\mathbf{r}')$ obeys the bounds (19) and (21), wherein $\rho(\mathbf{r})$ on the right equals $\Gamma(\mathbf{r}|\mathbf{r})$. The Lieb and Zumbach approaches ensure just the existence of an antisymmetric ψ (leading to a given, fixed density ρ), such that the inequalities (24) and (31) hold good. In the MY treatment, the N -representability of the density matrix is assumed, and the result is limited only to ground states, owing to the use of the variational principle. The Lieb and Zumbach results, however, are valid in a wider domain, i.e. for any (not necessarily the ground state) given well-behaved density. It may be reiterated, however, that in general, arbitrary wave functions leading to a given ρ do not conform to the bounds (24) and (31).

We have reviewed above some upper bounds to the kinetic energy functional. Lower bounds to the kinetic energy (fermions or bosons) were derived by the Hoffmann-Ostenhofs /15/ and later also by Lieb /28/. Starting with the definition of the one - particle density

$$\rho_{\psi}(\mathbf{r}_1) = N \int d^3\mathbf{r}_2 d^3\mathbf{r}_3 \dots d^3\mathbf{r}_N |\psi(\mathbf{r}_1, \mathbf{r}_2, \dots, \mathbf{r}_N)|^2, \quad \dots (32)$$

one obtains $\nabla_1 \rho(\mathbf{r}_1) = N \int d^3\mathbf{r}_2 d^3\mathbf{r}_3 \dots d^3\mathbf{r}_N (\psi^* \nabla_1 \psi + \psi \nabla_1 \psi^*)$.

Use of the Cauchy-Schwarz inequality leads to the bound

$$T[\psi] \geq T_w[\rho_{\psi}], \quad (33)$$

which means that the kinetic energy is bounded from below by the corresponding full Weizsäcker term.

The equidensity orbitals /52/ (cf. Eq. (26)) which differ only in their phases ensuring orthonormality, have further been put to use in the literature for obtaining the kinetic energy density. For example, Ghosh and Parr /102/ systematically constructed such a set of orthonormal orbitals, for the case involving exclusively spherically symmetric s-type atomic orbitals. With the choice $\psi_k(r) = (\rho(r)/N)^{1/2} \exp [2\pi i k \lambda(r)]$, they noted that k can, in addition to integral values, take half odd-integral values as well. Here, $\lambda(r)$ is the fractional charge $= \int_0^r dr' \rho(r') 4\pi r'^2 / N$, contained in a sphere of radius r . Thus, they obtained an approximation to the (nonlocal) kinetic energy density $t(r, \rho) = (d\rho/dr)^2 / (8\rho) + 2\pi^4 (1 - 4/N^2) r^4 \rho^3 / 3$. This result holds when N , the number of electrons equals $4n + 2$ for nonnegative integral values of n . They also obtained a similar result for other arbitrary integral N -values, and further generalized their result to three dimensions. Ghosh and Parr also proved the molecular virial theorem in a form particularly suited to DFT. Note that Harriman /52/ and Ghosh and Parr /102/ have exploited the equidensity orbitals for obtaining bounds to the kinetic energy. For a critical appraisal of these orbitals, refer to Ludeña /103/ and Capitani et al. /104/.

Yet another lower bound to $T[\psi]$ for spin-1/2 fermions, was derived by Lieb /14/ in his celebrated work on the stability of matter. This bound reads

$$T[\psi] \geq T_0[\rho_\psi]/(4\pi)^{2/3}. \quad (34)$$

For a general fermion-system with q spin-states, an additional factor of $q^{2/3}$ appears in the denominator of the right side of the inequality (34). Implicit in the derivation of the above result is the assumption that the wave function is normalized to unity. The proof of (34) is based on the following theorem (Theorem 2 of Lieb /14/ ; see Section 5 for a discussion of related works).

Let $V(\mathbf{r})$ be a nonpositive, local, multiplicative one-body potential. Let $N_E(V)$ denote the number of eigenvalues (counting the appropriate multiplicity whenever degenerate) of the operator $-\nabla^2 + V(\mathbf{r})$, that are all less than or equal to a prescribed negative energy value E (for this derivation we deviate from using Hartree units), is bounded from above as

$$N_E(V) \leq (4\pi)^{-1} (2|E|)^{-1/2} \int d^3r |V(\mathbf{r}) - E/2|_-^2, \quad (35)$$

where $|f(\mathbf{r})|_- = |f(\mathbf{r})| \Theta(-f(\mathbf{r}))$, Θ being the Heaviside unit-step function. The proof of the kinetic energy inequality (34) then proceeds as follows : construct an N -particle Hamiltonian $\hat{H}_N = \sum_i (-\nabla_i^2 + V(\mathbf{r}_i))$, with the choice $V(\mathbf{r}) = -\alpha \rho^{2/3}(\mathbf{r})$ (with $\alpha > 0$). Evidently, \hat{H}_N describes a noninteracting model Hamiltonian. Note that the fermion ground state energy $E = q \sum_i^{\text{occ}} \epsilon_i \geq q \sum_k \epsilon_k$, where the latter k -sum sweeps through all the bound ($\epsilon_i < 0$) eigenvalues of \hat{H}_N . On the other hand, the variational principle dictates that $E_0 \leq T[\rho_\psi] - \alpha \int d^3r \rho_\psi^{5/3}$. Setting $\alpha = (3\pi/(2q))^{2/3}$ and with the use of a result due to Lieb /14/, namely,

$$\sum_j |\epsilon_j| \leq (4/(15\pi)) \alpha^{5/3} \int d^3r \rho_\psi^{5/3}, \quad (36)$$

the desired inequality (34) is obtained. The bound (34) forms a crucial step in Lieb's work on stability of matter. For earlier related works, consult Lieb and Thirring /105, 106/. The inequality (34) has subsequently been made tighter by a factor of

1.496 by Lieb /107/. Unlike the inequalities (24) and (31) due to Lieb /28/ and Zumbach /101/ respectively, the lower bounds (33) and (34) are applicable to all antisymmetric wave functions yielding a given density ρ . We now turn to the density based bounds to the kinetic energy and its ingredients.

3.3. Lower Bounds to the Weizsäcker Correction

Since the explicit form of kinetic energy functional $T[\rho]$ is unknown, several attempts, starting with HK, have been made to approximate it. Usually, for a slowly varying density, $T[\rho]$ is expanded as /108, 109/

$$T[\rho] = T_0[\rho] + T_w[\rho]/9 + T_4[\rho] + \dots \quad (37)$$

In this "gradient expansion", the second term $T_w/9 \equiv T_2$ appears as the first-order correction to the leading TF kinetic energy T_0 . Thus, it is also pertinent to obtain bounds to T_w . Different lower bounds to T_w have been reported in the literature /110/. By use of the three-dimensional Sobolev inequality /111, 112/ viz.

$$\int d^3r |\nabla\phi|^2 \geq 3(\pi/2)^{4/3} \left\{ \int d^3r |\phi|^6 \right\}^{1/3}, \quad (38a)$$

one obtains/110,113/

$$T_w[\rho] \geq 3 \pi^{4/3} \left(\int d^3r \rho^3 \right)^{1/3} / 2^{7/3}. \quad (38b)$$

A more restricted result valid for spherically symmetric densities reads

$$T_w[\rho] \geq \langle r^{-2} \rangle / 8 = \pi \int_0^\infty dr \rho(r) / 2. \quad (39)$$

This bound is obtained by using a standard theorem in the monograph by Hardy, Littlewood and Pólya /114/, viz.

$$\int_0^\infty dr [4(dy/dr)^2 - (y/r)^2] \geq 0; \text{ for all } y(r) \text{ such that } y(0) = 0.$$

Here, the prescription employed is $y(r) = r \rho^{1/2}$. The result (39) was generalized by Gadre and Chakravorty /115, 116/ to include general non-spherically-symmetric densities as well. Their

derivation was founded on an inequality due to Redheffer /150/. In fact, it turns out /117/ that $T_w[\rho]$ can be connected to the leading term $T_0[\rho]$ itself, via

$$T_w[\rho] \geq 5 (12N)^{-2/3} T_0[\rho], \quad (40)$$

showing that the "correction" T_2 is not necessarily insignificant. Similar relationships between the first two terms of the gradient expansion for the exchange-correlation energy were also shown to exist /117/.

A successive application of Sobolev and Hölder inequalities yields some further connections such as /118/ :

$$T_0 \leq 4 (3N/2)^{2/3} T/5 \quad (41)$$

which is seen to be tighter, for $N \leq 12$, than the Lieb-Thirring /105/ bound (i.e. the inequality (34)); whereas the Lieb-Thirring bound becomes tighter with increasing N , beyond $N = 12$.

Dehesa and Galvez /119/ and Galvez and Dehesa /120/ have recently obtained bounds to $T_0[\rho]$ and also those to the Dirac-Slater exchange energy. A further connection of the kinetic energy with the direct Coulomb energy functional $J[\rho]$ was established /121/ :

$$J[\rho] \geq \pi^2 \langle r^{-1} \rangle^3 / (144 T_w[\rho]) \geq \pi^2 \langle r^{-1} \rangle^3 / (144 T[\rho]), \quad (42)$$

once again, linking J to one-electron functionals such as T_w and $\langle r^{-1} \rangle$. In deriving this result, some earlier inequalities due to Galvez and Dehesa /119, 120/ were employed.

Apart from the density-based inequalities discussed above, the atomic and molecular kinetic energy functional has links with many other diverse entities. One such remarkable connection is offered in the realm of information theory, as may be seen in the following Section.

3.4. Information Theory and Kinetic Energy

During the last decade, there has been an increasing interest in the application of information theory to a variety of quantum - mechanical problems /122-132/. Shannon /133/ axiomatically obtained the "uncertainty" or "entropy" associated with a probability distribution $P = \{p_1, p_2, \dots, p_n\}$ with $\sum_i p_i = 1$ and $p_i \geq 0$, as $S[P] = - \sum_i p_i \ln p_i$. He immediately proposed a generalization of this definition for the continuous case as $S[p] = - \int dx p(x) \ln p(x)$. The entropy for the continuous case is not invariant to the co-ordinate frame chosen and could also assume negative values (in contrast to the discrete case). From a physical point of view, the N-particle probability densities in conjugate spaces, viz. $|\psi(r_1, r_2, \dots, r_N)|^2$ and $|\phi(p_1, p_2, \dots, p_N)|^2$ may be utilized for computation of "entropies" for general quantum mechanical systems. In particular, an inequality due to Białynicki-Birula and Mycielski /130/ provides an interesting, general uncertainty-type relation in the position and momentum - spaces (and for complementary spaces, in general) in terms of an inequality

$$- \langle \ln |\psi|^2 \rangle - \langle \ln |\phi|^2 \rangle \geq 3N (1 + \ln \pi), \quad (43)$$

The transcription of (43) in terms of the respective one-particle densities $\rho(r)$ and $\gamma(p)$ reads /128/ :

$$S[\rho] + S[\gamma] \geq 3N (1 + \ln \pi) - 2N \ln N \quad (44)$$

where, the information "entropy" $S[\rho]$ is given by $S[\rho] \equiv - \int d^3r x \rho(r) \ln \rho(r)$, with a similar definition for $S[\gamma]$. Maximization of $S[\gamma]$ subject to a given value of the kinetic energy and the number of electrons, N , leads to /134/

$$S[\gamma] \leq 3N (1 + \ln \pi)/2 - N \ln N - 3N \ln(3N/(4T))/2 ; \quad (45)$$

whence, it follows, on use of (44), that

$$S[\rho] \geq 3N (1 + \ln \pi)/2 - N \ln N - 3N \ln(3N/(4T))/2. \quad (46)$$

Similar bounds to $S[\rho]$ and $S[\gamma]$ were obtained by constraining the $\langle r^2 \rangle$ -value. The most interesting result given in terms of an inequality involving the entropy-sum, is that

$$S[\rho] + S[\gamma] \leq 3N (1 + \ln \pi) + 3N \ln(4\langle r^2 \rangle \langle p^2 \rangle / 9) / 2 - 5 N \ln N. \quad \dots (47)$$

Here, we have a novel lower bound to the kinetic energy of a system in terms of the uncertainty sum in conjugate spaces. Exploiting (44) in conjunction with (47) yields /134/ for atomic systems :

$$\langle r^2 \rangle \langle p^2 \rangle \geq 9 N^2 / 4, \quad (48)$$

which matches the earlier bound derived by Gadre and Chakravorty /116/ and that by Tsapline /135/ and is essentially a three - dimensional generalization of the Heisenberg uncertainty principle.

3.5. Kinetic Energy Anisotropies

A straightforward generalization of the lower bound to the kinetic energy, viz. $T_w \leq T$ /15/ was carried out by Gadre, Koga and Chakravorty /136/ for obtaining bounds to "directional" kinetic energies. They obtained a bound :

$$\begin{aligned} \langle T_z \rangle &= \langle p_z^2 \rangle / 2 = \int d^3p \gamma(\mathbf{p}) p_z^2 / 2 \\ &\geq (1/8) \int d^3r (\partial \rho(\mathbf{r}) / \partial z)^2 / \rho(\mathbf{r}). \quad \dots (49) \end{aligned}$$

This result is of special importance in the context of directional Compton profile measurements of solids whereby directional kinetic energies can be readily computed /137/. For example, $\langle p_z^2 \rangle / 2 = 3 \int_0^\infty J(p_z^2) p_z dp_z$, where $J(p_z)$ is the directional Compton profile. For measurements in gas phase,

however, the experimental results of the Compton profile data and the momentum density are intrinsically spherically symmetric, with no anisotropies. In that case, the Hoffmann-Ostenhofs'/15/ bound is the best possible result so far. Incidentally, a relation, reciprocal to the inequality (33) connecting the diamagnetic susceptibility to the electron momentum density has also been derived recently /138/.

Incidentally, the \mathbf{r} -space local-kinetic energy density $t(\mathbf{r})$ is defined only up to an additive term of the form $\nabla \cdot \mathbf{A}$ where \mathbf{A} is an arbitrary vector function that has all the required derivatives existing and further, vanishes at infinity. A particular definition of $t(\mathbf{r})$ often used in the literature is : $t(\mathbf{r}) = (1/2) \sum_i n_i \nabla \psi_i^*(\mathbf{r}) \cdot \nabla \psi_i(\mathbf{r})$, ψ_i being the appropriate orbitals in a single-particle description and n_i being their occupancies. With this definition, it follows that $t(\mathbf{r}) \geq 0$: a strong and useful requirement indeed (Parr and Yang /24/). Further inequalities involving the kinetic energy are derivable via the constrained search procedure, as described in what follows.

3.6. Applications of the Constained Search Procedure

Levy and Perdew /139, 140/ formulated the constrained search procedure to investigate the behavior of various energy density functionals within the density functional framework. The basic idea here is that by constraining the domain of search, the minimum value of a given functional is necessarily greater than or equal to the actual (unconstrained) minimum.

For example, by employing the Harriman /52/ construction for two doubly occupied orthonormal spin-orbitals, an upper bound to the Levy functional, $Q[\rho]$ elaborated in Section 2 may be obtained /139-141/

$$Q[\rho] \leq (1/8) \int d^3r (\nabla \rho)^2 / \rho + 3 \int d^3r \rho(\mathbf{r}) |\nabla f|^2 \\ + (1/2)(4-1/4) \int d^3r d^3r' \rho(\mathbf{r}) \rho(\mathbf{r}') / |\mathbf{r}-\mathbf{r}'|, \quad \dots \quad (50)$$

where the function $f(\mathbf{r})$ is defined by Eq. (27).

Levy and Perdew /139, 140/ for the first time in DF literature, explicitly demonstrated, via the constrained search procedure, the non-negativity of the quantity $(T - T_s)$, which is the kinetic piece incorporated in the Kohn-Sham (KS) exchange-correlation energy. Here, $T[\rho] = \langle \psi_\rho^{\min} | \hat{T} | \psi_\rho^{\min} \rangle$ (ψ_ρ^{\min} being the ground state wave function), and $T_s[\rho] = \langle \phi_\rho^{\min} | \hat{T} | \phi_\rho^{\min} \rangle$ where, it is assumed that ρ is a ground state density for some noninteracting $\hat{H} = \hat{T} + \sum_{i=1}^N v(\mathbf{r}_i)$. The function ϕ_ρ^{\min} is that normalized antisymmetric function which yields ρ and simultaneously minimizes $\langle \hat{T} \rangle$. Thus, the inequality

$$T[\rho] \geq T_s[\rho] \quad (51)$$

readily follows. Further, if one introduces $\tilde{T}_s[\rho] = \text{Min} \{ \langle \psi | \hat{T} | \psi \rangle | \psi \Rightarrow \rho \}$ where ψ is an N -particle, antisymmetric normalized wave function, it readily follows that $\tilde{T}_s[\rho] \leq T_s[\rho] \leq T[\rho]$. The former inequality is obtained noting that the domain of ψ 's in the definition of $\tilde{T}_s[\rho]$ is a superset of those in the definition of $T_s[\rho]$ (cf. Parr and Yang /24/, pp.152). Moreover, the use of the Coulombic virial theorem for the equilibrium nuclear configuration leads to $E_{g.s.} \leq -T_s[\rho]$, ρ here being the ground-state density. It is noteworthy that within the X_α -theory (cf. Section 2.3), the functional $E_{xc}[\rho]$ is approximated by an "exchange-only" term. The latter scales purely as potential energy, thus leading to no kinetic energy piece incorporated in $E_{xc}[\rho]$, leading to $T = T_s$.

Levy and Perdew /140/ applied the Hellmann-Feynman theorem, viz.

$$dE_\lambda/d\lambda = \langle \psi_\lambda | \partial \hat{H}_\lambda / \partial \lambda | \psi_\lambda \rangle \quad (52)$$

where the Hamiltonian \hat{H} includes a parameter λ and $\hat{H}_\lambda \psi_\lambda = E_\lambda \psi_\lambda$, to obtain certain rigorous vector relations involving ρ and ∇v , under the integral sign. By expanding $v_\lambda(\mathbf{r}) = v(\mathbf{r} + \hat{\mathbf{u}}) = v(\mathbf{r}) + \lambda \hat{\mathbf{u}} \cdot \nabla v(\mathbf{r}) + \dots$ in a Taylor series, with $\hat{\mathbf{u}}$, an arbitrary unit

vector, one obtains, invoking homogeneity and isotropy of space, respectively :

$$\int d^3r \rho(\mathbf{r}) \nabla v(\mathbf{r}) = 0 \quad (53)$$

and

$$\int d^3r \rho(\mathbf{r}) [\mathbf{r} \times \nabla v(\mathbf{r})] = 0 \quad (54)$$

These two relationships, respectively imply invariance of the total energy under arbitrary translations and infinitesimal rotations of the entire system. In deriving equation (54), smallness of λ has been implicitly assumed in the expansion of $v(\mathbf{r} + \lambda \mathbf{r} \times \hat{\mathbf{u}})$, leading to an invariance w.r.t. infinitesimal rotations. Levy and Perdew further studied the scaling properties of various density functionals with the scaled density $\rho_\lambda(\mathbf{r}) = \lambda^3 \rho(\lambda \mathbf{r})$. By defining $\psi_\rho^{\min}(\mathbf{r}_1, \mathbf{r}_2, \dots, \mathbf{r}_N)$ as that antisymmetric function which yields the scaled density $\rho(\mathbf{r})$ and simultaneously minimizes $\langle \hat{T} + \hat{U} \rangle$, they showed that $\lambda^{3N/2} \psi_\rho^{\min}(\lambda \mathbf{r}_1, \lambda \mathbf{r}_2, \dots, \lambda \mathbf{r}_N)$ is that antisymmetric function which yields $\rho_\lambda(\mathbf{r})$ and simultaneously minimizes the entity $\lambda^{-2} \langle \hat{T} + \lambda \hat{U} \rangle$. Here, and in what follows, the operators \hat{T} and \hat{U} involve the unscaled co-ordinates, viz. $\mathbf{r}_1, \mathbf{r}_2, \dots, \mathbf{r}_N$ unless otherwise specified explicitly. Following the constrained search approach, one readily obtains the strict inequalities

$$\lambda^2 T[\rho] + \lambda U[\rho] > T[\rho_\lambda] + U[\rho_\lambda] \quad (55)$$

and

$$\lambda^2 T[\rho] + \lambda^2 U[\rho] < T[\rho_\lambda] + U[\rho_\lambda] \quad (56)$$

for $\lambda \neq 1$. Note that relations (55) and (56) involve equalities in the usual wavefunction theory. Recently, Levy /142/ has pointed out that the above results are rather counterintuitive. However, it must be borne in mind that the definitions used in this treatment are slightly different than those employed in the wavefunction theory, resulting in the above inequalities.

The inequalities (55) and (56) could be written separately as

$$\begin{aligned} U[\rho_\lambda] &< \lambda U[\rho] \\ T[\rho_\lambda] &> \lambda^2 T[\rho] \quad (\lambda < 1) ; \end{aligned} \quad (57a)$$

and

$$\begin{aligned} U[\rho_\lambda] &> \lambda U[\rho] \\ T[\rho_\lambda] &< \lambda^2 T[\rho] \quad (\lambda > 1) . \end{aligned} \quad (57b)$$

In the same spirit, Levy /142/ further pointed out that $T_s[\rho_\lambda]$ exactly equals $\lambda^2 T_s[\rho]$, i.e. the single-particle KS kinetic energy scales properly, as is intuitively required by the wave function theory.

3.7. Kinetic Energy and Pointwise Electron Densities

King recently /143, 144/ derived rigorous bounds to the atomic, spherically averaged, exact as well as Hartree-Fock atomic densities $\rho(r)$, in terms of the kinetic T , by means of several inequalities. He employed a one-dimensional inequality due to Block /145/, viz.

$$|y(t)|^2 \leq M(t) \int_a^b dx \left\{ f(x) [y'(x)]^2 + g(x) y^2(x) \right\}, \quad (58)$$

where $M(t)$ is independent of the function y and is given by

$$\begin{aligned} M(t) &= \int_a^b dx \left\{ f(x) [w'(x,t)]^2 + g(x) w^2(x,t) \right\} \\ &= w(t,t) + f(b) w'(b) w(b) - f(a) w'(a) w(a) ; \end{aligned} \quad (59)$$

with the prime denoting differentiation, w.r.t. x .

In the above two results, $a < t < b$ and $w(x,t)$ satisfies

$$(i) \quad (fw')' - gw = 0 \quad \begin{cases} a \leq x < t \\ t < x \leq b \end{cases}$$

(ii) $w(x,t)$ is continuous for $a \leq t \leq b$

(iii) $\lim_{\epsilon \rightarrow 0^+} [w'(t-\epsilon, t) - w'(t+\epsilon, t)] f(t) = 1$

$$(iv) \quad f(a) w'(a)y(a) = f(b) w'(b)y(b).$$

With these rather stringent conditions and with the prescription $y(r) = r \rho^{1/2}(r)$ and various choices for f and g compatible with the above requirements, King /143/ obtained the desired upper bound estimates for $\rho(r)$ locally, i.e. point-by-point. Especially noteworthy is the bound

$$\rho(r) \leq T/(2\pi r) \quad . \quad (60)$$

Even though this bound becomes singular only at the nucleus (i.e. at $r = 0$) and as the numerical studies evince, grossly overestimates the density, it must, however, be noted that nontrivial upper bounds to the density are hard to derive. In this sense, it is gratifying that King's bounds give a direct connection between the electron density of an atomic system and its kinetic energy (which also is the magnitude of the total energy) vide the Coulombic virial theorem for optimal densities. King and Dykema /146/ proved the result (60) also at the Hartree-Fock level. Even if these bounds may not have any impact on the enhancement of the level of accuracy in atomic structure calculations, they provide rigorous constraints on the density ρ in terms of the kinetic energy T of an atomic system. It may also be remarked that ρ and T are measurable from two separate experiments (e.g. coherent, elastic X-ray scattering leading to atomic form factors and Compton profile measurements, respectively), in the conjugate spaces of r and p . King /144/ also obtained another bound, viz.,

$$\rho(0) < 4 [T + \{2TN[(N-1)^2 + 4Z^2]\}^{1/2}] \times \\ [T + \{1 + (1 - 2T/(NZ^2))^{1/2}\}]^{1/2}/\pi \quad \dots \quad (61)$$

which connects, for Coulombic systems, the electron density at the nucleus to the system kinetic energy, through an inequality.

3.8 Interconnections Between Kinetic and Potential Energies

A fundamental relationship between the kinetic and potential energies of a given system is offered by the virial theorem (See, for example, Löwdin /147/). For instance, $2\langle\hat{T}\rangle = -\langle\hat{V}\rangle$, is satisfied by Coulombic systems in their equilibrium nuclear geometries. Some further relationships between T and V were established by Kinoshita /148,149/ via a novel approach. Consider, for a two-electron system, a well-behaved but otherwise arbitrary function $f(\mathbf{r}_1, \mathbf{r}_2)$ where \mathbf{r}_1 and \mathbf{r}_2 are the coordinates of electrons. Transforming to the center-of-mass frame : $\mathbf{u} = \mathbf{r}_1 - \mathbf{r}_2$; $\mathbf{R} = (\mathbf{r}_1 + \mathbf{r}_2)/2$; and setting $\hat{K} = -(\nabla_1^2 + \nabla_2^2)/2$ and with the identities $\nabla_{\mathbf{u}} \cdot (\hat{\mathbf{u}} \cdot \mathbf{f}^2) = \mathbf{f}^2(\nabla_{\mathbf{u}} \cdot \hat{\mathbf{u}}) + 2 \hat{\mathbf{u}} \cdot \mathbf{f} \nabla_{\mathbf{u}} \mathbf{f} = 2\mathbf{f}^2/\mathbf{u} + 2\hat{\mathbf{u}} \cdot \nabla_{\mathbf{u}} \mathbf{f}$ [$\hat{\mathbf{u}} \equiv \mathbf{u}/\mathbf{u}$]; $\nabla_1 \mathbf{f} = \nabla_{\mathbf{R}} \mathbf{f}/2 + \nabla_{\mathbf{u}} \mathbf{f}$; $\nabla_2 \mathbf{f} = \nabla_{\mathbf{R}} \mathbf{f}/2 - \nabla_{\mathbf{u}} \mathbf{f}$; so that $((\nabla_1 \mathbf{f})^2 + (\nabla_2 \mathbf{f})^2)/2 = (2(\nabla_{\mathbf{R}} \mathbf{f})^2 + (\nabla_{\mathbf{u}} \mathbf{f})^2)/2$, in the relative- and center of mass co-ordinates. A use of the Cauchy-Schwarz inequality gives

$$\begin{aligned} \langle f | 1/r_{12} | f \rangle &= - \int d^3u \, d^3R \, (\hat{\mathbf{u}} \cdot \nabla_{\mathbf{u}} \mathbf{f}) \\ &\leq \left\{ \int d^3u \, d^3R \, \mathbf{f}^2 \right\}^{1/2} \left\{ \int d^3u \, d^3R \, (\nabla_{\mathbf{u}} \mathbf{f})^2 \right\}^{1/2} \dots \quad (62) \end{aligned}$$

whence it turns out that

$$\langle f | 1/r_{12} | f \rangle \leq \langle f | \hat{K} | f \rangle^{1/2} \quad (63)$$

Thus, with the identification $f = \psi(\mathbf{r}_1, \mathbf{r}_2)$ for a two-electron system, a relationship between the kinetic energy and the electron-electron repulsion may be established. Kinoshita's result, i.e. the inequality (63), can be easily generalized to yield

$$U \leq N^{1/2} (N-1) T^{1/2} / 2^{1/2} \quad (64)$$

for an N -electron system.

Kinoshita derived some further inequalities among the kinetic energy, the electron-electron repulsion energy as well as the

electron-nuclear attraction energy. Generalizations of Kinoshita's results, though admittedly rigorous, cannot be expected to be tight for large values of N , still, they provide conditions on the values of the energy ingredients through inequalities. Some other interconnections for two-electron atoms derived by Kinoshita, are the following :

$$\langle V_1 f \mid V_2 f \rangle \leq 8 \langle f \mid \hat{K} \mid f \rangle \quad (65)$$

$$\langle Vf \mid Vf \rangle \leq 44 \langle f \mid \hat{K} \mid f \rangle \quad (66)$$

$$\langle V_1 f \mid V_1 f \rangle \leq 16 \langle f \mid \hat{K} \mid f \rangle \quad (67)$$

where $V_1 = Z/r_1$; $V = -(V_1 + V_2) + V_{12}$ with $V_{12} = 1/r_{12}$. Incidentally, it may be pointed out that using the results derived by Kinoshita, Redei/150/ obtained pointwise limits of error for atomic (spherically symmetric) $\rho(r)$ as well as on atomic form factors in terms of expectation values of the kinetic energy operator.

Yue and Janmin /151/ transcribed King's /143,144/ results to momentum-space. Further, they noticed that starting with the operator identity $i[(\mathbf{p}/p) \cdot \mathbf{r} - \mathbf{r} \cdot (\mathbf{p}/p)] = 2/p$ (caps on the operators are omitted here), with the Cauchy-Schwarz inequality, the following inequality is obtained.

$$\langle 1/p \rangle \leq \langle (\mathbf{p}/p) \cdot (\mathbf{p}/p) \rangle \langle r^2 \rangle^{1/2} = \langle r^2 \rangle^{1/2} . \quad (68)$$

With the identification $i(\mathbf{p} p^{-2} \cdot \mathbf{r} - \mathbf{r} \cdot \mathbf{p} p^{-2}) = p^{-2}$, one is led to

$$\langle p^{-2} \rangle \leq 4 \langle r^2 \rangle . \quad (69)$$

A transcription of the above results to the momentum-space yields the following bounds to the kinetic energy :

$$\langle r^{-1} \rangle^2 / 4 \leq T \quad (70)$$

$$\langle r^{-2} \rangle / 8 \leq T . \quad (71)$$

It is worth noting that Blau, Rau and Spruch /152, 153/ in their classic papers, had already employed a commutator identity $i(\mathbf{p} \cdot (\mathbf{r}/r) - (\mathbf{r}/r) \cdot \mathbf{p}) = 2/r$, exactly reciprocal to the one noted above (due to Yue and Janmin /151/). This identity, with a use of Cauchy-Schwarz inequality gives, as expected, a relation reciprocal to (68). In addition to these inequalities, the classic works of Blau, Rau and Spruch /152, 153/ contain a host of upper and lower bounds to matrix elements of a general hermitian operator. The above inequalities not only emerge as rigorous results but they also furnish certain bridging relationships between the conjugate spaces viz. \mathbf{r} and \mathbf{p} , which are not obvious at the outset, and materialize only as inequalities.

Having discussed inequalities for the (one-body) kinetic energy operator, we now embark upon an exposition of the bounds to the ubiquitous (two-body) electron-electron repulsion energy ingredient for atomic and molecular systems.

4. Bounds to Electron Repulsion Energies

It has been noted in Section 2 that the Hohenberg-Kohn energy functional, $E[\rho]$, in addition to the interaction term with the external potential, viz. $\int d^3r \rho v$, is comprised of the direct Coulomb repulsion piece $J[\rho]$ and the yet unknown functionals $T[\rho]$ and $E_{xc}[\rho]$. The respective wavefunction-based functionals, however, bear a completely known universal form. At the operational level, actual computation of the electron-repulsion energy within the wavefunction-based approach calls for an evaluation of a mammoth number of electron repulsion integrals (ERI's), consuming a good deal of computer time /4, 154, 155/ (see also Section 1 for further references). On the other hand, purely density-based approximations such as the X_α -method, yield decent estimates for various physical quantities of interest, even though they do not represent the functional $E_{xc}[\rho]$ exactly. It is gratifying to note that the connections of J and E_{xc} (cf. Section 1)

with simple, one-electron integrals that are local-density-functionals, are brought out only by the bounds to these quantities, and will never be realized, in the sense of a strict equality. This Section will be devoted to elaborate on the themes of bounds to direct (Section 4.1) and indirect (Section 4.2) Coulomb energies and also to various types of ERI's (Coulomb, exchange etc.) as well as those to electrostatic potentials.

4.1. Bounds to Direct Coulomb Energies

Schrader and Prager /156/ made a pioneering attempt towards employing electrostatic variational principles in the context of quantum-chemical molecular energy calculations. They showed that the Thomson principle of classical electrostatics can be utilized to obtain upper bounds to $J[\rho] = \int d^3r d^3r' \rho(\mathbf{r}) \rho(\mathbf{r}') / (2|\mathbf{r}-\mathbf{r}'|)$, by invoking the minimization of $J[\rho] = \int d^3r E^2 / (8\pi)$, where $\mathbf{E} = -\nabla V$ is an arbitrary electrostatic field, subject to the constraint $\nabla \cdot \mathbf{E} = -4\pi\rho$ (Note that the electron charge density is $-\rho$). Since the second variation of $\int d^3r E^2$ is always positive, one has

$$J \leq \int d^3r E^2 / (8\pi) \quad (72)$$

for all \mathbf{E} satisfying $\mathbf{E} = -\nabla V$ and $\nabla \cdot \mathbf{E} = -4\pi\rho$.

A lower bound to J was obtained by Schrader and Prager via the minimization of the functional

$$W[V] = \int d^3r [-2\rho V - (\nabla V)^2 / (4\pi)] \quad (73)$$

where V is an arbitrarily chosen scalar function subject to the Dirichlet boundary condition of existence of a surface S (including the case where it extends to infinity) on which $\nabla V = 0$. If this condition is not satisfied, extra surface terms will contribute to the right hand side of Eq. (73). Of course, this condition is satisfied automatically by atoms and molecules as they are intrinsically infinite in extent and have an

asymptotically decaying electron charge density. The minimizing condition is provided by the Poisson equation, $\nabla^2 V = 4\pi\rho$, for the electron density. Noting that the second variation of W is always nonpositive, leads to a lower bound to J , viz.

$$J \geq \int d^3r [-\rho V - (\nabla V)^2]/(8\pi) . \quad (74)$$

This, essentially, is the Dirichlet condition which has been fruitfully exploited in electrostatics for variational calculations of capacitances. It may also be worth noting here that such lower bounds to J are rather rare in the literature. The equality in relation (74) is attained only if V is precisely the electrostatic potential arising from the charge density $-\rho$. (Caution : Schrader and Prager use exactly the opposite sign convention for V to that normally employed in the literature). A combination of (73) and (74) leads to a bound

$$\begin{aligned} & \int (1/2) d^3r_1 d^3r_2 \rho_1(r_1) \rho_2(r_2)/r_{12} \\ & \geq (1/8) \int d^3r [2(-\rho_1 - \rho_2)V - (\nabla V)^2/(4\pi)] \\ & - \int d^3r E^2/(8\pi) \quad \dots (75) \end{aligned}$$

Here, $\nabla \cdot E = 4\pi (-\rho_1 + \rho_2)$.

Okniński /157-159/ derived inequalities for electron repulsion integrals, in general. He pointed out that the two-electron integrals defined by $(a|b) = \int d^3r_1 d^3r_2 a^*(r_1, r_2) \times b(r_1, r_2)/r_{12}$ and $(p|q) = \int d^3r_1 d^3r_2 p^*(r_1)q(r_2)/r_{12}$ could be treated as inner products /160-162/ in the appropriately defined spaces. Non-negativity of $[p|p]$ was proven directly by the use of Fourier convolution theorem /163/.

Use of the Gram-determinantal inequality gives the nonnegativity of J_{ij} and K_{ij} :

$$J_{ij} = \langle ii|jj \rangle \geq 0 \quad \text{and} \quad K_{ij} = \langle ij|ji \rangle \geq 0 , \quad (76)$$

while the Cauchy-Schwarz inequality yields the results

$$K_{ij} = \langle ij | ji \rangle \leq \langle ii | jj \rangle^{1/2} \langle jj | ii \rangle^{1/2} = J_{ij}, \quad (77)$$

showing that an exchange type integral can never exceed the direct Coulomb one, when both are formed out of the same orbitals i and j ; and also that the inequality

$$|\langle ij | kl \rangle|^2 \leq J_{ij} J_{kl} \quad (78)$$

holds rigorously. The results (76) through (78) were also obtained earlier by Power and Pitzer /164/. The square integrability of the orbitals does not, in general, guarantee the boundedness of a general electron repulsion integral. Such an existence condition for an electron-repulsion-type integral $I = \int d^3r_1 d^3r_2 p^*(\mathbf{r}_1) q(\mathbf{r}_2)/r_{12}$ is given by the use of the Sobolev inequality /165/, viz.

$$I \leq C_{\alpha\beta} \|p\|_{\alpha} \|q\|_{\beta} \quad (79)$$

where $C_{\alpha\beta}$ is a constant; $\alpha, \beta > 1$ and $1/\alpha + 1/\beta = 5/3$; whence the existence of the norms in the inequality (79) ensures finiteness of I . Based on these considerations, Okniński derived a bound

$$|\langle ij | kl \rangle| \leq 3 (\pi/2)^{1/3} (\int d^3r |ij|)^{2/3} (\int d^3r |kl|)^{2/3} \\ (\int d^3r |ij|^2)^{1/6} (\int d^3r |kl|^2)^{1/6} \quad \dots (80)$$

The derivation of this bound hinges upon the remarkable theorem due to Simon /165/, which is stated as follows.

Let $V \in L^1 \cap L^2$, then

$$\|V\|_R \equiv \int d^3r_1 d^3r_2 |V(\mathbf{r}_1) V(\mathbf{r}_2)|/r_{12}^2 \leq 3^{1/2} (2\pi) \|V\|_2^{2/3} \|V\|_1^{1/3} \\ \dots (81)$$

Here, $\|V\|_R$ stands for the Rollnik/166/ norm.

The inequality (80) connects the absolute magnitude of a general ERI to simple, one-electron integrals similar to the

overlap-type ones : a rigorous relation, possible only in the form of an inequality. For further comments, refer to Section 4.2.

Thulstrup and Linderberg /167/ derived bounds to direct Coulomb energies and further developed and applied the integral approximation method by Harris and Rein /168/. Thulstrup and Linderberg started with the three dimensional Sobolev inequality, giving, directly

$$\begin{aligned} 4\pi J &= 2 \int d^3r \rho(r) \phi(r) = \int d^3r |\nabla\phi|^2 \\ &\geq 3(\pi/2)^{4/3} \left(\int d^3r |\phi|^6 \right)^{1/3} \end{aligned} \quad (82)$$

where ρ is the electron density and ϕ , the electronic part of the classical electrostatic potential, $\phi(r) = \int d^3r' \rho(r')/|r-r'|$. A further application of the Hölder inequality to (82), leads to

$$J[\rho] \leq (4/3) (2/\pi)^{1/3} \left(\int d^3r \rho^{6/5} \right)^{1/3} \quad (83a)$$

which can be cast into a more flexible form by a subsequent application of the Hölder inequality, giving an upper bound to the right-hand-side integral in (82), viz.

$$\int d^3r \rho^{6/5} \leq \|f\|_m \|\rho^{6/5} f^{-1}\|_n \quad (83b)$$

where the function f is an arbitrary function such that the norms on the right in (83b) are finite, $m, n > 1$ and $1/m + 1/n = 1$. A host of further bounds to J were generated by these authors from the inequality (83b). Calculus of variations gives the 'best' constant sought for, by minimizing the ratio of a given upper bound, to the corresponding quantity under examination. For example, a result that one thus arrives at is

$$J[\rho] \leq (3/2) \pi^{-1/3} N^{4/3} \left(\int d^3r \rho^2 \right)^{1/3} \quad (84)$$

The result (83b) of the Thulstrup-Linderberg work was exploited by Gadre, Bartolotti, and Handy /16/ who obtained an upper bound in a desirable 'local' form, viz.

$$J[\rho] \leq 1.0918 N^{2/3} \int d^3r \rho^{4/3} . \quad (85)$$

The optimal constant in (85) was computed by calculus of variations /17/. Using the results due to Schrader and Prager /156/, Gadre et al. /16/ also computed lower bounds to J . By substituting $V = \rho^{1/3}$ in (74) one is led to

$$J[\rho] \geq \left(\int d^3r \rho^{4/3} \right)^3 / (N T_W[\rho]) . \quad (86)$$

The upper and lower bounds (85) and (86) respectively, to $J[\rho]$, obtained by Gadre et al. were tested for densities derived from the near Hartree-Fock atomic data due to Clementi and Roetti /169/, revealing that both these bounds are fairly tight. Incidentally, the results (83a,b) and (84) subscribe to the more general form $J \leq (\text{const.}) \{N^{(5k-3)/3} \int d^3r \rho^{1+k/3}\}^k$ as observed by Pathak et al. /170/.

The most attractive feature of the inequality (85) is that it connects the Coulomb repulsion energy to the most popular approximation for the exchange energy, viz. the Dirac-Slater exchange /43, 171, 172, 67/. An immediate interesting application of (85) was reported by Perdew and Zunger /75/ for the estimation of the self-interaction correction within the X_α -theory. By use of the bound (85) in the sense of an equality, the correction was estimated by them to be approximately /75/ $0.16 \sum_{i\sigma} \int d^3r \rho_{i\sigma}^{4/3}$ where the subscripts i and σ respectively stand for orbital (occupied) and spin indices. Along these lines, Gadre and Bendale /173/ further suggested that the Coulomb and total electron repulsion energies could be modelled as simple, gradient-free functionals of the one-particle density. Some forms explored by them were : $N^{2/3} \int d^3r \rho^{4/3}$, $(\int d^3r \rho^{6/5})^{5/3}$, $(\int d^3r \rho^2)^{1/3} N^{4/3}$ and $N^{3/2} (\int d^3r \rho^3)^{1/6}$. They observed that all these forms lead to remarkably linear fits to J and U when near Hartree-Fock (NHF) data /169/ for density were utilized.

In the spirit of Schrader and Prager's /156/ work, Gadre and Pathak /174/ implemented variational calculations on the He atom

and H_2 molecule by replacing $J[\rho]$ by its upper bound given by the inequality (85). Such a replacement, in the case of the helium atom, leads to a total energy higher by about a mere one per cent as compared to its NHF counterpart, while the H_2 molecule exhibits binding around the true equilibrium internuclear distance for a simple James-Coolidge type model and here too, the sacrifice in energy turned out to be just 0.2 per cent. Further, Pathak et al. /61/ modelled the atomic total electron-repulsion energy U as a local functional viz. $(AN^{2/3}-B) \int d^3r \rho^{4/3}$, (A and B are empirical constants) towards the construction of an atomic model in momentum-space. Semiclassical phase-space considerations /175, 176/ had earlier revealed that $\int d^3r \rho^{4/3}$ is approximately proportional to the expectation value of the magnitude of the linear momentum. By a prescription of the nuclear-electron attraction energy in the quasiclassical spirit, these authors developed the above simple atomic local density functional model in momentum space, analogous to an earlier co-ordinate-space one, due to Parr et al. /177/. This first-ever concrete density-based model in momentum space yields a remarkably simple form for the momentum space properties and further, gives quick yet decent estimates of several quantities of physical interest.

Golden /178/ applied the bound (83) due to Linderberg and Thulstrup /167/ to obtain

$$\begin{aligned} \sum_{n=1}^{N_{\uparrow}} \int d^3r_1 d^3r_2 |\psi_n(\mathbf{r}_1)|^2 |\psi_n(\mathbf{r}_2)|^2 / r_{12} \\ \leq (2^{10/3} / (3\pi^{1/3})) \int d^3r \rho_{\uparrow}^{4/3} \end{aligned} \quad (87a)$$

Here, N_{\uparrow} denotes the number of spin-up electrons and

$$\rho_{\uparrow}(\mathbf{r}) = \sum_{n=1}^{N_{\uparrow}} |\psi_n(\mathbf{r})|^2. \quad (87b)$$

employing his earlier result, Golden /179/ derived a bound to the exchange part of the electron-repulsion energy. These results are valid within the independent electron models such as the

Hartree-Fock theory. On the other hand, general bounds to the indirect part of electron repulsion, viz. $E_{xc}[\rho]$ were derived by Lieb /180/ and Lieb and Oxford /17/. These works, well-deserving a detailed exposition, will be treated in Section 5.2.

Chakravorty and Gadre /121/ were able to demonstrate interesting interconnections among apparently unrelated physical quantities such as Coulomb energy, X-ray scattering intensities and the average electron density $\langle \rho \rangle = \int d^3r \rho^2$ and the $\langle r^n \rangle$ expectation-values. For example, they showed that for atomic densities,

$$J[\rho] \leq (1/2) N \langle r^{-1} \rangle = N V_{ne} / (2Z) ; \quad (88)$$

and further obtained a lower bound to $J[\rho]$, viz.

$$J[\rho] \geq \pi^2 \langle r^{-1} \rangle^3 / (18 \langle r^{-2} \rangle) \quad (89)$$

For the sake of completeness, it may be pointed out that besides the rigorous treatments reviewed herein, there also exist some approximate upper bounds to ERI's reported in the literature (the reader may consult Pipek /181/ and references therein). However, these works fall outside the scope of this review, which limits itself exclusively to the discussion of rigorous inequalities.

In a study due to Weinstein et al. /182/, numerical tests on a number of atoms (see /183/, /184/ and /185/ for further extensions) within the HF approximation indicate that the spherically averaged atomic density $\rho(r)$ is, without exception, indeed a monotone decreasing function, i.e. $d\rho/dr \leq 0$. No general rigorous proof for this observation yet exists. It is, however, possible to establish rigorously the monotone decrement of the resulting spherically symmetric atomic (neutral atoms as well positive ions) total electrostatic potential, viz. $\phi(r) = Z/r - \int d^3r' \rho(r')/|\mathbf{r}-\mathbf{r}'|$. Use of the Poisson equation, for this spherically symmetric situation leads to

$$\phi'' + 2 \phi'/r = 4 \pi \rho \geq 0 \quad (90)$$

Now, assume that there exists a local maximum at $r = R$. This means that $\phi'(R) = 0$, implying from (90) above, that $\phi''(R)$ cannot be negative. Thus, $\phi(r)$ cannot have local maxima and hence must be a monotone decreasing function of r .

More recently, Sen and Politzer /186/ have shown that an atomic negative ion, however, exhibits a minimum in $\phi(r)$ at some $r = r_m < \infty$, such that the charge enclosed inside a sphere of radius r_m exactly equals, in magnitude, the nuclear charge. The proof to this effect readily follows from the definition of $\phi(r)$ and Eq. (90) above. Sen and Politzer further identified r_m with the ionic radius. The nonexistence of strict local maxima for the much wider domain viz. molecular electrostatic potential has been recently established by Gadre and Pathak /187/. They also proved /188/ that the total molecular electrostatic potential for any negative molecular ion must exhibit a negative-valued (directional) minimum at a finite distance in any arbitrary direction. The validity of these theorems has been numerically tested out for several molecular anions such as OH^- , CN^- , NH_2^- , NO_3^- etc.

Incidentally, the monotonicity of atomic $\gamma(p)$, the spherically averaged electron momentum density, has also been explored in several recent studies /189-193/. Here, however, it turns out that a given ground state atomic $\gamma(p)$ is generally nonmonotonic if there are more than two valence p- or d- electrons in an atom/ion. Even though no rigorous explanation of this fact exists except (heuristically speaking) for the preponderance of p- or d- occupancy resulting into nonmonotonicity, it appears that this behavior is intrinsic and not an artefact of a particular basis-set.

We now conclude this Section on the studies of bounds to direct, i.e. classical, electronic Coulomb-repulsion energies. Rigorous inequalities involving the indirect (viz. quantal) part are discussed in the following Subsection.

4.2. Bounds to Indirect Coulomb Energies

A derivation akin to that by Gadre et al. /16/ leads to an upper bound to the exchange integral (the u_i 's are the canonical Hartree-Fock orbitals)

$$K_{ij} \equiv \int d^3r d^3r' u_i^*(\mathbf{r}) u_j^*(\mathbf{r}') u_i(\mathbf{r}') u_j(\mathbf{r}) |\mathbf{r}-\mathbf{r}'|^{-1}, \quad (91)$$

as demonstrated by Pathak /194/. Defining the "differential overlap" as $F_{ij}(\mathbf{r}) = u_i^*(\mathbf{r}) u_j(\mathbf{r})$, the exchange integral can be cast into the form $K_{ij} = \int d^3r |\phi_{ij}(\mathbf{r})|^2 / (4\pi)$, (clearly implying the non-negativity of it, as seen earlier vide Section 4.1.) with the complex "potential" $\phi_{ij}(\mathbf{r})$ identified with $\int d^3r' |\mathbf{r}-\mathbf{r}'|^{-1} F_{ij}^*(\mathbf{r}')$. Application of the three-dimensional Sobolev inequality and that of the Cauchy-Schwarz inequality in succession, yields

$$K_{ij} \leq (8/3) (2/\pi)^{1/3} \left[\int d^3r |F_{ij}(\mathbf{r})|^2 \right]^{2/3} \times \\ \left[\int d^3r |F_{ij}(\mathbf{r})|^{4/3} \right] \leq \int d^3r |F_{ij}(\mathbf{r})|^{4/3} \quad \dots (92a)$$

The inequality on the extreme right follows from the fact that

$$\int d^3r |u_i u_j| \leq \left[\int d^3r |u_i|^2 \right]^{1/2} \left[\int d^3r |u_j|^2 \right]^{1/2} = 1. \quad (92b)$$

Multiplication by $(-1/2)$ and summing over i and j ($i \neq j$) in (92a), leads to a lower bound to the HF-exchange energy for closed-shell systems in terms of simpler one-electron integrals.

An extremely important versatile lower bound to E_{ind} , the 'indirect' or purely quantal part of the electron-electron repulsion energy U , (viz. $E_{ind} = U - J$, for electrons, $E_{ind} = E_{xc}$) for a system of like charges $e_1, e_2, e_3, \dots, e_N > 0$ (or all < 0) obeying arbitrary dynamics and statistics, was derived by Lieb /180/. In his elegant work, Lieb derived a lower bound to the electron-electron repulsion operator U ($\equiv U$) itself, namely,

$$U \equiv \sum_{i < j} e_i e_j / r_{ij} \geq -D[\rho, \rho] + \sum_{i=1}^N (2D[\rho, \mu_i] - D[\mu_i, \mu_i]) \\ \dots (93)$$

where, $D[f, g] = \int d^3r d^3r' f(r) g(r') / (2|r-r'|)$, and the functions $\mu_i(r)$ are arbitrary but for the constraints (i) $\mu_i(r) \geq 0$; (ii) $\mu_i(r) \equiv \mu_i(|r-r_i|)$, they are spherically symmetric around r_i ; (iii) $\int d^3r \mu_i \leq e_i$. The picture of the μ_i 's is that of a number of spherical "scoops" taken out of a given density distribution ρ . Notice that the dependence of the right hand side of the inequality (93) on the position vectors r_i ($i = 1, 2, \dots, N$) comes implicitly through that of the functions μ_i . The functions μ_i as prescribed by Lieb were :

$$\mu_i(r, r_i) = \bar{\rho}_\psi(r) \Theta(R_i(r_i) - |r-r_i|) \quad (94a)$$

where

$$\bar{\rho}_\psi = (4\pi)^{-1} \int d\Omega_{(r-r_i)} / |r-r_i| \rho_\psi(r-r_i), \quad (94b)$$

is the spherical average of ρ_ψ around r_i and $R_i(r_i)$ are the radii of spheres centered at r_i that encompass a total charge exactly equal to e_i , for each label i . Setting $I[\psi] \equiv \langle \psi | \sum_{i < j} e_i e_j / r_{ij} | \psi \rangle$, the total Coulomb repulsion for the state ψ , Lieb proved that

$$E_{\text{ind}}[\psi] = I[\psi] - D[\rho_\psi, \rho_\psi] \geq -C \left\{ \int d^3r \rho_\psi^{4/3} \right\}^{1/4} \left\{ \int d^3r \left[\sum_{i=1}^N e_i^{2/3} \rho_\psi^i(r) \right]^{4/3} \right\}^{3/4} \dots \quad (95)$$

The contribution ρ_ψ^i to the total density is given by $\rho_\psi^i(r_i) = e_i \sum_\alpha \int d^3r_1 d^3r_2 \dots d^3r_{i-1} d^3r_{i+1} \dots d^3r_N |\psi(r_1, r_2, \dots, r_N)|^2$; α denoting the degrees of freedom apart from the spatial ones (e. g. spin). Evidently, $\rho_\psi(r) = \sum_{i=1}^N e_i \rho_\psi^i(r)$. For electrons $|e_i| = 1$ in Hartree units and the constant C , occurring in the inequality

$$E_{\text{ind}} \geq -C \int d^3r \rho^{4/3}(r) \quad (96)$$

turns out to be $C = \pi^{1/12} 3^{11/12} 2^{3/2} \approx 8.52$. It is gratifying that this rigorous lower bound to the indirect Coulomb energy is a simple local functional of the density and is qualitatively

similar in form to its major ingredient, viz. $E_{\text{exch}} = -C_{\text{ex}} \times \int d^3r \rho^{4/3}$ (with the constant $C_{\text{ex}} = 3(3\pi)^{1/3}/4 \approx 0.7386$), which is the celebrated Dirac-Slater approximation to the exchange energy. Also of interest is the connection of $J[\rho]$ to the above local exchange energy, via an inequality (cf. inequality (85)).

The choice of the auxiliary functions μ_i in (93) is not the best one in the sense that the flexibility offered in the choice of μ_i is not fully exploited, as Lieb and Oxford /17/ demonstrated by making the inequality (96) tighter. Furthermore, the use of the "maximal function" /180/ was bypassed. Lieb and Oxford started from the operator inequality (93) and proposed the following choice for μ :

$$\mu_{\mathbf{r}}(\mathbf{r}') \equiv \lambda^3 \rho_{\psi}(\mathbf{r}) \mu(\lambda) \rho_{\psi}^{1/3}(|\mathbf{r}-\mathbf{r}'|) \quad (97)$$

with the positive scaling constant λ suitably determined. The inequality (93) is then rewritten as

$$\begin{aligned} \sum_{i < j=1}^N e_i e_j / r_{ij} \geq & -D[\rho_{\psi}, \rho_{\psi}] + 2 \sum_{i=1}^N D[\rho_{\psi}, e_i \delta_{\mathbf{r}_i}] \\ & - 2 \left(\sum_{i=1}^N D[\rho_{\psi}, e_i \delta_{\mathbf{r}_i} - e_i \mu_{\mathbf{r}_i}] + \sum_{i=1}^N D[e_i \mu_{\mathbf{r}_i}, e_i \mu_{\mathbf{r}_i}] \right) \\ & \dots \quad (98) \end{aligned}$$

with $\delta_{\mathbf{r}}(\mathbf{r}) \equiv \delta(\mathbf{r}-\mathbf{r}_i)$, the usual three-dimensional Dirac δ -distribution, representing a unit point charge located at \mathbf{r}_i . The introduction of the δ -distribution, by virtue of its being the single-particle density operator, leads naturally to ρ_{ψ}/N for its expectation value in the state ψ . The inequality thus engendered reads

$$\begin{aligned} I[\psi] \geq & D[\rho_{\psi}, \rho_{\psi}] - \left\{ \sum_{i=1}^N \int d^3r_i \ 2 D[\rho_{\psi}, \delta_{\mathbf{r}_i} - \mu_{\mathbf{r}_i}] \rho_{\psi}^i(\mathbf{r}_i) \right. \\ & \left. + \sum_{i=1}^N \int d^3r_i \ D[\mu_{\mathbf{r}_i}, \mu_{\mathbf{r}_i}] e_i \rho_{\psi}^i(\mathbf{r}_i) \right\} . \quad \dots \quad (99) \end{aligned}$$

Next, Lieb and Oxford prescribed a choice for μ , with the introduction of a parameter λ in the definition of $\mu \equiv \mu_{\mathbf{r}}(\mathbf{r}') =$

$\lambda^3 \rho_\psi(\mathbf{r}) \mu(\lambda \rho_\psi^{1/3}(\mathbf{r})(\mathbf{r}-\mathbf{r}'))$ for $|\mathbf{r}-\mathbf{r}'| \leq \lambda^{-1} \rho_\psi^{1/3}(\mathbf{r})$ and $\mu_{\mathbf{r}}(\mathbf{r}') = 0$, otherwise. The difference with Lieb's /180/ earlier treatment is that, here, $\int d^3r' \mu_{\mathbf{r}}(\mathbf{r}')$ equals unity. Such a construction also provides a handle (through the flexibility of $\lambda > 0$) for optimizing the bound, which eventually yields

$$E_{\text{ind}}[\psi] \geq -1.68 \left[\int d^3r \sum_{i=1}^N e_i \rho_\psi^1(\mathbf{r})^{4/3} \right]^{1/2} \left[\int d^3r \rho_\psi^{4/3}(\mathbf{r}) \right]^{1/2}. \quad \dots (100)$$

For a many electron system, $E_{\text{ind}}[\psi] \geq -1.68 \int d^3r \rho^{4/3}(\mathbf{r})$. This lower bound is a marked improvement over Lieb's earlier inequality (96), but the coefficient of 1.68 is still numerically far larger than $C_{\text{ex}} \approx 0.7386$ occurring in the Dirac-Slater exchange energy estimate. However, the result (100) is a rigorous general result for Coulombic interactions; independent of spin and statistics, a fact that endows elegance to it. It must be pointed out here that strict negative semidefiniteness of E_{ind} has not yet been established for an arbitrary many-electron system. However, for Coulombic interactions E_{ind} is intuitively expected to conform to this property.

Hertel, Lieb and Thirring /195/ had earlier considered the problem of seeking a lower bound (in terms of a single-electron operator) for the operator $U \equiv \sum_{i < j} 1/r_{ij} = \sum_{i \neq j} 1/(2r_{ij})$, of the form

$$U \geq \sum_{i=1}^N \phi(r_i) - \Lambda, \quad (101)$$

where ϕ is an arbitrary real integrable function, Λ being a constant. The derivation of the inequality (101) rests on finding a subsidiary potential $v(\mathbf{r})$ with the properties

$$1/r \geq v(\mathbf{r}) \equiv \int d^3k e^{i\mathbf{k} \cdot \mathbf{r}} \tilde{v}(\mathbf{k}) / (2\pi)^3, \quad (102)$$

with $\tilde{v}(\mathbf{k}) \geq 0$, denoting the Fourier transformation of $v(\mathbf{r})$. The inequality (102) physically means that the potential $v(\mathbf{r})$ decays faster than the Coulombic one, yielding a lower bound to the

operator U , viz.

$$U \geq \sum_{i,j} v(\mathbf{r}_i - \mathbf{r}_j) - N \tilde{v}(0)/2, \quad (103)$$

Defining $\mu(s)$ to be a measure, the Cauchy-Schwarz inequality may be used to give

$$\int d\mu(s) |f(s)|^2 \geq \left[\int d\mu(s) |f(s)| \right]^2 \int d\mu(s) \quad (104)$$

Here, s is a generic symbol for a space with arbitrary dimensions. With the substitutions $d\mu \equiv d^3k \tilde{\phi}^2(\mathbf{k}) / \{(2\pi)^3 \tilde{v}(\mathbf{k})\}$; $f \equiv \sum_{i=1}^N e^{i\mathbf{k} \cdot \mathbf{r}_i} \tilde{v}(\mathbf{k}) / \tilde{\phi}(\mathbf{k})$ (Here, 'tilde' denotes the Fourier-transformed quantity) along with the assumption of reality and non-negativity of $\tilde{\phi}(\mathbf{k})$ and $\tilde{v}(\mathbf{k})$. One then obtains

$$U \geq \sum_{i=1}^N \phi(\mathbf{r}_i) - \int d^3k \left\{ \tilde{\phi}^2(\mathbf{k}) / \tilde{v}(\mathbf{k}) - N \tilde{v}(\mathbf{k}) \right\} / (2(2\pi)^3). \quad \dots (105)$$

This interesting result gives a lower bound to U in terms of two arbitrary, local one-body functions, ϕ and a function v (both leading to real and non-negative Fourier transforms).

Hertel et al. also demonstrated the usefulness of their bound (105) for some model potentials. For the actual Coulomb problem, the choice $v(|\mathbf{r}|) = 1/r$ obviously leads to divergences, but the modified screened Coulomb choice $v(|\mathbf{r}|) = [1 - \exp(-\alpha r)]/r$ (with $\alpha > 0$) for the subsidiary potential leads to non-trivial lower bounds for the electron-electron repulsion energy. This work gives yet another instance where bounds to a two-body interaction energy occur in terms of simpler, one-body integrals. Incidentally, it may be remarked that Löwdin /196,197/ has obtained lower bounds to electronic Coulomb integrals by the method of inner projections, simplifying the actual evaluation of electron repulsion integrals.

4.3. Bounds to Electron Repulsion Integrals (ERI) over Gaussian Basis-Sets

We now turn our attention to the extremely practical problem of obtaining rigorous bounds to ERI's over Gaussian basis-sets. As noted earlier (cf. Section 1), the number of ERI's is $\sim N^4/8$ for basis-sets comprising of N primitive Gaussians. However, it is known that a large fraction of the electron-repulsion integrals (ERI's) are negligibly small in magnitude. Clementi and co-workers carried out a systematic study of the computer time needed for the evaluation of various types of ERI's such as $\langle ii|jj \rangle$, $\langle ij|ji \rangle$, $\langle ii|ij \rangle$, $\langle ii|ii \rangle$ etc. over Gaussian basis-sets. These studies reveal that even for a relatively small molecule such as ethane, a significant fraction of three or four center integrals are "negligible", i.e. smaller in magnitude than a pre-chosen cutoff value (which usually is set to be $\sim 10^{-8}$, $\sim 10^{-10}$ etc.). Clementi /198/ put forth the strategy of 'differential accuracy' for the computation of ERI's. Habitz and Clementi /199/ further analyzed the statistical distribution of various types of ERI's for large molecules such as Sugar-Phosphate-Guanine complex, benzopyrene, etc. Dupuis et al./200/ discussed certain storage and evaluation strategies for the ERI's based on the estimation of their numerical values. Schlegel /201/, Obara and Saika /202/ as well as Head-Gordon and Pople /203/ have given certain recursion relations facilitating the evaluation as well as storage of ERI's for Gaussian basis-sets. More recently, Clementi and Corongiu /4/ have given a detailed treatment of molecular ERI's, used by them in their versatile molecular package, KGNMOL.

Despite the above mentioned studies, very few rigorous upper and lower bounds to the absolute value of the general electron repulsion integral, viz. $|\langle ij|kl \rangle|$ appear in the literature. These bounds may be obtained in terms of upper and lower bounds to the special functions $F_m(t) = \int_0^1 du u^{2m} \exp(-tu^2)$, introduced by Boys /204/ and later used by Shavitt /205/. We enlist in the

Appendix some of these upper and lower bounds as summarized by Gadre et al. /206, 207/. The work due to Ahlrichs /9/ had earlier utilized the simplest of these results, viz. $F_0(t) \leq 1$ for extracting an upper bound to the integrals involving exclusively s-type Gaussians. Later, Gadre and Pathak /206/ presented a general set of upper as well as lower bounds to ERI's involving s-, p- as well as d-type primitive Gaussian functions. These authors also established detailed connections of these results with the density-based works mentioned in Section 4.3. Recently Gadre, Kulkarni and Pathak /207/ have further obtained rigorous bounds to molecular electrostatic potentials (MESP). These bounds have been gainfully exploited for the development of an efficient algorithm for the computation of MESP maps. The use of these bounds to ERI's and MESP's need not be overemphasized. Here, one has upper and/or lower bound criteria which may lead to substantial savings in CPU time as well as disk-space. On the other hand, as these bounds are rigorous, their use is theoretically completely justifiable.

5. BOUNDS TO TOTAL ELECTRONIC ENERGIES FOR COULOMB SYSTEMS

The themes of bounds to kinetic- and electron-electron-repulsion energy functionals encompassing a vast amount of literature have been presented in Section 3 and 4 respectively. In addition, there are several inequality-related significant works which form a class by themselves and thus require a detailed exposition. Section 5.1 reviews works on the stability of atomic and molecular negative ions pioneered by Lieb. In Section 5.2, non-binding theorems within the Thomas-Fermi and related domains will be discussed. Bounds to the number of eigenvalues for a discrete spectrum of Hamiltonians for bound systems will be presented in Section 5.3. These studies form the background for the study on stability of matter (Section 5.4). A constrained

search approach to energy functionals will be presented in Section 5.5 followed by yet another remarkable study, of Coulomb systems, by Lieb (cf. Section 5.6). Inequalities in connection with molecular electronic energies form the theme of Section 5.7.

5.1. Stability of Negative Ions

Empirically, it is well-known that the maximum degree of negative ionization of any neutral atom is just two; e.g. O^{--} , S^{--} , etc. Benguria and Lieb /208/ explored the general problem of stability of negative ions vis-a-vis the roles played by the Pauli exclusion- and uncertainty principles. It was found that only limited instability of negative-ions is accounted for, by the former.

Lieb /26/ derived a rigorous upper bound to the maximum number of negative particles (fermions or bosons or a mixture of both) of charges $-q_j |e|$ ($q_j > 0$, $j = 1, 2, \dots, N$) that can be stably bound to an atomic nucleus of charge $+Z|e|$ (we take $|e| = 1$). Lieb's classic proof now follows : Consider a system of N particles with the Hamiltonian

$$\hat{H}_N = \sum_j (\hat{T}_j - q_j V(r_j)) + \sum_{i < j} q_i q_j / |r_i - r_j| \quad , \quad (106)$$

with $\hat{T}_j = -\nabla_j^2 / (2m_j)$ and $V(r_j)$ the external (nuclear-electron) potential. Isolate some j^{th} particle rendering the decomposition $\hat{H}_N = \hat{H}'_{N,j} + \hat{h}_j$ with $\hat{h}_j = \hat{T}_j - q_j Z/r_j + \sum_{k \neq j} q_j q_k / |r_j - r_k|$ for the j^{th} particle. Denote the entire configuration space, viz. (r_1, r_2, \dots, r_N) by R , and by R_j , the set of coordinates of all but the j^{th} particle. The variational principle then yields

$$\langle r_j | \psi | \hat{H}_{N,j} | \psi \rangle \geq E'_{N,j} \langle r_j | \psi | \psi \rangle \quad , \quad (107)$$

for a fixed r_j . Now, with the assumption that $E_N \leq E'_{N,j}$ for the respective ground states, and noting that $\int d^{3N}R |\psi| \hat{H} \psi = E_N \int d^{3N}R |\psi|^2$ for real ψ , one has

$$\int d^{3N-3}R_j d^3r_j |r_j| \psi \hat{H}'_{N,j} \psi + \int d^{3N-3}R_j d^3r_j |r_j| \psi \hat{h}_j \psi \\ = E_N \langle |r_j| \psi | \psi \rangle \leq E'_{N,j} \langle |r_j| \psi | \psi \rangle ; \quad \dots (108)$$

whence it follows that

$$\langle |r_j| \psi | \hat{h}_j | \psi \rangle \leq 0 . \quad (109)$$

Now, setting $g(r) = |r|f(r)$, and $t = \int d^3r |r| f(r) \nabla^2 f(r) = - \int d^3r g(r) \nabla^2(g(r)/r)$, one has

$$t = \int d^3r (\nabla^2 g(r))^2 / r + 2\pi g^2(0) > 0 . \quad (110)$$

Thus the positivity of $\langle |r| \psi | \hat{T} | \psi \rangle$ is established. Now, using the triangle inequality $|r_j| + |r_k| \geq |r_j - r_k|$, Lieb established that

$$(1/2) \int d^{3N}R \psi^2 \sum_{k \neq j} q_j q_k (|r_j| + |r_k|) / |r_j - r_k| \\ \geq \sum_{k \neq j} q_j q_k / 2 = Q^2 / 2 - \sum_j q_j^2 / 2 , \quad \dots (111)$$

with the identification

$$q_j \langle |r_j| \psi | V(r_j) | \psi \rangle = Z \sum_j q_j \equiv Z Q \quad (112)$$

for atoms, with $V(r) = -Z/r$, the inequalities (110)-(112) together yield a condition that the relation (109) is valid only if the inequality

$$Q^2 - \sum_j q_j^2 < 2 Z Q \quad (113)$$

strictly holds. For atoms, this readily gives

$$N < 2 Z + 1 \quad (114)$$

An immediate appealing consequence of (114) is that H^{2-} is not stable, since $N = 3$ and $Z = 1$ would violate the bound (114).

Incidentally, H^{2-} ion has recently been reported as a metastable species in CaO and MgO crystals /209,210/. However, this does not

violate the validity of the above result, since this experimental finding applies to a crystalline environment and not to free species. For larger atomic systems, the result (114) is not tight, since the derivation of the above inequality is mitigated by the total neglect of the kinetic-like contribution.

Lieb further generalized his results to molecules:

$$N < 2Z + K - 1 \quad (115)$$

where K is the number of atoms in a given molecule and Z is the sum of all the corresponding nuclear charges. Lieb, Sigal, Simon and Thirring /27/ arrived at a result that the ratio $N(Z)/Z \rightarrow 1$ as $Z \rightarrow \infty$, for atomic systems. Here, $N(Z)$ denotes the number of electrons that a nucleus of charge Z binds (within the non-relativistic quantum theory). Incidentally, it may be noted that Hill /211/ rigorously demonstrated that the (nonrelativistic) H^- (hydride) ion has only one bound state. A noteworthy study of Drake /212/ showed that the 3P state arising from $2p^2$ configuration is a bound one. However, the work of Hill does not apply to 3P states. In a more general context, rigorous upper bounds to the number of bound eigenvalues have also been formulated in the literature. For a further discussion of these bounds, refer to Section 5.3.

5.2. Nonbinding Theorems within Statistical Theories

A rigorous general proof of molecular nonbinding within the Thomas-Fermi (TF) theory and its variants was given by Teller/29/. This confirmed the earlier conjecture by Sheldon /213/ which was based purely on numerical computations for the case of the nitrogen molecule. Teller's /29/ proof begins with the TF description of the atomic electrostatic potential $V(\mathbf{r})$, leading to the TF equation

$$\nabla^2 V(\mathbf{r}) = V^{3/2}(\mathbf{r}) - \rho_+, \quad (116)$$

ρ_+ being the nuclear (positive) charge density. Eq. (116) is obtained by introducing proper distance-scaling factors so as to yield a unit coefficient for the first term. Teller's molecule-building process goes as follows : add a localized, infinitesimal positive charge density $\xi(\mathbf{r})$ at a fixed point \mathbf{R} ($\mathbf{R} \neq 0$) and an equal (but opposite in sign) diffuse negative charge distribution rendering the composite system electrically neutral. Further, this new two-center system is assumed to conform to the TF theory. This process is repeated bit by bit, adding the localized positive and distributed negative charges to eventually build a TF-"molecule". After the very first addition of charges, one has

$$\nabla^2 V(\mathbf{r}) + \nabla^2 \epsilon(\mathbf{r}) = [V(\mathbf{r}) + \epsilon(\mathbf{r})]^{3/2} - \left\{ \rho_+(\mathbf{r}) + \xi(\mathbf{r}) \right\} \dots (117)$$

where $\epsilon(\mathbf{r})$ is the resultant infinitesimal change in the electrostatic potential as a consequence of the above addition of charge distributions. Linearization of Eq. (117) with a use of Eq. (116) leads to

$$\int_{\Omega} d^3r \nabla^2 \epsilon = \int_S dS \cdot \nabla \epsilon = (3/2) \int_{\Omega} d^3r V^{1/2} \epsilon \quad (118)$$

the surface S encloses the volume Ω containing neither the nucleus nor the additional positive charge. Eq. (118) implies that $\epsilon(\mathbf{r})$ has the same sign throughout the entire space, which in fact turns out to be positive (otherwise a contradiction results : Assuming that $\epsilon > 0$ outside S and $\epsilon < 0$ inside, the surface integral becomes positive, the volume integral still remaining negative, violating Eq. (118)). Further, the net change in the total energy, viz. δE for the process is

$$\begin{aligned} \delta E &= \delta E_v^{\text{elec}} + \delta Q \int d^3r \rho_+(\mathbf{r})/|\mathbf{r} - \mathbf{R}| \\ &= \int d^3r \left\{ \delta E_v^{\text{elec}} / \delta \rho(\mathbf{r}) \right\} \delta \rho(\mathbf{r}) + \int d^3r (\delta E_v^{\text{elec}} / \delta v(\mathbf{R})) \times \\ &\quad \left\{ -\epsilon(\mathbf{r}) \right\} + \delta Q \int d^3r \rho_+(\mathbf{r})/|\mathbf{r} - \mathbf{R}| \dots (119) \end{aligned}$$

where $\delta Q = \int d^3r \xi$ and v is the external potential (i.e. of the positive species). Further, $\epsilon(r) = \delta Q/|r-R| \geq 0$ and $\delta E/\delta \rho(r) = \mu = 0$, since, the chemical potential for a neutral TF system always vanishes. Thus, $\delta E_{\text{total}} = \delta Q \int d^3r (\rho_+(R) - \rho(R))/|r-R| \equiv \delta Q V(R)$, where $V(R)$ denotes the electrostatic potential at R . Teller further proved that $V(R)_{\text{"molecule"}} > V(R)_{\text{"separated atoms"}}$. We give a rather different proof: Assuming spherical symmetry to start with, one observes, with $\rho_+ = Z \delta(r)$ that $V(R) = Z/R - \{ \int_0^R dr \rho(r) 4\pi r^2 / R + \int_R^\infty dr \rho(r) 4\pi r \}$. For the very last term, $r \geq R$ so that $1/r \leq 1/R$, making the quantity in the curly brackets smaller than $\int_0^\infty dr \rho(r) 4\pi r^2 / R = Z/R$, implying the non-negativity of $V(R)$. Thus, the first order-change $\delta E_{\text{total}} > 0$, which thereby rules out any stable molecule within the TF domain.

Balázs/30/ extended the domain of validity of Teller's theorem. He proved that: No theory, within which $\rho(r)$ is a function exclusively of the electrostatic potential $V(r)$ at the same location r , can describe stable molecules. Unlike Teller's arguments which are based on energetics, Balázs' proof employs electrostatic-field considerations: If the combined electrostatic force produced by the electrons and the other nucleus in a diatom is repulsive, there is no binding. In a homonuclear diatomic molecule AB , the force on the nucleus A , viz. F_A , is given by

$$F_A = \int d^3r \rho_A \tilde{E} \quad (120)$$

with \tilde{E} denoting the electrostatic field. Enclosing one of the nuclei, say A , by two surfaces, S (curved) and S' (flat) (see Fig. 1) one forms the region of interest, Ω . The surface S' for this homonuclear diatom is evidently perpendicular to the electrostatic equipotential surfaces. The surface S , upon which the electric field identically vanishes may even have to be located at infinity. The Poisson equation $\rho_A(r) = -\nabla^2 V(r)/(4\pi) + \rho(r)$ in conjunction with $\tilde{E} = -\nabla V$ gives the force on the nucleus A which has the (positive) nuclear charge distribution ρ_A .

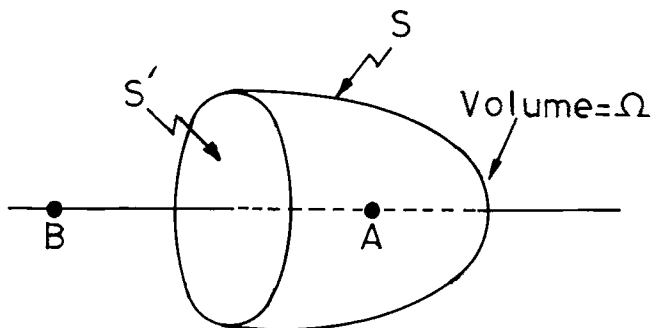


Figure 1. Balázs' construction of surfaces S (curved) and S' (flat), for a homonuclear diatomic molecule AB . A and B denote the respective nuclear positions.

Simplifying,

$$F_A = \oint_{S+S'} [dS \cdot \nabla V] [\nabla V] / (4\pi) - \oint_{S+S'} dS (\nabla^2 V) / (8\pi) - \int_{\Omega} d^3r \rho \nabla V, \quad (121)$$

by virtue of the vector form of Gauss' theorem. Since, on S , the field is zero and on S' , $\nabla V \cdot dS = 0$, the first term as well as the S -contribution to the second term vanishes; thus the first two terms, on the net, lead to a repulsive force. The third term, owing to the fact that $\rho = f(V) \geq 0$ can be transformed as indicated by the following string of arguments :

$$\begin{aligned} - \int_{\Omega} d^3r \rho \nabla V &= - \int_{\Omega} d^3r f(V) \nabla V = - \int_{\Omega} d^3r \nabla \int^V dV' f(V') = \\ &= - \oint_{S+S'} dS \int^V dV' f(V') = - \int_S dS \int^V dV' f(V'), \end{aligned}$$

which also contributes a force in the positive direction. This readily follows from the fact that f is a non-negative function and further, that all the surface elements dS on S' point in the direction AB leading to a force in the direction BA , tending to pull the nucleus A apart. Thus, within any theory where the density at every point is a local function of the electrostatic

potential at that point, molecular binding is not possible. Incidentally, Balázs also demonstrated that with the introduction of the first inhomogeneity, or the Weizsäcker correction, an attractive force between the two atoms results at large separations favoring binding. Balázs' nonbinding arguments /30/ are also generalizable to heteronuclear systems.

5.3. Inequalities for Number of Bound Eigenvalues for a Discrete Spectrum

As has already been pointed out in Section 4.2, Lieb /14/ and Lieb and Thirring /105, 217/ obtained a lower bound to the kinetic energy (the inequality (34) Section 4.2). Their derivation was founded on the upper bounds to the number of bound eigenstates for a given potential /214-216/ derived earlier. A comprehensive treatment of these results has been presented by Thirring /165/, which now follows.

Notation : Let $N(\hat{H})$ denote the number of nonpositive eigenvalues, of a Hamiltonian $\hat{H} = \hat{\mathbf{p}}^2 + \hat{V}$; $\hat{V} = V(\mathbf{r})$ being a one-body multiplicative potential. Here, we deviate from the usual Hartree units to keep in conformity with Thirring's notation.

Theorem : $N(\hat{\mathbf{p}}^2 + \lambda \hat{V})$ is a monotonically increasing function of $\lambda > 0$. By the operator inequality $\hat{H}_1 \leq \hat{H}_2$, we have, since the energy levels of the latter could never fall below those of the former, that $N(\hat{H}_1) \geq N(\hat{H}_2)$. Also, $N(\lambda \hat{H}) = N(\hat{H})$, i.e. scaling the Hamiltonian by a positive scaling parameter does not alter the number of bound eigenstates. Hence it follows that

$$N(\hat{\mathbf{p}}^2 + \lambda_1 \hat{V}) \geq N(\lambda_1 (\hat{\mathbf{p}}^2 + \lambda_2 \hat{V}) / \lambda_2) = N(\hat{\mathbf{p}}^2 + \lambda_2 \hat{V}) ,$$

for $\lambda_1 \geq \lambda_2$ (122)

The Birman-Schwinger /214, 215/ bound reads

$$N(\hat{\mathbf{p}}^2 + \hat{V} + c^2) \leq \left\{ \left\| (\hat{\mathbf{p}}^2 + c^2)^{-1/2} |\hat{V}|_-(\hat{\mathbf{p}}^2 + c^2)^{-1/2} \right\|_q \right\}^q$$

... (123)

where c is a real constant, $N(\hat{H} + c^2)$ denotes the number of eigenvalues of \hat{H} below $-c^2$, $q \geq 1$ and $|\hat{V}|_- = V \Theta(-V)$, following Lieb's /14/ notation (cf. Sec. 4). Note that the Hamiltonian $H \equiv \mathbf{p}^2 + \hat{V} + c^2 \geq \mathbf{p}^2 + |\hat{V}|_- + c^2 \equiv \hat{H}'$, since, by construction, $-|\hat{V}|_-$ will have any positive part in V chopped off. The (bound) eigenvalues of $\mathbf{p}^2 - \lambda |\hat{V}|_-$ are continuous, decreasing functions of λ .

Exploiting the continuity as well as monotonicity of the energy eigenvalues in λ , any given eigenvalue of $\mathbf{p}^2 - \lambda |\hat{V}|_-$ can be made to sweep through a range of values, and will definitely cross $-c^2$ (from above) for some choice of λ , $0 < \lambda \leq 1$. Since $\mathbf{p}^2 + c^2$ is a positive definite operator for $c \neq 0$, $\mathbf{p}^2 + c^2$ is invertible. Thus, the eigenvalue equation

$$(\mathbf{p}^2 - \lambda |\hat{V}|_-) \psi = -c^2 \psi \quad (124)$$

can always be cast into the form $(\mathbf{p}^2 + c^2)^{-1/2} |\hat{V}|_- (\mathbf{p}^2 + c^2)^{-1/2} \phi = (1/\lambda) \phi$. Therefore, $N(\mathbf{p}^2 - |\hat{V}|_- + c^2)$ equals the number of eigenvalues of the form $1/\lambda_i \geq 1$ of the Birman-Schwinger operator on the left hand side of the above eigenvalue equation, which resembles its variant discussed by Lieb /14/, viz. $B_E(V) = |\hat{V}|^{1/2} (\mathbf{p}^2 + |E|)^{-1} \times |\hat{V}|^{1/2}$. One therefore has a bound

$$N(\mathbf{p}^2 - |\hat{V}|_- + c^2) \leq \sum_i (1 / \lambda_i)^q \equiv \left\{ \text{Tr} (\mathbf{p}^2 + c^2)^{-1/2} |\hat{V}|_- (\mathbf{p}^2 + c^2)^{-1/2} \right\}^q, \quad \dots (125)$$

for $q \geq 1$; Tr herein denotes the trace. The above result has interesting consequences. For spherically symmetric potentials $V(\mathbf{r}) \equiv V(r)$, the angular momentum l is a good quantum number and hence one may project out on to each angular-momentum state separately. In particular, for $l=0$, i.e. bound s-states, and with the choice $q = 1$,

$$\begin{aligned}
\|(\hat{\mathbf{p}}^2 + c^2)^{-1/2} |\hat{V}|_-(\hat{\mathbf{p}}^2 + c^2)^{-1/2}\|_1 &= \text{Tr} |\hat{V}|_-(\hat{\mathbf{p}}^2 + c^2)^{-1} \\
&= \int d^3r \, d^3r' \langle \mathbf{r} | |\hat{V}|_- | \mathbf{r}' \rangle \int d^3p' \, d^3p'' \langle \mathbf{r}' | \mathbf{p}' \rangle \times \\
&\quad \langle \mathbf{p}' | (1/(\hat{\mathbf{p}}^2 + c^2)) | \mathbf{p}'' \rangle \langle \mathbf{p}'' | \mathbf{r} \rangle = \int d^3r \, d^3r' |V(r)|_- \delta(\mathbf{r}-\mathbf{r}') \\
&\quad \int d^3p \, e^{i\mathbf{p} \cdot \{\mathbf{r}-\mathbf{r}'\}} / (\mathbf{p}^2 + c^2) \int_0^\infty dr \, r^2 |V(r)|_- \int d^3r' \, \delta(\mathbf{r}-\mathbf{r}') \times \\
&\quad \int d\Omega \exp[-c|\mathbf{r}-\mathbf{r}'|] / (4\pi|\mathbf{r}-\mathbf{r}'|), \quad \dots (126)
\end{aligned}$$

in which case the integral, upon contour-integration gives the required trace to be $\int_0^\infty dr \, r^2 |V(r)|_- \int d^3r' \, \delta(\mathbf{r}-\mathbf{r}') \{ \sinh(rc) \times \exp(-r'c) \Theta(r'-r) + \sinh(r'c) \exp(-rc) \Theta(r-r') \} / (crr') = \int_0^\infty dr \, |V(r)|_- (1 - \exp(-2rc)) (2c)^{-1}$. Here, Θ denotes, as before, the Heaviside unit step distribution. For $c = 0$, in particular, this leads to an upper bound to the number of bound states : this number can never exceed /218/ the value $\int_0^\infty dr \, r \, V(r)$. For the choice $q = 2$, one is led to

$$\begin{aligned}
N(\hat{\mathbf{p}}^2 + c^2) &\leq (1/4\pi) \int d^3r \, d^3r' |V(\mathbf{r})|_- |V(\mathbf{r}')|_- \\
&\quad \exp(-2c|\mathbf{r}-\mathbf{r}'|^2) / |\mathbf{r}-\mathbf{r}'|^2, \quad \dots (127)
\end{aligned}$$

for a general binding potential $V(\mathbf{r})$ /14, 216/ The form of the integral on the r.h.s. of (127) is reminiscent of the Rollnik /166/ norm, as seen in Section 4. Further, invoking Young's inequality, one arrives at Lieb's elegant result (Inequality (35), Section 4.2) : $N_E(V) \leq (4\pi)^{-1} (2|E|)^{1/2} \times \int d^3r |V(\mathbf{r}) - E/2|_-^2$, which has been exploited by him /14/ in his classic paper on the Stability of Matter.

5.4. Stability of Matter

Ordinary matter, such as atoms, molecules and solids, despite the Coulombic attraction between the nuclei and the electrons, exhibits remarkable stability. Earlier works due to Kato /219/

and Dyson /220, 221/ have attributed this phenomenon to the Pauli exclusion principle. That the lower bound to the energy has a linear dependence on N , the number of constituent particles, was shown first by Dyson and Lenard /221/ and by Lenard and Dyson /222/. By "stability of matter", it is meant /14/ that the ground state energy of a system is finite. Thus, a question may be posed : for a hydrogenic atom with $\hat{H} = -\nabla^2/2 - Z/r$, does there exist an E_0 ($> -\infty$) such that $\langle \psi | \hat{H} | \psi \rangle / \langle \psi | \psi \rangle = E_0$? Lieb/14/ demonstrated that the Heisenberg uncertainty principle, viz. $\langle p^2 \rangle \langle r^2 \rangle \geq 9/4$ cannot account for the stability of such an atom. On the other hand, he invoked the three-dimensional Sobolev inequality to obtain a lower bound to the kinetic energy, viz. $T[\psi] \geq 3(\pi/2)^{4/3} \|\rho_\psi\|_3$ (cf. Section 3)[Inequalities in Lieb's work are given in terms of rather peculiar units, where $\hbar^2 = 2$, $m = 1$ and $|e| = 1$; thus one Rydberg unit equals $1/4$ in these units]. This leads to a lower bound, in Hartree units,

$$E_0 \geq -4Z^2/3 \quad (128)$$

Extension of this result to many fermion systems was also carried out by Lieb, wherein lower bounds to the kinetic (cf. Section 4.2; Inequality (35)) and electron repulsion energies were invoked. For the latter, the Thomas-Fermi theory enables one to give a lower bound to the electron repulsion operator, viz. (Theorem 10, Lieb /14/)

$$\begin{aligned} \sum_{i < j}^N |\mathbf{r}_i - \mathbf{r}_j|^{-1} &\geq (-1/2) \int d^3r \, d^3r' \, \rho(\mathbf{r}) \, \rho(\mathbf{r}') |\mathbf{r} - \mathbf{r}'|^{-1} \\ &+ \int d^3r \, \rho(\mathbf{r}) \, V_x(\mathbf{r}) - 2.21 N/\gamma - \gamma \int d^3r \, \rho^{5/3} \quad \dots (129) \end{aligned}$$

Here, $\gamma > 0$, $V_x(\mathbf{r}) = \sum_{j=1}^N |\mathbf{r} - \mathbf{r}_j|^{-1}$ and ρ is any non-negative function belonging to $L^1 \cap L^{5/3}$, ensuring, respectively, the finiteness of $\int d^3r \, \rho$ and that of $\int d^3r \, \rho^{5/3}$.

Employing these inequalities for extraction of a lower bound to $E_N^0 \equiv \langle \psi | \hat{H}_N | \psi \rangle$, the quantum mechanical energy of an N -fermion system, in its ground state, yields

$$E_N^0 \geq - (4.42) (4\pi q)^{2/3} (K^c)^{-1} [N + \sum_{j=1}^k Z_j^{7/3}] , \quad (130)$$

where $K^c = (3/5) (6\pi^2)^{2/3}$ and Z_j 's are the nuclear charges of the constituent atoms, q being the spin multiplicity.

By use of an improved prefactor in the kinetic energy bound /107/ the lower bound (130), for the case of $Z_j = 1$ (hydrogen atoms) and $N = k$ case, becomes (in Lieb's units)

$$E_N^0 \geq - 5.56 N , \quad (131)$$

which is equivalent to $-11.12 N$ in Hartree units. Note that the bound (131) depends linearly on N , which is indeed a desired characteristic, in that the quantities on the l.h.s. and r.h.s. are both size-consistent.

To summarize, Lieb's work forms a remarkable general study of the fundamental problem of the stability of matter : the results are independent of statistics of particles and also evince an improvement by orders of magnitude over the earlier studies /221,222/.

5.5. Scaling Properties of and Constrained Search Approach to Energy Functionals

Levy, Perdew and Sahni /18,139/ extensively applied the constrained search approach for obtaining rigorous inequalities for a variety of energy functionals. Some of these inequalities have been presented in earlier sections. The approach adopted in their derivation is based on the variational principle : constrain the domain of the functions over which the energy is minimized. Evidently, the minimum thus reached must be higher than, or, in the least, equal to the unconstrained minimum value.

Sahni and Levy /18/ obtained a variety of bounds to exchange and correlation energies as well as to the correlation potential. They introduced the following definitions :

$$E_c[\rho] = E[\rho] - E_{x_0}[\rho] \quad (132)$$

where $E[\rho] = \langle \psi | \hat{T} + \hat{U} + \sum_{i=1}^N v(\mathbf{r}_i) | \psi \rangle$ comes from a ψ , the interacting g.s. N-electron wave function and the "exchange-only" energy functional

$$E_{x_0}[\rho] = \langle \phi | \hat{T} + \hat{U} + \sum_{i=1}^N v(\mathbf{r}_i) | \phi \rangle \quad (133)$$

In the above definition, ϕ is the single-determinantal wave function (leading to ρ , the ground state density) constructed, a posteriori from the Kohn-Sham orbitals, and simultaneously minimizes the expectation value defined by Eq.(133).

Similarly, let

$$E'_{x_0}[\rho] = \langle \phi' | \hat{T} + \hat{U} + \sum_{i=1}^N v(\mathbf{r}_i) | \phi' \rangle \quad (134)$$

Here, ϕ' is that single determinant which is constrained to be g.s. of some noninteracting Hamiltonian $\hat{h}_{eff} = \hat{T} + \sum_{i=1}^N v_s(\mathbf{r}_i)$ and which minimizes the expectation value in (134). The g.s. density extracted from ϕ' is, in general, different from ρ . Now introduce the correlation energy functional

$$E'_c[\rho] = E[\rho] - E'_{x_0}[\rho] \quad (135)$$

In similar fashion, one defines the Hartree-Fock (HF) energy functional $E_{x_0}^{HF}[\rho]$ as

$$E_{x_0}^{HF}[\rho] = \langle \phi^{HF} | \hat{T} + \hat{U} + \sum_{i=1}^N v(\mathbf{r}_i) | \phi^{HF} \rangle \quad (136)$$

where ϕ^{HF} is a single Slater determinant which minimizes the expectation value in (136) with no further restrictions. The corresponding g.s. density is $\rho^{HF} \neq \rho$ in general.

Taking into account these definitions and applying the constrained-search formalism, one gets a set of interconnecting inequalities. First,

$$\langle \phi' | \hat{T} + \hat{U} + \sum_{i=1}^N v(\mathbf{r}_i) | \phi' \rangle > \langle \phi | \hat{T} + \hat{U} + \sum_{i=1}^N v(\mathbf{r}_i) | \phi \rangle ; \quad (137)$$

Whereby,

$$E'_{x_0}[\rho] - E_{x_0}[\rho] = \delta_1 > 0 \quad (138)$$

If the function $v_c(r)$ employed within the KS potential is a constant, then δ_1 will turn out to be zero.

Also, since ϕ is the energy minimizing KS determinant,

$$\begin{aligned} \langle \phi' | \hat{T} + \hat{U} + \sum_{i=1}^N v(r_i) + \sum_{i=1}^N v_c(r_i) | \phi' \rangle - \langle \phi | \hat{T} + \hat{U} + \sum_{i=1}^N v(r_i) \\ + \sum_{i=1}^N v_c(r_i) | \phi \rangle = \delta_2 > 0 \quad \dots (139) \end{aligned}$$

By addition of (137) and (139), one obtains

$$\int d^3r [\rho'(r) - \rho(r)] v_c(r) = \delta_1 + \delta_2 > 0 \quad (140)$$

Similarly, from (139) and (140),

$$E_{x_0}[\rho] - E'_{x_0}[\rho] = \int d^3r [\rho' - \rho] v_c - \delta_2 > 0 \quad (141)$$

is obtained, thereby yielding

$$0 < E'_c[\rho] - E_c[\rho] < \int d^3r [\rho' - \rho] v_c \quad (142)$$

Also, for general many-electron systems, the inequalities read

$$E_c[\rho] < E'_c[\rho] < E_c^{HF}[\rho]. \quad (143)$$

Savin, Stoll and Preuss /223/, in their work on application of correlation energy density functionals to atoms and molecules have derived rather similar results. Define $E_c[\rho] = E[\rho] - E^{HF}[\rho]$ and $E_c = E[\rho_0] - E^{HF}[\rho_{HF}]$, where ρ , ρ_0 and ρ_{HF} are respectively trial, g.s. and HF electron-densities. Then, by the variational principle, one obtains in general, the ordering of energies shown schematically in Fig. 2. Note, however, that the relative position of $E[\rho_{HF}]$ is uncertain, except that it lies above $E[\rho_0]$. Presuming the ordering of energies as depicted in Fig. 2, one has

$$E_c[\rho_0] < E_c < E_c[\rho_{HF}] \quad (144)$$

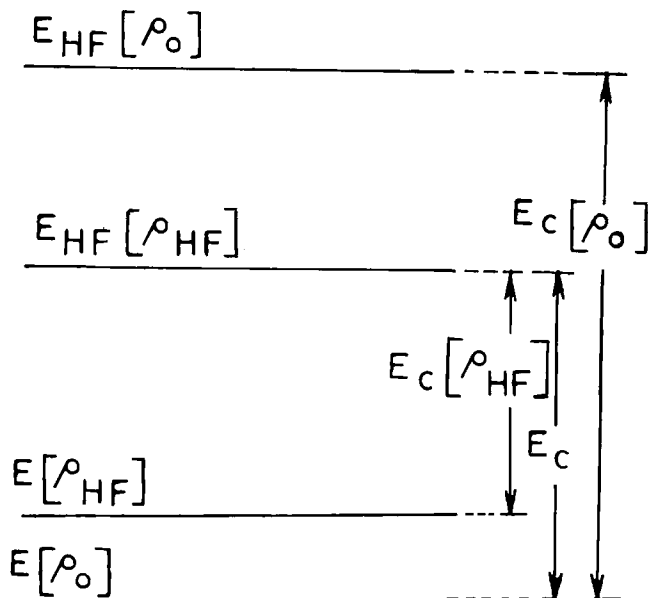


Figure 2. A Schematic diagram showing the relative magnitudes of various energy functionals as defined in Section 5.5.

In general, note that $E_c[\rho_0]$ as well as E_c are nonpositive. Notice further that the relative position of $E[\rho_{HF}]$ as shown in Fig. 2 is for definiteness. Even if it lies anywhere above $E_{HF}[\rho_{HF}]$ the inequality (144) still remains valid, since $E_{HF}[\rho_{HF}]$ then becomes a positive quantity. Thus the result (144) is valid in general.

Levy and Perdew /140/ and Levy /142/ in their works on scaling behavior of energy density functionals, obtained rigorous scaling properties of $E[\rho]$. For example,

$$(2\gamma - \gamma^2) E_c[\rho] + (\gamma - \gamma^2) \int d^3r \rho(\mathbf{r}) [\mathbf{r} \cdot \nabla v_c(\rho(\mathbf{r}); \mathbf{r})] - E_c[\rho_\gamma] > 0 \quad (145)$$

This implies that $E_c[\rho_\gamma] = \gamma E_c[\rho]$ only for $\gamma = 1$. Also, akin to the scaling properties of $T[\rho]$ and $U[\rho]$ as outlined in Section 3, one has

$$E_c[\rho_\gamma] < \gamma E_c[\rho] \quad (\gamma < 1) \quad (146)$$

and

$$E_c[\rho_\gamma] > \gamma E_c[\rho] \quad (\gamma > 1) \quad (147)$$

Similar inequalities hold for the Kohn-Sham exchange-correlation functional, $E_{xc}^{KS}[\rho]$. For computational purposes, however, the appropriate functionals should be made, by construction, to satisfy these inequalities. However, the literature to date, to the authors' knowledge, lacks such practical computational tests and further, their applications. However, the constrained search approach is quite valuable due to its formal aesthetic appeal.

Siedentop /100/ devised a practical scheme to obtain an upper bound to the lowest eigenvalue of a many-electron atom. His approach is based on the use of the so-termed Hellmann functional which treats the angular part quantum-mechanically whereas the radial part is treated semiclassically. The radial part prescribed by Siedentop reads $f_n(r) = \zeta_{lm}^{1/2}(r) \psi_n(\zeta_{lm}(r))$, with $\zeta_{lm}(r)$ as the contribution to the fractional charge contained in a sphere of radius r , by the electron orbitals labelled by the angular quantum numbers l, m . Further, the functions $\psi_n(q) = \exp(i\pi k_n q)$, with a finite number of choices for k_n were constructed. Siedentop subsequently constructed the determinantal (trial) wave function using the above recipe for construction of orbitals. After computation of the energy ingredients, the exchange contribution (which is always nonpositive) was dropped out leading to the upper bound to the total energy for the N -electron atom in question.

Siedentop and Weikard /224/ further introduced the Hellmann-Weizsäcker functional to obtain an upper bound to the quantum-mechanical ground state energy. Their theorem states that $E_0(Z, Z) \leq Z^{7/3} E_1^{TF(1)} + 8q_Z^2 + O(Z^2)$. Here, $E_Z^{TE(N)}$ is the corresponding Thomas-Fermi energy, $E_0(Z, N)$ is the total quantum mechanical energy for an atomic system with N the total number of

electrons and Z , the nuclear charge. This result is in agreement with Scott's /225/ conjecture that the leading correction to the TF energy goes as Z^2 .

5.6. Density Functionals for Coulomb Systems /28/

In his pioneering work, Lieb /28/ studied interconnections between many-particle wave functions and the single-particle density. He introduced certain functionals which circumvent the problem of V -representability and also discussed their properties in detail. Further rigorous bounds to the energy density functionals were also presented. We outline below Lieb's general treatment on Coulomb systems. First, we acquaint ourselves with the terminology, starting with the following definitions :

- (i) $\sqrt{\rho} \in H^1(R^3)$ if $\sqrt{\rho} \in L^2(R^3)$ and $\nabla\sqrt{\rho} \in L^2(R^3)$;
- (ii) $I_N = \left\{ \rho \mid \rho(\mathbf{r}) \geq 0, \sqrt{\rho} \in H^1(R^3), \int d^3r \rho = N \right\}$;
- (iii) $R_N = \left\{ \rho \mid \rho(\mathbf{r}) \geq 0, \int d^3r \rho = N, \rho \in L^3(R^3) \right\}$.

Then, $R_N \supset I_N$ by the three dimensional Sobolev inequality,

$$\text{viz. } \int d^3r |\nabla f|^2 \geq 3(\pi/2)^{4/3} \left(\int d^3r |f|^6 \right)^{1/3}.$$

Substituting $f = \sqrt{\rho}$ yields the following sequence of inequalities:

$$T[\psi] \geq T_w[\rho] \geq (3\pi^{4/3} 2^{7/3}) \left(\int d^3r \rho^3 \right)^{1/3}. \quad (148)$$

It is rather simple to prove that both R_N and I_N are convex sets, i.e. if ρ_1 and $\rho_2 \in R_N$ then $\lambda\rho_1 + (1-\lambda)\rho_2 \in R_N$ for $0 \leq \lambda \leq 1$.

Definition : A function (or functional) f is convex if

$$f(\lambda x + (1-\lambda)y) \leq \lambda f(x) + (1-\lambda)f(y) \quad (149)$$

for all $0 \leq \lambda \leq 1$ and for every pair (x,y) in the domain of f . In particular, it may easily be shown that, $\int d^3r (\nabla\sqrt{\rho})^2$ is convex.

Lieb further obtained an upper bound to the kinetic energy, $T[\psi]$, in terms of this convex functional. As it may be recalled,

this bound, along with its refinement by Zumbach /101/ was presented earlier in Section 3. As pointed out earlier, the map from ψ to ρ is a map from $H^1(R^{3N})$ onto $H^1(R^3)$, but it is not 1:1 ; different ψ 's can generate the same ρ . Lieb proved the following complicated theorems rigorously, answers to which are intuitively in the affirmative. We shall merely enunciate the theorems here.

Theorem 1 : The map from $H^1(R^{3N})$ to $H^1(R^3)$ is continuous i.e. for a fixed ψ and $\{\psi_j\}$ if there is a sequence such that $\|\psi - \psi_j\|$ and $\|\nabla\psi - \nabla\psi_j\|$ both $\rightarrow 0$, then $\|\rho^{1/2} - \rho_j^{1/2}\|$ and $\|\nabla\rho^{1/2} - \nabla\rho_j^{1/2}\|$ both $\rightarrow 0$.

Theorem 2 : Given a sequence $\rho_j^{1/2}$ which converges to $\rho^{1/2}$ [in the $H^1(R^3)$ sense], there exists a sequence ψ_j that converges to ψ [in the $H^1(R^{3N})$ sense] such that ρ_j and ρ are respectively generated by these wave functions.

Theorem 3 : There does exist an N-particle density matrix $\Gamma^{(N)}$ which, on integration yields a one particle spinless density matrix Γ , such that

$$\Gamma(r|r') = N \int \frac{d^3r}{\sigma} \int d^3r_2 \dots d^3r_N \psi[(r, \sigma_1), \dots, (r_N, \sigma_N)] \times \\ \psi^*[(r', \sigma'_1), \dots, (r'_N, \sigma'_N)] \quad \dots (150)$$

$\text{Tr } \Gamma = N$ and Γ must satisfy appropriate symmetry requirements /86/.

Lieb /28/ further studied the class of permissible external potentials. He pointed out that since $\rho \in L^1 \cap L^3$, $\rho \in L^p$ for all p satisfying $1 \leq p \leq 3$. Thus, the integral $\int d^3r \rho v$ is well-defined (i.e. is finite) if $v \in L^{3/2} + L^\infty$ i.e. v can be expressed as a sum $v = v_1 + v_2$, where $v_1 \in L^{3/2}$ and $v_2 \in L^\infty$ (i.e. v_2 is a bounded function). The class $L^{3/2} + L^\infty$ includes the Coulombic potential since $1/|r| = \tilde{\Theta}(|r|)/|r| + (1 - \tilde{\Theta}(|r|))/|r| = v_1 + v_2$, say, where $\tilde{\Theta}(r) = 1$ if $r \leq 1$ and zero otherwise, is a shifted Heaviside unit-step function. The function $v_1 \in L^{3/2}$ since $4\pi \int_0^1 dr (r^2/r) = 4\pi (1/2) = 2\pi < \infty$, and $v_2 < 1$, whence $v_2 \in L^\infty$.

There, of course, does exist a wider class of potentials which do not belong to $L^{3/2} + L^\infty$, but $\int d^3r \rho v$ still remains

finite. For example, consider the potential $v = kx^2/2$. Even though this v does not belong to $L^{3/2} + L^\infty$, $\int_{-\infty}^{\infty} dx \rho v$ is finite for the eigenfunctions of the one-dimensional harmonic oscillator.

Lieb proved the following properties of $E[v]$ that follow from the variation principle : $E[v] = \inf\{ \langle \psi | \hat{H}_v | \psi \rangle \mid \|\psi\| = 1 \}$ and $T[\psi] < \infty$ where $\hat{H}_v = \hat{T} + \hat{U} + \sum_{i=1}^N v(\mathbf{r}_i)$.

- (i) $E[v]$ is concave in v , i.e. $E[v] \geq \lambda E[v_1] + (1-\lambda) E[v_2]$ for $v = \lambda v_1 + (1-\lambda)v_2$ for all v_1, v_2 and $0 \leq \lambda \leq 1$
- (ii) $E[v]$ is monotone decreasing, i.e. for $v_1 \leq v_2$ (at all \mathbf{r}), $E[v_1] \leq E[v_2]$
- (iii) $E[v]$ is continuous in the $L^{3/2} + L^\infty$ norm and is locally Lipschitz.

The domain of $F[\rho] = E[v] - \int d^3r \rho v$ is the set $A = \{ \rho \mid \rho \text{ comes from a ground state and } \int \rho d^3r = N \} : A_N \neq I_N$ and further, is not convex. Thus, apart from F_{HK} being unknown, there still remain some conceptual problems, e.g. F_{HK} is not convex (for, strict convexity implies uniqueness of minima). Also, the domain of F_{HK} , viz. A_N is not convex.

Levy /53/ defined a functional $Q[\rho]$ over I_N , as was reviewed earlier in Section 2. Lieb /28/ put this work on a more rigorous footing by defining

$$\begin{aligned} \tilde{F}[\rho] = \inf \left\{ \langle \psi | \hat{T} + \hat{U} | \psi \rangle \mid \psi \Rightarrow \rho, \|\psi\| = 1 \right. \\ \left. \text{and } \langle \psi | \hat{T} | \psi \rangle < \infty \right\} . \end{aligned} \quad (151)$$

The basic difference between the definitions due to Levy and Lieb being that "min" in the former is replaced by the more appropriate "inf" in the latter. Lieb subsequently proved the theorem that for each $\rho \in I_N$ there exists a ψ with the attributes that $\|\psi\| = 1$ and $\langle \psi | \hat{T} | \psi \rangle < \infty$, such that $\tilde{F}[\rho]$, given by $\tilde{F}[\rho] \equiv \langle \psi | \hat{T} + \hat{U} | \psi \rangle$, i.e. the infimum in (151) is in fact a minimum. The main problem associated with \tilde{F} is that it is not convex either.

According to Lieb /28/, one may introduce an alternative choice

$$F_L[\rho] = \text{Sup} \left\{ E[v] - \int d^3r \rho v \mid v \in L^{3/2} + L^\infty \right\} \quad (152)$$

The functional F_L defined for all $\rho \in R_N$, is convex (since it is a supremum of a family of linear functionals) and depends explicitly on N through the energy functional $E[v]$. Lieb also established a rigorous inequality connecting \tilde{F} and F_L viz. $F_L[\rho] \leq \tilde{F}[\rho]$ for all $\rho \in I_N$. A further conjecture was made on the joint convexity of F_L in N and ρ , that is,

$$F_L[N+1, \rho_1] + F_L[N-1, \rho_2] \geq 2 F_L[N, (\rho_1 + \rho_2)/2] \quad (153)$$

The convexity was explored further by Lieb in the form of following theorem. Assume that (i) $F_L[N, \rho]$ is jointly convex (as in the inequality (153)). (ii) $E[N, v]$ is convex in N for all fixed v , i.e. $E[N+1, v] + E[N-1, v] \geq 2 E[N, v]$; then

- (a) In view of the definition (152), (ii) implies (i).
- (b) If $E[v] = \text{Inf} \{ F_L[\rho] + \int d^3r v \rho \mid \rho \in L^3 \cap L^1 \}$ or $E[v] = \text{Inf} \{ E[\rho] + \int d^3r v \rho \mid \rho \in I_N \}$ holds, then (i) implies (ii).

Further, Lieb summarized the bounds to the Kohn-Sham kinetic energy, the March-Young and Lieb-Thirring kinetic energy bounds, (cf. Section 3) as well as the bound to the indirect Coulomb energy functional (cf. Section 4).

To sum up, it may be remarked that the elegant and profound work of Lieb that appeals to the mathematical structure of the density functional formalism indeed represents a milestone in the formal development of DFT. His classic paper /28/ presents detailed studies on the structure of DFT and the convexity and boundedness properties of a variety of energy density functionals.

5.7. Monotonicity of Molecular Electronic Energy in Nuclear Co-ordinates

Lieb and Simon /226/ addressed the problem of monotonicity of electronic contribution to the Born-Oppenheimer energy of a

one-electron diatomic molecule. Let $E(R) \equiv$ the ground state energy of such a system (with Z_A and Z_B as the nuclear charges), and let $e(R) \equiv E(R) - Z_A Z_B / R$, denote the corresponding electronic contribution. Lieb and Simon /226/ established that $e(R)$ increases as R does, via the following theorems.

Theorem 1 : Let $e(R) = e(R_1, R_2)$ with $R = R_1 - R_2$.

Then $dE/dR \geq 0$ for an arbitrary $R > 0$. This result was established by these authors, with the use of correlation inequalities as well as by employing the theory of log-concave functions. This theorem was later generalized to arbitrary one-electron polyatomic molecules.

Theorem 2 : Fix the nuclear positions at R_1, R_2, \dots, R_N . For a single electron moving in such an external potential generated by this nuclear configuration, $e(\lambda) = e(\lambda R_1, \dots, \lambda R_N)$ is monotone nondecreasing function of λ , as λ increases.

Theorem 3 : The quantity $e(R_1, \dots, R_N)$ attains its minimum value when all $|R_i|$'s are equal, for fixed N and positive nuclear charges Z_1, Z_2, \dots, Z_N . The proof of this theorem employs the fact that $E(Z)$ is jointly concave since the Hamiltonian (electronic part only) is linear in all Z_i . This result has earlier been proven by Narnhofer and Thirring/227/. For further work generalizing this result, see Lieb /228/.

Mezey (/229, 230/ and references therein) in a series of contributions studied the topology of energy hypersurfaces of atoms and molecules. Of particular interest are two studies /231, 232/ that deal with "electronic energy level set topologies" in the abstract nuclear charge space Z of molecular systems. For this purpose, Mezey introduced the following definitions. Let the electronic energy E be a map from $R^n \times Z' \rightarrow R^1$ ($n = 3N$, N being the number of electrons), where Z' denotes a set of nonnegative integral nuclear charges at a fixed nuclear geometry, denoted by a generic symbol γ . In fact, Z' is a subset of $Z = \{x \mid z_i \geq 0, \text{ for } i = 1, 2, 3, \dots, w\}$, i.e. x denotes a collection of nuclear charges z_i . The "level set" of E^0 is defined /231, 232/ as

$$F_E^0(r) = \left\{ x \mid E(r, x) \geq E^0 \right\} . \quad (154)$$

Here, E^0 denotes a given (arbitrary) value of the electronic energy corresponding to $H_{elec}(r, x) = -(1/2) \sum_i \nabla_i^2 - \sum_{i\alpha} z_\alpha / r_{i\alpha} + \sum_{i < j} 1/r_{ij}$, which is the electronic part of the Hamiltonian. Equipped with these definitions, we outline the proof of Mezey's theorem that, $F_E^0(r)$ is a convex subset of Z' for a fixed geometry r . For this purpose, consider two vectors $x^{(1)}$ and $x^{(2)} \in F_E^0$; i.e. $E^{(1)} \geq 0$ and $E^{(2)} \geq E^0$. Now, assume, without loss of generality that $E^{(2)} \geq E^{(1)}$. With the prescription $x = \alpha_1 x^{(1)} + \alpha_2 x^{(2)}$, along with $\alpha_1, \alpha_2 \geq 0$, $\alpha_1 + \alpha_2 = 1$ and further, by invoking the linearity of H_{elec} w.r.t. x , it follows that

$$\begin{aligned} E(r, x) &= \langle \psi | H_{elec} | \psi \rangle = \alpha_1 \langle \psi | H_{elec}(r_1, x^{(1)}) | \psi \rangle \\ &+ \alpha_2 \langle \psi | H_{elec}(r_2, x^{(2)}) | \psi \rangle . \end{aligned} \quad \dots (155)$$

A subsequent use of the variational principle yields

$$E(r, x) \geq \alpha_1 E^{(1)} + \alpha_2 E^{(2)} \geq (\alpha_1 + \alpha_2) E^{(1)} = E^{(1)} > E^0 . \quad \dots (156)$$

Furthermore, F_E^0 is a connected set, i.e. is not a set of isolated points in Z but rather is a continuous one, since every point joining $x^{(1)}$ and $x^{(2)}$ also belongs to F_E^0 , vide convexity.

Next, Mezey proved an important general inequality connecting the electronic energies of isoelectronic molecules. What is remarkable in this bound is that it holds for arbitrary molecular geometries. We merely enunciate this result, after introducing the following terminology.

Let x denote an ordered w -tuple with nonnegative integral nuclear charges for its components x_i . The hypercube C_z^0 and the pyramid P_z^0 are defined by

$$C_z^0 = \left\{ x \mid x_i \leq z^0, i = 1, 2, \dots, w; x \in Z' \right\} \quad (157)$$

and

$$P_z^0 = \left\{ x \mid x = \sum_{i=1}^w \alpha_i z^{(i)}; \sum_{i=1}^w \alpha_i = 1; \alpha_i \geq 0 \right\}. \quad (158)$$

Evidently, $C_z^0 \supset P_z^0$. We illustrate the above two definitions schematically in Fig. 3 for a two dimensional case. The

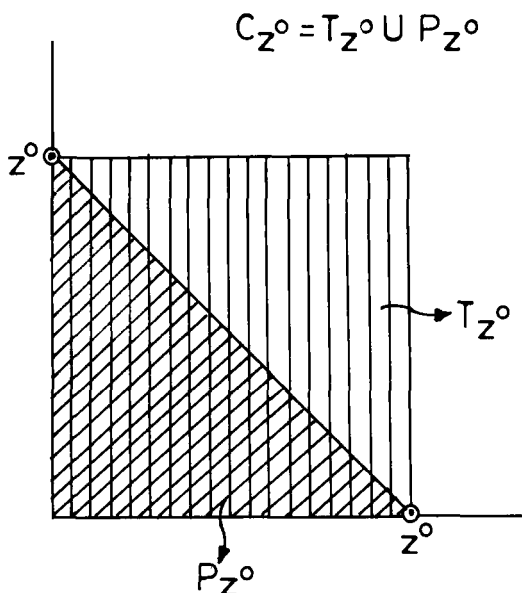


Figure 3. A schematic geometrical construction of the hypercube C_z^0 and the hyperpyramid P_z^0 illustrated for a two-dimensional case. T_z^0 denotes the upper triangle, i.e. the region not belonging to P_z^0 but within C_z^0 (cf. Section 5.7).

following theorem was then established : For isoelectronic pair of molecules $M^{(1)}(r^{(1)}, x^{(1)})$ and $M^{(2)}(r^{(2)}, x^{(2)})$, with $r^{(1)}, r^{(2)}$ denoting arbitrary geometries and with the nuclear charges w -tuples $x^{(1)}, x^{(2)} \in Z'$, such that $x^{(1)} \in P_z^0$ and $x^{(2)} \in C_z^0$ (the superscript "c" denotes the complement), for some fixed z^0 , the ground state electronic energies satisfy

$$E^{(1)} \geq E^{(2)}, \quad (159)$$

for arbitrary nuclear configurations. As an illustration, one may obtain, with a possible choice $z^0 = 2.5$, $N = 2$, the bound

$$E_{H_2} \geq E_{Li} + , \quad (160)$$

for all possible geometries for the respective molecules. Mezey applied the above theorem to compare the electronic energies of molecular species PCl_2I , PBr_2Cl and the ion pair $K^+ PSbCl^-$.

Arteca and Mezey /233/ have more recently studied simple inequalities for the electronic energies of diatomics. They have, further examined the boundaries defining the electronic energy level set topologies in abstract nuclear charge-space of molecular systems /19, 234/. Later, these relations have been used to extract bounds to the internuclear distances at which the electronic energy of a diatomic molecule reaches a specified value. In summary, the works of Mezey and co-workers clearly bring out the applicability of topological arguments to the study of molecular electronic energies.

5.8. Other Miscellaneous Works

While preparing this article, some recent works have come to our notice. Here, we make a brief mention of them along with earlier related articles.

Recently, Ghosh /235/ has derived a bound within DFT, viz.

$$\partial^2 E_\lambda / \partial \lambda^2 \leq \int d^3r (\partial^2 V_\lambda(r) / \partial \lambda^2) \rho_\lambda(r) \quad (161)$$

where λ parameterizes the external potential, $V_\lambda(r)$, thereby inducing a λ -dependence into the ground state density $\rho_\lambda(r)$ and the ground state energy, E_λ . Note that for the first derivative, the well-known Hellmann-Feynman theorem engenders an equality: $(\partial E_\lambda / \partial \lambda) = \langle \psi_\lambda | \partial \hat{H}_\lambda / \partial \lambda | \psi_\lambda \rangle / \langle \psi_\lambda | \psi_\lambda \rangle$, for a general Hamiltonian \hat{H}_λ characterized a parameter λ . Within the wavefunction domain, Silverman and van Leuven /236/ as well as Deb /237/ had earlier

derived an upper bound relation

$$\partial^2 E_\lambda / \partial \lambda^2 \leq \langle \psi_\lambda | \partial^2 \hat{H}_\lambda / \partial \lambda^2 | \psi_\lambda \rangle / \langle \psi_\lambda | \psi_\lambda \rangle \quad (162)$$

While (162) is rigorously valid relation, its transcription (161) due to Ghosh needs rectification (Eq. (7) in his paper has the second-order "cross-term" missing in the Taylor-expansion of $\Delta E(N, \lambda)$).

Mention also must be made of the very recent works due to Chen and Spruch /238, 239/ which address the question of lower bounds to the ground state energies and the accompanying necessary conditions for the existence of bound states.

6. CONCLUDING REMARKS

In this article, we have endeavored to present a comprehensive survey of inequalities involving atomic and molecular energy functionals. Indeed, such inequalities are encountered at every turn in quantum chemistry as well as atomic and molecular physics. In the mathematical literature, the topic of inequalities has been given a special status and several classic monographs dedicated to this topic have been produced. However, the topic of "Inequalities" is yet to join the club of accepted keywords in physics and chemistry. In the quantum theory of atoms, molecules and solids, equalities are rather rare and what one can achieve at best in most of the situations, is a rigorous inequality. The state of affairs is even more aggravated within the density-functional context, since the exact forms of kinetic and exchange-correlation energy density functionals have remained unknown. However, upper as well as lower bounds to these functionals or their ingredients can indeed be derived as demonstrated in the earlier Sections of this work. In particular, the connection between electron-electron repulsion energy functional and its ingredients with simpler, one-electron ones, is

possible only via the medium of inequalities. Such bounds appear in the wavefunction, as well as single-particle density domains. It is such inequalities that enable one the study of fundamental problems such as stability of negative ions, molecules and that of matter in general. Topological concepts can also be gainfully employed for obtaining bounds to molecular electronic energies. Thus inequalities are indeed all-pervading in the vast literature of quantum chemistry. To conclude, we earnestly express a hope that this article has brought out the power and versatility of inequalities in the quantum theory of atoms and molecules.

APPENDIX

Bounds to $F_m(t)$

Expressions for electron repulsion integrals over Gaussian basis-sets involve special functions /204, 205, 207, 240, 241/

$$F_m(t) \equiv \int_0^1 u^{2m} \exp(-tu^2) du. \quad (A.1)$$

A variety of upper and lower bounds to F_0 , F_1 and F_2 will be derived here. A reference may be made to Gadre, Shrivastava and Kulkarni /241/ for full details.

1. Bounds to $F_0(t)$

Note that $F_0(t)$ is a monotone decreasing function, since $F'_0(t) \leq 0$ for finite $t \geq 0$. The maximum value attained by F_0 is 1, viz. $F_0(0) = 1$. Hence, a trivial bound is

$$F_0(t) \leq 1. \quad (A.2)$$

Another bound is obtained by the following considerations :

$$F_0(t) \geq \int_0^1 e^{-t} du = e^{-t} \quad (A.3)$$

For $t \leq 0.1$, the following bounds are obtained by series expansion

$$F_0(t) \leq 1 - t/3 + t^2/10 \quad (\text{A.4a})$$

and

$$F_0(t) \leq 1 - t/3 + t^2/10 - t^3/42 + t^4/216. \quad (\text{A.4b})$$

The r.h.s. of the bound (A.4b) also serves as a good approximation to $F_0(t)$ for $t \leq 0.1$ with an error estimate of less than 10^{-8} .

Of particular interest is the bound

$$F_0(t) \leq (\pi/t)^{1/2}/2 \quad (\text{A.5})$$

which estimates the function with an error less than 1.25×10^{-7} for $t \geq 14$.

2. Bounds to $F_1(t)$

$$F_1(t) = \int_0^1 u^2 \exp(-tu^2) du \leq \int_0^1 u \exp(-tu^2) du = -(1/(2t)) \exp(-tu^2) \Big|_0^1 = (1-e^{-t})/(2t) \quad (\text{A.6})$$

Yet another upper bound to $F_1(t)$ may also be readily derived :

$$F_1(t) = \int_0^1 u^2 \exp(-tu^2) du \leq \int_0^1 u^2 \exp(-tu) du = (2/t^3) - (2 + 2t + t^2) \exp(-t)/t^3$$

Some simpler upper bounds to F_1 and F_2 are given by : $F_1 \leq 1/3$ and $F_2 \leq 1/5$ and in general,

$$F_m \leq 1/(2m + 1) \quad (\text{A.7})$$

These bounds have been successfully employed /241/ for devising an efficient algorithm for molecular electrostatic potential mapping. An upper bound serving as a useful approximation to $F_1(t)$ is given by :

$$F_1(t) \leq (\pi/t)^{1/2}/(4t) \quad (\text{A.8})$$

The r.h.s. of (A.8) estimates the function with an error less than 10^{-8} for $t \geq 14$.

3. For some further inequalities, note that $x \leq \exp(x-1)$. Substitute $x = tu^2$ to obtain $tu^2 \leq \exp(tu^2-1) = \exp(tu^2)/e$. Hence, $etu^2 \leq \exp(tu^2)$, yielding $\exp(-tu^2) \leq (etu^2)^{-1}$. This leads to the result

$$F_1(t) = \int_0^1 u^2 \exp(-tu^2) du \leq 1/(et) \quad (\text{A.9})$$

The bounds to $F_m(t)$ discussed here are of general practical interest since they may be gainfully employed for estimating the electron repulsion integrals as well as electronic properties of molecular systems whenever Gaussian basis functions are employed.

Acknowledgments

Financial assistance from the Indian National Science Academy (INSA), New Delhi, in the form of a Research Fellowship to SRG is gratefully acknowledged. We also thank the University Grants Commission (UGC), New Delhi and the Center for the Development of Advanced Computing (C-DAC), Pune, for support. We have immensely benefited by correspondence/discussions with Dr. P.P.

Thankachan. Further, we are grateful to Professors R. Ahlrichs, E. Clementi, S. Golden, W. Kutzelnigg, M. Levy, E.H. Lieb, P.-O. Löwdin, A. Okniński, R.G. Parr, J.P. Perdew, V. Sahni and V.H. Smith, Jr. for their valuable suggestions. We also thank Dr. A. Shanthi, Mr. A. Taspas, Ms. Indira Shrivastava, Mr. Sudhir Kulkarni, Mr. Rajendra Shirsat, Mr. Ajay Limaye and Ms. Sangeeta Bapat for proofreading the typescript. We further thank Mr. Vinay Vaidya for carefully creating the typescript.

REFERENCES

1. Szabo, A. and Ostlund, N. (1982). Modern Quantum Chemistry : Introduction to Advanced Electronic Structure Theory, MacMillan.
2. Mukherjee, D. (1989). Ed. Aspects of Many-Body Effects in Molecules and Extended Systems, Lecture Notes in Chemistry, Vol. 50, Springer-Verlag.

3. Ostlund, N.S. (1989) The Hypercube Inc. Product Release of CHEMPUTERTM-501.
4. Clementi, E. (1989). Ed. MOTECC-89 : Modern Techniques in Computational Chemistry , ESCOM Science Publishers.
5. Colwell, S.M., Marshall, A.R., Amos, R.D. and Handy, N.C. (1985). Chem. in Britain 21, 655.
6. Almlöf, J., Faegri, K., Jr. and Korsell, K. (1982). J. Comp. Chem. 3, 385.
7. Cremer, D. and Gauss, J. (1986). J. Comp. Chem. 7, 279.
8. Clementi, E. and Mehl, J. (1974). In Chemical and Biochemical Reactivity : The Jerusalem Symposium on Quantum Chemistry and Biochemistry VI, Israel Acad. Sci.
9. Ahlrichs, R. (1974). Theoret. Chim. Acta (Berl.) 33, 157.
10. Ahlrichs, R. (1988). Private communication to R.K.P.
11. Clementi, E. (1988). Private communication to S.R.G.
12. Hohenberg, P. and Kohn, W. (1964). Phys. Rev. 136, B864.
13. Kohn, W. and Sham, L.J. (1965). Phys. Rev. 140, A1133.
14. Lieb, E.H. (1976). Rev. Mod. Phys. 48, 553.
15. Hoffmann-Ostenhof, M. and Hoffmann-Ostenhof, T. (1977). Phys. Rev. A16, 1782.
16. Gadre, S.R., Bartolotti, L.J. and Handy, N.C. (1979). J. Chem. Phys. 72, 1034.
17. Lieb, E.H. and Oxford, S. (1981). Intern. J. Quantum Chem. 19, 427.
18. Sahni, V. and Levy, M. (1986). Phys. Rev. B33, 386.
19. Artega, G.A. and Mezey, P.G. (1987). Phys. Rev. A35, 4044.
20. Epstein, S.T. (1974). The Variation Method in Quantum Chemistry, Academic.
21. Parr, R.G. (1983). In Annual Reviews of Physical Chemistry, 34, 631. Ed. Rabinovich, B.S.
22. March, N.H. and Lundqvist, S. (1983). Ed. Theory of the Inhomogeneous Electron Gas, Plenum.
23. Dreizler, R.M. and Providencia, J. da (1985). Ed. Density Functional Methods in Physics, NATO ASI Series, Plenum.
24. Parr, R.G. and Yang, W. (1989). Density Functional Theory of Atoms and Molecules. International Series of Monographs on Chemistry Vol. 16. Oxford Univ. Press, New York.
25. Lieb, E.H. (1983). Phys. Rev. Letters 52, 315.
26. Lieb, E.H. (1984). Phys. Rev. A29, 3018.
27. Lieb, E.H., Sigal, I.M., Simon, B. and Thirring, W. (1984). Phys. Rev. Letters 52, 994.
28. Lieb, E.H. (1983). Intern. J. Quantum Chem. 24, 243.
29. Teller, E. (1962). Rev. Mod. Phys. 34, 627.
30. Balázs, N.L. (1967). Phys. Rev. 156, 42.
31. Thomas, L.H. (1927). Proc. Camb. Phil. Soc. 23, 542.
32. Fermi, E. (1927). Rend. Lincei 6, 602.
33. Fermi, E. (1928). Z. Physik 48, 73.
34. Gombás, P. (1956). Statistische Behandlung des atoms in Atoms II, Vol. XXXVI of Handbuch der Physik, Flugge, S., Ed. Springer, Berlin.

35. March, N.H. (1960). Self Consistent Fields in atoms, Pergamon.
36. Lieb, E.H. (1981). Phys. Rev. Letters 46, 457; (1981). Erratum 47, 427.
37. Lieb, E.H. (1981). Rev. Mod. Phys. 53, 603 and references therein.
38. Parr, R.G., Donnelly, R.A., Levy, M. and Palke, W.E. (1978). J. Chem. Phys. 68, 3801.
39. Katriel, J., Appelhof, C.J. and Davidson, E.R. (1981). Intern. J. Quantum Chem. 19, 293.
40. Englisch, H. and Englisch, R. (1981). Physica 121A, 253.
41. Gombás, P. (1949). Die Statistische Theorie des Atoms und Ihre Anwendungen, Springer, Wien. See also March, N.H. (1957). Proc. Phys. Soc. A70, 169.
42. Slater, J.C. (1960). Quantum Theory of Atomic Structure, Vol. II, McGraw Hill.
43. Dirac, P.A.M. (1930). Proc. Camb. Phil. Soc. 26, 376.
44. Lieb, E.H. and Simon, B. (1973). Phys. Rev. Letters 31, 681.
45. Lieb, E.H. and Simon, B. (1977). Adv. in Math. 23, 22.
46. Benguria, R. and Lieb, E.H. (1985). J. Phys. B18, 1045.
47. Stoll, H. and Savin, A. (1985). In Density Functional Methods in Physics, NATO ASI Series, Ed. R.M. Dreizler and J. da Providencia, Plenum. p. 177.
48. Lang, N.D. (1985). In Density Functional Methods in Physics, NATO ASI Series, Ed. R.M. Dreizler and J. da Providencia, Plenum; p. 233.
49. Epstein, S.T. and Rosenthal, C.M. (1974). J. Chem. Phys. 64, 247.
50. Smith, D.W. (1968). in Reduced Density Matrices with Applications to Physical and Chemical Systems Ed. Coleman, A.J. and Erdahl, R.M., Queen's papers on pure and applied mathematics, No. 11.
51. Gilbert, T.L. (1975). Phys. Rev. B12, 2111.
52. Harriman, J.E. (1981). Phys. Rev. A24, 680.
53. Levy, M. (1979) Proc. Nat. Acad. Sci. (USA). 76, 6072.
54. Percus, J.K. (1978). Intern. J. Quantum. Chem. 13, 89.
55. Levy, M. (1982). Phys. Rev. A26, 1200.
56. Henderson, G.A. (1981). Phys. Rev. A23, 19.
57. Pathak, R.K. (1984). Phys. Rev. A29, 978.
58. Smith, V.H., Jr. (1980). Presented at the Mexico City Conference on Quantum Chemistry. We are thankful to Professor Smith for bringing this reference to our notice.
59. Smith, V.H., Jr. (1982). In Local Density Approximations in Quantum Chemistry and Solid State Physics, Ed. J.P. Dahl and J. Avery, Plenum.
60. Smith, V.H., Jr. (1989). Private communication to the authors.
61. Pathak, R.K., Panat, P.V. and Gadre, S.R. (1982) Phys. Rev. A26, 3073.
62. Kohn, W. (1983). Phys. Rev. Letters 51, 1596.
63. Kohn, W. (1985). In Density Functional Methods in

- Physics, NATO ASI Series, Ed. R.M. Dreizler and J. da Providencia, Plenum, p. 233.
64. Hadjisavvas, N. and Theophilou, A. (1984). Phys. Rev. A30, 2183.
65. Gáspár, R. (1974). Acta. Phys. Hung. 35, 213.
66. Schwarz, K. (1972). Phys. Rev. 135, 2466.
67. Slater, J.C. (1979). The Calculation of Molecular Orbitals, Wiley and references therein.
68. Janak, J.F. (1977). Phys. Rev. B18, 7165.
69. Gopinathan, M.S., Whitehead, M.A. and Bogdanovic, R. (1976). Phys. Rev. A14, 1.
70. Vaidehi, N. and Gopinathan, M.S. (1984). Phys. Rev. A29, 1679.
71. Vijayakumar, M., Vaidehi, N. and Gopinathan, M.S. (1989). Phys. Rev. A40, 6834.
72. Barth, U. von and Hedin, L. (1972). J. Phys. C5, 1629.
73. Rajagopal, A.K. and Callaway, J. (1973). Phys. Rev. B7, 1912;
74. Gunnarsson, O. and Lundqvist, B.I. (1976). Phys. Rev. B13, 4274.
75. Perdew, J.P. and Zunger, A. (1981). Phys. Rev. B23, 5048.
76. Bartolotti, L.J., Gadre, S.R. and Parr, R.G. (1980). J. Amer. Chem. Soc. 73, 416.
77. Parr, R.G. and Pearson, R.G. (1983). J. Amer. Chem. Soc. 105, 7512.
78. Sen, K.D. and Jorgensen, C.K. (1987). Ed. Electronegativity, Springer-Verlag, Structure and Bonding. Vol. 66.
79. Perdew, J.P., Parr, R.G., Levy M. and Balduz, J. (1982). Phys. Rev. Letters 49, 1691.
80. Perdew, J.P. and Levy, M. (1983). Phys. Rev. Letters 51, 1884.
81. Valone, S.M. and Capitani, J.F. (1981). Phys. Rev. A23, 59.
82. Theophilou, A.K. (1979). A Course in Mathematical Physics. Vol. III, pp. 159-162. Springer-Verlag.
83. Katriel, J. (1980). J. Phys. C13, L375.
84. Szasz, L., Berrios-Pagan, I. and McGinn, G., Naturforsch, Z. (1975). A30, 1516.
85. Slater, J.C. (1933). J. Chem. Phys. 1, 687.
86. Löwdin, P.-O. (1955). Phys. Rev. 97, 1474; 1490; 1590.
87. Marc, G. and Mcmillan, W.G. (1985). Adv. Chem. Phys. 58, 209.
88. Mermin, N.D. (1965). Phys. Rev. 137A, 1441.
89. Löwdin, P.-O. (1988). Intern. J. Quantum Chem. Symp. 22, 337.
90. Peuckert, V. (1978). J. Phys. C11, 4945.
91. Bartolotti, L.J. (1981). Phys. Rev. A24, 1661.
92. Deb, B.M. and Ghosh, S.K. (1982). J. Chem. Phys. 77, 342.
93. Runge, E. and Gross, E.K.U. (1984). Phys. Rev. Letters 52, 997.
94. March, N.H. and Young, W.H. (1958). Proc. Phys. Soc. (London) 72, 182.
95. Macke, W. (1955). Phys. Rev. 100, 992.
96. Macke, W. (1955). Ann. Phys. Lpz. 17, 1.

97. Weizsäcker, C.F. von (1935). Z. Physik 96, 431.
98. Lieb, E.H. (1980). In Osterwalder, K., Mathematical Problems in Theoretical Physics. pp. 91 - 102. Springer-Verlag.
99. Müller, A.M.K. (1978). Ausgewählte Methoden und Probleme der Mehrteilchentheorie, Lecture Notes (unpublished).
100. Siedentop, H.K.H. (1981). Zeit. Phys. A302, 213.
101. Zumbach, G. (1985). Phys. Rev. A33, 1922.
102. Ghosh, S.K. and Parr, R.G. (1985). J. Chem. Phys. 82, 3307.
103. Ludeña, E.V. (1983). J. Chem. Phys. 79, 6174.
104. Capitani, J.F., Chang, B. and Harriman, J.E. (1984). J. Chem. Phys. 81, 349.
105. Lieb, E.H. and Thirring, W.E. (1975). Phys. Rev. Letters 35, 687;
106. Lieb, E.H. and Thirring, W.E. (1975). in Studies in Mathematical Physics : Essays in Honor of Valentine Bargmann, Ed. Lieb, E.H., Simon, B. and Wightman, A.S., Princeton University Press.
107. Lieb, E.H. (1978). Bull. Am. Phys. Soc. 23, 24.
108. Murphy, D.R. and Parr, R.G. (1979). Chem. Phys. Letters 60, 377.
109. Wang, W.-P. and Parr, R.G. (1977). Phys. Rev. A16, 891.
110. Gadre, S.R. and Pathak, R.K. (1982). Phys. Rev. 25, 668.
111. Sobolev, S.L. (1938). Math. Sbornik 4, 471.
112. Rosen, G. (1971). Siam J. Appl. Math. 21, 30.
113. Csavinsky, P. (1983). Phys. Rev. A27, 1184.
114. Hardy, G.H., Littlewood, J.E. and Pólya, G. (1934). Inequalities, Cambridge.
115. Gadre, S.R. and Chakravorty, S.J. (1986). Chem. Phys. Letters 132, 535.
116. Gadre, S.R. and Chakravorty, S.J. (1986). J. Chem. Phys. 84, 7051.
117. Pathak, R.K. and Gadre, S.R. (1982). Phys. Rev. A25, 3426.
118. Pathak, R.K. and Bartolotti, L.J. (1985). Phys. Rev. A31, 3557.
119. Dehesa, J.S. and Galvez, F.J. (1985). Phys. Rev. Letters B156, 287.
120. Galvez, F.J. and Dehesa, J.S. (1987). Phys. Rev. A35, 2384.
121. Chakravorty, S.J. and Gadre, S.R. (1987). Chem. Phys. Letters 142, 205.
122. Partovi, M.H. (1983). Phys. Rev. Letters 50, 1883.
123. Deutsch, D. (1983). Phys. Rev. Letters 50, 631.
124. Shimony, A.A. (1985). Phys. Rev. Letters 55, 1030.
125. Tikoshinsky, Y., Tishby, N.Z. and Levine, R.D. (1985). Phys. Rev. Letters 52, 1357.
126. Blankenbecker, R. and Partovi, M.H. (1985). Phys. Rev. Letters 54, 373.
127. Gadre, S.R. and Sears, S.B. (1979). J. Chem. Phys. 71, 432.
128. Gadre, S.R., Sears, S.B., Chakravorty, S.J. and Bendale, R.D. (1985). Phys. Rev. A32, 2602.
129. Koga, T. (1983). J. Chem. Phys. 79, 1933.

130. Białynicki-Birula, I. and Mycielski, K. (1975). *Commun. Math. Phys.* 44, 129.
131. Sears, S.B., Parr, R.G. and Dinur, U. (1980). *Israel. J. Chem.* 19, 165.
132. Parr, R.G., Ghosh, S.K. and Rupnik, K. (1986). *Phys. Rev. Letters* 56, 555.
133. Shannon, C.E. (1948). *Bell Systems Tech. J.* 27, 379 : 623.
134. Gadre, S.R. and Bendale, R.D. (1987). *Phys. Rev.* A36, 1932.
135. Tsapline, B. (1970). *Chem. Phys. Letters* 6, 596.
136. Gadre, S.R., Koga, T. and Chakravorty, S.J. (1987). *Phys. Rev.* A36, 4155.
137. Williams, B.G. (1978). *Compton Scattering*, McGraw Hill.
138. Gadre, S.R. and Pathak, R.K. (1990). *J. Chem. Phys.* 92, 4327.
139. Levy, M. and Perdew, J.P. (1985). in *Density Functional Methods in Physics* NATO ASI Series, Ed. R.M. Dreizler and J. da Providencia, Plenum; p. 11.
140. Levy, M. and Perdew, J.P. (1985). *Phys. Rev.* A32, 2010.
141. Levy, M., Nee, T.-S. and Parr, R.G. (1975). *J. Chem. Phys.* 63, 316.
142. Levy, M. (1987). *In Single-Particle Density in Physics and Chemistry* Ed. N.H. March and B.M. Deb, Academic, p. 45.
143. King, F.W. (1983). *J. Chem. Phys.* 78, 2459.
144. King, F.W. (1983). *J. Chem. Phys.* 78, 3091.
145. Block, H.D. (1957). *Proc. Am. Math. Soc.* 8, 844.
146. King, F.W. and Dykema, K.J. (1983). *J. Phys.* B16, 2071.
147. Löwdin, P.-O. (1959). *J. Mol. Spectry.* 3, 46.
148. Kinoshita, T. (1957). *Phys. Rev.* 105, 1490.
149. Kinoshita, T. (1959). *Phys. Rev.* 115, 366.
150. Redheffer, R. (1966). *J. Math. Anal. Appl.* 16, 219;
Redei, L.B. (1963). *Phys. Rev.* 130, 420.
151. Yue, W. and Janmin, L. (1984). *Physica Scripta* 30, 414.
152. Blau, R., Rau, A.R.P. and Spruch, L. (1973). *Phys. Rev.* A8, 119.
153. Blau, R., Rau, A.R.P. and Spruch, L. (1973). *Phys. Rev.* A8, 131.
154. Beebe, N.H.F. and Linderberg, J. (1977). *Intern. J. Quantum Chem.* 12, 683.
155. Momose, T. and Shida, T. (1987). *J. Chem. Phys.* 87, 2832.
156. Schrader, D.M. and Prager, S. (1962). *J. Chem. Phys.* 37, 1456.
157. Okniński, A. (1974). *Chem. Phys. Letters* 27, 603.
158. Okniński, A. (1974). *J. Chem. Phys.* 60, 4098.
159. Okniński, A. (1976). *Bull. Acad. Pol. Sci. (Ser. Chimiques)* 24, 263.
160. Löwdin, P.-O. (1970). *Adv. Quantum Chem.* 5, 185.
161. England, W. (1972). *Intern. J. Quantum Chem.* 5, 683.
162. Sims J.S. and Hagström S. (1971) *Phys. Rev.* A4, 908.
163. Kay, K.G. and Silverstone, H. (1969). *J. Chem. Phys.* 51, 4287.

164. Power, J.D. and Pitzer, R.S. (1974). Chem. Phys. Letters 24, 478. For an earlier derivation of the results $0 \leq K_{\leq J} \leq (J_+ + J_-)/2$, see Roothaan, C. C. J. (1951). Rev.¹Mod. Phys. 23, 169. ¹J
165. Simon, B. (1971). Quantum Mechanics for Hamiltonians Defined as Quadratic Forms, Princeton Series in Physics.
166. Rollnik, H. (1956). Z. Phys. 145, 639.
167. Thulstrup, P.W. and Linderberg, J. (1979). Intern. J. Quantum Chem. Symp. 13, 39.
168. Harris, F.E. and Rein, R. (1966). Theoret. Chim. Acta (Berl) 6, 73.
169. Clementi, E. and Roetti, C. (1974). At. Data Nucl. Data Tables 14, 177.
170. Pathak, R.K., Sharma, B.S. and Thakkar, A.J. (1986). J. Chem. Phys. 85, 958.
171. Slater, J.C. (1930). Phys. Rev. 36, 57.
172. Slater, J.C. (1951). Phys. Rev. 81, 385.
173. Gadre, S.R. and Bendale, R.D. (1983). J. Chem. Phys. 78, 996.
174. Gadre, S.R. and Pathak, R.K. (1981). J. Chem. Phys. 75, 4740.
175. Gadre, S.R. and Pathak, R.K. (1981). Phys. Rev. A24, 2906.
176. Pathak, R.K. and Gadre, S.R. (1981). J. Chem. Phys. 74, 5925.
177. Parr, R.G., Gadre, S.R. and Bartolotti, L.J. (1979). Proc. Nat. Acad. Sci. (USA). 76, 2522.
178. Golden, S. (1980). Intern. J. Quantum Chem. Symp. 14, 135.
179. Golden, S. (1979). J. Phys. Chem. 83, 1388.
180. Lieb, E.H. (1979). Phys. Letters A70, 444.
181. Pipek, J. (1984). Chem. Phys. Letters 111, 430.
182. Weinstein, H., Politzer, P. and Srebrenik, S. (1975). Theoret. Chim. Acta. (Berl). 38, 159.
183. Sperber, G. (1971). Intern. J. Quantum Chem. 5, 189.
184. Nemade, S.P. (1983). 'Some Investigations on Atomic Electron Densities', M.Sc. Project, University of Poona (unpublished).
185. Simas, A.M., Sagar, R.P., Ku, A.C.T. and Smith, V.H., Jr. (1988). Can. J. Chem. 66, 1923.
186. Sen, K.D. and Politzer, P. (1989). J. Chem. Phys. 90, 4370.
187. Gadre, S.R. and Pathak, R.K. (1990). Proc. Ind. Acad. Sci. (Chem. Sci.) 102, 189.
188. Gadre, S.R. and Pathak, R.K. (1990). J. Chem. Phys. 93, 1770.
189. Weyrich, W., Pattison, P. (1979). Chem. Phys. 41, 271.
190. Thakkar, A.J. (1982). J. Chem. Phys. 76, 747.
191. Gadre, S.R., Chakravorty, S.J. and Pathak, R.K. (1983). J. Chem. Phys. 78, 4581.
192. Harmalkar, A., Simas, A.M., Smith, V.H., Jr. and Westgate, W.M. (1983). Intern. J. Quantum Chem. 23, 811.
193. Westgate, W.M., Simas, A.M. and Smith, V.H. Jr. (1985). J. Chem. Phys. 8, 4054.
194. Pathak, R.K. (1984). J. Chem. Phys. 80, 583.

195. Hertel, P., Lieb, E.H. and Thirring, W. (1975). J. Chem. Phys. 62, 3355.
196. Lowdin, P.-O. (1986). Intern. J. Quantum Chem. 29, 1651.
197. Lowdin, P.-O. (1989). Private communication to the authors.
198. Clementi, E. (1972). Proc. Natl. Acad. Sci. (USA). 69, 2942.
199. Habitz, H. and Clementi, E. (1982). ETO Multicenter Integrals, Ed. C.A. Weatherford and H.W. Jones, pp. 157-169. Reidel.
200. Dupuis, M., Rys, J. and King, H.F. (1976). J. Chem. Phys. 65, 111 and references therein.
201. Schlegel, H.B. (1982). J. Chem. Phys. 77, 3676.
202. Obara, S. and Saika, A. (1986). J. Chem. Phys. 84, 3963.
203. Head-Gordon, M. and Pople, J.A. (1988). J. Chem. Phys. 89, 5777.
204. Boys, S.F. (1950). Proc. Roy. Soc. (London), A200, 542.
205. Shavitt, I. (1963). In Advances in Computational Physics. Ed. B. Adler, Vol. 2. p.1. Academic.
206. Gadre, S.R. and Pathak, R.K. (1988). Proc. Ind. Acad. Sci. (Chemical Sci.) 100, 583.
207. Gadre, S.R., Kulkarni, S.A. and Pathak, R.K. (1989). J. Chem. Phys. 91, 3596.
208. Benguria, R. and Lieb, E.H. (1983). Phys. Rev. Letters 50, 1771.
209. Orera, V.M. and Chen, Y. (1987). Phys. Rev. B36, 1244.
210. Orera, V.M. and Chen, Y. (1987). Phys. Rev. B36, 5576.
211. Hill, R.N. (1977). Phys. Rev. Letters 38, 643.
212. Drake, G.W.F. (1970). Phys. Rev. Letters 24, 126.
213. Sheldon, J.W. (1955). Phys. Rev. 99, 1291.
214. Schwinger, J. (1961). Proc. Nat. Acad. Sci. (USA). 47, 122.
215. Birman, M.S. (1961). Mat. Sbornik. 55, 124; (1966) Am. Math. Soc. Translation.
216. Ghirardi, G.C. and Rimini, A. (1965). J. Math. Phys. 6, 40.
217. Lieb, E.H. and Thirring, W.E. (1976). Phys. Rev. Letters 35, 1116(E).
218. Bargmann, V. (1952). Proc. Nat. Acad. Sci. (USA). 38, 961. Series II. 53, 23.
219. Kato, T. (1951). Trans. Am. Math. Soc. 70, 195.
220. Dyson, F.J. (1967). J. Math. Phys. 8, 1538.
221. Dyson, F.J. and Lenard, A. (1967). J. Math. Phys. 8, 423.
222. Lenard, A. and Dyson, F.J. (1968). J. Math. Phys. 9, 698.
223. Savin, A., Stoll, H. and Preuss, H. (1986). Theoret. Chim. Acta (Berl). 70, 407.
224. Siedentop, H. and Weikard, R. (1987). Commun. Math. Phys. 112, 471.
225. Scott, J.M.C. (1952). Phil. Mag. 43, 859.
226. Lieb, E.H. and Simon, B. (1978). J. Chem. Phys. B11, L537.
227. Narnhofer, H. and Thirring, W. (1975). Acta. Phys. Aust. 41, 281.
228. Lieb, E.H. (1982). J. Phys. B15, L63.
229. Mezey, P.G. (1983). J. Chem. Phys. 78, 6182.
230. Mezey, P.G. (1985). J. Mol. Str. (Theochem) 123, 171.

- 231. Mezey, P.G. (1982). Intern. J. Quantum Chem. 22, 101.
- 232. Mezey, P.G. (1983). Intern. J. Quantum Chem. 24, 523.
- 233. Arteca, G.A. and Mezey, P.G. (1987). Phys. Lett. A122, 483.
- 234. Arteca, G.A. and Mezey, P.G. (1987). J. Chem. Phys. 87, 5882.
- 235. Ghosh, S.K. (1990). Chem. Phys. Letters 172, 77.
- 236. Silverman, J.N. and van Leuven, J.C. (1970). Chem. Phys. Letters 7, 37.
- 237. Deb, B.M. (1972). Chem. Phys. Letters 17, 78.
- 238. Chen, Z. and Spruch, L. (1990). Phys. Rev. A42, 127.
- 239. Chen, Z. and Spruch, L. (1990). Phys. Rev. A42, 133.
- 240. Christoffersen, R.E. (1972). Adv. Quantum Chem. 6, 333.
- 241. Gadre, S.R., Shrivastava, I.H. and Kulkarni, S.A. (1990). Chem. Phys. Letters 170, 271.

Note added in proof

We note that during the preparation of this article, some excellent reviews, viz. by Jones and Gunnarsson, in The Reviews of Modern Physics, 1989; and the entire Volume 21 of the Advances in Quantum Chemistry, 1990, devoted to the Density Functional Theory, have appeared. We also have to make a mention of an earlier article by Weinhold (Vol. 6 of Adv. Quantum Chem.) that deals with bounds to quantal expectation values for many-electron systems.

ATOMIC NATURAL ORBITAL (ANO) BASIS SETS FOR QUANTUM CHEMICAL CALCULATIONS

Jan Almlöf

Department of Chemistry and
Minnesota Supercomputer Institute
University of Minnesota
Minneapolis, MN 55455
USA

Peter R. Taylor[†]

ELORET Institute
Palo Alto, CA 94303
USA

1. INTRODUCTION

1.1. Atomic orbitals and molecular orbitals

The molecular orbital (MO) theory of electronic structure is the most fruitful concept introduced into quantum chemistry. Its simple interpretation of structure, bonding, and spectroscopy in terms of one-electron functions not only provides great qualitative physical insight, but also leads naturally to a variety of schemes for the quantitative calculation of molecular properties. Since, in general, the

[†]Mailing address: NASA Ames Research Center, Moffett Field, CA 94035, USA

functional form of the MOs is unknown, some suitable scheme for approximating them must be found. Expanding unknown functions in a fixed basis set is a standard mathematical technique in the physical sciences, and in the earliest qualitative schemes MOs were represented as arising from overlapping atomic orbitals (AOs) — a linear combination of atomic orbitals (LCAO) model. This model has a very clear and straightforward physical interpretation. In most molecular systems, the forces acting on the electrons are approximately the same as in the free atoms, and the total electronic energy in a molecule therefore seldom differs by more than a small fraction from the sum of atomic energies. (In other words, the heat of atomization for a molecule is small compared to the total energy). It is therefore a commonly accepted notion that a molecule can be considered as assemblage of atoms with chemical bonding as a small perturbation. Consistent with that view, the molecular orbitals in an electronic structure model can be formed from atomic orbitals with small additional adjustments, and the LCAO MO model is consequently a cornerstone of quantum chemistry.

The simplest example of the MO model (for the case of more than one electron) is the H_2 molecule. Here the ground state arises from two electrons occupying a bonding MO of σ_g symmetry; in the simple LCAO representation the σ_g MO is a symmetric combination of $1s$ AOs on the individual hydrogens. This picture is qualitatively satisfactory, but for quantitative predictions it suffers from two well-known disadvantages. First, approximating the wave function by a single electron configuration neglects the detailed correlation of the electronic motion: the orbital model is a mean-field treatment (the Hartree-Fock approximation). Second, while any function such as an MO can be expanded in some suitable complete set of basis functions (say, AOs), naive valence AO combinations like the one suggested above for H_2 will not necessarily be adequate. Hence for quantitative accuracy we must be concerned both with AO basis sets that extend beyond the occupied ground-state AOs of the atoms, and with a treatment of the many-particle problem that goes beyond the Hartree-Fock approximation. Further, since the exact AOs are not available for any atom beyond hydrogen (and even in that case have a complicated analytical form),

additional approximations are necessary. We shall discuss some consequences of these concerns in the following subsections.

1.2. LCAO MOs and the Hartree-Fock approximation

We begin with an approximation to the N -electron molecular wave function Ψ as a single Slater determinant of orthonormal molecular spin orbitals $\{\psi\}$

$$\Psi_0 = \begin{vmatrix} \psi_1(1) & \psi_1(2) & \psi_1(3) & \dots & \psi_1(N) \\ \psi_2(1) & \psi_2(2) & \psi_2(3) & \dots & \psi_2(N) \\ \vdots & \vdots & \vdots & \ddots & \vdots \\ \psi_N(1) & \psi_N(2) & \psi_N(3) & \dots & \psi_N(N) \end{vmatrix} = |\psi_1 \psi_2 \psi_3 \dots \psi_N\rangle. \quad (1)$$

The LCAO expansion provides a simple solution to approximating the orbitals $\{\psi\}$

$$\psi_i = \sum_{\lambda} \chi_{\lambda} C_{\lambda i}. \quad (2)$$

Here $\{\chi\}$ is a set of AOs: functions centered on the various nuclei. If the summation in (2) is restricted to run over only those shells of AOs occupied in the free ground-state atoms, we speak of a minimal basis set. In certain small symmetric systems the LCAO coefficients C for a minimal basis are determined by symmetry, but in more complicated cases (larger systems and/or more AOs) some condition must be used to determine C . Given the clamped-nucleus Born-Oppenheimer Hamiltonian (in atomic units)

$$H = -\frac{1}{2} \sum_i \nabla_i^2 - \sum_{i,A} \frac{Z_A}{|r_i - R_A|} + \sum_{i < j} \frac{1}{|r_i - r_j|} + \sum_{A < B} \frac{Z_A Z_B}{|R_A - R_B|}, \quad (3)$$

where i and A span the range of electron and (fixed) nuclear coordinates, respectively, a condition for C can be found by taking the expectation value of the

approximate wave function (1) over the Hamiltonian (3), inserting the expansion (2) in the resulting functional and making the energy stationary with respect to all variations of \mathbf{C} that preserve orthonormality of the $\{\psi\}$. This gives the matrix equation

$$\mathbf{FC} = \mathbf{SC}\epsilon, \quad (4)$$

where \mathbf{S} is the overlap matrix over the AO basis $\{\chi\}$, ϵ is a matrix of Lagrange multipliers arising from the orthonormality constraints, and

$$F_{\mu\nu} = h_{\mu\nu} + \sum_{\lambda\sigma} P_{\lambda\sigma} [(\mu\nu|\lambda\sigma) - (\mu\sigma|\lambda\nu)]. \quad (5)$$

Here $h_{\mu\nu}$ is a one-electron integral and $(\mu\nu|\lambda\sigma)$ a two-electron integral in Mulliken notation, i.e.

$$(\mu\nu|\lambda\sigma) = \iint \chi_{\mu}^{*}(r_1) \chi_{\nu}(r_1) \frac{1}{r_{12}} \chi_{\lambda}^{*}(r_2) \chi_{\sigma}(r_2) dr_1 dr_2 \quad (6)$$

over the basis $\{\chi\}$. \mathbf{P} is the density matrix: if we restrict ourselves to the closed-shell case (where α and β spin-orbitals have the same spatial part) we have

$$P_{\mu\nu} = 2 \sum_i C_{\mu i} C_{\nu i}. \quad (7)$$

and

$$F_{\mu\nu} = h_{\mu\nu} + \sum_{\lambda\sigma} P_{\lambda\sigma} [(\mu\nu|\lambda\sigma) - \frac{1}{2}(\mu\sigma|\lambda\nu)], \quad (8)$$

in a space orbital notation. The LCAO self-consistent field (SCF) equations (4) were first derived for the case of a closed-shell molecule with doubly-occupied spatial orbitals independently by Roothaan [1] and by Hall [2], and were

extended to the case of a single determinant of spin-orbitals by Pople and Nesbet [3]. There have been numerous subsequent extensions to open-shell systems — further references are given in Ref 4.

It is evident that optimizing the expansion coefficients $\{C_{\lambda i}\}$ in (2) using (4) requires the evaluation of one- and two-electron integrals over the AOs. The form chosen for the AOs therefore has a crucial influence on the computational complexity and feasibility of the LCAO SCF scheme. A complete (i.e., infinite) set of AOs would yield the *Hartree-Fock limit* result, but utilizing such a set is not feasible in practice. From comparisons with accurate (numerical) atomic Hartree-Fock calculations, a Slater-type orbital (STO), centered at \mathbf{R}_A ,

$$\chi(n, l, m, \zeta) = |\mathbf{r} - \mathbf{R}_A|^{n-1} \exp(-\zeta |\mathbf{r} - \mathbf{R}_A|) Y_{lm}(\theta_A, \phi_A) \quad (9)$$

involving an exponential radial term (Y_{lm} is a spherical harmonic) is known to be one of the best single-term approximations to an atomic orbital. The exponential radial term reproduces the correct cusp behavior at an atomic nucleus if the exponent ζ is chosen appropriately; the correct asymptotic decay can also be described with a suitable (in general different) choice of ζ . STOs would thus appear to be a good choice for the AO basis. A minimal basis set of such STOs is sometimes referred to as a single zeta basis. After the Roothaan-Hall equations were derived, much effort was devoted to evaluating the two-electron integrals over STOs [5]. Unfortunately, these integrals were found to be mathematically complicated and computationally time-consuming, especially where functions on more than two centers are involved, and where the system has symmetry lower than cylindrical. In fact, there is still no method for computing multicenter STO integrals accurately when higher angular momentum functions are involved. These problems were greatly exacerbated by the early realization that the MOs obtained from minimal STO basis sets are of rather poor quality. If two independent STOs are used to represent each occupied AO, the resulting “double zeta basis” MOs were substantially improved, but at a cost of generating and handling some 16 times as many two-electron integrals.

The basis set deficiencies were only partly overcome by using double zeta sets. A consequence of the lower symmetry of molecules, as compared to atoms, is that AOs that are unoccupied in the atomic ground state at the Hartree-Fock level, such as *d* type functions for first-row atoms, can (and do) contribute to the occupied MOs. Such higher angular momentum functions are referred to as polarization functions since they allow for polarization of electron density in chemical bonds. Adding polarization functions to a double zeta (or larger) STO basis obviously further increases the computational labour, and although a number of large basis set STO studies of diatomic and linear polyatomic systems were performed the need for an alternative to STOs was clear.

Boys [6,7] and Preuss [8] had earlier suggested the use of basis functions with a Gaussian radial form:

$$\chi(\lambda, \mu, \nu, \alpha) = (x - X_A)^\lambda (y - Y_A)^\mu (z - Z_A)^\nu \exp(-\alpha |\mathbf{r} - \mathbf{R}_A|^2). \quad (10)$$

These functions are termed Cartesian Gaussian functions because of the use of polynomials in *x*, *y*, and *z* to generate the angular dependence. Two-electron integrals over such Gaussian-type orbitals (GTOs) can be evaluated with little difficulty, even for nonlinear polyatomic species. Early experience with small Gaussian basis sets had been discouraging [9]; this is perhaps not surprising, since a Gaussian function can satisfy neither the nuclear cusp condition nor the asymptotic behavior of atomic wave functions. An alternative use of GTOs was to use them for expansions of STOs in order to overcome the integral evaluation problems associated with the latter [10]. This approach, although frequently used later in the popular STO-nG basis sets [11], is not free from difficulties. In fact, GTOs themselves could be used in LCAO calculations once it was appreciated that, because of their less satisfactory properties, MO expansions in GTOs would be more slowly convergent than MO expansions in STOs [12]. That is, more GTOs would be required for a given level of accuracy. Finally, it was realized that many GTOs appeared with very similar relative weights for the same element in different molecules: for example, those high exponent GTOs that were required to approximate the nuclear cusp condition satisfactorily. In such

cases a single function formed as a fixed linear combination of GTOs — a contracted Gaussian (CGTO) [13] — could be used as a basis function, thus substantially reducing the length of the LCAO expansions of the MOs.

The nodal structure of the Gaussians in (10) is equivalent to that of atomic orbitals with quantum numbers $n = l+1$, that is, radially nodeless functions of the form $1s, 2p, 3d, 4f$, etc, where the Cartesian “angular momentum” value $L = \lambda + \mu + \nu$ is used instead of the regular l value for atomic functions. The correct radial nodal structure of other atomic orbitals is achieved either by the choice of the contraction coefficients or by using several basis functions with appropriate relative phases.

It is appropriate at this point to discuss how the role of the “atomic basis functions” in molecular Hartree-Fock calculations has changed in the light of these developments. In the early minimal basis set studies, essentially the same basis functions that would be used in a qualitative LCAO MO model were being used in the SCF calculations — single-term approximations to atomic orbitals. There was thus an intimate connection between the SCF calculation and the interpretative model. However, as the atomic basis sets in common use have expanded, whether to double zeta STO sets or to extended sets of CGTOs with multiple polarization functions, the connection with the simple interpretative model has been considerably weakened. In the vast majority of extended basis set SCF calculations carried out today, it is seldom possible to identify any of the CGTOs with functions resembling atomic orbitals, except for core orbitals which are usually uninteresting for chemical interpretation. The “AO” in LCAO has come to mean little more than “Gaussian basis function”, with a concomitant loss of simple physical interpretability in the calculation. To a large extent this arises from confusing a mathematical expansion basis (CGTOs) used largely for its computational convenience with a physically motivated set of basis functions (AOs). This point has been addressed particularly by Raffennetti [14] and by Ruedenberg and coworkers [15], who first showed how accurate LCAO SCF calculations could be carried out in a basis of high-quality AOs, while retaining the computational convenience of an underlying CGTO expansion basis. Later in this review we shall describe an LCAO approach in which the AOs used are of greater

physical significance than the rather arbitrary CGTO combinations employed in most calculations.

1.3. The correlation problem

Löwdin [16] has defined the correlation energy as the difference between the exact non-relativistic energy of a system and the Hartree-Fock energy. This difference arises because the exact wave function cannot be represented as a single determinant like (1). As the correlation energy is a small fraction of molecular total energies, we may expect the Hartree-Fock determinant (or a combination of a few determinants) to dominate the wave function, which is conveniently expanded using the MOs $\{\psi\}$ as a configuration-interaction (CI) expansion

$$\Psi = \Psi_0 + \sum_i \sum_a \Psi_i^a c_i^a + \sum_{i<j} \sum_{a<b} \Psi_{ij}^{ab} c_{ij}^{ab} + \sum_{i<j<k} \sum_{a<b<c} \Psi_{ijk}^{abc} c_{ijk}^{abc} + \dots \quad (11)$$

The configurations Ψ_i^a , Ψ_{ij}^{ab} ... are obtained by exciting one, two, ... electrons from the occupied MOs (indexed i, j, \dots) to empty “virtual” MOs (a, b, \dots) that arise because the expansion basis is invariably larger than the number of occupied MOs. Of course, the functional form of these empty MOs will reflect the functional form of the underlying expansion basis. We should note that we have tacitly assumed a spin-orbital formulation of the CI problem in (11), although most efficient computational formulations are spin-adapted.

In practice it is often convenient to distinguish between two types of correlation effects [17,18]. *Nondynamical* correlation arises when several configurations are nearly degenerate and interacting, and therefore become simultaneously important in the expansion of the wave function. This situation arises, for example, in breaking chemical bonds and in many electronically excited states, and can lead to qualitatively incorrect predictions from Hartree-Fock calculations. Nondynamical correlation can usually be accounted for by extending the wave function from one to relatively few terms, i.e., a multiconfigurational

SCF (MCSCF) treatment. In general, the convergence of MCSCF results with the atomic basis set size is similar to that of SCF calculations.

Dynamical correlation arises from the cusp condition in r_{ij} that is satisfied by the exact wave function. Convergence of the dynamical correlation energy with excitation level, that is, with respect to successive terms in (11), has been shown by explicit calculations to be fairly rapid, single and double excitations being the most important (see, for example, Refs. 18–20). In cases where nondynamical correlation is important, the expansion (11) must be redefined so that all important configurations appear as reference functions. In contrast to the rapid convergence with excitation level, convergence with respect to the size and nature of the atomic expansion basis set is very slow [18,21]. This is not surprising — reproducing a two-electron cusp in the wave function by products of one-electron orbitals is a slowly convergent procedure. In addition, describing such cusp behavior requires functions with higher angular momenta than the occupied AOs, and the correlation energy contributions of these higher angular functions converge much more slowly with angular quantum number than their SCF contributions in molecules.

A CI expansion like (11) is not the only approach to calculating dynamical correlation energies in which an “ N -particle basis” is built up as products of one-electron orbitals. Other related methods like perturbation-theoretic and coupled-cluster techniques have their own advantages and disadvantages [22]. For present purposes, we note only that all of these methods naturally show the same slow convergence of dynamical correlation energy with atomic expansion basis. We also note that the convergence of the N -particle and one-electron expansions will be coupled to some extent, although for most extended basis sets this coupling appears to be rather weak.

1.4. Considerations for basis set design

We have briefly reviewed a number of aspects of the calculation of molecular SCF and correlation energies that are relevant to the design and construction

of atomic basis sets. Several other issues are also important. If, for example, accurate atomic or molecular properties are required, the basis set must contain angular functions suitable for describing the effect of an applied perturbation (e.g., electric field, if the property of interest is the dipole moment) on the wave function. Accounting for all these considerations makes basis set design a complicated and demanding task. It is clear from 1.2 and 1.3 that obtaining accurate correlation energies will be much more demanding of the atomic expansion basis than the computation of SCF energies, so one strategy is to concentrate on the design of basis sets for describing dynamical correlation effects, assuming that such sets will perform adequately at the SCF level or in describing nondynamical correlation. This is the strategy we will pursue in the remainder of this review. We will show that it is indeed possible to obtain basis sets for accurate SCF calculations as a consequence of the accurate treatment of dynamical correlation. In the next section we review some formal properties of wave functions and orbitals that are required for our later development. In section 3 we discuss a variety of computational aspects of basis set contraction and the evaluation of Gaussian integrals. Section 4 contains a detailed analysis of the performance of our proposed basis set designs, while in section 5 a number of different applications to accurate calculations of atomic and molecular properties are described. Several recent alternative approaches are discussed in section 6, and our conclusions are given in section 7.

2. NATURAL ORBITALS

2.1. Properties of Natural Orbitals

For molecular SCF wave functions it may be acceptable to use an LCAO representation based on occupied SCF AOs (although computed properties in minimal SCF AO basis sets can be poor [23]). However, for correlated wave functions such small basis sets are even less desirable, and additional basis functions need to be defined. Unfortunately, the form of the virtual SCF AOs can change dramatically as the expansion basis is changed, so little in the way of physical interpretation can be based on the SCF AOs from extended basis sets. It is desirable to find some set of orbitals whose definition is less dependent on the expansion basis at the correlated level. Consider the first-order reduced density kernel [24] from an N -electron wave function Ψ :

$$\gamma(1'1) = N \int \Psi(1', 2, \dots, N) \Psi^*(1, 2, \dots, N) d\tau_2 \dots d\tau_N. \quad (12)$$

In an arbitrary (orthonormal) spin-orbital basis $\{\phi\}$ we can expand $\gamma(1'1)$ as

$$\gamma(1'1) = \sum_k \sum_l \phi_k^*(1') \phi_l(1) \gamma_{kl}, \quad (13)$$

where γ is the first-order reduced density matrix. γ is a square Hermitian matrix and can be diagonalized by a unitary transformation. This property can therefore be used to write $\gamma(1'1)$ in the diagonal representation

$$\gamma(1'1) = \sum_k \eta_k^* \eta_k n_k, \quad (14)$$

Löwdin has termed the set $\{\eta\}$ *natural spin-orbitals* (NSOs) [25]. The n_k are occupation numbers of the NSOs; in the normalization of (11) we have

$$0 \leq n_k \leq 1. \quad (15)$$

In practice, it is more common to sum over the spin coordinate in (13) and (14), giving the spinless first-order reduced density matrix, and its eigenvectors, the *natural orbitals* (NOs). The occupation numbers of the NOs so defined lie between zero and two.

Natural orbitals have a number of special properties. SCF orbitals are themselves NOs — for a closed-shell system the occupied orbitals have occupation numbers of two and the virtuals have occupation zero. For a two-electron system, the NOs can be shown [26] to yield the most rapidly convergent CI expansion of the wave function, and truncation of the orbital space by eliminating the NOs with the smallest occupation number produces the smallest least-squares error in the wave function. For many-electron systems these properties do not apply rigorously, but there is considerable empirical evidence to support the contention that the occupation number of an NO provides a useful measure of its importance in the wave function [24]. Hence if we are interested in developing methods for truncating one-particle basis sets, NOs and their occupation numbers are certainly worth investigating.

2.2. Natural Orbitals for Neon Atom

Let us consider the neon atom NOs. Figure 1 displays the occupation numbers for the NOs of an SDCI wave function, correlating the eight valence electrons, in an uncontracted (18s 13p 6d 5f 4g 3h 2i) GTO basis set. (This basis set should account for about 97–98% of the complete basis set limit valence correlation energy for a given N -particle space treatment.)

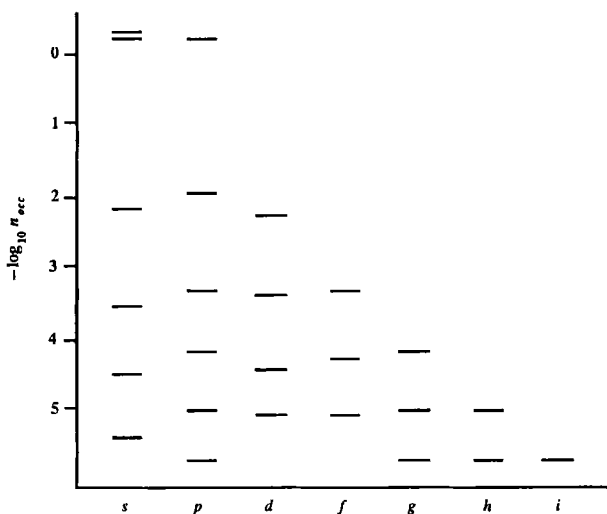


Figure 1. Ne natural orbital occupation numbers.

Occupation numbers for NOs not shown in Fig. 1 are smaller than 2×10^{-6} . There is some regularity in the larger occupation numbers, but this is gradually lost as the occupation numbers decrease. A systematic pattern can also be discerned in the *s* and *p* NOs, i.e., the ones mainly describing radial correlation, and a different one in the high *l* occupation numbers. Since the occupation number of an NO is a direct measure of its importance in the wave function, we can expect to obtain a systematic sequence of truncated orbital spaces by eliminating the NOs with occupation numbers below different selection thresholds. For example, at an occupation number threshold of 10^{-3} , we retain *3s 2p 1d* NOs, at 10^{-4} *4s 3p 2d 1f* and at 10^{-5} *5s 4p 3d 2f 2g 1h* or *5s 4p 3d 2f 1g 1h* (the second *g* NO occupation number is in fact almost exactly 10^{-5}). However, below a threshold of 10^{-5} the pattern becomes more complicated. The fifth *p* NO has an occupation number very close to 10^{-5} ; and the fourth *d* and third *f* occupation numbers are only slightly smaller, although the size of the GTO basis is probably not large enough to define these occupation

numbers reliably. At occupation numbers of 10^{-6} and smaller, the NOs take on an increasingly oscillatory behavior because of the nodal structure enforced by orthogonality. However, these very weakly occupied NOs obviously contribute little to the wave function and do not affect the energy significantly (see below). At thresholds around 10^{-5} and larger, therefore, the NO occupation numbers seem to provide a very convenient scheme for truncating the one-particle space. We shall now consider the consequences of this truncation for the total energy.

In Table 1 we list energy results for several truncated NO expansions for Ne.

Table 1. Ne atom NO expansion energy truncation errors (E_h)^a.

Primitive basis sets		E_{SCF}	E_{SDCI}
(18s 13p 6d 5f 4g 3h 2i)		-128.547094	-128.850926
(18s 13p 6d 5f 4g 3h)		-128.547094	-128.849475
(18s 13p 6d 5f 4g)		-128.547094	-128.845632
(18s 13p 6d 5f)		-128.547094	-128.833422
Threshold	Truncated NO expansions	ΔE_{SCF}	ΔE_{SDCI}
1×10^{-6}	6s 6p 4d 3f 3g 2h 1i	0.000017	0.006476
^b	6s 6p 5d 4f 3g 2h 1i	0.000017	0.005897
1×10^{-5c}	5s 4p 3d 2f 2g 1h	0.000068	0.006382
1×10^{-5c}	5s 4p 3d 2f 1g 1h	0.000068	0.008472
1×10^{-5}	5s 4p 3d 2f 1g	0.000068	0.007298
1×10^{-4}	4s 3p 2d 1f	0.000162	0.016939

^a Truncation error measured with respect to primitive set with the same highest angular momentum.

^b "Canonical" sequence — see text.

^c Occupation number of second g NO is almost exactly 10^{-5} .

For the primitive basis sets we give the total SCF and SDCI energy, while for the NO sets we give the *truncation error*, defined as the difference between the energy in the truncated NO set and the energy in the primitive set, which of course corresponds to using all NOs. The truncation errors in Table 1 are referenced to the primitive basis with the same highest angular momentum. The primitive basis results in Table 1 show that to within the common criterion of 1 kcal/mol — “chemical accuracy” — in the SDCI energy, it is necessary to include *i* type functions ($l = 6$). The contribution of *h* type functions is several times larger. Turning to the truncated NO expansion results, we note first that the truncation error in the SCF energy is effectively zero for all the basis sets listed. For the SDCI energy, the truncation errors are naturally much larger, ranging from 6 to 9 mE_h. For the largest truncated set, *6s 6p 4d 3f 3g 2h 1i*, the average error is approximately 1 mE_h per *l* value, or a little over 0.5 kcal/mol. If the selection threshold is increased to 1×10^{-5} the truncation error remains almost unchanged, since although energy is lost by using a smaller NO set, there is a compensating reduction in the primitive basis energy from the omission of *i* functions. We can see a similar effect when *h* functions are omitted, by comparing the *5s 4p 3d 2f 1g 1h* and *5s 4p 3d 2f 1g* results. Included also in Table 1 is a result from a *6s 6p 5d 4f 3g 2h 1i* truncated NO space. This does not correspond to any strict selection by occupation number threshold, but it represents the final stage (within this primitive space) of the “canonical” sequence *3s 2p 1d, 4s 3p 2d 1f*, etc. (The seventh *s* NO is a highly oscillatory orbital with a very small occupation number, it was therefore excluded.) This *6s 6p 5d 4f 3g 2h 1i* set improves the energy by only 0.6 mE_h compared to the *6s 6p 4d 3f 3g 2h 1i* set.

These observations support the contention that NO truncation is a useful method for excluding unimportant orbitals. However, while a primitive Gaussian basis that is essentially complete for all *l* values up to and including $l = 6$ is useful to establish these convergence properties, it would be impractically large for correlated calculations on polyatomic molecules. To illustrate that the same behavior is observed for smaller, more practical primitive basis sets we give in Table 2 NO truncation errors for a smaller (*13s 8p 6d 4f 2g*) primitive basis.

The results of Table 2 are very similar to those of Table 1. The truncation error in the SCF energy is negligible, while the truncation error in the SDCI energy is relatively small at an occupation number threshold of 10^{-5} , although it becomes noticeable at a threshold of 10^{-4} .

Table 2. Ne atom NO expansion energy truncation errors (E_h)^a.

Primitive basis sets		E_{SCF}	E_{SDCI}
(13s 8p 6d 4f 2g)		-128.546574	-128.843807
(13s 8p 6d 4f)		-128.546574	-128.832550
(13s 8p 6d)		-128.546574	-128.798756
Threshold	Truncated NO expansions	ΔE_{SCF}	ΔE_{SDCI}
1×10^{-5}	5s 4p 3d 2f 1g	0.000063	0.006059
1×10^{-5}	5s 4p 3d 2f	0.000063	0.004126
1×10^{-4}	4s 3p 2d 1f	0.000166	0.016691
1×10^{-6}	6s 5p 4d	0.000057	0.000731
1×10^{-5}	5s 4p 3d	0.000063	0.002337
1×10^{-4}	4s 3p 2d	0.000166	0.009408

^a Truncation error measured with respect to primitive set with the same highest angular momentum.

We note again the importance of higher angular functions: the *f* and *g* spaces are less well saturated than in the larger primitive set used in Table 1, but even here *g* type functions contribute more than 11 mE_h to the energy. Overall, occupation number truncation at a threshold of 10^{-5} produces an energy effect of little more than 0.5 kcal/mol per *l* value (on average), while truncation at the 10^{-4} threshold leads to an average energy loss of about 2 kcal/mol per *l* value. Interestingly, the NO truncation patterns closely parallel the importance of polarization functions for the correlation energy in molecular calculations, pointed out by Jankowski *et*

al. [27]. They emphasize the need for “balanced” polarization sets, which they found to follow the sequence $1d$, $2d1f$, and $3d2f1g$. Dunning has arrived at similar conclusions in basis set optimization studies [28].

We should perhaps note one aspect of expanding NOs in primitive Gaussian functions here. Traditionally, the $(13s\ 8p)$ set would be regarded as “valence triple zeta” [29], since only the outermost three s primitives contribute substantially to the outer lobe of the $2s$ AO (the remainder have small coefficients from the requirement of orthogonality to the $1s$). From this point of view, one would then expect such a basis to be capable of describing only three valence s AOs, plus the $1s$ core, yet the primitive set appears to be capable of describing at least the first *four* s NOs, as well as the core. In fact, the fourth outermost primitive in the $(13s)$ set has almost zero coefficient in the $2s$ AO because of the position of the radial node; this primitive contributes substantially to higher valence s NOs. Comparisons of the overlap between s NOs expanded in a $(13s)$ set with those expanded in an $(18s)$ set also demonstrate that the former can describe at least four valence s NOs, although only the $(18s)$ set would normally be regarded as quadruple zeta in the valence shell. Thus designations like “triple zeta” are best reserved for the SCF level only.

The utility of NOs in providing a set of orbitals with desirable truncation properties is, of course, well known in quantum chemistry [23,30]. NO transformations of SCF MOs have long been popular in reducing the number of orbitals that must be included in the orthonormal basis to be used in a CI calculation, but this is a transformation performed at the MO level [30]. NOs have also occasionally been used to define atomic orbital basis sets: for polarization functions by Pettersson and Siegbahn [31], and in a series of small basis set comparisons on H_2CO by Feller and Davidson [32]. These investigations, however, were isolated special cases, and the possibilities associated with using a systematic truncation by occupation number were not explored. The results shown in Tables 1 and 2 suggest that the NOs of an atom provide a well-defined AO basis that could be used in molecular calculations, and that occupation number truncation may be appropriate for determining which NOs should be used.

We therefore propose that if it is desired to perform LCAO calculations of correlated molecular wave functions, an appropriate AO representation, by analogy with the use of SCF AOs for molecular Hartree-Fock calculations, will be obtained by using NOs for the atoms — *atomic natural orbitals* (ANOs) [33]. These will normally be expanded in Gaussian functions, but that is a computational convenience, not a mathematical requirement. In order to verify whether this is a reasonable choice of AO basis, we must explore its use in molecular calculations and evaluate its performance, and this aspect is treated comprehensively in section 4. A number of computational considerations also arise, and these merit discussion first. So far, we have paid scant attention to the details of the expansion basis, or to the computational implementation of any LCAO method. We now turn to these aspects, in particular to the distinction we wish to make between the AO basis and an underlying set of expansion functions, and how that distinction affects the generation of integrals over the AOs.

3. EXPANSION BASIS

3.1. Basis Set Contraction

The practice of contracting Gaussian basis sets [13,34], that is, the use of fixed linear combinations of primitive Gaussian functions as the one-particle basis, rather than individual Gaussians, can be viewed as a method of reducing the dimensionality of the computational problem by projecting out less essential parts of the expansion basis. By transforming the Gaussians to a new, intermediate set of functions which better represent the problem, the number of degrees of freedom involved in representing the MOs is reduced. This contraction procedure serves several purposes. First, it reduces the size of the final basis set and therefore reduces the computer time requirements for the wave function calculation. This is especially important for calculations of the correlation energy because of their strong (N^5 and higher) dependence on basis set size. Second,

contraction reduces the size of matrices that must be kept in computer memory during a calculation: Fock and density matrices (eqs. 4–6) in the case of an SCF calculation, for example. Third, contraction reduces the length of the two-electron integral files that need to be stored externally in all conventional approaches to atomic and molecular electronic structure calculations. With modern computers, the size of the Fock or density matrices is not normally of great concern, and the real storage bottleneck that calls for basis set contraction is the size of the integral list.

The most common way to determine contraction coefficients has been to carry out an atomic SCF calculation in the primitive basis [34]. Often, the exponents for the primitive Gaussians (α in (10)) are also optimized in these calculations. The SCF coefficients of the atomic orbitals are then used as contraction coefficients. Another scheme, popular for developing small basis sets and for polarization functions, is to expand STOs in a set of primitive Gaussians to obtain basis functions [11]. In either case, the standard approach to contraction has been to let each primitive function contribute to exactly one contracted function. Hence the transformation

$$X^{\text{CGTO}} = \chi^{\text{GTO}} \mathbf{T} \quad (16)$$

that gives the contracted basis $X^{\text{CGTO}} \{X_1, X_2, \dots\}$ in terms of the primitive basis $\chi^{\text{GTO}} \{\chi_1, \chi_2, \dots\}$ is blocked in such a way that only one element is non-zero in every row of the rectangular transformation matrix \mathbf{T} — see Fig. 2.

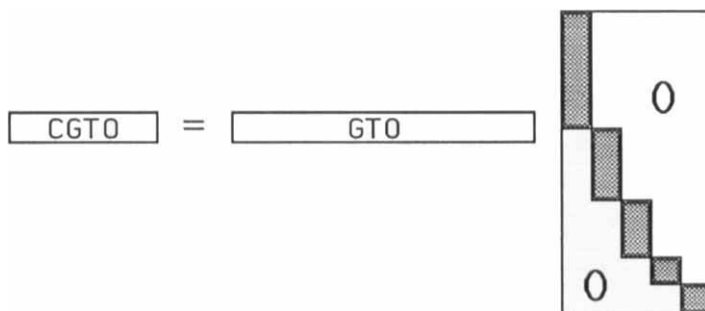


Fig. 2. Segmented contraction scheme

This restriction on the contraction transformation is referred to as a *segmented contraction* scheme. It has several disadvantages; perhaps the greatest being that it is difficult to apply to heavy elements and/or large basis sets, since in these cases one primitive function often contributes significantly to several AOs [35]. With segmented contraction schemes the segmentation becomes ambiguous, in the sense that the primitive function can be assigned to any of the contracted functions to which it contributes strongly, but no choice will give a contracted basis set that adequately approximates the AOs in the original primitive basis. In such a case there is little recourse but to include the same primitive Gaussians in several contracted functions. If a transformation of the form of Fig. 2 is still required (this is commonly the case for computational reasons, as discussed later in 3.4), the particular primitive Gaussian(s) will have to be duplicated, increasing the size of the primitive basis. A much more satisfactory solution is to use a more flexible scheme than segmented contraction. In the *general contraction* scheme of Raffanetti [14], the transformation \mathbf{T} in (16) is simply a rectangular matrix (Fig. 3).

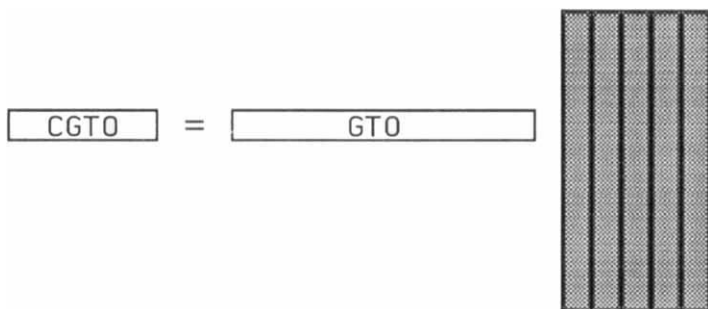


Fig. 3. General contraction scheme

One considerable advantage of the general contraction scheme is that the CGTOs reproduce exactly the desired combinations of primitive functions. For example, if an atomic SCF calculation is used to define the contraction coefficients in a general contraction, the resulting minimal basis will reproduce the SCF energy obtained in the primitive basis [14]. This is not the case with segmented contractions. There are other advantages: for example, it is possible to contract inner-shell orbitals to single functions with no error in the atomic energy, making calculations on heavy elements much easier [36]. Another advantage is a conceptual one, much exploited by Ruedenberg and co-workers [15,37]. Using a general contraction, it is possible to perform calculations in which the one-particle space is a set of atomic orbitals, a true LCAO scheme, rather than being a segmented grouping of a somewhat arbitrary expansion basis. The MOs can then be analyzed very simply, just as for the original qualitative LCAO MO approach, but in terms of “exact AOs” rather than crude approximations. In this respect, general contraction is uniquely able to meet one of our criterion from section 1: that the one-particle space should retain the conceptual simplicity of the original LCAO approximation.

The segmented contraction scheme is simpler to implement and has therefore gained certain popularity, indeed, the vast majority of Gaussian-based *ab initio* calculations carried out to date have used segmented basis sets. Nevertheless, we advocate here the use of a general contraction scheme, that is,

one in which no restrictions are placed on the elements in T other than those imposed by orthogonality and normalization. In doing so, we allow the basis function to resemble AOs as closely as the primitive expansion allows.

It is, of course, possible to combine some features of the two contraction schemes, as in Fig. 4.

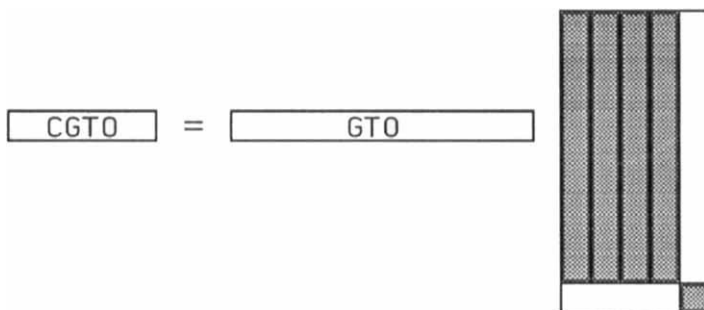


Fig. 4. Modified general contraction scheme

This approach is useful where it is desired to “uncontract”, say, the outermost primitive functions from the contraction, i.e., to let them constitute basis functions on their own [14,15]. We shall discuss this possibility in more detail below. For our present purposes we regard the modified contraction of Fig. 4 as simply a general contraction, paying no special attention to the zero elements in the contraction matrix.

With general contraction in mind, we now consider aspects of basis set choice for use in molecular calculations with correlated wave functions.

3.2. Extended Basis Sets

A basis set that provides a good description of the atoms is a necessary, though by no means sufficient, condition for balanced calculations on molecules. A scheme based on atomic SCF calculations defines only a minimal basis, and to

obtain sufficient flexibility for a molecular calculation additional functions will be required. In addition to describing the atoms well, the basis must have the necessary flexibility to account for the deformation that the atoms undergo when a molecule is formed, as discussed in 1.2. For the calculation of molecular properties, the basis must also be able to account for the change of the wave function caused by an external perturbation. We consider first the extension of the basis for molecular SCF calculations to include angular functions unoccupied in the atoms, a topic we have already touched on briefly in 1.2.

The center of a basis function (R_A in Eqs. 8 and 9) is usually chosen to coincide with an atomic nucleus. For calculations on atoms this is a natural choice, but for molecules, where the local environment of an atom has lower than spherical symmetry, this position is not necessarily optimal. Now, it is easily shown that the derivative of a Gaussian with respect to its center is a combination of Gaussians with the same exponent but with higher and lower l values:

$$\frac{\partial \chi(\lambda, \mu, \nu, \alpha)}{\partial X_A} = \lambda \chi(\lambda-1, \mu, \nu, \alpha) - 2\alpha \chi(\lambda+1, \mu, \nu, \alpha). \quad (17)$$

Hence if functions having similar exponents to the valence orbitals, but different l values, are added to the basis, they will be able to describe the effect of displacing the basis functions from the nuclei. A first necessity for an accurate molecular SCF wave function is therefore to add higher angular functions to the basis to describe this "polarization" effect. In addition, as we have already pointed out, a minimal basis of AOs does not have the flexibility to describe the relaxation of the AOs in the molecule, and the basis must also be augmented with additional functions of the same angular type as the occupied AOs to account for this. Since chemical bonding affects only the valence AOs substantially, additional flexibility is required primarily in the valence region. A segmented contraction of the type shown in Fig. 2 commonly has this flexibility imposed on it to avoid excessive duplication of functions. The situation for general contractions is discussed below.

We have pointed out in section 1.3 that the basis set requirements for correlated calculations are even more demanding than for SCF calculations. Functions with the same l value as the occupied AOs, but with more radial nodes, are required to describe atomic radial correlation, while functions with higher l values are required to describe atomic angular correlation [38,39]. We note again that convergence of the correlation energy with basis set size is slow, especially with respect to angular quantum number. The polarization effect described above and dynamical electron correlation are two quite different physical effects, and there is no reason to expect that the basis sets required to account for these effects will be the same. In practice, however, it is found that the requirements on polarization functions are less critical than those on correlation functions, and that the error in the correlation energy due to basis set limitations is much larger than the deviation from the Hartree-Fock limit, at least for practical basis sets. The basis is thus effectively "saturated" with respect to the Hartree-Fock level by the time it is adequate for describing correlation, as we shall see in sections 4 and 5. In schemes where the original contracted basis is determined by atomic SCF calculations, neither polarization nor correlating basis functions are defined by any systematic method, and in some cases these functions are chosen by what is no more than an educated guess.

There are thus several deficiencies in the usual methods of determining exponents and contraction coefficients for atomic basis sets. These are commonly based on atomic SCF calculations, and thus reflect nothing of the requirements for describing electron correlation, nor for augmentation of the basis to describe polarization. Such effects involve angular functions that are not occupied in the SCF atomic ground state, and hence to incorporate them systematically it will be necessary to turn our attention to correlated treatments of the atom.

Making the assumption, as discussed above, that an adequate set of correlating basis functions will also provide the requisite polarization functions, we can restrict ourselves to determining the former. In close analogy with using atomic SCF calculations to determine basis sets for molecular SCF calculations, we may use correlated calculations for atoms to determine basis sets for more sophisticated molecular calculations. This could be done by optimizing a

correlated wave function for an atom with respect to the LCAO coefficients of some primitive Gaussian basis, i.e., an atomic MCSCF treatment [40]. However, since we wish to describe dynamical correlation, a very large external space would be required in these calculations, and the MCSCF configuration space in a large uncontracted basis set would rapidly become prohibitive. Instead, we propose to utilize the convergence properties of ANOs, as discussed in section 2 above. We can perform a CI (or, in principle, a coupled-cluster or perturbation-theoretic) calculation on the atom of interest using a primitive Gaussian basis, and then generate the NOs of this wave function. As we have discussed, the NO occupation numbers provide a sequence for systematic truncation of the NO space, to give a hierarchy of contracted basis sets; each such set will be a proper subset of the larger sets. We also regain our connection with traditional LCAO methods, as the one-particle basis will once again comprise well-defined atomic functions — atomic natural orbitals.

3.3. Primitive Basis Sets

As we have already noted, the calculation of the correlation energy using basis set methods has a higher power dependence on the size of the basis set than integral evaluation or the SCF calculation, and in high-quality calculations of electronic structure the computer time and other resource requirements are dominated by the correlation energy. The time for two-electron integral evaluation, once a major bottleneck, is insignificant by comparison. This dominance of the correlation energy calculation is accentuated as the systems studied and/or the basis sets become larger. As a consequence, the cost of a calculation is largely determined by the size of the contracted basis, and this should thus be kept as small as possible. In contrast, the size of the primitive set only affects the integral time, which usually accounts for a marginal fraction of the cost for a calculation when modern methods for integral evaluation are used. Large primitive sets can therefore be used to allow for as accurate an expansion of the AOs as desired, in order to maximize the quality of the calculation within the

constraints given by the size of the contracted basis. In calculations involving no or low-level correlation (such as second-order perturbation theory), integral time is still of some concern, and basis sets are usually chosen with the economy of integral evaluation in mind. In highly correlated calculations, however, other aspects of the basis become increasingly more important than the size of the primitive set. The most desirable approach is then to ensure that the primitive basis effectively saturates the atomic radial space for each angular momentum included in the basis. A brute-force approach to this problem, taken in many of the applications presented below, is to employ a non-optimized even-tempered expansion for the exponents, simply ensuring that the primitive sets are large enough [33]. Obviously, there ought to be more efficient approaches, and Dunning [28] has recently determined large energy-optimized primitive sets, very useful in their own right and well suited to ANO contraction.

Accurate primitive *sp* basis sets for first-row atoms have been available for some time in the compilation of van Duijneveldt [29]. His large (13s 8p) sets reproduce numerical Hartree-Fock atomic energies to within 0.5 mE_h in the worst case (Ne). These primitive sets are suitable for the generation of ANOs. For even higher accuracy, Partridge has generated sets of size up to (18s 13p) for the first-row atoms [41]. For heavier elements, basis sets of accuracy similar to (13s 8p) for the first row have only recently become available, in work by Partridge [41,42] and by Partridge and Fægri [43]. Of course, before contraction it is necessary to supplement these *sp* sets with polarization functions. For the even-tempered sequences used here the exponents are of the form $\alpha\beta^k$, with $0 \leq k \leq n$. In order to ensure that the angular spaces are saturated, we have used values of n large enough that primitive functions with $k=0$ and $k=n$ make little contribution to the ANOs we retain, although Dunning's recent work [28] indicates that this is an unnecessarily conservative approach. For first- and second-row atoms, the values of α and β are determined as follows. First, we use the formulas

$$\eta_{opt} = 0.02 Z^2 \tag{18}$$

for the first row, and

$$\eta_{opt} = 0.077 Z - 0.69 \quad (19)$$

for the second row, to determine molecular correlation-optimized single Gaussian d exponents η_{opt} for an atom of atomic number Z . These formulas were originally given by Ahlrichs and Taylor [44], from fitting of optimized exponents, and are used to define the geometric mean of the sequence $\alpha\beta^k$ for the d primitive set. β is taken to be 2.5, which is approximately the ratio between successive terms of a high-quality optimized sp basis; α then follows from η_{opt} and n . The geometric mean exponent of a higher angular set is then taken to be $1.2^{l-2}\eta_{opt}$, for whatever l value is desired. This approach was derived from the observation that the optimum (correlation-optimized) single f exponent is approximately 1.2 times that of the optimum d , and similarly for the ratio of g exponent to f exponent [27]. Such qualitative behavior is also observed in the more recent work of Dunning [28].

A similar approach can be taken for heavier atoms: optimizing a single correlating function exponent for the lowest polarization function angular momentum, scaling it by 1.2 for each additional higher unit of angular momentum, and then expanding even-tempered sequences about these “optimized” mean exponents. If the conservative approach to verifying saturation of each angular quantum number is followed, large primitive polarization spaces will be obtained. This will return some of the overall computational burden to the integral evaluation. Many improvements have been made (and continue to be made) in methods for the evaluation of integrals over Gaussian functions, and the reader is referred elsewhere for details [45–47], but some aspects of the computational methodology that are particularly relevant to general contractions and the use of large primitive sets and large polarization spaces are discussed in the Appendix.

3.4. Basis Set Superposition Error

For most chemical applications relative energies are more important than absolute ones, and for any type of bonding it is important that deficiencies that may exist in the description of the fragments are not accidentally removed when the bond is formed. Unfortunately, this is not always the case. Deficiencies in the description of one fragment can be reduced by the presence of basis functions on the other fragment [48,49]. This effect is referred to as basis set superposition error (BSSE) [50]. It is most commonly known as a problem of one-particle basis incompleteness, although there are also effects arising from N -particle space incompleteness [51]. While the common view is that BSSE is dominantly a problem encountered in the calculation of weak intermolecular interactions (because here the BSSE is a substantial fraction of the interaction energy), BSSE pervades the quantum chemical calculation of energy differences. The spurious "improvement" can be minimized by ensuring that the description of the monomer fragments is as good as possible, although practical considerations also mandate keeping the basis sets small. Where the fragments are atoms, we may expect that ANOs will satisfy this criterion better than most basis sets, because the basis set is constructed with an accurate description of the atom in mind. Even so, for the highest accuracy, it is desirable to estimate the BSSE by, for example, a "counterpoise" calculation in which both fragment basis sets are used to describe each fragment [49].

The BSSE is often significant at the SCF level, and this is a situation often discussed in the literature [48,52]. However, a similar situation occurs at the correlated level. The presence of neighboring molecules provides an additional virtual space and increases the effective many-particle basis set for a molecule involved in intermolecular interaction, with a resulting lowering of the energy. For several reasons, the magnitude of this superposition effect in correlated calculations is often more severe than at the SCF level. First, a typical calculation recovers a much greater fraction of the SCF energy than of the correlation energy, leaving more room for improvement in the correlated case. Second, most of the residual energy in an SCF calculation is due to an imperfect description of the

core, which is not easily recovered with orbitals from neighboring molecules. In contrast, the deficiencies in correlation treatment are mostly due to a lack of high angular momentum functions, which can often be approximately modelled by diffuse orbitals from the neighboring atoms. Third, the correlation contribution to intermolecular forces is usually of most interest when weak interactions are considered, a situation where small errors are particularly serious [51]. Finally, the basis functions are usually optimized in SCF calculations for the atoms, and the effect can therefore be very small at the SCF level, but still rather large at the correlated level.

The concept of BSSE also applies to strongly bound systems, that is, to covalent bonds. The mechanism in that case is similar, with the interaction energy overestimated due to an improvement of the atomic description by neighboring atomic orbitals. The net effect of BSSE is to artificially overestimate the intermolecular or interatomic interaction. However, since LCAO basis sets usually lack the flexibility to describe a molecule as accurately as the constituent atoms, calculated bond energies are routinely too small. In that case, BSSE is often seen to bring the results in seemingly better agreement with experiment, and it has been common practice to ignore the effect rather than correcting for it. However, if the aim of a calculation is chemical understanding these effects should not be ignored. Correcting for BSSE, whenever possible, will provide a less uncertain approximation to the solution of the Schrödinger equation, and is likely to contribute more to our chemical understanding.

3.5. Core Correlation

Our discussion so far has been confined to correlation effects involving the valence electrons of a molecule. In general, for chemical binding and for most properties, correlation of the core electrons makes a minor contribution only, although this can be crucial in very accurate calculations (see, for example, Ref. 20). The calculation of correlation effects involving core electrons is very demanding. If core orbitals are not correlated, such as in an SCF calculation, they

can often be represented by only one or two basis functions per orbital, whereas at the correlated level the basis set must be substantially expanded to include higher angular functions with the same radial extent as the core orbitals [53]. Thus very large basis sets, both primitive and contracted, are required to provide an adequate description of core correlation. It is natural to ask whether NOs can provide a route to compact contracted basis sets capable of describing core correlation effects.

Correlation effects involving the $1s$ electrons of first-row atoms are qualitatively different from those of the valence electrons [18]. The $1s^2$ pair correlation energy is essentially constant from Li to Ne, and a simple perturbation theory argument shows that the occupation numbers of core-correlating NOs must therefore decrease as Z increases. The requirement that the NOs form an orthonormal set will then mix core-correlating NOs with weakly occupied valence-correlating NOs, and truncation by occupation number will clearly be unsuitable in that case. If core-correlating NOs are determined separately they can be merged into the valence ANO basis, but this does not necessarily provide orbitals appropriate for describing core-valence inter-shell correlation, which is probably the most important contribution to core correlation effects on spectroscopic constants. Computing core, core-valence and valence ANOs separately leads to large basis sets that suffer from near linear dependencies [54]. Thus it would appear that ANO contractions do not provide a very satisfactory solution to the problem of core correlation, at least for first-row atoms.

For heavier elements, assuming that core correlation involves only the outermost of the core orbitals, the problems are less severe. For example, for a second-row atom the differences in correlating NO occupation numbers between the L and M shells is much less than between the K and L shells for first-row atoms. It is then easier to use ANO contractions to determine contracted basis sets capable of accounting for both core and valence correlation effects [33,55].

not form full sets of partner functions for degenerate representations. For example, the NOs of a CI wave function for a component of the 3P state of carbon atom will comprise mixtures of l values (of the same parity, i.e., sd or pf), and will not display rotational equivalence among the AOs of (nominal) p symmetry, etc. The simplest way to recover the desired atomic symmetry properties is to impose *symmetry and equivalence restrictions* [57] on the density matrix, before diagonalizing to give NOs [58]. This corresponds to projecting the totally symmetric component out of the density matrix. An alternative computational means to the same end is to compute density matrices for *all* components of a degenerate state, and then to average these before diagonalizing. This is much more expensive, however.

Another difficulty not yet addressed arises when constructing an ANO basis set for one-valence-electron atoms like hydrogen or the alkali metals. The use of SCF orbitals provides a possible solution for the core and valence orbitals, but of course cannot provide data for correlation or polarization functions. An alternative, which has the advantage of sampling a molecular environment, is to obtain NOs for the homonuclear diatomic system, such as H_2 , in the primitive basis [33]. The ANOs are then taken from the NO coefficients of, say, the σ_g , π_u , δ_g , etc orbitals. Another alternative would be the use of negative ion NOs, such as those of H^- or Li^- [59]. The former approach is probably the more satisfactory for the alkali metals and for hydrogen in covalent molecules, while the latter might be preferred for hydrogen in ionic hydrides.

It should be noted that the case of hydrogen is somewhat special. It is well known [60] that hydrogen $1s$ functions are not optimum for use in a minimal basis calculation on, for example, H_2 , and that the SCF energy is a minimum for a scaling of the orbital exponents by a factor of about 1.2 in this case. By analogy, Gaussian exponents optimized for hydrogen atom are usually scaled by a factor of 1.2–1.4 when used in molecular calculations. With the molecule-optimized “ANOs” the reverse problem is encountered: the $1s$ function derived from the strongly occupied H_2 σ_g NO is not optimum for H. The “ANOs” derived from H_2 display contraction errors similar (if somewhat smaller) to those in other first-row atoms. Hence a $[3s]$ ANO contraction of van Duijneveldt’s $(8s)$ primitive

4. CONTRACTION ERRORS

As discussed in the previous section, for a given correlation treatment the ultimate accuracy is determined by the initial expansion basis. For almost all current calculations, this means the primitive GTO basis chosen. We define the *contraction error* in a calculated quantity as the difference between the value computed in the primitive basis and in the particular contracted basis. In the context of atomic wave functions and NOs, the contraction error is identical to the truncation error defined in 2.2. In this part of our discussion, we shall concentrate on procedures to reduce the contraction error in our LCAO calculations, using the primitive basis result as our comparison standard. It is *not* appropriate at this stage to compare with experiment — although we shall eventually do that — as there are other sources of error in our calculations that we need to explore. Accurate atomic correlation energies are certainly a necessary, if not a sufficient, condition for accurate molecular correlation energies. Further, if ANOs are to be a useful basis for LCAO expansions, we must establish that the contraction errors converge quickly enough for truncated ANO sets of a practical size to perform acceptably.

4.1. Construction of ANO basis sets

We have already presented details of the contraction error in the correlation energy of neon atom, in 2.2 (Tables 1 and 2). The NOs were obtained from one of the simplest correlation treatments: configuration interaction including all single and double excitations from the Hartree-Fock determinant (usually denoted SDCl). In general, this is how the ANO sets used in the examples here have been generated [33]. The only complication arises for open-shell atoms, or, more specifically, for spatially degenerate atomic states. As discussed in detail by McWeeny and Kutzelnigg [56], or Davidson [24], the NOs of an atom display spherical symmetry only for *S* states. For degenerate states the NOs do not span irreducible representations of the rotation group in three dimensions, and they do

4.2. N₂ spectroscopic constants

Table 3 contains total energies for N₂ (at a bond length of 2.0 a_0) and N atom obtained with an uncontracted (13s 8p 6d 4f) primitive Gaussian basis set and several different ANO contraction schemes [33]. These are all based on SDCI natural orbitals for the ⁴S atomic ground state.

Table 3. N and N₂ total energies and contraction errors^a (E_h)

Basis	N atom	N ₂ molecule
(13s 8p 6d 4f)	-54.400790	-108.995877
	-54.522139	-109.354902
[6s 5p 4d 3f]	0.000007	0.000794
	0.000252	0.001914
[5s 4p 3d 2f]	0.000016	0.001543
	0.000890	0.005017
[4+1s 3+1p 2+1d 1+1f]	0.000009	0.001879
	0.002115	0.008435
[4s 3p 2d 1f]	0.000048	0.003724
	0.003822	0.016937

^a Upper numbers SCF, lower numbers SDCI

The set denoted [4+1s 3+1p 2+1d 1+1f] is derived from the [4s 3p 2d 1f] ANO set, augmented by the outermost primitive Gaussians (uncontracted) of each symmetry type. The atomic SCF energies display almost no contraction error for any of the sets listed, and even for the molecular SCF energies the contraction errors are less than 4 mE_h. The results in the [5s 4p 3d 2f] ANO set are actually somewhat better than our observation for Ne in 2.2 that the contraction error at this level is about 1 kcal/mol per *l* value. For the atomic SDCI energies the contraction errors are also less than 4 mE_h, and for the larger ANO sets the contraction error is even smaller. The contraction errors in the molecular SDCI energies are larger, of course; even in the [6s 5p 4d 3f] ANO set the contraction error is 2 mE_h, rising to 17 mE_h in the [4s 3p 2d 1f] set. Uncontracting the

basis [29] has a contraction error of 0.6 kcal/mol. However, segmented contractions for H, even in scaled primitive sets, commonly have enough flexibility that the contraction error is zero. For H it may be preferable to use either a [4s] ANO set, which has a negligible contraction error [33], or to uncontract the outermost primitive function from the [3s] set. Otherwise H in the molecule may be described better than the free atom.

Another case requiring special attention arises for species such as transition-metal atoms, in which several low-lying states arise from different atomic configurations (such as $d^n s^2$ and $d^{n+1} s$). In general, the orbitals for these different occupations have very different radial extents, so that, for example, ANOs for a $d^n s^2$ state will give a poor description of a $d^{n+1} s$ state. One solution to this problem is to obtain ANOs for an average of the states of interest [61]. As a rule, the errors in atomic separations for the average ANOs are much smaller than the errors associated with using the ANOs of one state for the other. Analogous problems arise for species like the alkaline-earth atoms, where the strong sp near-degeneracy effects require that the definition of the valence shell be extended to include the p orbitals; ANOs can then be generated by, say, averaging the NOs for the ground 1S and excited 1P or 3P state [55,62]. The same situation is encountered again in treating molecules with strong ionic character; for electronegative atoms it is useful to use ANOs averaged for the neutral atom and its negative ion [63]. (The original neutral atom ANOs usually work well for a positive ion.) This technique of using averaged ANOs has been investigated in detail by Widmark *et al.* [64], and is discussed in sections 5 and 6 below.

In general, the contraction errors in the energy for individual atoms follow a very similar pattern to Ne above, although the actual contraction errors are somewhat smaller since Ne has one of the largest valence correlation energies. Rather than list data for a variety of atoms, we shall proceed to the investigation of contraction error in molecular energies and spectroscopic constants.

outermost primitives in this set reduces the error to 9 mE_h, but the results of Table 3 show that this is not as effective a way of reducing contraction error in the energy as adding an additional ANO of each symmetry type.

Table 4 lists spectroscopic constants obtained at the SDCI level for N₂. The r_e and ω_e values were obtained from quadratic fits in r^{-1} to three points around r_e . The “dissociation energies” are simply differences between the N₂ energy at the computed r_e and twice the N atom SDCI energy in the same basis. This approach is not size-consistent, and does not give “ D_e ” values to be meaningfully compared with experiment directly, but they should still be adequate for studies regarding contraction errors.

Table 4. Contraction errors in N₂ spectroscopic constants

Basis	r_e (Å)	ω_e (cm ⁻¹)	“ D_e ” (eV) ^a
(13s 8p 6d 4f)	1.085	2516	8.51
[6s 5p 4d 3f]	1.086	2514	8.48
[5s 4p 3d 2f]	1.086	2513	8.43
[4+1s 3+1p 2+1d 1+1f]	1.087	2512	8.41
[4s 3p 2d 1f]	1.089	2507	8.28

^a See text.

Consider first the r_e values. The two largest ANO sets both agree with the uncontracted result to within 0.001 Å, and even the [4s 3p 2d 1f] set is within 0.004 Å of the uncontracted result. The [4+1s 3+1p 2+1d 1+1f] set gives a bond length contraction error slightly larger than the [5s 4p 3d 2f] ANO set. The harmonic frequencies show a similar pattern of contraction error — the largest ANO sets are in very close agreement with the uncontracted set, but even in the worst case the contraction error is less than 10 cm⁻¹. Finally, the contraction error in D_e varies from 0.03 eV in the largest ANO set to 0.23 eV in the smallest. Due to a partial cancellation of contraction error in the total molecular energy with contraction error in the atom (see Table 3), the contraction error in D_e

is considerably less than that in the total energy. N_2 , with its triple bond and its large correlation contribution to D_e , is one of the more difficult systems to describe accurately. Bearing this in mind, the contraction errors in spectroscopic constants obtained here paint a very encouraging picture.

4.3. H_2O Properties

We now consider calculations on the water molecule [65]. Results for the energy, dipole, and quadrupole moments are listed in Table 5.

Table 5. H_2O properties and contraction errors (a.u.)^a

Basis	Energy	μ_z	Θ_{xx}	Θ_{yy}
(13s 8p 6d 4f/8s 6p 4d)	-76.067080	0.7792	1.7962	-1.8844
	-76.340323	0.7337	1.8019	-1.8762
[5s 4p 3d 2f/4s 3p 2d]	0.000636	0.0085	-0.0246	0.0215
	0.003490	0.0180	-0.0307	0.0283
[4+1s 3+1p 2+1d 2f/ 3+1s 2+1p 2d]	0.000572	0.0002	-0.0032	-0.0001
	0.005150	0.0053	-0.0016	-0.0018
[4s 3p 2d 1f/3s 2p 1d]	0.002508	0.0112	-0.0676	0.0714
	0.014127	0.0196	-0.0878	0.0947
[3+1s 2+1p 2d 1f/2+1s 2p 1d]	0.001252	0.0030	-0.0052	0.0010
	0.023035	0.0018	-0.0038	-0.0015
[3s 2p 1d/2s 1p]	0.008466	0.0371	-0.0750	0.0290
	0.064935	0.0403	-0.1412	0.0986
[5s 4p 3d 2f/4s 3p 2d] segmented	0.005367	0.0029	0.0008	-0.0010
	0.016241	0.0068	0.0032	-0.0017
[4s 3p 2d 1f/3s 2p 1d] segmented	0.058075	0.0299	-0.0002	-0.0079
	0.082060	0.0301	0.0014	-0.0112
[3s 2p 1d/2s 1p] segmented	0.069596	0.0528	-0.1512	0.1217
	0.129705	0.0609	-0.2097	0.1864

^a Upper numbers SCF, lower numbers SDCI

To establish a standard we first compute an SDCl wave function using a (13s 8p 6d 4f) primitive set on O and (8s 6p 4d) on H. We then compare results obtained with this wave function to results obtained with different contractions of this primitive basis. It will usually be convenient to quote the uncontracted results explicitly and then to give contraction errors for the other sets.

We note first that the contraction errors in the SCF and correlation energies are much smaller for ANO basis sets than for segmented contracted sets of the same size, just as we observed for Ne. (The segmented sets were obtained by grouping the innermost functions into one term and leaving the outermost primitives uncontracted. For polarization functions the contraction coefficients are actually from the atomic NOs.) In the largest ANO set, [5s 4p 3d 2f/4s 3p 2d], the contraction error in the SDCl total energy is only 3.5 mE_h, five times less than that of a segmented contracted set of the same size. The contraction error in the energy for the [4s 3p 2d 1f/3s 2p 1d] segmented set is very large: actually larger than for the [3s 2p 1d/2s 1p] ANO contraction.

For the dipole moment of H₂O, somewhat different behaviour is observed. The contraction errors for the [5s 4p 3d 2f/4s 3p 2d] ANO basis set are almost three times larger than for the segmented set, at both the SCF and SDCl levels, and are unacceptably large (over 2% at the SDCl level). We can readily understand this result. The permanent moments of a molecule are determined by the wave function at relatively large distances from the nuclei, and thus to keep the contraction error small it will be necessary to retain the maximum flexibility in this region. Since segmented sets invariably have the outermost primitives uncontracted, this flexibility appears as a by-product of trying to keep contraction errors manageable while using segmented contractions. Conversely, general contractions determined from energy considerations alone, like ANOs, reduce the emphasis on the outermost regions of the wave function, and hence the contraction error in the dipole moment is larger. The apparent superiority of segmented contractions here, however, is strongly dependent on the size of the basis: the [4s 3p 2d 1f/3s 2p 1d] ANO basis shows a *smaller* contraction error in the dipole moment than the segmented set of the same size. The contraction of

one more primitive into the core orbital in this segmented set clearly drastically affects the valence part of the wave function, even though the original primitive set is regarded as triple zeta valence quality [29]. Similar considerations apply to the quadrupole moments, where the results obtained with unmodified ANO basis sets show comparatively large errors.

The smallest dipole moment contraction errors tabulated are obtained with ANO sets in which the outermost primitive functions have been uncontracted. Even the smaller $[3+1s\ 2+1p\ 2d\ 1f/2+1s\ 2p\ 1d]$ set, with the polarization functions fully contracted, shows a negligible contraction error in the dipole moment. This simple approach to increasing the flexibility of the wave function in its outer region is clearly very effective [61,65,66]. We discuss below its application to the dipole polarizability.

A somewhat different perspective on contraction error is obtained by considering the electric field gradient (EFG) at the nuclei in H_2O , values for which are given in Table 6. The contraction errors for the hydrogen EFG are uniformly smaller for the ANO sets than for segmented contracted sets of the same size. For oxygen, the contraction errors are similar for the two contraction schemes, except that the $[4s\ 3p\ 2d\ 1f/3s\ 2p\ 1d]$ ANO set produces an anomalously large contraction error. This is a genuine effect, but its origins are unclear.

Table 6. Contraction error in H_2O electric field gradients (a.u.)^a

Basis	O _{xx}	O _{yy}	H _{xx}	H _{yy}	H _{xz}
(13s 8p 6d 4f/8s 6p 4d)	-1.6200	1.8021	-0.2265	0.2621	-0.3177
	-1.5057	1.6878	-0.2313	0.2658	-0.3234
[5s 4p 3d 2f/4s 3p 2d]	-0.0355	0.0350	-0.0028	0.0035	-0.0039
	-0.0343	0.0342	-0.0031	0.0040	-0.0043
[4+1s 3+1p 2+1d 2f/ 3+1s 2+1p 2d]	-0.0456	0.0577	-0.0025	0.0015	-0.0020
	-0.0420	0.0544	-0.0029	0.0020	-0.0027
[4s 3p 2d 1f/3s 2p 1d]	-0.1415	0.1454	-0.0095	0.0101	-0.0158
	-0.1538	0.1625	-0.0107	0.0114	-0.0178

Table 6 (continued)

Basis	O _{xx}	O _{yy}	H _{xx}	H _{yy}	H _{xz}
[3+1s 2+1p 2d 1f/ 2+1s 2p 1d]	-0.0513 -0.0329	0.0516 0.0317	-0.0075 -0.0097	0.0090 0.0113	-0.0139 -0.0172
[3s 2p 1d/2s 1p]	-0.0792 -0.0680	0.0978 0.0914	-0.0276 -0.0293	0.0371 0.0386	-0.0460 -0.0464
[5s 4p 3d 2f/4s 3p 2d] segmented	-0.0304 -0.0238	0.0292 0.0231	-0.0062 -0.0075	0.0067 0.0081	-0.0110 -0.0131
[4s 3p 2d 1f/3s 2p 1d] segmented	-0.0649 -0.0301	0.0365 -0.0039	-0.0091 -0.0115	0.0095 0.0122	-0.0152 -0.0191
[3s 2p 1d/2s 1p] segmented	-0.0840 -0.0656	0.0679 0.0551	-0.0448 -0.0469	0.0579 0.0602	-0.0766 -0.0782

^a Upper numbers SCF, lower numbers SDCI

Polarizability results for H₂O in different ANO contractions of a (13s 8p 6d/8s 6p) primitive set are given in Table 7. The polarizability is sensitive to the description of the outer regions of the charge density, and is easily seen from perturbation theory to require higher angular functions diffuse enough to polarize the charge density in this region.

Table 7. Contraction error in H₂O dipole moment and polarizability (a.u.)

	Energy	μ	α_{xx}	α_{yy}	α_{zz}
(13s 8p 6d/8s 6p)	-76.065465	0.780	9.17	7.81	8.43
	-76.313308	0.738	9.68	8.69	9.10
[4+1s 3+1p 2+1d/ 3+1s 2+1p]	0.000844	0.000	-0.03	-0.03	-0.05
	0.005416	0.001	-0.06	-0.02	-0.06
[5s 4p 3d/4s 3p]	0.000716	0.008	-0.55	-1.69	-0.80
	0.003103	0.013	-0.75	-2.17	-1.03

As would be expected, the most diffuse primitives must be left uncontracted to achieve the necessary flexibility. In the $[5s\ 4p\ 3d/4s\ 3p]$ ANO set the contraction error in the SDCI dipole moment is 2%, which may be acceptable for some purposes, but the errors in the polarizability tensor components are as large as 20%, which is clearly unacceptable. Replacing the most weakly occupied ANO by the outermost primitive in each shell reduces the contraction error in the polarizabilities to considerably less than 1%, and the contraction error in the dipole moment is insignificant [61,65]. The contraction error in the energy increases when this is done, but this is probably less important in calculations where a good polarizability is the prime concern.

This examination of N_2 and H_2O , while brief, illustrates essentially all aspects of ANO basis performance. A variety of additional molecules and properties are analyzed in greater detail in Refs. 33 and 65, providing further confirmation of the conclusions given above. In summary, we may expect ANO contractions to perform very well in the calculation of total energies, spectroscopic constants, and for properties that do not depend strongly on the outer regions of the wave function. The simple modification of releasing the outermost primitive from the contraction is usually all that is required to eliminate contraction errors in multipole moments and dipole polarizabilities.

5. APPLICATIONS OF ANO BASIS SETS

There have been numerous applications of large-scale correlated calculations using ANO basis sets. Several of these applications have been discussed in illustrative detail in Ref. 20. Here, we shall consider a few specific applications with special features of interest.

5.1. Binding energies

One of the earliest applications of ANO basis sets was in the prediction of the D_e value for the molecule NH by Bauschlicher and Langhoff [67]. These authors used a multireference CI treatment of electron correlation, calibrated against full CI calculations in a relatively small $[5s\ 4p\ 2d\ 1f/4s\ 2p]$ ANO basis. They then employed their MRCI treatment in a very large $[5s\ 4p\ 3d\ 2f\ 1g/4s\ 3p\ 1d]$ ANO basis. By computing also the dissociation energy of CH and OH (again using MRCI wave functions calibrated against full CI), and comparing these values to experiment, they estimated the NH D_e value to be 3.37 ± 0.03 eV. Their value fell exactly between the earlier estimates of Meyer and Rosmus (3.40 eV) [68] and Melius and Binkley (3.35 eV) [69], although their estimated uncertainty encompassed both of these values. At the time, the dissociation energy had not been established experimentally to better than the range 3.29–3.47 eV, three times larger than the theoretical uncertainty. The most recent [70] experimental estimate is 3.40 ± 0.03 eV, which agrees with the theoretical value within the stated uncertainties. Hence experiment and theory for this case appear to agree to considerably better than 1 kcal/mol for the NH binding energy.

A more challenging binding energy calculation is the dissociation energy of the CN radical. In a set of investigations of first-row diatomic binding energies [71,72], elaborate MRCI wave functions in conjunction with large ANO basis sets were shown to yield dissociation energies for C_2 , N_2 , O_2 , and F_2 in error by a maximum of 0.18 eV, and by extrapolating the computed values to account for errors in the correlation treatment and the basis, it appeared to be possible to compute D_e for CN to within 0.1 eV. Since the available experimental values ranged from 7.63 to 8.53 eV [73], an accuracy of 0.1 eV from theory should assist in eliminating some experimental results.

The CN radical is too large to permit meaningful full CI calibrations with realistic one-particle basis sets at present. One approach to estimating the accuracy of the computed D_e , and to extrapolating to the exact value, is then to compare with computed results for C_2 and N_2 . Since there may be problems calibrating an

extrapolation procedure for a heteronuclear diatomic against homonuclear diatomics, it is also advantageous to compare with NO. Finally, since the electron affinity (EA) of CN is very well established experimentally, we can obtain D_e for CN by computing D_e for CN^- , and correcting by the experimental EAs of C and CN. An advantage of this procedure is that CN^- dissociates to C^- and N, both of which have $2s^2 2p^3$ (4S) ground states. The $2s2p$ near-degeneracy in the 3P ground state of C atom, which is almost absent in the CN molecule and which is difficult to describe to the same level of accuracy across the potential curve, is therefore absent.

Table 8 displays computed binding energies for these various diatomic molecules [73], obtained in different ANO basis sets and with multireference CI

Table 8. MRCI+Q D_e values (eV) for CN, CN^- , N_2 , C_2 , and NO.

Molecule	Basis	D_e
CN	[4s 3p 2d 1f]	7.44
	[5s 4p 3d 2f 1g]	7.65
CN^-	[4s 3p 2d 1f] + (1p)	9.95
	[5s 4p 3d 2f 1g] + (1p)	10.19
N_2	[4s 3p 2d 1f]	9.38
	[5s 4p 3d 2f 1g]	9.74
	Expt ^a	9.90
C_2	[4s 3p 2d 1f]	6.02
	[5s 4p 3d 2f 1g]	6.19
	Expt ^b	6.29
NO	[4s 3p 2d 1f]	6.38
	[5s 4p 3d 2f 1g]	6.62
	Expt ^a	6.73

^a Ref 74

^b Ref 75

wave functions (including Davidson's correction for the effects of higher excitations). The MRCI wave functions were based on references selected from a valence-shell CASSCF calculation, at a threshold of 0.01 for CN and C₂, and on CASSCF reference spaces for the other molecules in the table. Discrepancies between experiment and the best computed results are also given. The increase in D_e on going from a [4s 3p 2d 1f] to a [5s 4p 3d 2f 1g] ANO basis is remarkably similar for all species listed (about 0.2 eV) except N₂, for which the effect is considerably larger. The discrepancy with experiment in the larger basis is 0.12 eV in NO, 0.16 eV in N₂, and 0.10 eV in C₂.

Bauschlicher and co-workers used two different formulas for extrapolating the computed data to the basis set limit [73]; these give 7.74 and 7.78 eV by extrapolating using the CN data, and 7.75 and 7.81 by extrapolating using the CN⁻ data. They recommended a value of 7.78±0.06 eV, with an estimated confidence of 80% based on their basis set and correlation methodology studies. To within a 99% confidence limit D_e was asserted to be 7.78±0.10 eV. As noted above, experimental results range from 7.63 to 8.53 eV, although Arnold and Nicholls [76] suggested the true value should lie between 7.9 and 8.1 eV, consistent with most of the data available at that time, as well as their own experimental estimate of 8.02±0.13 eV. Such a value is considerably outside the estimate of Bauschlicher and co-workers. A more recent experimental study by Engleman and Rouse [77] gives 7.78±0.05 eV, in much better agreement with the theoretical number. Further, use of the oscillator strengths for the CN red system, calculated by Bauschlicher and co-workers, in the analysis of solar spectra by Lambert [78] suggests a D_e value of 7.82±0.05 eV. Thus recent experimental evidence supports the current theoretical value for the dissociation energy of CN.

Many studies, in addition to the two discussed explicitly above, have stressed the severe basis set requirements for computing accurate binding energies; see, for example, Refs. 27 and 79. Recently, Almlöf and co-workers have investigated the convergence of the N₂ D_e value with basis set [80], focussing particularly on the contribution from high angular momentum basis functions. A selection of their results is displayed in Table 9. These were

obtained with MRCI wave functions in which all occupations from a six-electron, six active orbital CASSCF calculation were used as references.

Table 9. MRCI D_e values (kcal/mol) for N_2 .

Basis	D_e
(13s 8p 6d 4f 2g) primitive set	
[4s 3p 2d 1f]	216.0
[5s 4p 3d 2f]	219.6
[6s 5p 4d 3f]	220.8
[6s 5p 4d 3f] + (1s 1p)	221.0
[5s 4p 3d 2f 1g]	222.1
[6s 5p 4d 3f 2g]	223.6
(18s 13p 6d 5f 4g 3h 2i) primitive set	
[6s 5p 4d 3f 2g]	223.7
[6s 5p 4d 3f 2g 1h]	224.5
[6s 5p 4d 3f 2g 2h 1i]	225.0

The rather slow convergence of binding energy with basis set angular momentum is well illustrated by these results. Functions of h type contribute something more than 1 kcal/mol, the common definition of thermochemical accuracy, but it appears that i and higher angular types together will contribute no more than half this. Diffuse s and p functions make very little contribution. The expansion of the spd or $spdf$ contractions from [5s 4p 3d 2f] to [6s 5p 4d 3f] affects the binding energy by more than 1 kcal/mol, but the results of section 4.2 suggest that further expansion of the contracted set will hardly change the result.

It is not really appropriate to compare the best result from Table 9, 225.0 kcal/mol, with the experimental value of 228.4. As discussed in Ref. 80, the MRCI result is not size-consistent, and inclusion of the multireference Davidson correction increases the computed D_e value by about 0.5 kcal/mol.

Further, core correlation (mainly core-valence correlation) increases D_e , by about 0.7 kcal/mol in Refs. 79 and 80. Additional basis set expansion was estimated in Ref. 80 to increase by no more than 1 kcal/mol, although it should be noted that even the largest basis used in that work suffers from BSSE of about 0.3 kcal/mol, so this basis set extension effect might be an overestimate. Adding all these contributions and subtracting a counterpoise correction for BSSE gives a “theoretical” D_e value of some 226.8 kcal/mol, or about 1.6 kcal/mol smaller than experiment — somewhat outside chemical accuracy, but a relative accuracy of considerably better than 1%. Very recently, Werner and Knowles have performed an additional series of basis set investigations on the binding energy of N_2 [81]. They obtain 228.1 kcal/mol, in even better agreement with experiment. Their core correlation contribution is considerably larger than that computed in Refs. 79 and 80 and their correlation treatment gives a somewhat larger binding energy than that obtained by Almlöf and co-workers [80]. The differences due to the (valence) basis set used are very small.

5.2. Dipole moments

In many applications of electronic structure theory, it is important to have a balanced description of the different parts of the molecule, rather than a calculation that is independently optimum at any one point. This is especially true for the calculation of reliable electric moments. A balanced description of the different parts of the molecule is imperative to get the right polarity. Based on both variational and perturbational arguments it can be shown that a local improvement of the wave function will increase the electron density in that region of space. This applies to the addition of both one-particle basis functions and reference configurations. Improvement of the basis set on one atom in a molecule will therefore affect the polarity of the system, and, consequently, if one atom in a molecule has a better basis set than the others the calculation of a dipole moment will be biased. An approach in the ANO spirit, which optimizes the atomic description is therefore likely to perform very well in this context. Further, the

incremental improvement of the ANO basis by successive addition of new functions without altering the previous set is likely to yield a stable description, as well as a test of the convergence of the basis set expansion.

Calculations of the dipole moment for the $^2\Sigma^+$ ground state of the diatomic molecule CP will be discussed as one example of such an approach [82]. A primitive basis set of size (18s 13p 6d 4f 2g/13s 8p 6d 4f 2g) was used, contracted according to three different schemes that are shown in Table 10, together with total energies and dipole moments.

Table 10. CP total energy and dipole moment^a

Basis	Energy (E_h)	μ (a.u.)
[5s 4p 2d 1f/4s 3p 2d 1f]	-378.481947	0.3059
	-378.746669	0.3559
[5+1s 4+1p 3d 2f/4+1s 3+1p 3d 2f]	-378.482821	0.3128
	-378.752308	0.3629
[5+1s 4+1p 3d 2f 1g/4+1s 3+1p 3d 2f 1g]	-378.483264	0.3129
	-378.758078	0.3599

^a Upper numbers SCF, lower numbers SDCI. Bond length 2.9517 a_0

The energy improvements obtained on enlarging the contracted basis are negligible at the SCF level, but several mE_h at the SDCI level. The dipole moment is more affected: uncontracting the outermost *s* and *p* primitives increases the SCF and SDCI dipole moments by 0.007 a.u., while the further addition of a *g* ANO has no effect on the SCF dipole moment but decreases the SDCI result by 0.003 a.u. The similarity of the dipole moment results of Table 10 suggests that this quantity is essentially converged with respect to further extensions of the one-particle basis. Further, the SDCI dipole moment was computed both as an expectation value and as an energy derivative with respect to an applied electric field and excellent agreement between the two methods was obtained (a difference of less than 0.001 a.u. in the largest contracted basis). While these two approaches are

not equivalent for truncated CI [83], even in a complete basis, experience shows that they do not differ significantly for SDCI wave functions unless the one-particle basis is deficient or non-dynamical correlation effects are important.

In order to improve the accuracy of their dipole moment prediction, Rohlfing and Almlöf [82] employed the $[5+1s\ 4+1p\ 3d\ 2f/4+1s\ 3+1p\ 3d\ 2f]$ basis in a succession of MRCI calculations. They found it necessary to include the phosphorus $3d_\pi$ orbitals in the reference space for the MRCI, and the $3d_\sigma$ orbitals were almost as strongly occupied. Similar effects have been previously observed in calculations on CCl and ClF [31] — it is clearly crucial to have an adequate d basis when effects like these are important, and ANOs can satisfy this requirement very compactly. The most elaborate calculation of the dipole moment in Ref. 82 gave a value of 0.351 a.u., which can be assumed to be at least 0.003 a.u. too large because of the omission of the g ANOs. By considering a sequence of MRCI selection thresholds Rohlfing and Almlöf inferred that reference selection led to overestimating μ by another 0.003 a.u., leading to a predicted CP dipole moment of 0.34 ± 0.005 a.u. after an estimate for core-valence correlation effects.

5.3. The bond distance in CH₄

The CH bond length in methane has been a contentious issue in quantum chemistry. The first accurate, correlated determination of this quantity was the work of Meyer [84], at the pair-natural orbital (PNO) CI and CEPA level using an extended basis. He obtained a bond length of 1.091 Å, 0.005 Å longer than the experimental estimate at that time. This was a larger discrepancy than would have been expected at this level of treatment, and Meyer suggested it might originate from an overestimation of the cubic anharmonicity of the CH stretch in the experimental analysis [85]. However, later theoretical work [86] and reanalysis of experiment [87] showed that although the anharmonicity had indeed been overestimated, this had almost no consequence for the bond length. Further experiments and refined analyses (including both *ab initio* and experimental force

field data) [88] confirmed a bond length of 1.086 ± 0.001 Å, and it was hypothesized that the source of the discrepancy between the best theoretical value and experiment must be a deficiency in the calculations, either in the basis set or correlation treatment. Several subsequent theoretical studies were performed, including a very detailed investigation by Siegbahn [89], but apart from indicating that core-valence correlation reduced the computed bond length by between 0.001 and 0.002 Å, the results of the calculations were little different from Meyer's. Handy and co-workers [90] investigated very large basis sets at the MP2 level and pointed out a significant basis set issue: *p* functions on H with high exponents (larger than 1.0) were required to obtain an MP2 geometry close to the basis set limit. In view of this finding it appeared desirable to perform a systematic investigation of basis set extension at a suitable high level of correlation treatment, and Bowen-Jenkins *et al.* [91] therefore re-examined the CH₄ bond length using successively larger ANO basis sets at the MRCI and CPF levels.

Bowen-Jenkins *et al.* used a primitive (14s 9p 6d 3f 2g) Gaussian expansion basis on carbon and an (8s 6p 3d) set on hydrogen [91]. These expansion basis sets were contracted using ANOs for the ⁵S state of C and NOs from H₂ (as described above). The final basis sets were of the form [4+1s 3+1p 3d 2f 1g/ 4s 3p 1d] and [5s 3p 2d 1f/4s 3p]. Optimized bond lengths using these basis sets and a variety of correlation treatments are given in Table 11. At the (externally contracted) MRCI level, these basis sets gave bond lengths of 1.088 Å and 1.089 Å, respectively, compared with 1.090 Å obtained earlier by Siegbahn [89] from a segmented [9s 5p 4d 1f/4s 2p 1d] set and the same correlation treatment. After correction for core-valence correlation effects, a result of slightly over 1.086 Å was obtained, in perfect agreement with experiment [88]. Using the same ANO basis sets in CPF (and MCPF) calculations gave essentially the same results.

Table 11. CH₄ bond lengths (Å)

Method	Basis	r_e
CCI	[5s 3p 2d 1f/4s 3p]	1.089
	[4+1s 3+1p 3d 2f 1g/4s 3p 1d]	1.088
	[9s 5p 4d 1f/4s 2p 1d]	1.090
+ CV ^a		1.089
CCI+Q	[5s 3p 2d 1f/4s 3p]	1.090
	[4+1s 3+1p 3d 2f 1g/4s 3p 1d]	1.089
	[9s 5p 4d 1f/4s 2p 1d]	1.091
+ CV ^a		1.090
CPF	[5s 3p 2d 1f/4s 3p]	1.088
	+ CV ^a	1.087
CPF	[4+1s 3+1p 3d 2f 1g/4s 3p 1d]	1.087
	+ CV ^a	1.086
PNO-CEPA ^b	[8s 5p 2d 1f/4s 2p]	1.091
SDCI	[5s 3p 2d 1f/4s 3p]	1.085
SDCI+Q	[5s 3p 2d 1f/4s 3p]	1.089
MP2 ^c	[8s 6p 3d 1f/6s 3p]	1.083
Expt ^d		1.086±0.001

^a Core valence correction from Ref. 89^b Ref. 84^c Ref. 90^d Ref. 88

Investigation of BSSE showed that it affected the computed bond length by no more than 0.0005 Å. Studies involving a systematic reduction of the ANO basis by successively deleting functions (see Table 12) established convergence of the bond length with respect to the one-particle space to within about 0.0005 Å [91].

Table 12. Basis set dependence of CH₄ MCPF bond lengths (Å)

Basis	r_e
[5s 3p 2d 1f/4s 3p]	1.088
[4+1s 3+1p 3d 2f 1g/4s 3p 1d]	1.087
[4+1s 3+1p 2d 1f/3s 2p 1d]	1.089
[4+1s 3+1p 2d/3s 2p 1d]	1.088
[4+1s 3+1p 2d/3s 2p]	1.088
[4+1s 3+1p 1d/3s 2p]	1.088
[4+1s 3+1p 1d/3s 1p]	1.093

These basis set investigations also showed that deleting (from the smaller ANO set) the *f* ANO and the second *d* ANO on carbon or the *d* from hydrogen affected the computed bond length by less than 0.001 Å, but deleting the second *p* ANO from hydrogen lengthened the bond by 0.004 Å. This observation supports the contention of Handy and co-workers [90] that the earlier studies used basis sets with deficiencies in the hydrogen *p* space, although the source of this deficiency in Siegbahn's largest set [89] is unclear. Hence these results resolve the discrepancy between theory and experiment: earlier calculations, even in large CGTO basis sets, suffered from lack of basis set saturation. The ANO sets used by Bowen-Jenkins *et al.* [91] perform well in allowing for basis set saturation without the basis set size becoming unmanageable.

5.4. Ne atom polarizabilities

We have already referred to the problems associated with computing properties such as polarizabilities, which are very sensitive to the description of the outer valence charge distribution, if AO sets obtained by energy optimization are used. Segmented contraction of large primitive sets has usually involved leaving most of the outer primitive GTOs uncontracted, as otherwise there is an

unacceptable loss of energy. This was shown in 4.3 for H_2O , and is discussed in more detail in Refs. 65 and 66. When using general contractions (not only ANO sets) one approach, as we have described at length, is to uncontract the outermost primitive GTOs; Widmark *et al.* [64] suggest the somewhat more elegant alternative of determining the ANOs from a calculation in which a field has been applied. Either of these techniques works well for dipole moments and dipole polarizabilities. However, for higher polarizabilities the results become progressively more dependent on the outer reaches of the valence charge density. Since an energy-optimized primitive GTO expansion basis does not include exponents that sample these outer regions, no contraction scheme will be able to produce useful results. We shall explore here the requirements for extending a high-quality ANO basis set to predict higher polarizabilities for the neon atom, using results from the recent study by Taylor *et al.* [92].

Some information on augmentation of energy-optimized basis sets can be obtained by considering the functional form of the applied perturbation and the energy derivative to which the property corresponds, as discussed briefly in 3.2 above. It is obvious, for example, that at the SCF level a dipole perturbation (a static homogeneous electric field) will couple to one higher unit of angular momentum than is required in the unperturbed wave function. Further, as the resulting new basis function is required to polarize the outer valence charge density, it will be relatively diffuse. Similarly, a quadrupole perturbation (a static electric field gradient) will couple to two higher units of angular momentum. Hence we see the well-documented requirement (see, for example, Ref. 93 and references therein) for rather diffuse *d* functions for dipole polarizabilities and *f* functions for quadrupole polarizabilities in first-row atoms, for example. The static dipole hyperpolarizability of an atom is a fourth derivative of the energy, so for first-row atoms it must be expected that diffuse *f* functions will be required. In addition, as the order of the perturbation increases, the contribution to the perturbed energies of the outer regions of the charge density increases. Hence it may also be necessary to augment the *sp* basis with diffuse functions. Finally, we reiterate that this analysis corresponds to the SCF case. Since correlation generates (small) populations in the higher angular functions, it is possible that in

correlated studies diffuse functions of even higher angular types will have to be included.

The perturbed energy of a closed-shell atom in a homogeneous field F and field gradient F' is

$$E(F, F') = E_0 - \frac{1}{2}\alpha F^2 - \frac{1}{24}\gamma F^4 - \frac{1}{4}BF^2F' - \frac{1}{4}CF'^2 \quad (20)$$

which defines the dipole polarizability (α) and hyperpolarizability (γ), the dipole-dipole-quadrupole hyperpolarizability (B), and quadrupole polarizability (C) [94]. Table 13 displays these polarizabilities for Ne at the SCF level [92].

Table 13. Ne SCF polarizabilities (a.u)

Basis	α	γ	B	C
A ^a	2.15	17.5	-5.92	2.28
A + (1s 1p)	2.34	49.2	-10.10	2.34
A + (2s 2p 1d)	2.34	56.3	-10.55	2.35
A + (2s 2p 1d 1f)	2.34	66.9	-12.87	3.10
A + (2s 2p 1d 2f)	2.34	70.2	-13.33	3.20
A + (3s 3p 2d 3f)	2.34	71.9	-13.39	3.20
A + (3s 3p 2d 3f 2g)	2.34	72.2	-13.42	3.20
A + (3s 3p 2d 3f 2g 1h)	2.34	72.2	-13.42	3.20
A + (3s 3p 2d 3f 3g) ^c	2.34	72.2	-13.42	3.20
B ^b + (3s 3p 2d 3f)	2.34	72.2	-13.38	3.20
C ^d + (3s 3p 2d 3f)	2.38	71.2	-13.25	3.21

^a Basis A: [4+1s 3+1p 2+1d 1+1f].

^b Basis B: [4+1+1s 3+1+1p 2+1d 1+1f].

^c Includes a tighter, correlation-optimum g function

^d Basis C: [4+1+1s 3+1+1p 2+1+1d 1+1f].

The main source of error in α from the modified ANO contraction (denoted A) is the omission of diffuse s and p functions, which affects α by about 10%. Uncontracting the second outermost d as well as the first increases α by 2%, and this result is now at the Hartree-Fock limit. Convergence of the SCF value for γ is clearly much slower. The value does not begin to stabilize until at least two diffuse s , p , and f functions and a diffuse d function are added. The reason more diffuse f functions than d functions are required reflects the original primitive set, which has 6 d functions, but only 4 f functions whose mean exponent is tighter than the mean d exponent. Hence uncontracting the outermost f primitive is less effective at describing field polarization than is uncontracting the outermost d . Uncontracting the second outermost d function has less effect on γ than on α , consistent with our reasoning above. The polarizabilities that involve field gradient perturbations show similar basis set convergence behaviour to γ .

For accurate values of polarizabilities it has long been established that correlation effects must be included. In Table 14 we list values for the various polarizabilities in a succession of ANO-derived basis sets [92], using the coupled-cluster method with single and double excitations (CCSD). The basis set convergence of α follows a very similar trend to the SCF level, although where basis set extension affects the results the changes are somewhat larger. We may note that the addition of more diffuse f functions has almost no effect on α , nor does the addition of diffuse g (or h) functions. A tighter g function increases the correlation energy but does not affect α . Overall, correlation increases α by about 10% at the CCSD level, and this is essentially independent of basis set size.

The convergence of γ with basis set at the CCSD level is again much slower than for α . This results partly from the very large correlation contribution — almost 40% — which converges even more slowly than the SCF value. Not until a (3s 3p 2d 3f) diffuse set has been added has the CCSD value of γ stabilized to within 1%.

Table 14. Ne CCSD polarizabilities (a.u)

Basis	α	γ	B	C
A ^a	2.35	22.4	-6.95	2.49
A + (1s 1p)	2.60	68.7	-12.59	2.59
A + (2s 2p 1d)	2.60	83.8	-13.51	2.60
A + (2s 2p 1d 1f)	2.60	97.2	-16.56	3.52
A + (2s 2p 1d 2f)	2.60	103.1	-17.32	3.67
A + (3s 3p 2d 3f)	2.61	107.3	-17.46	3.67
A + (3s 3p 2d 3f 2g)	2.61	108.1	-17.54	3.68
A + (3s 3p 2d 3f 2g 1h)	2.61	108.2	-17.55	3.68
A + (3s 3p 2d 3f 3g) ^c	2.61	107.5	-17.48	3.67
B ^b + (3s 3p 2d 3f)	2.61	109.9	-17.43	3.67
C ^d + (3s 3p 2d 3f)	2.64	108.7	-17.27	3.68

^a Basis A: [4+1s 3+1p 2+1d 1+1f].

^b Basis B: [4+1+1s 3+1+1p 2+1d 1+1f].

^c Includes a tighter, correlation-optimum *g* function

^d Basis C: [4+1+1s 3+1+1p 2+1+1d 1+1f].

The effect of diffuse *g* functions is not quite negligible (just under 1%), but a diffuse *h* function makes almost no contribution. This is also observed for the polarizabilities *B* and *C*, for which convergence with basis set is again similar to the SCF level.

The overall conclusions about the basis set dependence of correlated polarizabilities for Ne are a little surprising: the *diffuse* functions that must be added can be determined entirely at the SCF level. The inclusion of correlation does not appear to require any further extension of the diffuse functions, although *g* functions are almost important enough to be needed. Further, while the CCSD method itself yields polarizabilities that are not quite converged with respect to the correlation treatment (especially for γ), correcting the results for the effect of triple excitations appears to yield converged results, and the basis set conclusions still

hold [92]. Investigations of Be atom and of the other rare-gas atoms [95] indicate that these basis set conclusions are valid for other atoms as well. It will certainly be of interest to see whether they hold for molecules. It is clear that substantial computational economy results from “decoupling” the determination of the field response and correlation requirements of the basis set .

5.5. Ni(H₂O)

The ability of ANO basis sets to reduce basis set superposition error substantially, as well as to describe molecular properties accurately, has been exploited by Bauschlicher [61] in computing the interaction between a nickel atom and a water molecule. The interaction energy had previously been computed by a number of groups, with conflicting results [96-98]. Early calculations predicted quite large Ni-H₂O binding energies [96,97], but after correction for BSSE the binding was estimated to be around 3 kcal/mol (see discussion in Ref. 61), arising mainly from dipole-induced dipole interaction. However, experimental studies of transition metal-H₂O interaction [99] suggested that (unlike other late transition metals), Ni does *not* form a stable complex with H₂O, in contradiction to the theoretical results. Yet another conclusion was reached in calculations by Sauer *et al.* [100]: they obtained no Ni-H₂O binding at all in BSSE-corrected SCF calculations, but almost 11 kcal/mol in SDCI calculations (corrected only for the SCF BSSE). Their interpretation was that the metal-ligand binding therefore arose from dispersion, rather than electrostatic, interactions [100].

In order to try to resolve whether Ni binds to H₂O, and by what mechanism, CI calculations in a large basis set were undertaken by Bauschlicher [61]. The primitive Ni basis was the (20s 12p 9d) set of Partridge [41], augmented with three diffuse *p* functions to describe the Ni 4*p* orbital, and a diffuse *d* function to describe the contribution of the Ni 3d⁹4s configuration to the wave function properly. Six *f* primitives were added for polarization and correlation. This final (20s 15p 10d 6f) primitive set was contracted using SDCI ANOs averaged for the 3d⁸4s² (^{3F}) and 3d⁹4s (^{3D})

states. In order to improve the description of the Ni polarizability the outermost *s* and *p* primitives were uncontracted, giving a final contracted basis of the form [6+1*s* 5+1*p* 4*d* 3*f*]. For water, a basis similar to those discussed in 4.3 above was used, based on van Duijneveldt's primitive sets [29] and contracted to [5*s* 4*p* 3+1*d* 2*f*/4*s* 3*p*] + (1*s* 1*p*/) (that is, diffuse functions added to O only). At the SDCI+Q level the H₂O dipole moment was within two percent of experiment, while the *zz* component of the polarizability was about 7% smaller than experiment. The error in the Ni polarizability was estimated to be about 10%.

Computed binding energies for the Ni–H₂O complex [61] are given in Table 15.

Table 15. Ni–H₂O binding energies (kcal/mol).

Method	D_e	$D_e(\text{corrected})^a$
SCF	2.86	2.82
SDCI	4.84	4.36
SDCI+Q	5.30	4.75

^a Corrected for BSSE.

The SCF BSSE is seen to be almost zero, while at the correlated level the BSSE is about 0.5 kcal/mol. Explicit calculations show that about two-thirds of the BSSE arises from improvement in the Ni energy produced by the H₂O basis. Comparison of the BSSE-corrected SCF and SDCI+Q results shows that dispersion is responsible for less than 50% of the binding energy, and although the dispersion contribution would increase with improvements in the calculation it is unlikely to be more than 50% even in the limit of a complete CI. The contention of Sauer *et al.* [100] that at the SCF level the complex is unbound is not substantiated — the basis set of Ref. 100 is too small to describe the interaction correctly even at the SCF level. On the other hand, the CI result in that basis is much too large when corrected using only the SCF BSSE: CI superposition errors

can be an order of magnitude or more larger than SCF superposition errors, so using the latter only as a correction will severely overestimate the degree of binding. Bauschlicher's SCF result [61] is consistent with the earlier, smaller basis set studies, and it seems reasonable to assume that his correlated result, after BSSE correction, is a lower bound to the binding energy. Thus the various theoretical results can be understood in the light of the large basis investigations, although it is still unclear why the Ni-H₂O complex is not observed in matrix isolation experiments.

The use of a very large expansion basis is crucial to the success of this sort of investigation. While the counterpoise correction [49] for BSSE has been shown to be a physically reasonable and numerically reliable approach, it works best when the correction is small, as with any correction method. The only safe way to obtain small BSSEs is to use large basis sets, and these can be handled compactly via ANO contractions. As we discussed in 3.4, in general we recommend the use of counterpoise corrections even for strong interactions such as chemical bonding, although the situation here is more open to debate than for weak interactions such as van der Waals systems.

6. ALTERNATIVE APPROACHES

While the ANO contracted sets we have discussed are certainly no larger (and are commonly smaller) than more conventional CGTO sets of similar quality, the primitive sets from which they are obtained are larger than many others commonly used. As we have explained at some length in section 3, this has less consequence from the point of view of computation time than might be imagined, at least when an efficient integral evaluation scheme is used. Nevertheless, there is obviously much to be gained if the Gaussian expansion basis used to represent the AOs can be made smaller without materially affecting the results. On the one hand, the investigations of Ahlrichs and co-workers [27,79] give no ground for

optimism about this possibility, as we have discussed above. Dunning [28], however, has explored the use of carefully optimized primitive sets and reached much less pessimistic conclusions. By augmenting generally contracted sp sets for first-row atoms with additional uncontracted s , p and polarization functions whose exponents are optimized in atomic CI calculations, Dunning has obtained atomic energies as good as ANO sets of the same size. When these sets are used in molecular calculations, they also yield very good results [28,81,101]. While they do require augmentation for the calculation of some molecular properties [101], this is not really different from modification of ANO contraction schemes as discussed above. A very promising possibility is that optimization of polarization function exponents can reduce the size of the GTO expansions used for ANOs. It is also interesting to note that the optimized polarization exponents of Dunning are not radically different from those obtained from the formulas of Ahlrichs and Taylor [44] and the scaling relations for multiple primitives used in 3.3.

Another alternative, one we have already discussed in the context of representing AOs by Gaussian expansions, is to obtain the contraction coefficients not from natural orbitals (which could be regarded as a "maximum overlap" criterion for reducing the contraction error) but from energy optimization. For systems dominated by a single reference configuration, the AOs so obtained can be expected to be very similar to the ANOs. One advantage of using NOs is that virtually all CI codes produce natural orbitals as a normal by-product of the calculation, while the energy optimization requires an MCSCF calculation for a configuration space of SDCI type. Codes to perform this optimization are much less common than codes that yield CI NOs. The recent developments of restricted active space (RAS) CI methods [102,103], in which wave functions are defined by allocating electrons to different orbital spaces according to desired occupation number restrictions, and their extension to MCSCF orbital optimization in RASSCF methods, should allow a wider investigation of energy optimized contractions as opposed to ANO contractions. It would be useful if a scheme for including core correlation could be devised along these lines; a brute-force inclusion of the core orbitals into the RAS CI expansion will probably not do, as

the total correlation energy benefits so much more from core correlation than valence correlation that the RASSCF orbitals will be heavily biased in favour of core correlation.

Other variations on the ANO approach have been examined. Shavitt and co-workers [104] have constructed contracted sets that comprise the occupied SCF AOs, and correlating NOs obtained by performing, say, an SDCI calculation and then diagonalizing the first-order reduced density matrix projected into the unoccupied SCF AO space. In this way the AOs expected to contribute most to the molecular wave function are the original SCF AOs. For most purposes this is an unimportant distinction — the main benefit is that the AO set used for a given atom reproduces the original atomic SCF energy exactly with a minimal set. The resulting basis sets perform just as well as the true ANO sets in molecular applications. As we noted briefly above, Widmark *et al.* [64] have extended the scope of the calculations that define the ANOs. They include other electronic states (possibly including ionic states), and the ground state perturbed by an electric field, in a density matrix averaging procedure. This provides a compromise set of ANOs that should be able to describe the atom even in an ionic molecule, and also yields a better description of molecular properties like the dipole moment and polarizability, as we touched on in 4.3. This appears to be a very promising extension to techniques for generating ANO basis sets.

A somewhat different approach to using contracted basis sets that describe atomic correlation well in molecular calculations has been explored in considerable detail by Petersson and co-workers [105–107]. They use *pair-natural orbitals* (PNOs) of the atoms, rather than natural orbitals. PNOs are closely related to NOs for two-electron systems, and share the unique convergence properties of the latter [26]. Petersson and co-workers have exploited these convergence properties to develop sophisticated schemes for extrapolating computed molecular correlation energies to basis set limit values, with accompanying uncertainty estimates [106]. Hence the PNOs are used not only to provide a physically motivated AO basis for molecular calculations, but also to guide estimation of the “complete basis set” (CBS) correlation energies, as they

are termed by Petersson and co-workers. The extrapolation technique has been used to compute binding energies to high accuracy, for example [107].

All of the alternative approaches we have discussed so far have been concerned with modifications or improvements to “physical” LCAO schemes; that is, those which seek to perform a molecular calculation in a basis that has a clear connection to a physically illustrative description of the atom. There have been attempts to extend the more *ad hoc* traditional contraction schemes to incorporate correlation, without any special attention to physical interpretability. For example, correlation-optimized primitive exponents have been generated in atomic MP2 calculations by Krishnan *et al.* [108], and form the backbone of the larger basis sets used in calculations with the GAUSSIAN series of programs. There has been a number of attempts to exploit bond-centered sets rather than atom-centered polarization functions. There are several difficulties with such approaches, although by far the most important is the issue of superposition error, which has been discussed by several authors; see, for example, Ref. 109 and references therein — Ref. 110 describes a more recent investigation. Perhaps the least aesthetically appealing aspect of bond functions is that considerable evidence has accumulated since the earliest days of *ab initio* quantum chemistry that a major source of error in molecular calculations is the inability to describe correlation in the dissociated atom limit correctly [111], and it does seem more than plausible that atomic problems should be solvable within a one-center model. The spectacular successes of empirical correction schemes of “atoms-in-molecules” type [112] (see also Refs. 113 and 114 for more recent work) attest to the vital role atomic correlation and its correct description plays in molecules, as for that matter does the success of ANO basis sets.

Finally, it is always possible to define prescriptions (for correlation treatments as well as basis sets) for successful “prediction” of specific properties by exploiting cancellation of errors. For example, while we have sought to compute reliable binding energies by reducing the errors in both fragments and the bound system as much as possible, one can proceed by trying only to find a level that is equally inadequate for both limits. While some of the dangers in this procedure are obvious, it must be stressed that the primary problem is one of

predictive reliability. This question of predictive reliability also has consequences for error analysis in quantum chemistry: the *mean* deviation of a set of comparisons between computed and experimental data is one test of reliability, but it may be less useful than the *maximum* deviation. By analogy with a numerical analyst trying to write an accurate sine function routine, we must be interested in minimizing the maximum error, not in the less challenging and less interesting minimization of least-squares error, if we are to make reliable predictions.

7. CONCLUSIONS

We have reviewed here an approach to basis set design that is driven by the desire to use physically motivated atomic orbitals as basis functions for molecular calculations. The fact that the AOs are expanded as fixed contractions of Gaussian functions is a physically irrelevant computational device. For correlated calculations the natural orbitals derived from correlated atomic wave functions prove to be a compact, computationally efficient, and physically meaningful set of basis functions. The efficient evaluation of AO integrals over such basis sets imposes certain computational requirements on an integral code; we discuss in the Appendix how these requirements are implemented in evaluation of two-electron integrals over a generally contracted Gaussian basis set in the MOLECULE integral program [115]. We have shown how ANO basis sets are effectively able to exhaust the capabilities of the underlying Gaussian expansion basis — that is, to minimize the contraction error. Finally, we have enumerated several applications of quantum chemistry to problems in which the use of ANO basis sets has been instrumental in obtaining the required high accuracy.

APPENDIX: COMPUTATIONAL CONSIDERATIONS

A.1. Implementation of general contraction

Most techniques for Gaussian integral evaluation are designed for segmented contractions: since each integral over primitive functions contributes to only one integral over contracted functions there are various mechanisms for incorporating part of the segmented contraction process into the primitive integral evaluation. For an average “contraction ratio” $N_{prim}/N_{cont} = k$, the expected k^4 dependence of integral evaluation can be sharply reduced, for example [47]. We make no attempt here to discuss general aspects of Gaussian integral evaluation, nor to discuss segmented contractions, but concentrate instead on specific computational issues that arise when using general contractions, large primitive spaces, and high angular quantum number basis functions. We will assume that the usual efficiencies obtained by treating all members of a shell with the same angular quantum number together, and evaluating integrals using vector loops over exponent quadruplets, are already being exploited [45].

In terms of arithmetic operations, the computational overhead associated with performing a general contraction is not insignificant. Given the same average contraction ratio $N_{prim}/N_{cont} = k$, the number of operations needed per contracted integral is of the order of $2N_{prim}(k^4-1)/(k-1)$. This is usually significantly larger than in the segmented scheme, where it is only $2k^4$, even for the most naive implementation. This disadvantage is partly outweighed by the fact that the general contraction scheme lends itself well to vectorization in terms of matrix multiplications, where the effective vector length varies between $(N_{prim})^3$ and $(N_{cont})^3$ [116,117]. It should be noted, though, that the number of operations is linear in the number of primitive integrals, the ratio being of the order $2N_{prim}/(k-1)$.

Consistent with our assumption that the calculation of primitive integrals is vectorized, we assume that batches of primitive integrals arising from all exponents and all components of a set of four l values have been evaluated simultaneously, or at least handled in a specific sequence. The general contraction

transformation from the primitive basis $\{\alpha, \beta, \dots\}$ to the contracted basis $\{\mu, \nu, \dots\}$ is carried out in four steps [116],

$$(\alpha\beta|\gamma\delta) \rightarrow (\mu\beta|\gamma\delta) \rightarrow (\mu\nu|\gamma\delta) \rightarrow (\mu\nu|\lambda\delta) \rightarrow (\mu\nu|\lambda\sigma) \quad (\text{A1})$$

using as index quadruples

$$[\alpha, \beta, \gamma, \delta], [\beta, \gamma, \delta, \mu], [\gamma, \delta, \mu, \nu], [\delta, \mu, \nu, \lambda], [\mu, \nu, \lambda, \sigma], \quad (\text{A2})$$

respectively, where the index $[\alpha, \beta, \gamma, \delta]$ denotes storage with the first index varying fastest, etc. If the shells contain n_1, n_2, \dots primitive functions and m_1, m_2, \dots contracted functions, we can define a compressed index from the last three indices of the quadruple, say for $[\alpha, \beta, \gamma, \delta]$, as

$$p_1 = \delta + (\gamma - 1) * n_4 + (\beta - 1) * n_3 * n_4 \quad (\text{A3})$$

so that

$$A_{\alpha\beta\gamma\delta}^{(1)} = (\alpha\beta|\gamma\delta) = A_{\alpha, p_1}^{(1)} \quad (\text{A4})$$

The first quarter-transformation is then

$$\begin{aligned} A_{\beta\gamma\delta\mu}^{(2)} &= (\mu\beta|\gamma\delta) = A_{p_1, \mu}^{(2)} \\ &= \sum_{\alpha}^{n_1} (\alpha\beta|\gamma\delta) T_{\alpha\mu} = \sum_{\alpha}^{n_1} A_{\alpha, p_1}^{(1)} T_{\alpha\mu} = [\mathbf{A}^{(1)\dagger} \mathbf{T}]_{p_1, \mu}, \end{aligned} \quad (\text{A5})$$

or, in matrix notation

$$\mathbf{A}^{(2)} = \mathbf{A}^{(1)\dagger} \mathbf{T}. \quad (\text{A6})$$

Clearly, this step is a matrix multiplication with a vector loop length of $n_2 * n_3 * n_4$, if the “inactive” index p_1 is used for the innermost loop.

Next, consider the quarter-transformed integrals $(\mu\beta|\gamma\delta)$ as a two-dimensional array where now μ , β and γ are collapsed into a single index, p_2 .

$$A_{\beta\gamma\delta\mu}^{(2)} = (\mu\beta|\gamma\delta) = A_{\beta,p_2}^{(2)}. \quad (\text{A7})$$

It should be noted that no explicit data movement (that is, no reordering of data in computer memory) is necessary to go from $A_{p_1,\mu}^{(2)}$ to $A_{\beta,p_2}^{(2)}$. In both cases the array is a set of integrals $(\mu\beta|\gamma\delta)$ stored with β as the fastest varying index, μ as the slowest; the change is only one of notation. Again, the second step in the transformation is carried out as

$$\begin{aligned} A_{\gamma\delta\mu\nu}^{(3)} &= (\mu\nu|\gamma\delta) = A_{p_2,\nu}^{(3)} \\ &= \sum_{\beta}^{n_2} (\mu\beta|\gamma\delta) T_{\beta\nu} = \sum_{\beta}^{n_2} A_{\beta,p_2}^{(2)} T_{\beta\nu} = [\mathbf{A}^{(2)\dagger} \mathbf{T}]_{p_2,\nu}, \end{aligned} \quad (\text{A8})$$

or

$$\mathbf{A}^{(3)} = \mathbf{A}^{(2)\dagger} \mathbf{T}, \quad (\text{A9})$$

with a largest vector length of $n_3 * n_4 * m_1$. The last two quarter-transformations can be carried out in exactly the same way, with vector lengths of $n_4 * m_1 * m_2$ and $m_1 * m_2 * m_3$.

The above scheme thus allows computationally efficient use of a general, as opposed to a segmented, contraction scheme, and has been incorporated into the program MOLECULE [115]. It works well if the number of primitive functions in a shell is reasonably large, so that the number of primitive integrals, $n_1 * n_2 * n_3 * n_4$ is large. The effective vector length might often be less than optimal for many small basis sets, especially when basis sets contain polarization functions with a

single exponent for a given l -value. Unfortunately, therefore, the highest (and thus most time-consuming) l -values are likely to suffer most from these short vector lengths. A remedy for this problem can often be obtained by rearranging the basis sets to “superatoms”, i.e. groups of basis functions extending over several different centers. The only modification needed in the integral code is that coordinates must be assigned to each primitive function in the shell, rather than to the entire shell itself. The atoms contributing to a superatom can be of different type, though to facilitate the exploitation of molecular symmetry we normally require that they all have the same multiplicity with respect to the symmetry operations used. This procedure increases the effective vector length in the integral calculation, and improvements in integral time ranging from a factor of two to ten are typically seen on vector computers. In addition, the overhead involved in the integral evaluation is significantly reduced, and important savings are therefore seen also on hardware where vector length by itself is of no immediate concern.

A.2. Symmetry Properties of Basis Functions

GTOs for polyatomic calculations are usually defined in terms of their Cartesian components, as in Eq. (9). For s and p orbitals their angular parts are identical to the real spherical harmonics, but for $L > 1$ the space spanned by the Cartesian functions is larger than that spanned by the spherical harmonics with $l = L$. Hence for a given L the $\binom{L+2}{2}$ Cartesian functions, which form a linearly independent set, can be transformed to subsets which comprise not only the $(2l+1)$ orthogonal spherical harmonics of order l , but also sets of spherical harmonics with $l = L-2, L-4, \dots$. These “contaminants” are radially nodeless functions of the type $3s$ for $L = 2$, $4p$ for $L = 3$, $5d$ and $5s$ for $L = 4$, etc.

In the evaluation of many-center integrals over GTOs, the calculation is almost invariably carried out in terms of Cartesians. The basis is thus of larger dimension than it would be if the contaminants were excluded. The contaminants have not been chosen according to any optimization criterion, and are therefore not

necessarily well suited for the description of AOs with their particular n and l quantum numbers. In this sense, the integral list is needlessly lengthened by retaining the contaminants. In SCF calculations where integral time is the rate-determining step, and in which the basis set is small enough that storage of the integrals is not a problem, there may be arguments for retaining them [118], since their removal only increases the computation time. The near-linear dependence that may arise when these functions are added to an already large basis can be controlled with the same standard methods used to handle more general linear dependencies [119]. In correlated calculations, however, there is clearly an advantage in selecting each basis function carefully, as the cost of the entire calculation in that case depends largely on the size of the contracted basis set. The contaminants should therefore always be projected out of the basis. The final (i.e. spherical harmonic) CGTOs then become linear combinations of Cartesian CGTOs, and a transformation of Cartesian integrals to spherical harmonic integrals must be performed. In the MOLECULE program [115] this transformation is handled using the same scheme as described in 3.4 for general contraction. Lindh *et al.* [120] have developed schemes whereby the transformation to spherical harmonics can be amalgamated with the evaluation of primitive integrals in the same way as the contraction, resulting in significant savings. Explicit timing comparisons of integral evaluation and correlated wave function generation for Cartesian and spherical harmonic basis sets are given in Ref. 121.

There are additional computational techniques to be exploited in the calculation and manipulation of the two-electron integrals, at least when the molecule has spatial symmetry. Atom-centered basis functions are symmetry-related: they span reducible representations of the molecular point group. Hence integrals over the basis functions are symmetry-related, and only unique integrals need be evaluated; see, for example, Ref. 122 and references therein. This reduces the integral evaluation time, and can be used to reduce the computation time in other steps of the calculation. An even more powerful approach is to form linear combinations of the basis functions that transform according to irreducible representations of the point group [123–125]. Such symmetry adaptation leads to

an extensive blocking of the integral list and other arrays that are manipulated in the wave function calculation. In most implementations of symmetry in algorithms for electronic structure calculations, only point groups with real, one-dimensional representations are considered, that is, D_{2h} and its subgroups. While the theory for higher point groups is known [125], it has turned out difficult to design cost-effective implementations for general electronic structure codes. The symmetry adaptation of unique integrals can be formulated to require considerably less work than the (obvious) four-index transformation scheme, and as discussed in Ref. 121, the gain in computational efficiency in subsequent steps, such as transformation of integrals from the AO to MO basis, is considerable.

ACKNOWLEDGMENTS

The authors would like to thank many colleagues and collaborators for helpful discussions and comments. PRT was supported by NASA Grant NCC 2-371. Part of this work was supported by the National Science Foundation, Grant No CHE-8915629 (JA).

REFERENCES

1. C. C. J. Roothaan, *Rev. Mod. Phys.* **23**, 69 (1951).
2. G. G. Hall, *Proc. Roy. Soc. A* **205**, 541 (1951).
3. J. A. Pople and R. K. Nesbet, *J. Chem. Phys.* **2**, 571 (1954).
4. R. Carbó and M. Klobukowski, eds., *SCF Theory and Applications* (Elsevier, Amsterdam, 1990).
5. C. A. Weatherford and H. W. Jones, *ETO Multicenter Molecular Integrals* (Reidel, Dordrecht, 1982).
6. S. F. Boys, *Proc. Roy. Soc. A* **200**, 542 (1950).
7. S. F. Boys, G. B. Cook, C. M. Reeves, and I. Shavitt, *Nature* **178**, 1207 (1956).

8. H. Preuss, *Z. Naturforsch. A* **11**, 323 (1956).
9. R. K. Nesbet, *J. Chem. Phys.* **32**, 1114 (1960).
10. H. Taketa, S. Huzinaga, and K. O-ohata, *J. Phys. Soc. Japan* **21**, 2313 (1966).
11. W. J. Hehre, R. F. Stewart, and J. A. Pople, *J. Chem. Phys.* **51**, 2657 (1969).
12. M. Krauss, *J. Chem. Phys.* **38**, 564 (1963).
13. E. Clementi and D. R. Davis, *J. Comput. Phys.* **2**, 223 (1967).
14. R. C. Raffenetti, *J. Chem. Phys.* **58**, 4452 (1973).
15. M. W. Schmidt and K. Ruedenberg, *J. Chem. Phys.* **71**, 3951 (1979).
16. P. O. Löwdin, *Adv. Chem. Phys.* **2**, 207 (1959).
17. O. Sinanoglu, *Adv. Chem. Phys.* **14**, 237 (1969).
18. A. C. Hurley, *Electron Correlation in Small Molecules* (Academic Press, London, 1976).
19. K. P. Lawley, ed., *Adv. Chem. Phys.* (Vol 67 and 69, Wiley, New York, 1987).
20. C. W. Bauschlicher, S. R. Langhoff, and P. R. Taylor, *Adv Chem Phys.* **77**, 103 (1990).
21. F. Sasaki and M. Yoshimine, *Phys. Rev. A* **9**, 17 (1974).
22. R. J. Bartlett, *J. Phys. Chem.* **93**, 1697 (1989).
23. W. J. Hehre, R. Ditchfield, and J. A. Pople, *J. Chem. Phys.* **53**, 932 (1970).
24. E. R. Davidson, *Reduced Density Matrices in Quantum Chemistry* (Academic Press, London, 1976).
25. P. O. Löwdin, *Phys. Rev.* **97**, 1474 (1955).
26. P. O. Löwdin and H. Shull, *Phys. Rev.* **101**, 1730 (1956).
27. K. Jankowski, R. Becherer, P. Scharf, H. Schiffer, and R. Ahlrichs, *J. Chem. Phys.* **82**, 1413 (1985).
28. T. H. Dunning, Jr, *J. Chem. Phys.* **90**, 1007 (1989).
29. F. B. van Duijneveldt, *IBM Research Report RJ 945* (IBM, San Jose, 1971).

30. I. Shavitt, in *Methods of Molecular Electronic Structure Theory*, ed. H. F. Schaefer (Plenum, New York, 1977).
31. L. G. M. Pettersson and P. E. M. Siegbahn, *J. Chem. Phys.* **83**, 3538 (1985).
32. E. R. Davidson and D. Feller, *Chem. Rev.* **86**, 681 (1986).
33. J. Almlöf and P. R. Taylor, *J. Chem. Phys.* **86**, 4070 (1987).
34. T. H. Dunning, Jr and P. J. Hay, in *Methods of Molecular Electronic Structure Theory*, ed. H. F. Schaefer (Plenum, New York, 1977).
35. T. H. Dunning, Jr, *J. Chem. Phys.* **66**, 1382 (1977).
36. P. J. Hay and T. H. Dunning, Jr, *J. Chem. Phys.* **66**, 1306 (1977).
37. D. Feller and K. Ruedenberg, *Theoret. Chim. Acta* **52**, 231 (1979).
38. S. F. Boys, *Proc. Roy. Soc.* **A201**, 125 (1950).
39. S. F. Boys, *Proc. Roy. Soc.* **A217**, 136 (1950).
40. P. Jørgensen, private communication.
41. H. Partridge, *J. Chem. Phys.* **90**, 1043 (1989).
42. H. Partridge, *J. Chem. Phys.* **87**, 6643 (1987).
43. H. Partridge and K. Fægri, *Theoret. Chim. Acta.* in press.
44. R. Ahlrichs and P. R. Taylor, *J. Chim. Phys.* **78**, 315 (1981).
45. V. R. Saunders, in *Methods in Computational Molecular Physics*, eds. G. H. F. Diercksen and S. Wilson (Reidel, Dordrecht, 1983).
46. S. Obara and A. Saika, *J. Chem. Phys.* **84**, 3963 (1986).
47. M. Head-Gordon and J. A. Pople, *J. Chem. Phys.* **89**, 5777 (1988).
48. E. Clementi, *J. Chem. Phys.* **46**, 3851 (1967).
49. S. F. Boys and F. Bernardi, *Mol. Phys.* **19**, 553 (1970).
50. B. Liu and A. D. McLean, *J. Chem. Phys.* **59**, 4557 (1973).
51. B. Liu and A. D. McLean, *J. Chem. Phys.* **91**, 2348 (1989).
52. A. Johansson, P. Kollman, and S. Rothenberg, *Theoret. Chim. Acta* **29**, 167 (1973).
53. R. K. Nesbet, *Phys. Rev.* **175**, 2 (1968).
54. C. W. Bauschlicher, S. R. Langhoff, and P. R. Taylor, *J. Chem. Phys.* **88**, 2540 (1988).

55. H. Partridge, C. W. Bauschlicher, L. G. M. Pettersson, A. D. McLean, B. Liu, M. Yoshimine, A. Komornicki, *J. Chem. Phys.* **92**, 5377 (1990).
56. R. McWeeny and W. Kutzelnigg, *Int. J. Quantum Chem.* **8**, 707 (1968).
57. R. K. Nesbet, *Proc. Roy. Soc. A* **230**, 312 (1955).
58. C. W. Bauschlicher and P. R. Taylor, *Theoret. Chim. Acta* **74**, 63 (1988).
59. C. W. Bauschlicher, *J. Phys. B* **21**, 1413 (1988).
60. C. A. Coulson, *Valence* (Oxford University Press, London, 1953).
61. C. W. Bauschlicher, *Chem. Phys. Lett.* **142**, 71 (1987).
62. T. J. Lee, A. P. Rendell, P. R. Taylor, *J. Chem. Phys.* **92**, 489 (1990).
63. S. R. Langhoff, C. W. Bauschlicher, and P. R. Taylor, *J. Chem. Phys.* **88**, 5715 (1988).
64. P.-O. Widmark, P.-Å. Malmqvist, and B. Roos, *Theoret. Chim. Acta* **77**, 291 (1990).
65. J. Almlöf and P. R. Taylor, *J. Chem. Phys.* **92**, 551 (1990).
66. J. Almlöf, T. U. Helgaker, and P. R. Taylor, *J. Phys. Chem.* **92**, 3029 (1988).
67. C. W. Bauschlicher and S. R. Langhoff, *Chem. Phys. Lett.* **135**, 67 (1987).
68. W. Meyer and P. Rosmus, *J. Chem. Phys.* **63**, 2356 (1975).
69. C. F. Melius and J. S. Binkley, in *Twentieth Symposium on Combustion* (The Combustion Institute, Pittsburgh, 1984).
70. K. M. Ervin and P. B. Armentrout, *J. Chem. Phys.* **86**, 2659 (1987).
71. C. W. Bauschlicher and S. R. Langhoff, *J. Chem. Phys.* **87**, 2919 (1987).
72. S. R. Langhoff, C. W. Bauschlicher, and P. R. Taylor, *Chem. Phys. Lett.* **135**, 543 (1987).
73. C. W. Bauschlicher, S. R. Langhoff, and P. R. Taylor, *Astrophys. J.* **332**, 531 (1988).

74. K. P. Huber and G. Herzberg, *Constants of Diatomic Molecules* (Van Nostrand Reinhold, New York, 1979).
75. J. Kordis and K. A. Gingerich, *J. Chem. Phys.* **58**, 5058 (1973).
76. J. O. Arnold and R. W. Nicholls, *J. Quant. Spectrosc. Rad. Transf.* **12**, 1435 (1972).
77. R. Engleman, Jr and P. E. Rouse, *J. Quant. Spectrosc. Rad. Transf.* **15**, 831 (1975).
78. D. L. Lambert, B. Gustafsson, K. Eriksson, and K. H. Hinkle, *Astrophys. J. Suppl. Ser.* **62**, 373 (1986).
79. R. Ahlrichs, P. Scharf, and K. Jankowski, *Chem. Phys.* **98**, 381 (1985).
80. J. Almlöf, B. J. DeLeeuw, P. R. Taylor, C. W. Bauschlicher, and P. Siegbahn, *Int. J. Quantum. Chem. Symp.* **23**, 345 (1989).
81. H.-J. Werner and P. J. Knowles, *J. Chem. Phys.* **94**, 1264 (1991).
82. C. M. Rohlfing and J. Almlöf, *Chem. Phys. Lett.* **147**, 258 (1988).
83. J. Almlöf and P. R. Taylor, *Int. J. Quantum Chem.* **27**, 743 (1985).
84. W. Meyer, *J. Chem. Phys.* **58**, 1017 (1973).
85. K. Kuchitsu and L. S. Bartell, *J. Chem. Phys.* **36**, 2470 (1962).
86. P. Pulay, W. Meyer, and J. E. Boggs, *J. Chem. Phys.* **68**, 5077 (1978).
87. L. S. Bartell and K. Kuchitsu, *J. Chem. Phys.* **68**, 1213 (1978).
88. D. L. Gray and A. G. Robiette, *Mol. Phys.* **37**, 1901 (1979).
89. P. E. M. Siegbahn, *Chem. Phys. Lett.* **119**, 515 (1985).
90. N. C. Handy, J. F. Gaw, and E. D. Simandiras, *J. Chem. Soc. Faraday Trans. 2* **83**, 1577 (1987).
91. P. Bowen-Jenkins, L. G. M. Pettersson, P. Siegbahn, J. Almlöf, and P. R. Taylor, *J. Chem. Phys.* **88**, 6977 (1988).
92. P. R. Taylor, T. J. Lee, J. E. Rice, and J. Almlöf, *Chem. Phys. Lett.* **163**, 359 (1989).
93. G. Maroulis and A. J. Thakkar, *Chem. Phys. Lett.* **156**, 87 (1989).
95. J. E. Rice, P. R. Taylor, T. J. Lee, and J. Almlöf, *J. Chem. Phys.* **94**, 4972 (1991).

96. M. R. A. Blomberg, U. Brandemark, P. E. M. Siegbahn, K. Broch-Mathisen, and G. Karlström, *J. Phys. Chem.* **89**, 2171 (1985).
97. C. W. Bauschlicher, *J. Chem. Phys.* **84**, 260 (1986).
98. M. R. A. Blomberg, U. Brandemark, and P. E. M. Siegbahn, *Chem. Phys. Lett.* **126**, 317 (1986).
99. J. W. Kauffman, R. H. Hauge, and J. L. Margrave, *J. Phys. Chem.* **89**, 3541 (1985).
100. J. Sauer, H. Haberlandt, and G. Pacchioni, *J. Phys. Chem.* **90**, 3051 (1986).
101. S. R. Langhoff, C. W. Bauschlicher, and P. R. Taylor, *J. Chem. Phys.* **91**, 5953 (1989).
102. J. Olsen, B. O. Roos, P. Jørgensen, and H. J. Aa. Jensen, *J. Chem. Phys.* **89**, 2185 (1988).
103. P.-Å. Malmqvist, A. P. Rendell, and B. O. Roos, *J. Phys. Chem.* **94**, 5477 (1990).
104. D. C. Comeau, I. Shavitt, P. Jensen, and P. R. Bunker, *J. Chem. Phys.* **90**, 6491 (1990).
105. M. R. Nyden and G. A. Petersson, *J. Chem. Phys.* **75**, 1843 (1981).
106. G. A. Petersson, A. K. Yee, and A. Bennett, *J. Chem. Phys.* **83**, 5105 (1985).
107. G. A. Petersson, A. Bennett, T. G. Tensfeldt, M. A. Al-Laham, W. A. Shirley, and J. Mantzaris, *J. Chem. Phys.* **89**, 2193 (1988).
108. R. Krishnan, J. S. Binkley, R. Seeger, and J. A. Pople, *J. Chem. Phys.* **72**, 650 (1980).
109. C. W. Bauschlicher, *Chem. Phys. Lett.* **122**, 572 (1985).
110. J. M. L. Martin, J. P. François, and R. Gijbels, *J. Comput. Chem.* **10**, 152 (1989).
111. R. G. Parr, *Quantum Theory of Molecular Electronic Structure* (Benjamin, New York, 1964).
112. A. C. Hurley, *Rev. Mod. Phys.* **35**, 448 (1963).
113. K. Ruedenberg, M. W. Schmidt, M. M. Gilbert, and S. T. Elbert, *Chem. Phys.* **71**, 65 (1982).

- 114. M. W. Schmidt, M. T. B. Lam, S. T. Elbert, and K. Ruedenberg, *Theoret. Chim. Acta* **68**, 69 (1985).
- 115. J. Almlöf and P. R. Taylor, The MOLECULE Integral Program, unpublished work.
- 116. J. Almlöf and P. R. Taylor, in *Advanced Theories and Computational Approaches to the Electronic Structure of Molecules*, ed. C. E. Dykstra (Reidel, Dordrecht, 1984).
- 117. R. Ahlrichs, H.-J. Böhm, C. Ehrhardt, P. Scharf, H. Schiffer, H. Lischka, and M. Schindler, *J. Comput. Chem.* **6**, 200 (1985).
- 118. M. Sabio and S. Topiol, *J. Comput. Chem.* **10**, 660 (1989).
- 119. A. C. Hurley, *Introduction to the Electron Theory of Small Molecules* (Academic Press, London, 1976).
- 120. R. Lindh, U. Ryu, and B. Liu, *J. Chem. Phys.*, in press
- 121. P. R. Taylor, C. W. Bauschlicher, and D. W. Schwenke, in *Methods in Computational Chemistry, Vol. 3*, ed. S. Wilson (Plenum, New York, 1989).
- 122. M. Dupuis and H. F. King, *Int. J. Quantum Chem.* **11**, 613 (1977).
- 123. R. M. Pitzer, *J. Chem. Phys.* **58**, 3111 (1973).
- 124. J. Almlöf, MOLECULE Integral Program (University of Stockholm, Institute of Physics Report 74-29, 1974).
- 125. E. R. Davidson, *J. Chem. Phys.* **62**, 400 (1975).

A

Ab initio method, 149
 Absorption cross-section, 140
 Pt, 140–141
 ACCD, *see* Approximate coupled cluster doubles method
 ACP-D45, *see* Approximate coupled cluster doubles method
 Actinide compounds, 138
 Ag cluster, 148
 AGP, *see* Antisymmetrized geminal power
 Angular momentum, 48–49
 Langer modification, 45
 Annulenes resonance, 75, 81
 ANO, *see* Basis sets, atomic natural orbital
 Anticommuting complex variables, 35, 43
 Antisymmetrized geminal power, 169
 AO, *see* Atomic orbitals
 Approximate coupled cluster doubles method, 175
 Approximation methods, 9
 coupled cluster doubles polarization propagator approximation, 183
 coupled cluster polarization propagator approximation, 180–185
 coupled electron pair approximations, 168
 Dirac-Slater approximation, 261
 “Frozen-core” approximations, 127
 Gaussian approximation, 73, 75, 91
 Hartree-Fock approximation, 303
 higher random phase approximation, 181
 perturbation techniques, 9
 phase-integral approximation, 44
 random phase approximation, 177
 saddle-point approximation, 15, 74–75, 77, 84, 91, 111
 second order polarization propagator approximation, 169, 177–197
 self-consistent-multipolar approximation, 128
 semiclassical approximation, 9

stationary phase approximation, 91
 variational methods, 9
 WKB, 10, 44

Aromatic systems resonance, 78
 Atomic basis sets, *see* Basis sets, atomic
 Atomic interaction line, 130
 Atomic orbitals, 4–5, 15, 53, 55, 62, 65, 68, 74, 76, 81, 83, 85, 87, 127, 145, 301
 Pt₂, 145
 Au₆ complexes, 138
 γ -Al₂O₃, 146–147
 [110] surface, 146

B

Basis optimization, 127
 Basis sets
 atomic, 310
 atomic natural orbital, 301–373
 alkaline-earth atoms, 323
 H₂, 332
 transition metal atoms, 333
 contraction, 318–322
 general, 320
 segmented, 320
 contraction errors, 331–340
 H₂O, 336–340
 N atom, 334
 N₂, 334–336
 core correlation, 329–330
 expansion, 318–330
 extended, 322–325
 primitive, 325–327
 superposition error, 328–329
 Be atom, excitation energies, 187, 190
 Bifurcation and catastrophe theory, 15, 78, 82
 Binding energy
 C₂, 342
 CN, 342
 CN⁻, 342
 H₂, chemisorbed on Pt₄, 154

Binding energy (*continued*)

- N₂, 342
- NH, 341
- Ni(H₂O), 356
- NO, 342
- Pt₂, 144
- Pt₄H₂, 158
- Pt₄H₆, 158
- Pt₄H₈, 158
- Pt₄H₁₀, 158
- Pt₄H_x, 158–159
- Birman-Schwinger bound, 272
- Bond disruption process, 137
- Bond distance(length), 128
 - CH₄, 347–350
- Bond ellipticity, 130
 - H-H, 135
 - Ni-H, 135
 - Ni-Ni, 135
 - Ni₄, 136
- Bond formation process, 137
- Bond path, 130, 134, 136
 - H-H, 132–136
 - Ni-Ni, 134
- Bond strength, 136
 - TM-H, 138
 - TM-TM, 138
- Bonding, 2, 62, 82, 113
 - intermetallic, 125
- Bonds
 - covalent, 2
 - δ, 3
 - double, 4
 - π, 3
 - σ, 3
 - single, 4
- Bose operators, 105
- Bose systems, *see* Boson systems
- Boson
 - functional integral, 43
 - Goldstone, 81
 - partition function, 108
 - systems, 35, 92, 105
- Bound states, 127
 - energies, 44
- BP, *see* Bond path
- Brownian motion theory, 12
- BSSE, *see* Basis set superposition error
- Bulk metals
 - EAM study, 143
 - EAM-MD calculations, 143

C

- C₂
 - binding energy, 342
 - dissociation energy, 342
- C₂H₂ chemisorbed on Ni(111) surface, 132
- Carbon dimer, ground state, 3
- Carrier space, 106
- Cartesian Gaussian functions, 306
- CAS-SCF calculations, 150
- Catastrophe machine, Zeeman, 79
- Catastrophe theory, *see* Bifurcation and catastrophe theory
- CBS, *see* Correlation energy, complete basis set
- CC, *see* Coupled cluster method
- CCDPPA, *see* Coupled cluster doubles
 - polarization propagator approximation
- CCPPA, *see* Coupled cluster polarization
 - propagator approximation
- CCSD, *see* Coupled cluster equations, singles and doubles model
- CEPA, *see* Coupled electron pair approximations
- CGTO, *see* Contracted Gaussian type orbital
- CH⁺ ion
 - cluster amplitudes, 193
 - correlation coefficients, 193
 - excitation energy, 189, 191
 - oscillation strength, 192
 - radiative lifetime, 193
 - transition moment, 192
- CH₄, bond distance(length), 347–350
- Charge density, 180
 - contour interval, 131
 - contours, 131, 133
 - H-H, 135
 - H₂Ni₄, 133
 - Li clusters, 131
 - Na clusters, 131
 - Ni-H, 135
 - Ni-Ni, 135
 - Ni₄, 131, 136
 - Pt_n, 139
- Charge-density waves, 80
- Charge distribution, 130
- Chemical activity, 136
- Chemical bond, directionality, 136
- Chemical bonding, *see* Bonding
- Chemisorption,
 - C₂H₂ on Ni(111) surface, 132

H_2 on Pt_4 surface, 153
 Chemisorption path, 132
 CHF, *see* Coupled Hartree-Fock method
 CI, *see* Configuration-interaction expansion
 Closure relations, 84
 Cluster amplitudes, CH^+ ion, 193
 Cluster valency model, 150
 CN
 binding energy, 342
 dissociation energy, 342
 CN^-
 binding energy, 342
 dissociation energy, 342
 Coherent states, 16, 35
 Cohesion, 144, 145
 Cohesive energies, 126, 137
 Ni_4 , 128
 Pt_2 , 139
 Pt_n , 142
 Commutation superoperators, 93
 Complex formation, 130
 Compression energy, s bonds, 4
 Compton profile, directional, 242
 Configuration-interaction expansion, 308
 Configuration space, 45
 Conjugated hydrocarbons, CC distances, 4
 Constrained search procedure, 243–246
 Contracted Gaussian type orbital, 307
 Cooper pairs, 81
 Core orbitals, 145
 Correlation coefficients
 CH^+ ion, 193
 spin-adapted, first order, 174
 Correlation effects
 dynamical, 309
 nondynamical, 308
 Correlation energy, 174
 complete basis set, 359
 second order, 174
 third order, 174
 Correlation energy functional, 277–278
 atoms, 278
 molecules, 278
 Corresponding effective action, 15
 Coulomb potential, 44–47, 53, 56, 127
 Coulomb problem, 59
 Coulomb singularity, attractive potential, 44
 Coupled cluster doubles polarization
 propagator approximation, 183
 Be atom, excitation energies, 187, 190

CH^+ ion, excitation energies, 189
 extended, 184
 Coupled cluster equations
 singles and doubles model, 170
 spin-adapted, 170–209
 Coupled cluster method, 168
 Coupled cluster polarization propagator
 approximation, 180–185
 Coupled cluster polarization propagator
 method, 167–209
 analysis, 185–191
 list of calculations, 194
 Coupled electron pair approximations, 168
 Coupled Hartree-Fock method, 181
 Covalent bonding, 128, 148–149
 Pt_4 , 148, 152
 $\text{Pt}_4(\text{O}_2\text{CCH}_3)_8$, 149
 CP, *see* Critical points
 Critical points, 130
 dipole moment, 346
 energy, 346
 Cusp catastrophe surface, 79–81

D

D-MBPT(∞), *see* Linearized coupled cluster
 doubles
 Defect structures
 EAM study, 143
 TM oxides, 138
 Density functional theory, 213, 216–231
 constrained search procedure, 243–246
 electronegativity, 229
 hardness, 229
 N-representability, 221
 non-V-representability, 224
 pure state V-representability, 223–225
 self-interaction correction, 229
 Slater transition state method, 228
 spin-polarized, 229
 V-representability, 222
 X_α -method, 228
 Density functionals
 Coulomb systems, 281–284
 scaling properties, 245
 Density gradient field
 H_2Ni_4 cluster, 133
 Ni_4 cluster, 131
 Density matrix, 35, 45
 equivalence restrictions, 332
 Density operator, 42

Density of states
 partial
 Pt_{13} , 139
 $\text{Pt: Al}_2\text{O}_3$, 147
 partial spin
 Ni_4 , 129
 DFT, *see* Density functional theory
 Dipole moments, 345
 CP, 346
 H_2O , 336
 Dirac-Slater approximation, 261
 Dirac-Slater model, Pt_2 , 144
 Dirac-Slater moment-polarized relativistic
 scheme, 139
 Directional Compton profile, 242
 Discrete-variational X_α scheme, 126–127
 Dissociation energy
 C_2 , 342
 CN, 342
 CN^- , 342
 N_2 , 342
 NH, 341
 $\text{Ni}(\text{H}_2\text{O})$, 356
 NO, 342
 DV- X_α , *see* Discrete-variational X_α scheme
 Dyson equation, 72
 Dyson's time-ordering operator, 26, 36
 Dyson's U matrix theory, 92, 96

E

EAM, *see* Embedded atom method
 EAM-MD calculations, 143
 Effective core potentials, 127
 relativistic, 150
 EFG, *see* Electric field gradient
 Electric field gradient, H_2O , 338
 Electron-repulsion energy functional, 214
 bounds, 250–265
 bounds to direct Coulomb energies,
 251–258
 bounds to indirect Coulomb energies,
 259–263
 Electron-repulsion integrals, 213, 252
 bounds, 264–265, 290–292
 Electronegativity, atoms, 229
 Electronic density, 151–152
 pointwise, 246–247
 Electronic energies, total, 214
 bounds, Coulomb systems, 265–290
 Electronic energy level set topologies, 285
 Ellipticity, bond, *see* Bond ellipticity

Embedded atom method, 143
 Energy density functional, constrained search
 procedure, 243–246
 Energy functionals
 bounds to atomic and molecular, 211–300
 constrained search approach to, 276
 Hartree-Fock, 277
 scaling properties of, 276
 Thomas-Fermi, 219
 Energy hypersurface, topology, 285
 Energy propagator, 48–49, 58
 Energy truncation errors in
 Ne, 314, 316
 NO expansion, 314–316
 Equivalence restrictions, on density matrix,
 332
 ERI, *see* Electron-repulsion integrals
 Euclidean path integral, 63, 72
 Euler-angle coordinates, 50
 Evolution operator, 18–19, 26
 Evolution superoperators, 94
 in Liouville space, 15
 Exchange-correlation energy, 214
 bounds, 276
 Exchange-correlation potential, 127
 Exchange forces, 2
 Exchange integrals, molecular Coulombic, 70
 Excitation energies
 Be atom, 187, 190
 CH^+ ion, 189, 191
 Excitation operators, singlet, 171

F

Fermi energy, Ni_4 , 129
 Fermi levels, Ni_4 , 129
 Fermi systems, 16, 35–36
 Fermionic
 field operators, 92
 systems, 35, 92
 Fermions, 16, 36, 80
 interacting system, 35, 42
 propagator, 43
 Ferromagnetic cluster, 129
 Feynman functional integral, *see* Feynman
 path integral
 Feynman path integral, 7–123
 fermion particle system, 14
 field theories, 62
 gauge, 90
 time dependent mean, 84
 formulation of quantum mechanics, 62

hydrogen atom in four-dimensions, 14
 least-action mechanical principle, 9
 Liouville space, 92–98
 many electron systems, 62
 one-dimensional harmonic oscillator, 14
 partition function, 62
 propagator, 12–14, 16–20, 23, 25–26,
 28–30, 35, 38, 41–43, 52–54, 59,
 61, 63
 short-time propagators, 21, 41, 57, 66
 time-lattice subdivision process, 12
 Feynman superpropagator, 92, 104–105, 107
 Field operators, 92–110
 Finite many-body problem, equivalence
 between non-relativistic molecular
 system, 15
 First quantized Hamiltonians, 36
 Fluctuation potential
 second-order, 169
 third-order, 169
 Fluorine molecule, 3
 Fredholm's integral equation, 12, 102
 "Frozen-core" approximations, 127
 Functional calculus, 11
 Functional integrals, *see* Feynman path
 integral

G

Gaussian approximation, 73, 75, 91
 Gaussian integrals, 30, 45, 72, 111
 path integrals, 45
 Gaussian-type orbital, 306
 contracted, 307
 Generalized valence bond, 138
 ab initio method, 147–153
 orbitals, 148
 Pt₄, 148–152
 wave function, 151–152
 Pt₄, 152
 Gradient field
 H₂Ni₄, 133
 Ni₄, 131
 Gram-determinantal inequality, 252
 Green's functions, 12–13, 16, 44–45, 47,
 50–51, 72, 92, 110
 double-time retarded, 175
 energy dependent, 176
 Group theory classifications, 3
 GTO, *see* Gaussian-type orbital
 GVB, *see* Generalized valence bond

H

H-H bonds, 135
 charge density, 135
 ellipticity, 135
 Laplacian, 135
 H₂ adsorbed on Ni(111) surface, 132
 H₂ adsorbed on Ni₄ surface, 132
 H₂ chemisorbed on Pt₄ surface, 153
 binding energy, 154
 H₂Ni₄ cluster, 126, 128, 132–137
 charge density contour map, 133
 density gradient field, 133
 H₂O, 336–340
 contraction errors, 336–340
 dipole moment, 336
 electric field gradient, 338
 energy, 336
 polarizability, 339
 quadrupole moment, 336
 Hamiltonian superoperator, 177
 Harmonic oscillator, 29
 four-dimensional isotropic, 45
 Harmonic potential, 127
 Hartree-Fock approximation, 303
 Hartree-Fock calculations, 127
 Hartree-Fock determinant, 308
 Hartree-Fock equations, 85
 Hartree-Fock model
 non-linear, 82
 time-dependent, 84
 Hartree-Fock SCF orbitals, spatial, 171
 Hartree-Fock theory, 137
 time-dependent, 112
 Hartree product, 67
 Heaviside step function, 176
 Hellmann-Feynman theorem, 244
 Hellmann functional, 280
 Hellmann-Weizsäcker functional, 280
 Hermitian superoperators, *see* Superoperators,
 linear hermitian
 HF, *see* Hartree-Fock
 Higgs fields, 82
 Higher random phase approximation, 181
 HK functional, universal, 214, 218
 HK, *see* Hohenberg-Kohn
 Hohenberg-Kohn energy functional, 226
 Hohenberg-Kohn theorem, 213, 217–220
 Hopf fibration, 111
 HRP, *see* Higher random phase approxima-
 tion
 Hückel model, 62, 71, 75, 77, 111

Hückel model (*continued*)
 Gaussian, 81, 91
 partition function, 72–77
 Huygens-like principle, 102
 Hydrocarbon free radicals
 CH_2 , 4
 polyacetylene, 4
 Hydrocarbons, conjugated, CC distances, 4
 Hydrogen atom
 chemisorbed on Pt_4 , 154
 path integral theory, 44–61
 rotational invariance, 45
 Hydrogen bonding, double, 75, 78, 81
 Hydrogen molecular ion equation, 3
 Hydrogen molecule, 2, 4, 132
 Hydrogen- Pt_4 interaction, 147
 Hydrogen saturation, Pt_4H_x , 155–160
 Hydrogenic atomic orbitals, 55
 Hydrogenic oscillator, 45–47
 Hyperthyroidism, 78

I

Information theory, 241
 Infra-red vibrational spectra, 126
 Interatomic potential, 146
 Interatomic surface, 131
 Interface, metal-metal oxide, 126
 Intermetallic bonding, 125
 Ionic potentials, 146
 Ising model, 67, 75
 bidimensional continuum, 71
 continuum, 67, 72–73
 one-dimensional, 15, 64, 72, 111
 partition function, 64, 74

K

Kepler motion, 53
 Kernel, *see* Propagator
 Kinetic energy
 anisotropies, 242–243
 bosonic, 234
 bounds, density-matrix based, 232
 directional, 242
 fermionic, 234
 functional, 231–250
 pointwise electron density, 246–247
 Kinetic energy-density functional, 231
 constrained search procedure, 243–246
 r-space local kinetic energy density, 243

Kinetic-potential energies, interconnections, 248–250
 Kinetic repulsion energy functional, 214
 Klauder's continuous representation theory, 84, 88
 Kohn-Sham exchange-correlation energy functional, 226
 Kohn-Sham exchange-correlation functional, 280
 Kohn-Sham method, 226–230
 one-electron equations, 227
 Slater determinants, single, 227
 Kohn-Sham orbitals, 227
 Kohn-Sham-Slater exchange potential, 128
 Kohn-Sham transformation, 46, 49–50, 53, 56, 59–61, 111
 KS, *see* Kohn-Sham

L

Laplacian, 135
 H-H, 135
 Ni-H, 135
 Ni-Ni, 135
 Ni_4 , 135–136
 Lattice constant, 144
 LCAO, *see* Linear combination of atomic orbitals
 LCAO self-consistent field(SCF) equations, 304
 LCCD, *see* Linearized coupled cluster doubles
 LCCDPPA, *see* Linearized coupled cluster doubles polarization propagator approximation
 LD theory, 137
 LDF, *see* Local density functional calculations
 Lennard-Jones paper, 1–6
 auf-bau principle, 3
 hydrogen molecular ion equation, 3
 molecular orbital theory, 1–6
 Levi-Civita transformation, 60
 Lewis model, 2
 Li cluster, 148
 charge density topological analysis, 131
 Linear combination of atomic orbitals, 1, 85, 151, 302
 Linear hermitian operators, 94
 Linear muffin tin orbital method, 127
 Linear response function, 175
 Linearized CCD, *see* Linearized coupled cluster doubles
 Linearized coupled cluster doubles, 174

CH⁺ ion, excitation energy, 191
 Linearized coupled cluster doubles polariza-
 tion propagator
 approximation, 183
 CH⁺ ion, excitation energies, 191
 extended, 184
 Liouville superoperators, 94
 Lithium molecule, 4
 LMTO, *see* Linear muffin tin orbital method
 Local density functional calculations
 Pt₄, 152
 Pt₄H_x complex, 150
 wavefunctions, 152
 Local spin density
 calculations, 143
 jellium model, 143
 single particle theory, 126
 London force, 3
 Löwdin model, proton tunneling probabilities,
 11
 LSD, *see* Local spin density

M

Magnetic moment
 Ni, 137
 Pt₄, 139
 Magnetic resonance frequencies, protons, 82
 Magnetic susceptibility, 84
 Many body perturbation theory, 168–169,
 193, 212
 correlation coefficients, CH⁺, 193
 March-Young result, 232
 Markovian property, 25
 Matter, stability, 274–276
 MBPT, *see* Many body perturbation theory
 MCSCF, *see* Multiconfigurational self-
 consistent field
 MD, *see* Molecular dynamics
 Memory superoperators, 15, 92–110
 MESF, *see* Molecular electrostatic potentials
 Metal clusters
 in enzymatic reaction centers, 125
 in inorganic chemistry, 125
 in organometallic chemistry, 125
 in petroleum refining and chemical
 industries, 126
 in photographic process, 125
 Metal-ligand interaction, 147
 Metal-metal bonds, Pt₄, 148–149
 Metal-metal oxide interface, 126
 Metallic bonding, Pt₄(CO)₅, (PMe₂Ph)₅, 149

Mezey's theorem, 286
 MO, *see* Molecular orbitals
 Molecular-beam techniques, preparation of
 mass-separated Pt_n fluxes by, 142
 Molecular dynamics, 143
 Molecular electronic energy, monotonicity,
 284
 Molecular electrostatic potentials, bounds, 265
 Molecular nonbinding theorems, 268–272
 Molecular orbitals, 1–6, 301, 303
 Lennard-Jones paper of 1929, 1–6
 theory, 1–6,
 Molecular structure
 determining by intra-atomic relaxation
 mechanisms, 145
 theory of, 1
 MRCI, *see* Multireference configuration
 interaction
 MS-X_α, *see* Multiple scattering X_α method
 Mulliken populations
 Pt₄, 152, 155
 Pt₄H, 155
 Pt₄H_x, 158–159
 Multiconfigurational self-consistent field, 169,
 212
 Multiple scattering X_α method, Pt_n, 141
 Multireference configuration interaction, 341

N

N atom, contraction errors, 334
 N₂
 binding energy, 342
 contraction errors, 334–336
 dissociation energy, 342
 spectroscopic constants, 334–336
 Na cluster, 148
 charge density topological analysis, 131
 Natural orbitals, 311–318
 Ne atom, 312–318
 Natural spin-orbitals, 312
 Ne, 3
 natural orbitals, 312–318
 polarizability, 350–355
 Negative ions, stability, 266–268
 NH
 binding energy, 341
 dissociation energy, 341
 Ni(111) surface, pocket site, 132
 Ni(H₂O), 355–357
 binding energy, 356
 dissociation energy, 356

- Ni, magnetic moment, 137
 Ni-H bond
 charge density, 135
 ellipticity, 135
 Laplacian, 135
 Ni-H₂O interaction, 355–357
 Ni-Ni bond, 131, 134
 charge density, 135
 ellipticity, 135
 Laplacian, 135
 Ni₃ cluster, 132
 Ni₄ bonding, 129
 Ni₄ cluster, 126, 128–132, 148
 charge density, 131, 135–136
 density gradient field, 131
 ellipticity, 135
 Fermi energy, 129
 Fermi level, 129
 Laplacian, 135–136
 Ni₄H₂ cluster, 126, 128, 132–137
 NO
 binding energy, 342
 dissociation energy, 342
 Non-relativistic molecular system, equivalence between finite many-body problem, 15
 Nonbinding theorems, 268
 NR, *see* Density functional theory, N-representability
 NSO, *see* Natural spin-orbitals
 Nucleic bases, 75, 78, 81
- ## O
- Orbital expansion, 127
 Oscillator strength, CH⁺ ion, 192
 Oxygen
 ground state, 3
 structure, 3
- ## P
- Pair interactions, 168
 Pair-natural orbital, 359
 CH₄, 347
 Partition function, 65
 Partition functional for N-electrons, 68, 90
 Path integral method, *see* Feynman path integral
 Permutation operator, 173
 Permutation symmetry, 171
 Perturbation techniques, 9
 Perturbative polarization propagator methods, 175–180
 Phase-integral approximation, 44
 Phase-space representations, 10
 Phase transitions, 82
 Platinum valency model, 147
 PNO, *see* Pair-natural orbital
 Pointwise electron densities, 246–247
 Polarizability
 H₂O, 339
 Ne atom, 350–355
 Polarization propagator formalism
 coupled cluster wavefunction, 168
 response properties, 168
 Polarization propagator method, 167–209
 coupled cluster, analysis, 185–191
 coupled cluster, approximation, 180–185
 perturbative, 175–180
 second order, approximation, 169
 spin-adapted coupled cluster equations, 170–175
 Polaron problem, 11
 Polyacetylene, 4
 Potential expansions, 127
 Potts model, 74
 Projected generating functional, 87
 Propagator, 12–14, 16–20, 23, 25–26, 28–30, 35, 38, 41–43, 52–54, 59, 61, 63
 short-time, 21, 41, 57, 66
 Proto-atoms, 131
 Pseudo-atoms, 131
 PSVR, *see* Density functional theory, pure state V-representability
 Pt cluster, 138–145
 multiple scattering X_α method, 141
 Pt-ligand complex, 139
 Pt₂
 binding energy, 144
 nonrelativistic, 145
 relativistic effect, 145
 Pt₄, 147
 generalized valence bond orbitals, 147–152
 H, chemisorbed, 154
 local density functional wavefunctions, 152
 magnetic moment, 139
 Mulliken populations, 152, 155
 Pt: Al₂O₃, 138, 146
 density of states, partial, 147
 PtAl₅O₇⁺ cluster, 146
 Pt₄(CO)₅(PMe₂Ph)₅, metallic bonding, 149
 Pt₄H, Mulliken populations, 155

Pt_4H_2 cluster
 binding energies, 158
 Mulliken populations, 158
 Pt_4H_4
 binding energies, 158
 Mulliken populations, 158
 Pt_4H_6
 binding energies, 158
 Mulliken populations, 158
 Pt_4H_8
 binding energies, 158
 Mulliken populations, 158
 Pt_4H_{10}
 binding energies, 158–159
 Mulliken populations, 158
 Pt_4H_n cluster, 151
 binding energies, 158
 Mulliken populations, 158–159
 Pt_4H_x cluster, hydrogen saturation, 155–160
 $\text{Pt}_4(\text{O}_2\text{CCH}_3)_8$, covalent bonding, 149
 Pt_{13} cluster, 128
 density of states, partial, 139
 $\text{Pt}_{24}(\text{CO})_{22}(\mu_2\text{-CO})_8^{2-}$ dianion, 139
 Pt_n fluxes, mass-separated, preparation, 142

Q

Quadrupole moment, H_2O , 336
 Quantum field operators, 97
 Quantum field theoretic regime, 9
 Quantum field theory, 78, 81
 Quantum fluctuations, 15, 78, 81
 Quantum many-body propagator, 84
 Quasiclassical TF energy functional, 219
 Quaternionic polar coordinates, 50
 Quaternions, *see* Anticommuting complex variables

R

Radial path integral, 45
 Radiative lifetime, CH^+ ion, 193
 Random phase approximation, 177
 RASCI, *see* Restricted active space configuration interaction
 RASSCF, *see* Restricted active space self-consistent field methods
 Rayleigh-Schrödinger correlation coefficients, spin-adapted first order, 174
 Rayleigh-Schrödinger correlation energy, 174
 Rayleigh-Schrödinger perturbation theory, 174

Resonance
 annulenes, 75, 81
 aromatic systems, 78
 electron exchange, 2
 perturbation theory, 2
 Restricted active space configuration interaction, 358
 Restricted active space self-consistent field methods, 358
 Restricted active space self-consistent field orbitals, 359
 Roothaan's equations, 15, 84–91
 Roothaan-Hall equations, 305
 RPA, *see* Random phase approximation
 RS, *see* Rayleigh-Schrödinger
 RSPT, *see* Rayleigh-Schrödinger perturbation theory
 Runge-Lenz-Pauli vector, 49

S

Saddle-point approximation, 15, 74–75, 77, 84, 91, 111
 Saddle-point equations, 77
 Scattered wave method, 127
 SCC, *see* Self-consistent-charge scheme
 SCF, *see* Self-consistent field
 Schrödinger operators, 93
 SCM, *see* Self-consistent-multipolar approximation
 SDCl, *see* Single and double configuration interaction
 Second order polarization propagator approximation, 169, 177–197
 Be atom, excitation energies, 187, 190
 CH^+ ion, excitation energies, 189
 Second quantized hamiltonians, 13, 35–36, 42–43
 Self-consistent-charge scheme, 127–128, 151
 analysis, 129
 Self-consistent field
 ab initio method, 75, 213
 equations, 5
 Hamiltonian, 5
 potential, 127
 Self-consistent iteration process, 145
 Self-consistent-multipolar approximation, 128
 Self-consistent orbitals, 127
 Self-consistent perturbative DV- X_α approach, 144
 Self-energy and reactivity indices, 72

- Single and double configuration interaction, 312, 331
 Slater determinants, 68–69, 84–85, 88, 112
 single, 227, 277
 Slater transition-state method, 228
 Slater-type orbital, 305
 Sobolev inequality, 253
 three-dimensional, 239
 Soliton, 82
 SOPPA, *see* Second order polarization propagator approximation
 Spin density, local, 126
 calculations, 143
 Spin quantum numbers, 171
 Stark effect, 46, 55
 Stationary phase approximation, 91
 STO, *see* Slater-type orbital
 Superoperators
 identity, 101, 177
 linear hermitian, 94
 memory, 15, 92, 95–96, 98, 102
 mutually orthogonal projection, 94
 time-dependent, 94
 Surfaces
 EAM study, 143
 γ -Al₂O₃, 146
 Symmetry, 14, 46
 cylindrical, 130
 dynamical, 53
 geometrical, 53
 "hidden", 53
 permutation, 171
 spherical, 53
 Symmetry restrictions, on density matrix, 332
 Synergetics, links between critical phenomena and bifurcation theory, 82
- ### T
- TA, *see* Topological atom
 TDHF, *see* Time-dependent Hartree-Fock
 TF, *see* Thomas-Fermi
 TFD, *see* Thomas-Fermi-Dirac model
 TFDW, *see* Thomas-Fermi-Dirac-Weizsäcker model
 Thomas-Fermi-Dirac model, 219
 Thomas-Fermi-Dirac-Weizsäcker model, 219
 Thomas-Fermi energy functional, 219
 Thomas-Fermi theory, 268
 Thomson principle of classical electrostatics, 251
 Three-dimensional Sobolev inequality, 239
 Time-dependent Hartree-Fock, 177
 Time evolution equation, 103
 Time-ordering operator, *see* Dyson's time-ordering operator
 TM, *see* Transition metal
 TM magnetism
 chemisorbed atoms, 137
 chemisorbed molecules, 137
 quenching, 137
 TM-H bond, 138
 TM-TM bonds, 138
 Topological atom, 129
 analysis, 130
 charge density, Li clusters, 131
 charge density, Na clusters, 131
 transferability, 130
 Topology of energy hypersurfaces, 285
 Transfer matrix, 64
 one-electron, 69
 Transition metal clusters, 125–165
 bonding mechanism, 130
 electronic structure, 125
 interaction with external ligands, 125
 interaction with hydrogen and oxides, 125–165
 intermetallic bonding 125
 Transition metal oxides, defect structures, 138
 Transition moment, CH⁺ ion, 192
 Transition probabilities, in propagator or response methods, 168
 Transition state method, 228
 Tunnel effect, 80–81
- ### U
- U matrix theory, 92, 96
 Universal HK functional, 214, 218
- ### V
- Valency model, Pt, 147
 Variational principle, 217, 266
 Dirac, 74
 Hamilton, 79
 Virial theorem, 130, 248
 Volterra integral equation, 95
 VR, *see* Density functional theory, V-representability

W

Wave equations, non-linear, 78

Wave functions

bound states, 44

coupled cluster, 168–169

determinantal, 5

hydrogenic, 46, 54–55

microscopic Green's function approach, 12

molecular SCF, 311

multielectronic, of a p electron system, 79

N-electron molecular, 303

one-dimensional harmonic oscillator, 46, 52

one electron, 67–68, 72

path integral method, 12–13

single electron, 44

Weizsäcker correction, lower bounds, 233,
239–240

Wick rotation, 63, 107

WKB approximation, 10, 44

X

X-ray absorption near edge spectra, Pt clusters,
126, 138–142

X_α -scheme, 228

XANES, *see* X-ray absorption near edge spectra

Z

Zeeman effect, 46

Zwanzig-Feshbach projection space technique, 98